Effect of Limestone and Inorganic Processing Additions to Cement on the Strength and Durability of Concrete

BY

MUSTAPHA IBRAHIM
B.S., Lawrence Technological University, 2010

THESIS

Submitted as partial fulfillment of the requirements
for the degree of Doctor of Philosophy in Civil Engineering
in the Graduate College of the
University of Illinois at Chicago, 2016

Chicago, Illinois

Defense Committee:

Professor Mohsen Issa, Chair and Advisor
Professor Ahmed Shabana, Mechanical and Industrial Engineering
Professor Craig Foster
Professor Krishna Reddy
Professor Chien Wu

ACKNOWLEDGMENTS

I would like to thank my advisor Professor Mohsen Issa for his support and guidance throughout my PhD program. Professor Issa motivated me to advance my understanding of the framework of material and structural engineering. His deep knowledge and experience and his persevering nature have inspired and taught me to overcome numerous obstacles under enormous pressure.

I would also like to express my appreciation to my PhD committee members; Professor Ahmed Shabana, Professor Craig Foster, Professor Krishna Reddy, Professor Alexander Chudnovsky, and Professor Chien Wu. Their recommendation and advice in my research, was deeply appreciated.

I would also like to acknowledge the contributions of my colleagues and teammates in the ICT/IDOT research; Mustafa Al-Obaidi, Maen Farhat, Ibrahim Lotfy, and Momenur Rahman. Mustafa Al-Obaidi and Maen Farhat had major contribution as their help was vital in completing the experimental testing required in this research effort.

I would like to acknowledge the Illinois Center of Transportation and the Illinois Department of Transportation for sponsoring this research effort. Many thanks to the Chairman of the Technical Review Panel (TRP), Mr. John Huang, and the members of the TRP: Mr. Randy Riley (ACPA), Mr. Steve Kosmatka (PCA), Mr. Brian Borowski (LaFarge Cement), Mr. Douglas Dirks (IDOT), Mr. Nick Popoff (St Marys Cement), Mr. Raymond McVeigh (Great Lakes Cement Promotion Association), Mr. Brian Pfeifer (FHWA), and Mr. Paul Tennis (PCA). Also, special thanks are also extended to the Ozinga RMC Inc, Prairie Material, Holcim US Inc, St. Marys Cement, and W.R. Grace for procuring the materials for the study.

Finally, I would further like to express my deepest and sincere appreciation to my lovely family, especially my mother for her unconditional patience, support, encouragement, and love.

TABLE OF CONTENTS

LIST OF TABLES

LIST OF FIGURES

EXECUTIVE SUMMARY

The Illinois Department of Transportation (IDOT) has recently adopted making several changes to concrete mix designs, using revisions to cement specification ASTM C150/AASHTO M 85 and ASTM C465/AASHTO M 327 for the new IDOT Standard Specifications book. These proposed revisions may impact the department and the concrete industry. The addition of more than 5% limestone and Inorganic Process Additions (IPA) above the specified limit by ASTM C150 require strength and durability testing of concrete mixes using common cements with less than 5% and cements with more than 5% limestone and IPA. In addition to the limestone and IPA modification, the IDOT were interested in increasing the maximum permissible amount of insoluble residue (IR) in cement according to ASTM C150 from 0.75% to 1.5%. Therefore a comprehensive investigation was conducted to evaluate the strength and durability performance of concrete mixes for pavements and bridge decks when made with modified cement with higher quantities of limestone and IPA and IR amount exceeding what is recommended by ASTM C150/AASHTO M 85.

Twenty-six concrete mix combinations with total cementitious content of 535 lbs/yd^3 (317 Kg/m^3), which is the minimum amount of cementitious materials required by IDOT, were carried out. Different cementitious combinations and aggregates were used for this study. Three different cement sources were procured, provided with conventional and modified cement. Class C fly ash and ground granulated blast furnace slag (GGBF slag) were alternatively used as supplementary cementitious materials (SCMs) with 30% replacement by weight of the total cementitious content. Each cementitious combination was batched with one type of coarse aggregate (crushed limestone) and two types of fine

aggregates (natural sand and combined sand). The combined sand is a combination of 50% natural sand and 50% manufactured sand obtained as leftovers from the crushed limestone coarse aggregate quarries. The use of combined sand is recognized as part of the IDOT growing interest in producing sustainable concrete mix designs for pavements and bridge decks, by providing an effective method to secure limestone byproducts mainly from the processes of blasting and crushing required to produce crushed limestone in locally available quarries.

The study included measuring the fresh and hardened properties of concrete. The fresh properties included measuring the slump, air content, unit weight, and setting time. The hardened properties included measuring the strength and durability characteristics. The strength properties were measured in terms of compressive and flexural strength, and the durability performance was evaluated in terms of chloride ion penetration per salt ponding and diffusion test, rapid chloride penetration (RCP) test, water penetration (DIN 1048), freeze/thaw performance, and hardened air void parameters of the concrete mixes. The study found similar performance in terms of strength and durability of concrete between the conventional and modified cements and demonstrated their performance with SCMs replacements and fine aggregate types.

The freeze/thaw evaluation demonstrated series of premature failures in the specimens when the concrete mixes had sufficient entrained air content. Further investigation revealed that the cause of failure is attributed to aggregate popouts. This has raised some speculations on the adequacy of the minimum total cementitious content required (535 lbs/yd^3 [317 Kg/m^3]) to resist the freeze/thaw hostility. Based on the results of this study the IDOT has raised the bar for the minimum amount of Portland cement

content from 375 lbs/yd^3 (222 Kg/m^3) to 400 lbs/yd^3 (237 Kg/m^3) when 30% of fly ash or slag are used to replace the cement by weight of the total cementitious content.

Based on the experimental results, simplified analytical approaches to predict the water penetration coefficient in concrete based on the water penetration test results (DIN 1048), and the equivalent-steady state diffusion coefficient through the use of RCP test were developed. The penetration coefficient (K_w) of water penetrating in unsaturated concrete under hydrostatic pressure per DIN 1048 was estimated based on the average depth rather than the maximum depth of penetration. In addition, the equivalent-steady state diffusion coefficient (D_{c_rm}) based on the chloride migration rate per RCP test was estimated using the Nernst-Plank equation. By using this equation, the Arrhenius correction factor was applied to account for the "Joule effect". The results showed a reasonable relationship between the K_w and D_{c_rm}. Overall, a reliable method was established to predict the K_w based on the DIN 1048 test and a simplified equation based on the charge passed in RCP test was developed to estimate the D_{c_rm}.

In addition, on the basis of the chloride ion concentration test results, a diffusion model with time dependent surface chloride and diffusion coefficient was developed to predict the service life of concrete structures. The service life is predicted by determining the time to corrosion initiation in the steel reinforcement in concrete. The proposed model was compared with existing service life prediction software and models and showed promising results.

1. INTRODUCTION

1.1. Background

The primary environmental impacts associated with concrete production for civil infrastructure stem from the high carbon footprint of concrete. Among all the materials and stages required for concrete production, cement production represents the largest contributor to the overall greenhouse gas (GHG) emissions associated with concrete. Cement production is energy intensive and harmful to the environment because of the high temperatures required to burn the raw materials and also because of the emission of gaseous by-products during that process. On average, each ton of cement produced accounts for 0.92 tons of CO_2 emissions, 60% of which can be attributed to the calcination process used to process cement (Marceau et al., 2006). The remaining CO_2 emissions are generated during fossil fuel consumption by machinery for grinding and heating of the raw cementitious materials.

The increase in the cement and concrete production has pushed many organizations and agencies from all over the globe to find alternative solutions that can help to reduce the GHG emission without negatively affecting the cost on one hand, or the strength, durability and performance on the other hand. This is quite a challenge for state transportation agencies in the U.S., cement production plants, and the concrete industry. In view of that, the biggest concern for State transportation agencies is how to prescribe sustainable concrete mix designs for pavement and bridge decks made from locally available materials for the concrete industry that can provide a sustainable infrastructure.

The need to produce concrete with sustainable cement has pushed the Canadian Standard Association (CAN/CSA-A3000) to reduce the GHG emission in their cement

production. This took place by allowing cement producers to replace up to 15% of their typical Portland Cement (PC) mix with limestone and produce what is known as Portland Limestone Cement (PLC). The advantage of using PLC is the reduced energy and cost required to burn the raw materials for cement. This method has been adopted for use in Europe for decades, with quantities up to 35% replacement of cement by weight. The success in modifying cement production in both Europe and Canada prompted the United States to move toward a more sustainable approach in the cement production and concrete industries.

1.2. Problem Statement

The ASTM C150/AASHTO M 85 and ASTM C465/AASHTO M 327 has recently approved the use of limestone and inorganic process additions (IPA) with quantities more than 5% replacement to cement by weight. It is expected that these modifications in cement production will help to mitigate some environmental problems by reducing the amount of raw materials burned to produce cement and to reduce the carbon footprint by at least 3% to 4% of total CO_2 emissions. The modification will also help reduce the depletion of natural resources and will offer a low-cost, efficient method to secure waste materials. However, adding these materials can have detrimental effect on the strength and durability characteristics of concrete.

The Illinois Department of Transportation (IDOT) has recently adopted making several changes to concrete mix designs, using revisions to cement specification ASTM C150/AASHTO M 85 and ASTM C465/AASHTO M 327 for the new IDOT Standard Specifications book. These proposed revisions may impact the department and the concrete industry. The addition of more than 5% limestone and IPA above the specified limit by ASTM C150 require strength and durability testing of concrete mixes using common cements with less than 5% and cements with more than 5% limestone and IPA. In addition to the limestone

and IPA modification, the IDOT were interested in increasing the maximum permissible amount of insoluble residue (IR) in cement according to ASTM C150 from 0.75% to 1.5%. Therefore a comprehensive investigation is required to evaluate the strength and durability performance of concrete mixes for pavements and bridge decks when made with modified cement with higher quantities of limestone and IPA and IR amount exceeding what is recommended by ASTM C150/AASHTO M 85.

1.3. Research Objectives

Because of the lack of experimental test data for concrete with IDOT mix designs using more than 5% limestone and IPA and/or more than 0.75% IR, an experimental investigation must be conducted to assess the strength gain, ultimate strength, and durability characteristics of concrete mixes containing Portland cements with more than 5% limestone and IPA, and/or with IR exceeding 0.75%. Therefore, the main objective of this research is to evaluate the strength and durability properties of the IDOT concrete mixes with 535 lb/yd^3 (317 Kg/m^3) of cementitious materials content when the Portland cement contains more than 5% limestone and IPA and/or more than 0.75% IR for the purpose of accepting and recognizing current ASTM C150/AASHTO M 85 revisions and for ensuring that implementation of these revisions will not affect the performance of the economical concrete used by the department.

The primary objective of this study is to accept the new modifications in cement production and concrete mix designs by providing sustainable concrete for pavements and bridge decks without negatively affecting their strength and durability performance. The objectives of the study are summarized as follows

1. Provide sustainable concrete mixes by reducing the carbon footprint from the cement plants, and design concrete mixes with optimum performance.

2. Develop economical and practical concrete mixes when the total cementitious materials content (CMC) of the mix is 535 lb/yd^3 (317 Kg/m^3) while maintaining 0.42 w/cm ratio. This is performed by ensuring 2 – 6 in. (50 – 150 mm) slump and 5 – 8% (6.5%) fresh air content as an acceptance criteria for concrete.
3. Make use of locally available materials that has history of good performance.
4. Evaluate the fresh characteristics, strength properties, and durability performance of the concrete mixes when the Portland cement contains more than 5% (total) limestone and IPA content, and more than 0.75% IR.
5. Analyze the experimental results of the concrete mixes with Portland cement containing more than 5% limestone and IPA and compare them with concrete mixes made with conventional Portland cement.
6. Based on the findings, provide recommendations on the addition of limestone and IPA to Portland cement and the overall performance of concrete mixes when the cementitious materials content level is 535 lb/yd^3 (317 Kg/m^3).
7. Accept and recognize revisions to the current ASTM C150/AASHTO M 85 based on the findings of the project and ensure that these revisions do not affect the performance of concrete that is being accepted and used by IDOT.

Based on the results of the comprehensive experimental program the following investigation and analytical studies were performed:

1. Conduct a comprehensive program to study the factors influencing the freeze/thaw performance of concrete.
2. Develop simplified analytical approaches to predict the water penetration coefficient in concrete based on the water penetration test results, and the equivalent-steady state

diffusion coefficient through the use of rapid chloride penetration test.

3. Develop a mathematical model for service life prediction of concrete structures through the diffusivity of chloride, by taking into account time dependent surface chloride concentration and diffusion coefficient.

1.4. Thesis Organization

Chapter 1: This chapter gives a general background on the limestone, inorganic process additions, and insoluble residue use in cement production. It also presents the problem statement and the research objective of this report.

Chapter 2: This chapter presents a detailed description of the past literature research documenting the fresh properties, strength, and durability performance of concrete made with cement with added raw materials, such as limestone and insoluble residue, and replaced in certain quantities by supplementary cementitious materials, such as fly ash and GGBF slag.

Chapter 3: This chapter presents a detailed description of the physical and chemical properties of the materials procured for the study.

Chapter 4: This chapter presents the selected concrete mix combinations made with conventional and modified cement to study their fresh properties, strength, and durability performance.

Chapter 5: This chapter presents the experimental program outlining detailed description of the experiments used to study the fresh characterizes, strength properties, and durability performance of concrete with conventional and modified cement.

Chapter 6: This chapter presents the results of the fresh properties which includes the workability, fresh air content, and the initial and final setting times of concrete.

Chapter 7: This chapter presents the results of the strength properties in terms of the compressive and flexural strength of concrete.

Chapter 8: This chapter presents the durability performance of concrete in terms of the hardened air content parameters, freeze/thaw performance, chloride ion concentration, water penetration test, and rapid chloride penetration test.

Chapter 9: This chapter investigates the cause of a series of premature failures occurred in the freeze/thaw specimens tested in accordance with ASTM C666, Procedure A when the concrete mixes had sufficient entrained air content. Also, the effect of lignosulfonate based water reducing admixture on the fresh and hardened properties of air content was examined.

Chapter 10: In this chapter, analytical approaches were proposed, based on the experimental results, to predict the water penetration coefficient in concrete based on the water penetration test, and the equivalent-steady diffusion coefficient based on the RCP test.

Chapter 11: This chapter presents a proposed mathematical model to predict the service life of concrete structures through the diffusion of chloride by taking into account time dependent surface chloride and diffusion coefficient.

Chapter 12: This chapter presents a summary of the work presented in this study. It also contains the conclusions drawn and the anticipated future work.

It should be noted that a technical report for the ICT / IDOT has been published by Issa (2014) regarding the research of this dissertation and under the title: “Effect of Portland Cement (current ASTM C150/AASHTO M85) with Limestone and Process Addition (ASTM C465/AASHTO M327) on the Performance of Concrete for Pavement and Bridge Decks.”

2. LITERATURE REVIEW

2.1. Introduction

The studies done on adding IPA to cement were very limited for this research. Therefore, the literature review focused on studies investigated the addition of limestone to cement by either blending or intergrinding.

This review incorporates the studies that were conducted to investigate the use of alternative raw materials, such as limestone, and industrial by-products, such as slag or fly ash, to replace cement. Most studies were conducted in Europe and Canada to document the performance of Portland cement when replaced by alternative materials having different quantities and different properties. Studies that were conducted in Canada were initiated after the Canadian Cementitious Materials Compendium CAN/CSA A 3000 adopted the use of up to 15% Portland-limestone cement.

This literature review documents the performance of added raw materials to cement in the fresh and hardened stage of cement paste and concrete. The fresh properties include the effect on workability, fresh air content, and setting time. The hardened properties include the effect on strength and durability.

2.2. Materials Background

2.2.1. Limestone Waste

Limestone waste is a byproduct obtained as a leftover from the process of crushing limestone rocks to produce crushed limestone aggregates for concrete (see Figure 2-1). Using this waste in building materials such as in cement can alleviate some environmental problems and reduce the depletion of natural resources. Nowadays, limestone by-products are being used

extensively in the cement production as a potential cost effective approach to reduce the amount of virgin cementitious materials required and the associated GHG emissions due to their production. Also, it has been used in combination with natural sand as a fine aggregate material for concrete.

Figure 2-1. Excess crushed limestone usable for concrete

Limestone use in cement production has been adopted in Europe for decades, with up to 35% replacement to cement. The process of adding limestone to cement is illustrated in Figure 2-2. The cement manufacturing requires proportioning different raw materials (limestone, silica, alumina, and iron) to achieve the desired chemical composition. Once the materials are proportioned, they are blended together by grinding into a powder, after which they are

delivered to a rotary kiln where they get burned at a temperature between 2500 ºF and 2800 ºF (1400 ºC and 1550 ºC). This burning process changes the raw mix chemically to produce the cement clinker (roughly ¾ in. in diameter). The clinker is then ground with gypsum to produce the Portland cement. The limestone is added by either intergrinding or blending it with the cement. The process of intergrinding limestone takes place with the clinker and gypsum in the grinding mill, while blending takes place after grinding. According to ASTM C150 the limestone amount shall not be more than 5% by weight while being interground with the cement.

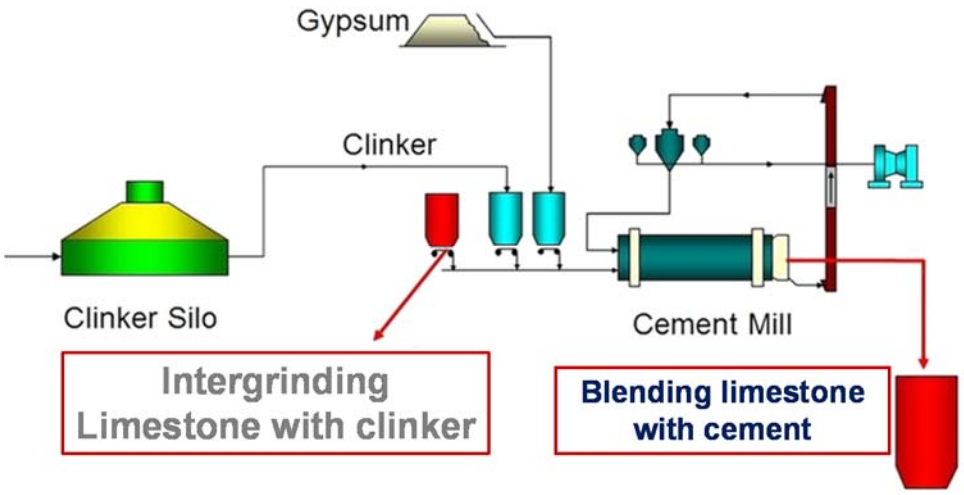

Figure 2-2 Process of blending or intergrinding limestone with cement

2.2.2. Inorganic Process Addition and Insoluble Residue

Processing additions are materials that are blended with the cement or interground with the clinker to aid in the production and handling process (ASTM C219). Inorganic process additions (IPA) are most notably used among processing additions in the cement production. The IPA materials can be in the form of granulated blast furnace slag, fly ash, bottom ash, limestone, cement kiln dust, and calcined byproducts (Dhir, 1994). The IPA additions can help

in optimizing the total grinding energy required for a given fineness of cement (Taylor, 2007). Such materials also aid in reducing the total energy required in the process of cement production and thereby reducing the total CO_2 emissions and other greenhouse gases. According to ASTM C150 the IPA content shall not be more than 5% by weight where it's permissible to be either interground or blended with the cement.

The insoluble residue (IR) are classified as impurities in cement, stemming mainly from the addition of gypsum (Kiattikomol et al., 2000). The current ASTM C150, limits the IR to 0.75% by weight of cement. The amount of IR can be determined by treating the cement with hydrochloric acid and sodium hydroxide (Neville, 1995). These insoluble residues are classified as inert materials and therefore higher IR content can reduce the strength characteristics of cement; this was confirmed by Kiattikomol et al. (2000). The need to increase IR content can be justified through the better quality of cement produced, nowadays, with higher C_3S content and higher fineness (Kiattikomol et al., 2000). Moreover, limestone and IPA can contain high quantities of IR that can reach up to more than 30% in natural limestone and fly ash (Gebhardt, 1995). Therefore, increasing the IR content can allow the cement producers to have more flexibility in increasing the amount of limestone and IPA to be inerground or blended with cement.

2.2.3. Fly Ash

ACI Committee 116 defines fly ash as "the finely divided residue resulting from the combustion of ground or powdered coal, which is transported from the firebox through the boiler by flue gases" (see Figure 2-3). It is a byproduct of the burnt coal required to generate electricity in coal-fired power plants. Fly ash has been shown to possess pozzolanic properties attributed to its large quantities of reactive silicates, which can help improve the durability,

strength and long-term performance of fly ash-amended concrete (Thomas, 2007; O'Brien et al., 2009). For example, it has been found that fly ash in concrete can reduce thermal cracking by lowering the heat of hydration (Malhotra, 2002). Additionally, fly ash concrete also tends to have low permeability and thus can better resist chemical weathering due to chlorides, sulfates and carbonates in rainwater (Dhir, 2006). Moreover, the sustainability of concrete can be improved since the incorporation of fly ash can reduce the amount of Portland cement needed for a given volume of concrete, thus reducing the overall carbon footprint of the fly ash-amended cement. An added benefit is that the fly ash that would have required disposal in a sanitary landfill now is diverted for use in a relatively safe and stable form once incorporated into concrete. Studies on fly ash have shown that its aforementioned advantages have gained worldwide attention on its possible use as SCM in concrete production (Ondova and Stevulova, 2012).

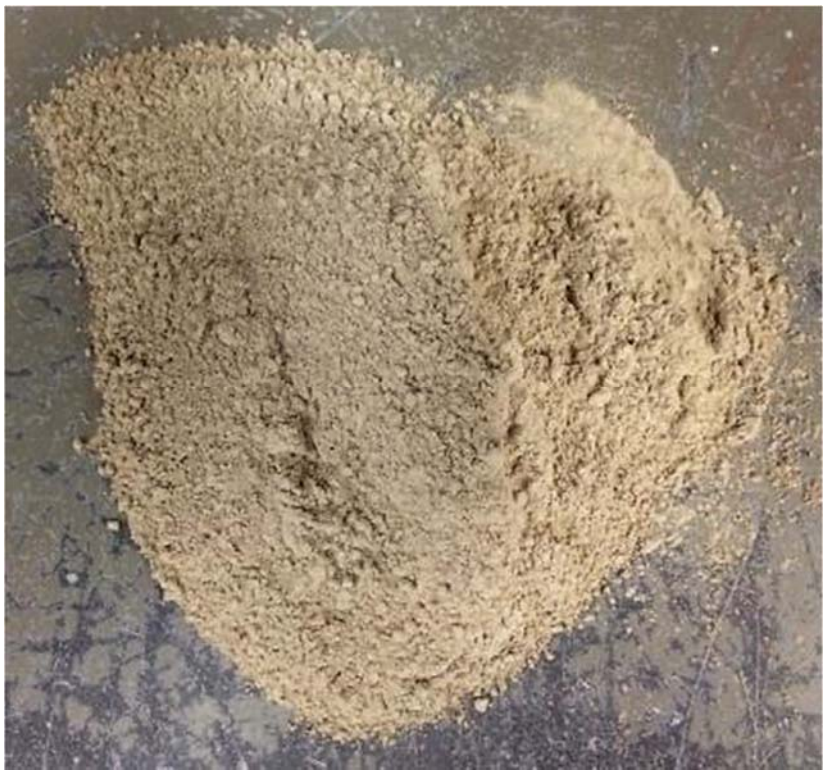

Figure 2-3. Class C fly ash

2.2.4. Ground Granulated Blast Furnace Slag

Slag is another industrial byproduct that has been used as an SCM in concrete. Its use in concrete dates back to the early 1900s (Aitcin, 2008), but it did not gain popularity in practice until the 1970's and 80's. Iron blast furnace slag – or simply slag - is formed during metal smelting when iron ore, coke, and flux are melted together at a temperature of about 2800 ºF (1550 ºC). Then the molten slag is cooled by quenching the material in water then grinding them to give the final form of ground granulated blast furnace slag (Kosmatka and Wilson, 2011; see Figure 2-4). Similar to fly ash, studies have shown added advantage to concrete performance made with slag such as improved durability characteristics and long-term strength properties (Cramer and Sippel, 2005; LaBarca et al., 2007).

Figure 2-4. Grade 100 ground granulated blast furnace slag byproduct

2.3. Effect of Adding Limestone and Alternative Cementitious Materials to Cement on the Fresh Properties of Concrete

This section provides a review on the effect of adding limestone to cement on the fresh properties of concrete mixtures. The fresh properties of the materials used in the research include the measurement of workability (slump) and setting time of concrete. The studies conducted in Canada and Europe revealed conflicting results because the results were influenced by the Blaine fineness of Portland-limestone cement, the method adopted to add limestone to cement, the amount of SCMs replacement, the type and gradation of aggregates, and the type of chemical admixtures used.

2.3.1. Workability

Studies show inconsistent results for the effect of limestone addition on the workability of cement and concrete. Most studies focus on the effect of the Blaine fineness of limestone and their particle size distribution with respect to the cement. Mathews (1994) observed that a higher water to cement ratio was needed to maintain the desired slump after the addition of the limestone. It was reported that an approximate 0.01 increase in w/cm ratio was needed for cement with less than 5% limestone addition while 0.02 increase in w/cm ratio was needed for cement with less than 25% limestone addition. Bonavetti et al. (2003) proved that the addition of limestone reduced workability as a result of administering more admixtures to get the desired slump. In contrast, Schmidt et al. (1993) found that the addition of limestone to cement with 13% to 17% content resulted in reducing the water cement ratio in comparison with regular Portland cement from 0.60 to 0.57.

Other studies failed to observe major changes in the slump as a result of limestone addition. Bucher et al. (2008) reported that concrete mixtures produced with conventional

Portland cement and with cement containing 10% interground limestone showed insignificant changes in the slump reading. Hooton and Thomas (2009), who investigated concrete mixtures with regular cement content and with cement including 12% limestone content, reported that the mixtures did not show any difference in their fresh properties, including workability, bleeding, and finishing.

2.3.2. Setting Time

Most studies showed that the initial and final setting of cement are influenced by the fineness and amount of limestone added to cement.

Vuk et al. (2001) reported that initial and final set times decreased with the increase of fineness. Hooton et al. (2007) reported that cement with finer limestone set faster than regular cement. Tsivilis et al. (1999a) found that the addition of finer limestone resulted in decreasing the setting time. In contrast, the study conducted by Moir and Kelham (1997) showed that the replacement of cement by 20% limestone with increased fineness prolonged the setting time.

On the other hand, El-Didamony et al. (1995) reported that the addition of a low quantity (up to 5%) of limestone to cement increased the setting time while the addition of higher quantities of limestone resulted in decreasing the setting time. Heikal et al. (2000) reported that the replacement of cement with up to 20% limestone having the same Blaine fineness resulted in decreasing the setting time. Bucher et al. (2008) also observed a decrease in the time set in cement having 10% limestone content. Mounanga et al. (2010) observed that the addition of limestone as filler reduced the setting time for concrete containing fly ash and blast furnace slag. On the other hand, a study conducted by Tsivilis et al. (2000) showed an increase in set time as a result of an increase in limestone content. Ezziane et al. (2010) also reported that the blended addition of limestone to cement increased the set time in mortar.

Other studies, such as Hooton and Thomas (2009), reported that no correlation was found between the addition of limestone to cement and the setting time of field concrete mixtures.

2.4. Effect of Adding Limestone and Alternative Cementitious Materials to Cement on the Strength Properties of Concrete

The effect of adding limestone to cement on the strength of concrete has been attributed to the quality and quantity of limestone used, production method, i.e. whether limestone was blended or interground with cement, distribution of cement particle size and shape, limestone and cement Blaine fineness, and addition of other cementitious and pozzolanic materials.

Studies investigating the addition of limestone to cement explored the strength of cement paste and concrete. Schiller and Ellerbrock (1992) conducted a study on cement containing 0, 10, and 20% limestone by mass. It was observed that in order to achieve 7250 psi (50 MPa) strength at 28 day with cement with limestone, the equivalent amount coarser than 30 μm for plain cement should be coarser than 26 μm for cement with 10% limestone and 14 μm for cement with 20% limestone. Sprung and Seibel (1991) found that replacing cement with limestone having up to 10% fineness would result in a strength increase because of improved particle distribution. The increase is noticed at early ages but will not improve long-term strength development. Sprung and Seibel (1991) also concluded that using large quantities of limestone would cause a reduction in strength because of the dilution effect; however, this setback could be compensated by increasing the fineness in the limestone cement. Similarly, Schmidt (1992a) concluded that cement with 5 to 10% limestone had little effect on strength reduction compared with regular cement. . Another major study conducted by Tsivilis et al. (1999a) showed the results of compressive strength of cement produced from two different clinkers, with four different levels of Blaine fineness each and with limestone contents ranging

from 5% to 35%. In this study, it was observed that cement with up to 10% limestone content having cement fineness up to a limit value showed insignificant strength reduction compared with pure cement while cement with higher limestone contents resulted in lower strength regardless of its fineness.

Kiattikomol et al. (2000) studied the effect of adding insoluble residue (IR) on the strength properties of concrete. Portland cement type I was prepared with 0%, 0.5%, 1.0%, 1.5%, 2.0%, 3.0%, 5.0%, and 7.0% replacement of IR by weight and with similar particle size distribution and shape of cement. Figure 2-5 shows a relationship between the compressive strength at different ages and the IR added to the cement. The results showed a strength drop ranging from 2 to 9.5% at 3 day, and 1.2 to 5.5% at 60 day for cement with 0.5 to 7% IR. It is therefore concluded that the higher the IR content, the lower the compressive strength. However, it was observed that the cement with the highest IR had a compressive strength exceeding the ASTM C150 limits at all ages, which limits the amount of IR to 0.75%.

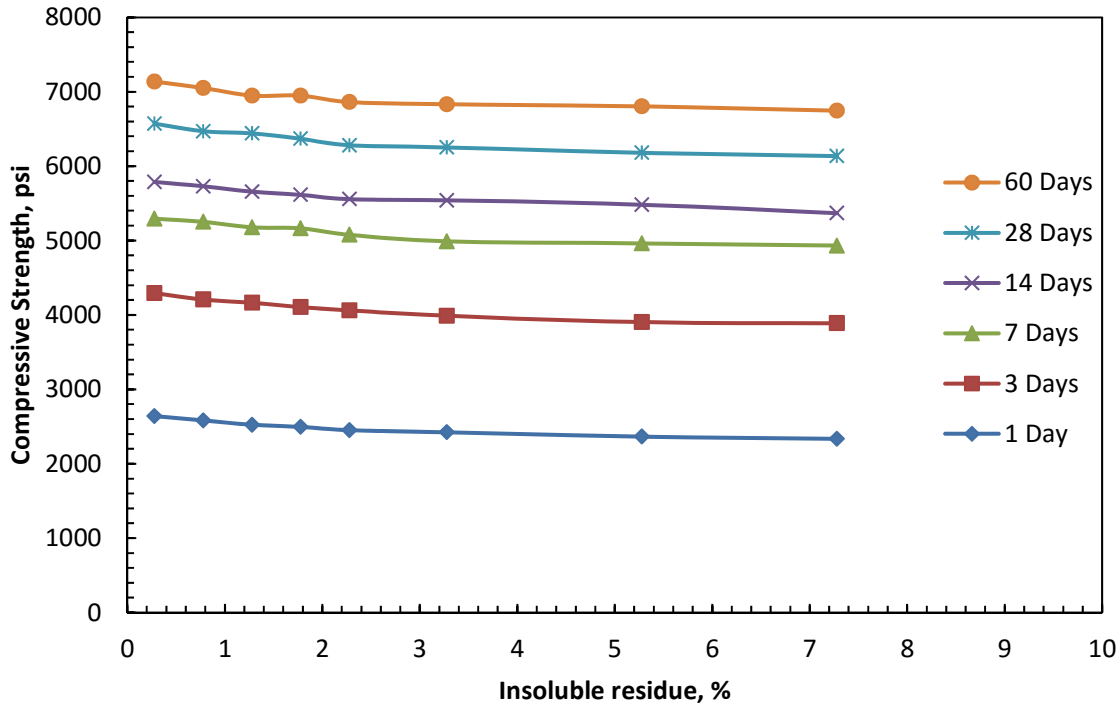

Figure 2-5. Effect of insoluble residue on compressive strength (Kiattikomol et al., 2000).

Studies showed a similar performance between strength development in concrete with limestone cement and strength development in cement paste with limestone. Bonavetti et al. (2003) observed that concrete with cement containing limestone showed better early strength than concrete made with plain cement at 7 day for cement with 10% limestone and 3 day for cement with 20% limestone, knowing that strength reduction was noticed after 28 day. Bonavetti et al. (2003) attributed the strength variation to the gel-space ratio concept: "The compressive strength of concrete depends on the effective w/cm ratio and the degree of hydration of cement. For the same Portland cement composition, the addition of filler creates changes in both gel–space ratio terms". Irassar et al. (2001) tested the compressive strength of concrete mixtures with cement containing 0, 9, and 18% limestone by mass. The study showed that the limestone filler improved the early strength of the mixes, but reduced the long-term strength because of the high fineness of the limestone cement. It was also observed in the same study that the use of blast furnace slag (20 % replacement by mass) improved the long-term strength of concrete. Dhir et al. (2007) evaluated the use of Portland-limestone cement in concrete construction. The study showed that for every 10% limestone added to cement, a reduction of 0.08 in the w/cm ratio of concrete mix was needed to attain the same strength with respect to Portland cement.

In addition to the studies mentioned above, three major studies were recently published in Canada to study the effect of limestone addition on strength development in concrete. The studies, which were conducted by Thomas et al. (2010a), Thomas et al. (2010b), and Hooton et al. (2010), are discussed in Section 2.6.

Most studies focusing on the tensile and flexural strength showed strength variation and development similar to compressive strength because of the addition of limestone to cement.

2.5. Effect of Adding Limestone and Alternative Cementitious Materials to Cement on the Durability Properties

2.5.1. Permeability

The permeability in concrete is mainly related to the pore structure, the size of pores, and the connectivity between pores in concrete. Deterioration of concrete structures is strongly related to its permeability. For example, corrosion in steel embedded in concrete is caused by the penetration of water, oxygen, and chloride ions. Freezing and thawing cycles are more hostile when concrete is saturated. Alkali-silica reactivity (ASR) and sulfate attack could be prevented by improving the porous structure and permeability in concrete. As a result, low permeability is required in aggressive environments to support longevity of concrete structures. Studies show that the effect of adding limestone and alternative materials to cement on permeability varies according to their particle size distribution and fineness and the addition of SCMs.

Moir and Kelham (1993) studied the permeability of oxygen in concrete with cement containing 0, 5, and 25% limestone. The results indicated a slight reduction in permeability caused by the addition of limestone. No difference was observed in the porosity and sorptivity for concrete with control and 5% limestone cement. Schmidt (1992b) used the water permeability test (DIN 1048) to study permeability in air-entrained concrete with and without limestone addition to cement. The results were comparable for concrete with both types of cement. Because of the limited number of studies, it is not confirmed whether the higher fineness of Portland-limestone cement contributes to lowering permeability or not.

Tsivilis et al. (1999b) investigated the effect of limestone addition to cement on air permeability, water absorption, and pore structure for concrete. In this study, cement was prepared from two clinkers with different chemical composition and strength development and with the addition of three different types of limestone. Tsivilis et al. (1999b) concluded that "limestone cement concrete, with optimum limestone content, can give lower gas permeability and water absorption rate as compared with pure cement concrete." Tsivilis et al. (2003) also investigated air permeability, water permeability, sorptivity, and porosity of limestone cement concrete. The limestone was interground with the cement to give Portland-limestone cement (PLC). The cement properties used for the study are shown in Table 2-1.

Table 2-1. Cement Properties (Tsivilis et al., 2003)

Sample	Composition (%)		Specific Surface (m^2/Kg)	Compressive Strength (psi)			
	Clinker	Limestone		1 Day	2 Day	7 Day	28 Day
LC1	100	0	260	1726	3089	5120	7411
LC2	90	10	340	1624	3031	5265	6947
LC3	85	15	366	1871	3292	5468	7034
LC4	80	20	470	2161	3524	5511	6976
LC5	80	20	325	1102	2495	4076	5773
LC6	75	25	380	1407	2582	4554	5802
LC7	65	35	530	1421	2466	3800	4772

1 psi = 0.00689476 MPa

All specimens were cured for 28 days prior to testing. Table 2-2 shows the results of all tests. First, gas permeability, K_g, increased with the increase of limestone content, except for the concrete produced with 35% limestone which showed the lowest gas permeability value. On the other hand, water permeability, K_w, and sorptivity, S, were among the highest for concrete with control cement, and were among the lowest for concrete with 15% limestone cement. The

results of porosity, *P*, were comparable with the control up to 15% limestone addition, but porosity increased with higher limestone content.

Table 2-2. Permeability Test Results for PLC Concrete (Tsivilis et al., 2003)

Code	w/cm	Strength 28 Day (psi)	Limestone (%)	K_g (10^{-17} m^2)	K_w (10^{-12} m/s)	S (mm/min$^{0.5}$)	P (%)
LC1	0.70	4627	0	2.26	2.39	0.237	12.48
LC2	0.70	3974	10	2.65	2.3	0.238	12.3
LC3	0.70	3960	15	2.8	2.22	0.226	12.31
LC4	0.70	4061	20	2.95	2	0.22	13.14
LC5	0.62	4090	20	3.03	1.81	0.228	12.94
LC6	0.62	3843	25	2.82	2.07	0.229	13.62
LC7	0.62	3858	35	2.1	2.23	0.224	14.64

K_g: gas permeability; K_w: water permeability; S: sorptivity; P: porosity

1 psi = 0.00689476 MPa

2.5.2. Chloride Penetration

Tezuka et al. (1992) used cement with 0, 5, and 10% limestone and Blaine fineness of 450 kg/m^2 to determine the chloride diffusion coefficient for mortar specimens. The diffusion coefficient for specimens with 5% limestone was the lowest, and the results for specimens with cement containing 0 and 10% limestone were also toward the low end. Moir and Kelham (1993) reported tests on the chloride penetration for concrete with cement containing up to 5% limestone. He found that compressive strength is the best indicator of chloride concentration. It was concluded that the higher the compressive strength, the lower the chloride concentration. Mathews (1994) measured the chloride concentration of reinforced concrete prisms placed for 5 years in a tidal zone in a marine exposure site. Five different sources of Portland cement were used in these mixes. One source was blended with 30% fly ash while another was

interground with 28% fly ash. In addition, one source was interground with 5 and 25% limestone while the rest were blended with 5 and 25% limestone. The chloride concentrations were measured up to 30mm depth and averaged for all mixes batched with the same amount of limestone or fly ash. The results were considerably lower for the fly ash mixes. Chloride concentrations were lower in concrete with cement containing 5% limestone compared with concrete with control cement; whereas, chloride concentrations were slightly higher in concrete with cement containing 25% limestone than in concrete with control cement. Alunno-Rosetti and Curcio (1997) used cement from two different plants, with and without 20% limestone, to test chloride concentration in concrete. The results, shown in Table 2-3, indicate that concrete with higher cement content has lower chloride penetration. However, the results for concrete with and without 20% limestone were inconsistent between the two sources of cement.

Table 2-3. Chloride Penetration in Concrete (Alunno-Rosetti and Curcio, 1997)

	Total Cement Content, kg/m^3	Limestone Content (%)	Chloride Penetration, mm	
			28 Days	60 Days
Plant B	270	0	43	63
		20	102	113
	330	0	38	49
		20	48	79
Plant G	270	0	212	281
		20	197	264
	330	0	115	183
		20	146	182

Rapid chloride permeability test (RCP test per ASTM C1202) was measured by Thomas et al. (2010a) in a comprehensive study on the effect of limestone and SCMs addition on the performance of concrete. Table 2-4 shows the mixture proportioning with the cementitious

content, w/cm ratio, and the RCP test results of this study. The study showed that the older specimen and the use of SCMs reduced the coulombs charged, but exhibited no significant difference between the specimens made with Portland cement (PC) or Portland-limestone cement (PLC) with 12% limestone. In another study by Thomas et al. (2010b), RCP test was conducted to determine the diffusion coefficient for cores taken from cast-in-place slabs after 35 days. Cement properties, SCMs replacement levels (two parts slag and one part fly ash), RCP test results, and the diffusion coefficient (per ASTM C1556) are shown in Table 2-5. It is noticed that the charge passed reduced significantly with the addition of SCMs, but showed insignificant difference between the PC and the PLC with 12% limestone.

Table 2-4. Mix Proportions and RCP Test Results (Thomas et al., 2010a)

	w/cm	Mix Proportion				Total Cem. (lb/yd^3)	RCP Test (Coulombs)	
		Cement Type	Limestone Content (%)	Fly Ash (%)	Slag (%)		28 Days	56 Days
Series C	0.40	PC	0	0	0	689	2030	1730
		PLC	12	0	0	696	2050	1910
Series B	0.45	PC	0	0	0	597	2570	2350
		PLC	12	0	0	603	2620	2360
		PC	0	0	35	599	1020	810
		PLC	12	0	35	600	940	710
		PC	0	20	0	603	1190	650
		PLC	12	20	0	604	1450	690

1 lb/yd^3 = 0.5933 Kg/m^3

Table 2-5. RCP Test Results and Diffusion Coefficients (Thomas et al., 2010b)

Cement Type	Limestone Content (%)	RCPT Results (coulombs)				D_a (10^{-12} m^2/s)			
		SCM Replacement Level, %				SCM Replacement Level, %			
		0	25	40	50	0	25	40	50
PC	0	2400	1410	570	490	15.0	3.8	1.5	1.3
PLC	12	2350	1310	620	520	11.9	2.9	1.2	1.8

1 m^2/s = 1550 in^2/s

Irassar et al. (2001) measured the chloride concentration and determined the diffusion coefficient of concrete specimens immersed in 3% NaCl solution for a period of 45, 180, and 360 days. Table 2-6 shows the results for diffusion coefficient (D_a) and surface chloride concentration (C_s) for concrete specimens with different amount of limestone in cement (Irassar et al., 2001). It was observed that the higher the w/cm ratio and limestone content, the higher the diffusion coefficient. The increase is attributed to the minimal contribution of limestone cement to the hydration process. Thomas et al. (2010b) noted that the diffusion coefficients for cores immersed for 42 days in chloride solution, shown in Table 2-5, indicated inconsistent performance of concrete whether made with PC or PLC, but showed lower D_a for concrete made with higher SCM content.

Table 2-6. Surface Chloride Concentration and Chloride Diffusion (Irassar et al., 2001)

Limestone Content in Cement (%)	C_s (%)			D_a (10^{-12} m^2/s)		
	w/cm			w/cm		
	0.4	0.5	0.6	0.4	0.5	0.6
0	0.12	0.15	0.15	5	6.9	25.7
10	0.13	0.12	0.18	11.2	20.3	21.6
20	0.14	0.15	0.25	10.5	23.8	41.4

C_s: surface chloride concentration (% by weight of concrete)

D_a: diffusion coefficient

2.5.3. Freeze/Thaw

Early studies on the effect of limestone addition to Portland cement have shown conflicting results as far as the freeze/thaw damage to concrete. Sprung and Seibel (1991) used the "cube" method to test the resistance of concrete with total cement content of 506 lb/yd^3 (300 kg/m^3) and w/cm ratio of 0.6 to frost damage. Siebel and Sprung (1991) also tested the frost resistance of concrete using the European round robin with three different Portland-limestone cements having 11%, 26%, and 12% limestone. Both studies concluded that the amount, quality, and strength of limestone used to replace the cement have a great effect on controlling frost damage to concrete. Albeck and Sutej (1991) reported that concrete made from Portland limestone could have the same frost resistance as concrete made from Portland cement as long as the organic materials in the limestone are less than 0.2% by mass. In contrast, Scmidt (1992b) showed that concrete specimens made from Portland-limestone cement with 13 to 17% limestone, showed similar or slightly better resistance to frost damage and de-icer scaling compared with concrete with Portland cement.

Section 2.6 discusses the effect of freeze/thaw on concrete made with PLC based on the studies conducted in Canada by Thomas el al. (2010a), Thomas et al. (2010b), and Hooton et al. (2010). The tests were conducted in accordance with ASTM C666 for freeze/thaw resistance and de-icer salt scaling (ASTM C672 or OPS LS-412). All three studies indicated adequate resistance to freeze/thaw for concrete specimens made with PLC and similar durability factors for concrete specimens made with PC.

Several investigations and long-term studies show a strong relation between cement fineness and cement freeze/thaw resistance. Mehta (1999) observed old concrete curbs and gutters that were in good condition despite being without air entrainment and exposed to severe

concrete weathering (heating, cooling, wetting, and drying). This observation is supported by his model which indicates that concrete starts to deteriorate when weathering damages the microstructure, thereby increasing the concrete's susceptibility to freeze/thaw attack. Burrows (1999) supports this correlation in his study of concrete specimens made from Portland cement with varying Blaine fineness that were tested to check their resistance to freeze/thaw cycles, as shown in Figure 2-6. The curves show the number of cycles needed to cause 25% mass loss in the concrete specimens. The blue curve indicates specimens stored indoors and the red-dashed curve indicates specimens stored indoors for 3 months and then outdoors in Denver Colorado for 9 months. Two conclusions were made: First, increased cement fineness reduces concrete resistance to frost damage by increasing the mass loss and, second, weathering drastically reduces resistance to frost damage for concrete made with higher Blaine fineness. These observations raise questions about the frost resistance of concrete made from Portland-limestone cement that has higher Blaine fineness than Portland cement.

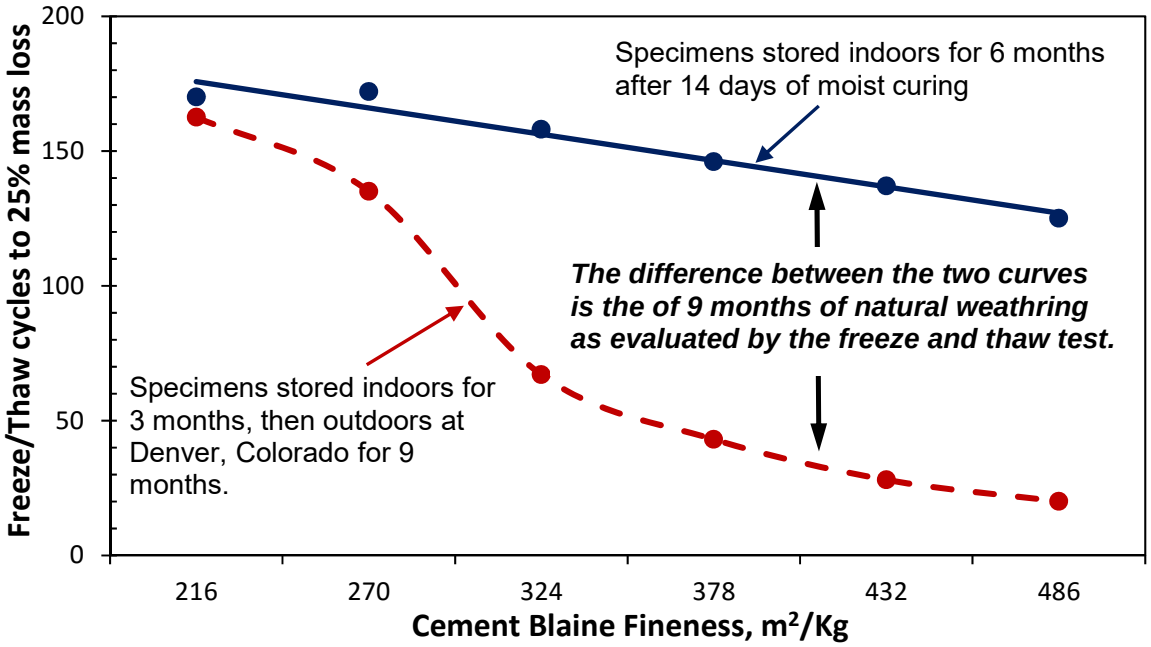

Figure 2-6. Effect of weathering on fineness of cement in concrete (Burrows, 1999).

2.6. Studies Conducted in Canada

The addition of up to 15% limestone to Portland cement was investigated in Canada in 2008. Extensive laboratory and field research have been conducted in Canada in recent years to compare the strength and durability of the PLC with that of PC. Three related laboratory and field trials that were documented in 2010 indicated comparable results in the strength and durability of PLC compared with PC. Two trials were conducted by the University of New Brunswick and Lafarge (Thomas et al., 2010a and 2010b) while the third trial was conducted by the University of Toronto and Holcim (Hooton et al., 2010):

- Equivalent Performance with Half the Clinker Content using PLC and SCM. (Thomas et al., 2010a)
- Field Trials of Concretes Produced with Portland-limestone cement. (Thomas et al., 2010b)
- Decreasing the Clinker Component in Cementing Materials: Performance of Portland-Limestone Cements in Concrete in Combination with SCMs. (Hooton et al., 2010)

2.6.1. Equivalent Performance with Half the Clinker Content Using PLC and SCM

Thomas et al., (2010a) examined the strength and durability of PLC with 12% limestone in comparison with PC with 3 to 4% limestone. Three series of mix proportions were prepared as shown in Table 2-7. Series A and C included pure PC (3 to 4% limestone) or PLC (12% limestone) cement with w/cm of 0.8 for Series A and 0.4 for Series C. Series B included PC and PLC mixes with w/cm of 0.45. The cement in Series B mixes was prepared with no SCMs, 20% fly ash replacement, and 30% slag replacement. The study tested the time of setting of

concrete per ASTM C403, compressive strength per ASTM C39, rapid chloride penetration per ASTM C1202, resistance to rapid freezing and thawing per ASTM C666, Procedure A, and scaling resistance to de-icing chemicals per ASTM C672.

The setting time results shown in Table 2-7 indicate that PLC mixes set faster than similar PC mixes. The compressive strength of each mix was measured at 1, 7, 28, and 56 day. The results of this study show insignificant variation in the compressive strength between the mixes with PC and PLC cement type. In most cases, the compressive strength was higher for PLC mixes at an early stage compared with PC mixes.

Table 2-7. Laboratory Mix Design (Thomas et al., 2010b)

Mix Proportion	**Series A lb/yd^3**		**Series B lb/yd^3**						**Series C lb/yd^3**	
w/cm	0.78	0.8	0.45	0.45	0.45	0.45	0.45	0.45	0.4	0.4
Cement Type	PC	PLC	PC	PLC	PC	PLC	PC	PLC	PC	PLC
Slag, %	na	na	na	na	35	35	na	na	na	na
Fly Ash, %	na	na	na	na	na	na	20	20	na	na
Total Cmt.	**396**	**396**	**597**	**603**	**599**	**600**	**603**	**604**	**689**	**696**
Water	310	317	268	271	270	270	271	271	276	278
Air, %	1.5	1.4	6.2	5.3	6	5.6	5.2	5	6.2	5.4
Slump, in.	4.75	4.5	4.75	4.75	4.25	4.25	5	4.25	5	4.5
Set Time, hrs:min	5:40	5:10	5:40	4:50	6:20	5:45	7:05	5:45	6:35	5:55

1 lb/yd^3 = 0.5933 Kg/m^3; 1 in. = 25.4 mm

A rapid chloride penetration test was conducted per ASTM C1202 on Series B and C mixes. The results showed no significant impact on replacing PC with PLC. However, a significant reduction in the charge passed in PC and PLC mixes with fly ash or slag content was observed.

The effect of limestone on the performance of concrete was inconsistent when the de-icer salt scaling test was conducted per ASTM C672. Mass loss increased with the increase of the amount of SCMs in PC and PLC mixes. . All mixes showed great performance after 300 cycles in the freeze/thaw test per ASTM C666 with high durability factors ranging from 98 to 102%.

The laboratory tests in this study showed good performance for concrete mixes with PLC cement with up to 12% limestone in terms of strength and durability and comparable results for the mixes with PC cement. It was also noticed that SCMs improved the durability of concrete mixes with PLC and PC cement.

2.6.2. Field Trials of Concrete Produced with Portland-Limestone Cement

Thomas et al. (2010b) examined the strength and durability of PLC with 12 % limestone content in comparison with PC with 3 to 4% limestone content. Eight concrete mixes were batched with total cementitious material content of 600 lb/yd^3 (356 Kg/m^3). Each batch contained either PC or PLC. For each type of cement, the SCM comprising two parts slag cement and one part fly ash by mass was used at replacement levels of 0, 25, 40, or 50%. The target air content was 6% and target slump was 4 in. (100 mm). The study tested the compressive strength per ASTM C39, rapid chloride penetration per ASTM C1202, apparent chloride diffusion coefficient per ASTM C1556, resistance to rapid freezing and thawing per ASTM C666, Procedure A, microscopic determination of air void system parameters per ASTM C457, and scaling resistance to de-icing chemicals per ASTM C672 and BNQ NQ 2621 Annex B.

The results for the compressive strength showed highest strengths for PC and PLC with 40 and 50% SCM; however, the concrete batched with PC and PLC showed insignificant

variation. The rapid chloride penetration test showed that the charge passed in 6 hours decreased with the increase of SCM content, and that there was insignificant difference in performance between concretes produced with PC and PLC. Moreover, all mixtures with PC and PLC showed satisfactory air void parameters with excellent durability factors after 300 cycles of freezing and thawing per ASTM C666, Procedure A. The scaling resistance per ASTM C672 showed that the mass loss increased with the increase of SCM content in the mix, regardless of the type of mix.

The study showed that adding SCMs to concrete may increase its strength and resistance to chloride ion penetration, regardless whether PC or PLC are used, and that replacing cement by SCMs in the range of 40 to 50% results in better performance. The study also showed that the content of limestone in cement could be increased to 12% while maintaining equivalent strength and durability, and that replacing cement by SCMs in the range of 40 to 50% results in better performance.

2.6.3. Decreasing the Clinker Component in Cementing Materials: Performance of Portland-Limestone Cement in Concrete in Combination with SCMs

In a study by Hooten et al. (2010), Portland cement clinker with 12% C_3A was interground with different levels of limestone. Tests were conducted on three types of cements; Portland cement with 3.5% limestone (GU), 10 % limestone (PLC10), and 15% limestone (PLC15). Each cement type was replaced with slag at 0, 30, and 50% of total cementitious content. The study tested the sulfate resistance per ASTM C1012 (sulfate-resistance expansion), alkali-silica reactivity test per ASTM C1567 (accelerated mortar bar test) and per ASTM C1293 (concrete prism test), and the following laboratory concrete tests: compressive strength per ASTM C39, de-icer salt scaling per OPS LS-412 similar to ASTM C672 and based on the

Ontario Ministry of Transport provisional standard, drying shrinkage per ASTM C157, rapid chloride penetration test per ASTM C1202, and obvious chloride diffusion coefficient per ASTM C1556.

Laboratory concrete tests were conducted at w/cm=0.4 and total cementitious materials of 607 lb/yd^3 (360 kg/m^3). Cement was replaced with slag at 0 and 30% of total cementitious content. The target air content was 5 to 8%, target compressive strength was 5080 psi (35 MPa) at 28 day, and target rapid chloride penetration was 1500 coulomb at 56 days.

Sulfate attack and alkali-silica reactivity are not part of the current project; however, it is important to show their effect on the performance of concrete with PLC.

In the sulfate-resistance test, mortar bars and cubes were cast and cured until their compressive strength reached 2850 psi (20 MPa). The bars were then immersed in a 50 g/litre of sodium sulfate (Na_2SO_4) solution and their length change was measured periodically for 1 year. According to ASTM C1157 (Standard Performance Specification of Hydraulic Cement) and the Canadian Standard Association, a cement is considered moderately sulfate resistant if the bar expansion is less than 0.1 % after 6 months and highly sulfate-resistant if the bar expansion is less than 0.05% after 6 months or 0.1% after 1 year. The results indicated that slag-free mixes failed to pass the test after 6 months, and that bar expansion increased with the increase in the amount of limestone. . However, all mixes that contained 30 and 50% slag showed high sulfate resistance.

The accelerated mortar bar test per ASTM C1567 and the concrete prism test per ASTM C1293 were both conducted to study alkali-silica reactivity. For ASTM C1567, siliceous limestone aggregates from the Spratt quarry near Ottawa, Ontario, were crushed to sand size to meet the specified particle size distribution. Mortar bars (1 × 1 × 12 in. [25 × 25 ×

300 mm]) were cast and cured, immersed in water, and heated in an oven at 80°C for 1 day. Then, the bars were immersed in sodium hydroxide solution and stored at 80°C. The length change was recorded periodically for 28 days in NaOH solution. According to the standard, expansion should be less than 0.1% at 14 days. All slag-free cements failed the test. The results indicated that mortar expansion was higher in PLCs than GU cement. On the other hand, the bar expansion for cements with slag failed at the 30% slag replacement, but all cements with 50% slag showed positive results.

The compressive strength results, shown in Table 2-8, were inconsistent compared with other studies where mixes with slag indicated higher strength. First, the compressive strength of mixes with PLC10 and PLC15 and for slag-free mixes was slightly higher than the compressive strength of GU mixes. However, a significant drop in the strength of all mixes with 30% slag replacement and a significant increase in the strength of PLC mixes were observed compared with to the GU mixes. Therefore, it was concluded that the reduction might be attributed to other factors, such as the air content in the concrete.

Table 2-8. Compressive Strength Results (Thomas et al., 2010b)

Concrete Mix	Compressive Strength (psi)			
	7 Day	28 Day	56 Day	91 Day
GU 100%	5700	6860	7281	8485
PLC10 100%	6179	7353	8238	8731
PLC15 100%	5860	7165	8108	8137
GU 70% SLAG 30%	2814	4351	4786	4873
PLC10 70% SLAG 30%	4351	6179	6701	7745
PLC15 70% SLAG 30%	4554	6237	6788	7832

1 psi = 0.00689476

The results for drying shrinkage in this study showed no variation in the length change for the three types of cement with 0 and 30% slag replacement.

In the rapid chloride penetration test, the charge passed for all slag-free mixes was higher than the maximum requirement of 1500 Coulombs at 56 days. However, the results were much lower with the 30% slag replacement. It was therefore concluded that there was no effect of limestone from both types of cement PLC10 and PLC15 when compared with GU cement.

The apparent chloride diffusion measurements were very compatible with the RCP test test results. The use of PLC cement in all mixes had no effect on chloride penetration, and the replacement of 30% slag reduced the percentage of chloride in all cements.

This study showed that the performance of PLC cement with up to 15% interground limestone is comparable to the performance of GU cement. It was also observed that slag improved the strength and durability of GU and PLC cements.

3. MATERIAL SELECTION

3.1. Procuring Sources of Materials

The sources of materials procured for the study are: three sources of cement, one source of Class C fly ash, one source of ground granulated blast furnace slag (GGBF slag), one source of coarse aggregate, and two sources of fine aggregates. The sources and types of materials are presented in Table 3-1.

3.2. Cementitious Sources and Properties

The provisions of ASTM C150 and AASHTO M85 both permit up to 5% inorganic processing additions (IPA) to be used as ingredients in Portland cement. Such materials must be qualified through testing by ASTM C465 (or AASHTO M 327) and the finished cement must meet all of the other chemical and physical requirements of ASTM C150/AASHTO M 85. The chemical limits often provide a secondary limit on the amount of inorganic processing additions. However, the Canadian specification CAN/CSA A3000 does not limit the amount of inorganic processing additions used in Portland cement to 5%. It does require that, when processing additions are used in amounts greater than 1%, the manufacturer identify and report the amount used.

Two sources of cement (C1 and C2) were prepared with limestone and IPA with different quantities less than and exceeding 5% by weight of cement. Ground granulated blast furnace slag was used as IPA for cement with more than 5% limestone and IPA. The C1 source was prepared by intergrinding limestone and partially intergrinding IPA at CTL laboratory in Skokie, Illinois. The conventional cement was designated as C1 and the modified cements were designated as C1IP1 and C1IP2. The C2 cement was produced by intergrinding limestone

and homogeneously blending IPA. The conventional cement in C2 cement was designated as C2 and the modified cement was designated as C2IP.

The insoluble residue (IR) content of ASTM C150/AASHTO M 85 Portland cements is limited per the specifications to a maximum of 0.75% by weight. According to the CSA A3000, while the insoluble residue for other types of Portland cement is limited to 0.75%, it permits a maximum insoluble residue of 1.5% for GU (general use) and HE (high early) portland cements. For C1 and the fly ash used in this research, the IR contents were 0.49% and 32.41%, respectively. Therefore, fly ash was blended with C1 as shown in Figure 3-1 to produce C3 as conventional cement with 0.75% IR and C3IR as modified cement with 1.5% IR. The amount of blended fly ash in the finished cement that would result in 0.75% IR (C3) was 0.81%, and the amount that would result in 1.5% IR (C3IR) was 3.17%.

The chemical properties of C1 and C2 cement sources as well as the Class C fly ash and GGBF slag used as supplementary cementitious materials are presented in Table 3-2. The amount of limestone, IPA, and IR used for each cement source are shown in Table 3-3. The Blaine fineness and the compressive strength of C1 and C2 cements are shown in Table 3-4. The Blaine fineness ranged between 378–408 m^2/Kg. The compressive strength properties were slightly higher for the modified cement in comparison with the conventional cement for C1 source, but were slightly lower for C2 cement source.

Table 3-1. Materials Source and Type

Material	Type	Supplier	Designation
Three sources of cement	Type I/II	First cement source: **Lafarge North America** **C1** has **4.2% limestone** **C1IP1** has **3.8% limestone** and **4.5% IPA** **C1IP2** has **3.2% limestone** and **6.7% IPA**	C1 C1IP1 C1IP2
		Second cement source: **St. Marys Cement** **C2** has **2.6% limestone** **C2IP** has **2.5% limestone** and **3% IPA**	C2 C2IP
		Third cement was produced by blending **C1** with **fly ash** to increase the **insoluble residue (IR)** as follows: • **C3: Low dose processing addition** using fly ash with LOI max 3% and IR Max 0.75%, and • **C3IR: High dose processing addition** using fly ash with LOI max 3.5% and IR Max 1.5%	C3 C3IR
Class C Fly Ash	Class C	Pleasant Prairie	Fly Ash
GGBF Slag	Grade 100	Holcim Skyway	Slag
One source of coarse aggregate	Crushed Limestone (3/4 in. Nominal max. size)	Hanson MS Thornton quarry The material is MS Thornton Aggregate Source: 50312-04 Material Code: CM 1101 BD.	CA
Two sources of fine aggregate	Natural Sand	Bluff City material in South Beloit, natural sand Aggregate Source: 52010-20 Material Code: 027FM02	NS
	Combined Sand	Hanson MS Romeoville, combined sand Aggregate Source: 51972-02 Material Code: 029FM20	CS
Water reducing admixture	ASTM C494, Type A	W.R. Grace WRDA 82	WRA
High-range-water-reducer	ASTM C494, Type F	ADVA Cast 575	HRWR
Air entrainment agent (AEA)	ASTM C260 AASHTO M 154	W.R. Grace AEA Daravair 1400	AEA

Figure 3-1. Preparing C3 cement by blending C1 cement with fly ash.

Table 3-2. Chemical and Physical Properties of Cement

Material	Type	Chemical Data, %											Blaine (m^2/Kg)
		SiO_2	Al_2O_3	Fe_2O_3	CaO	MgO	SO_3	Alkali	C_3S	C_2S	C_3A	C_4AF	
C1	Type I/II Cement	19.8	4.8	2.8	63.1	2.6	2.6	0.55	55	15	8	8	380
C1IP1		21	5.2	2.6	61.4	3.4	2.6	0.50	51	15	7	8	408
C1IP2		20.4	5.1	2.6	62.3	2.9	2.6	na	55	13	8	8	407
C2		19.2	4.7	2.7	62.1	3.8	3.9	0.93	56	13	8	8	385
C2IP		19.8	4.9	2.7	61.7	4	3.8	0.92	55	12	8	8	383
Fly Ash	Class C	38.7	20.3	5.6	22.9	4.0	2.2	1.90					
GGBF Slag	Grade 100	33.3	10.5	0.2	36.0	16.0	2.8	0.73					
IPA	Slag	33.3	10.5	0.2	36.0	16.0	2.8	0.76					

Table 3-3. Limestone, Inorganic Process Addition to Cement and IR Content

Cement	Limestone, %	Inorganic Process Addition, %		Total	Insoluble Residue (IR), %	Loss on Ignition (LOI), %
		Slag	Fly Ash			
C1	4.2	0	0	**4.2**	0.49	2.54
C1IP1	3.8	4.5	0	**8.3**	0.50	2.32
C1IP2	3.2	6.7	0	**9.9**	na	2.0
C2	2.6	0	0	**2.6**	0.20	1.5
C2IP	2.5	3	0	**5.5**	0.18	1.4
C3	4.2	0	0.81	5.01	**0.75**	2.54
C3IR	4.2	0	3.17	7.37	**1.5**	2.55

Note: C3 and C3IR were prepared by blending C1 with fly ash at UIC laboratory

Table 3-4. Blaine Fineness and Strength Properties of Cement

Cement Source	Blaine Fineness (m^2/Kg)	Compressive Strength, psi			
		1 Day	3 Day	7 Day	28 Day
C1IP2	408	na	3530	5020	na
C1	380	2070	3800	5020	6130
C1IP1	407	2010	3940	4650	6400
C2	378	2910	4043	4648	5973
C2IP	386	3183	4413	5220	6390

1 psi = 0.00689476 MPa

3.3. Aggregate Properties

Only aggregates demonstrating a history of good performance for durability concerns, such as D-Cracking and Alkali silica reactivity (ASR), are used in this study. The coarse aggregate was crushed limestone with a nominal maximum aggregate size of 3/4 in. (19 mm) obtained from Thornton quarry, IL. The crushed limestone had a minimum of 45% passing ½ in. (12.5 mm) sieve. Two types of sand were used: (1) natural river sand obtained from South Beloit, IL, and (2) combined sand, which is a combination of 50% natural sand and 50% crushed limestone obtained from Romeoville, IL. The use of combined sand was observed to have some environmental benefits. This was done by implementing a low cost and efficient method in securing limestone by-product obtained from the crushing process of limestone to produce coarse aggregates.

The properties of the coarse and fine aggregate materials are shown in Table 3-5 and Table 3-6, respectively. Gradation samples for both aggregates were prepared and measured according to IDOT specifications. The coarse aggregate samples were prepared using a mechanical splitting device, as shown in Figure 3-2, while the fine aggregate samples were

prepared by quartering the field sample, as shown in Figure 3-3. The gradation for fine and coarse aggregates was determined for each set of mix combinations to ensure that they are within the IDOT acceptable gradation limits. Gradation curves for the coarse aggregate are shown in Figure 3-4, and for the fine aggregates are shown in Figure 3-5.

Fine aggregates, both natural and combined sand, were prepared and stored in sealed buckets with a moisture content ranging between 2% and 5%. Coarse aggregates were prepared to maintain saturated surface dry (SSD) condition. First, the coarse aggregates were soaked in water for at least 24 hours to ensure complete saturation. The water was then drained and the aggregates were spread on the ground until the SSD condition was reached. The coarse aggregates were then placed in sealed buckets.

Table 3-5. Properties of Coarse Aggregate

Aggregate Type	Source	Material Code	SSD Specific Gravity	Oven-Dried Specific Gravity	Water Absorption, %
Hanson Material Service, Thornton, (CA_1)	50312-04	CM1101BD	2.697	2.654	1.6

Table 3-6. Properties of Fine Aggregate

Aggregate Type	Source	Material Code	SSD Specific Gravity	Oven-Dried Specific Gravity	Water Absorption, %
Bluff City natural sand, South Beloit (FA_1)	52010-20	027FM02	2.642	2.613	1.1
Hanson Material Service, combined sand, Romeoville, (FA_2)	51972-02	029FM20	2.674	2.634	1.5

Figure 3-2. Mechanical splitting device for coarse aggregate gradation sampling.

Figure 3-3. Quartering of fine aggregate for gradation sampling.

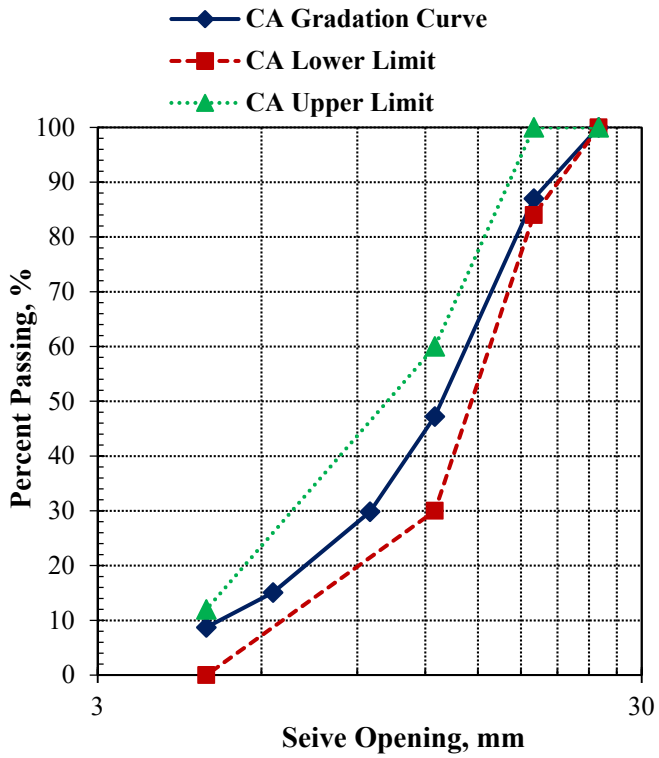

Figure 3-4. Gradation curve for the coarse aggregate (CA).

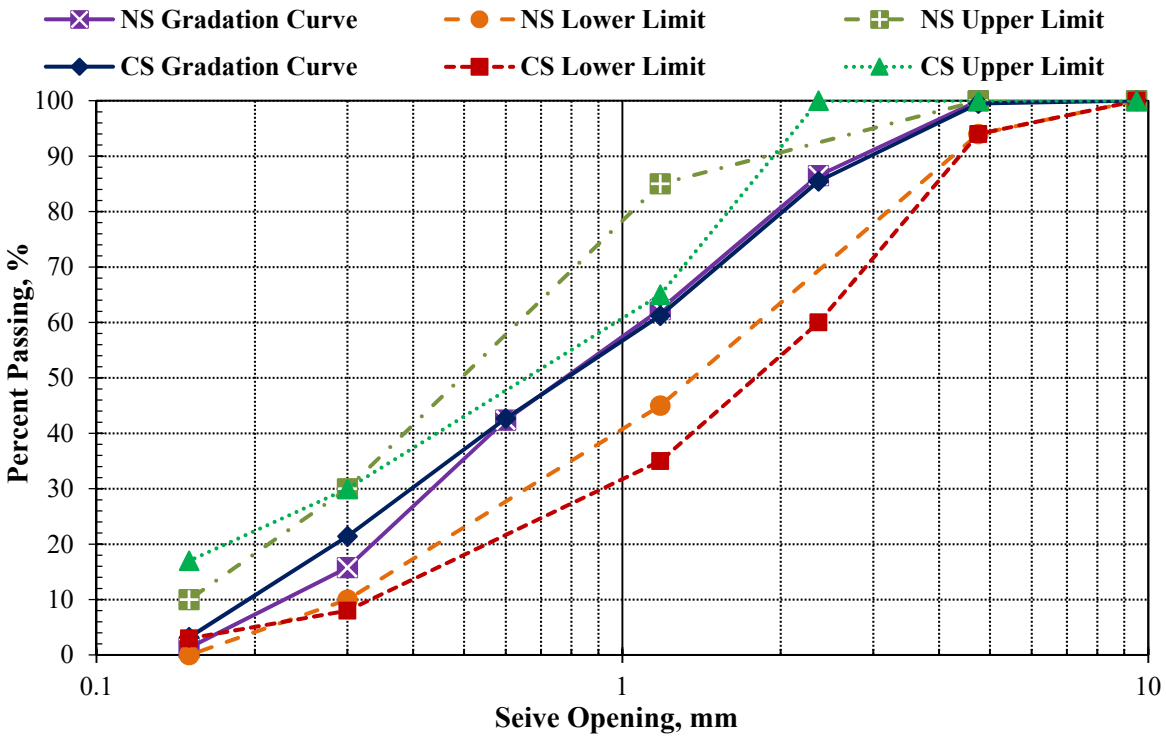

Figure 3-5. Gradation curve for the fine aggregates (natural sand [NS] and combined sand [CS])

3.4. Chemical Admixtures

Three types of chemical admixtures were used in the concrete mixes:

- A lignosulfonate based water reducing admixture (WRA) commercially known as WRDA® 82
- A polycarboxylate based high-range water reducer (HRWR) commercially known as ADVA® Cast 575
- A vinsol resin based air entraining admixture (AEA), commercially known as Daravair® 1400, was used to provide the entrained air in the concrete to ensure resistance against freeze/thaw attacks.

Manufacturer's guidelines were provided for all chemical admixtures with details about performance, addition rates, compatibility with other admixtures, and batching sequences.

The WRDA® 82 is an aqueous solution of modified lignosulfonates. The addition rate for the WRDA® 82 ranges from 3 to 5 fl oz. per 100 lbs of cement (cwt) and from 2 to 10 fl oz/cwt if local testing shows acceptable performance. It is recommended to add WRDA® 82 to the concrete mix near the end of the batch sequence and to avoid any contact between WRDA® 82 and other admixtures before and during the batching process to obtain optimum performance. WRDA® 82 is highly compatible with vinsol based AEA when both are used in the same mix. Using WRDA® 82 in a concrete mix might reduce the amount of air-entraining admixture by 25-50%.

The ADVA® Cast 575 was used as the polycarboxylate-based HRWR. The addition rate of the ADVA® Cast 575 varies between 2 to 10 fl oz/cwt. The dosage requirement for ADVA® Cast 575 might be affected by the mix proportions, cementitious content, and ambient

conditions. It is recommended to add ADVA® 575 to the concrete mix near the end of the batch sequence to obtain optimum performance.

The Daravair® 1400 is chemically similar to vinsol based products. The guideline of Daravair® 1400 does not specify a standard addition rate. A typical Daravair® 1400 addition rate ranges from ½ to 3 fl oz/cwt. The addition rate varies depending on several factors, including temperature, type of cement, sand gradation, and using extra fine materials such as fly ash and micro silica. It is, however, recommended to add Daravair® 1400 to the concrete mix at the beginning of the batch sequence by dribbling on the sand to obtain optimum performance.

4. CONCRETE MIX DESIGN AND BATCHING

4.1. Concrete Mix Design

Total of twenty six different concrete mixes with different mix proportions were made. Every cementitious combination was batched with crushed limestone coarse aggregate and natural sand or combined sand. The cementitious content for the concrete mixes was 535 lbs/yd^3 (317 Kg/m^3) which is the minimum amount required for central mixing by the Illinois Department of Transportation (IDOT) for concrete pavement and bridge decks. Each concrete mix was made with 375 lbs/yd^3 (222 Kg/m^3) of cement and 160 lbs/yd^3 (95 Kg/m^3) [30% replacement by weight] of class C fly ash or GGBF slag. All the concrete mixes were designed with a mortar factor of 0.88 which is within the acceptable range (0.70 – 0.90) of IDOT specification for pavement mix designs. The mortar factor is a measure of the ratio of mortar per volume of dry rodded coarse aggregate. A higher mortar factor is sometimes desirable to improve the workability of the concrete mix and finishability of the formed surface and to have better control on the entrained air distribution in concrete. The water-to-cementitious (w/cm) ratio ranged from 0.40 – 0.44 depending on the mix combination. The w/cm ratio target was 0.42 but it was slightly reduced to 0.40 for concrete mixes made with fly ash and batched with natural sand owing to its high workability, while it was increased to 0.44 for concrete mixes made with slag and batched with combined sand. This was owed to the failure to maintain required slump without exceeding the recommended admixtures content by the manufacturer. The lignosulfonate based water reducing admixture (WRA) and polycarboxylate based high-range water reducer (HRWR) were used to attain a slump in the range of 2 – 6 in. (50 – 150 mm). The vinsol resin based air entraining admixture (AEA) was used to provide 6.5 ± 1.5% air in the concrete to ensure resistance against freeze/thaw attacks. A summary of the mix

combinations for mixes batched with natural sand and combined sand are presented in Table 4-1 and Table 4-2, respectively.

Table 4-1. Concrete Mix Proportions Batched with Natural Sand

Mix Designation		Cementitious Combination lb/yd^3			Aggregates, lb/yd^3		Coarse/Fine Ratio	W/CM Ratio
		Cement	Fly Ash	Slag	Coarse	Fine		
Mixes batched with Natural Sand	C1-F-NS1	375	160	–	1823	1325	57.9 / 42.1	0.40
	C1-F-NS2	375	160	–	1823	1325	57.9 / 42.1	0.40
	C1IP1-F-NS	375	160	–	1823	1325	57.9 / 42.1	0.40
	C1IP2-F-NS	375	160	–	1823	1325	57.9 / 42.1	0.42
	C1-S-NS1	375	–	160	1823	1316	58.1 / 41.9	0.42
	C1-S-NS1	375	–	160	1823	1316	58.1 / 41.9	0.42
	C1IP1-S-NS	375	–	160	1823	1316	58.1 / 41.9	0.42
	C1IP2-S-NS	375	–	160	1823	1316	58.1 / 41.9	0.42
	C2-F-NS	375	160	–	1823	1294	58.5 / 41.5	0.42
	C2IP-F-NS	375	160	–	1823	1294	58.5 / 41.5	0.42
	C2-S-NS	375	–	160	1823	1316	58.1 / 41.9	0.42
	C2IP-S-NS	375	–	160	1823	1316	58.1 / 41.9	0.42
	C3-F-NS	375	160	–	1823	1325	57.9 / 42.1	0.40
	C3IR-F-NS	375	160	–	1823	1325	57.9 / 42.1	0.40
	C3-S-NS	375	–	160	1823	1316	58.1 / 41.9	0.42
	C3IR-S-NS	375	–	160	1823	1316	58.1 / 41.9	0.42

1 lb/yd^3 = 0.593276 Kg/m^3

Table 4-2. Concrete Mix Proportions Batched with Combined Sand

Mix Designation		Cementitious Combination lb/yd³			Aggregates, lb/yd³		Coarse/Fine Ratio	W/CM Ratio
		Cement	Fly Ash	Slag	Coarse	Fine		
Mixes batched with Combined Sand	C1-F-CS	375	160	–	1823	1308	58.2 / 41.8	0.42
	C1IP1-F-CS	375	160	–	1823	1308	58.2 / 41.8	0.42
	C1-S-CS	375	–	160	1823	1304	58.3 / 41.7	0.44
	C1IP1-S-CS	375	–	160	1823	1304	58.3 / 41.7	0.44
	C2-F-CS	375	160	–	1823	1308	58.2 / 41.8	0.42
	C2IP-F-CS	375	160	–	1823	1308	58.2 / 41.8	0.42
	C2-S-CS	375	–	160	1823	1304	58.3 / 41.7	0.44
	C2IP-S-CS	375	–	160	1823	1304	58.3 / 41.7	0.44
	C3-F-CS	375	160	–	1823	1308	58.2 / 41.8	0.42
	C3IR-F-CS	375	160	–	1823	1308	58.2 / 41.8	0.42
	C3-S-CS	375	–	160	1823	1304	58.3 / 41.7	0.44
	C3IR-F-CS	375	–	160	1823	1304	58.3 / 41.7	0.44

1 lb/yd^3 = 0.593276 Kg/m^3

All concrete mixes were batched according to ASTM C192/AASHTO T 126. The mixture design proportioning was based on one cubic yard. IDOT PCC Mix Design Version V2.1.2 was used for proportioning all the concrete mixes. An example of the IDOT PCC Mix Design is shown in Appendix A.

4.2. Trial Mixes

The earliest concrete mixes completed in this research were conducted using the WRDA® 82 and Daravair® 1400 chemical admixtures. They were observed to have very low hardened entrained air compared with their fresh air content. As a result, the concrete mixes failed to pass the freeze/thaw test per ASTM C666, procedure A. Due to this inadequacy, several 1 to 3

ft^3 trial batches were made for each mix and were calibrated to yield an air content ranging between 5 and 8% and a slump of approximately 2 – 6 in. (50 – 150 mm).

In order to check this inadequacy, a sensitivity study was conducted to investigate air stability in the fresh and hardened state. The study analyzed the effect of chemical admixtures on the air content of concrete mixes batched at the University of Illinois at Chicago (UIC). The results provided a description of the effect of chemical admixtures on the rate of air loss in concrete mixes in the fresh stage. It also demonstrated the effect of admixtures on each other and on the slump and air readings.

From the trial mixes it was concluded that the lignosulfonate based WRA, used in these mixes had a synergistic effect when it reacted with the vinsol resin based AEA. This reaction enhanced the air bubbles, but it increased the instability of air content in the mix and the variation in the rate of air loss. On the other hand, the addition of the polycarboxylate based HRWR showed an adverse effect when used with the AEA. The HRWR reduced and stabilized the air content in the mix by eliminating the effect of combining lignosulfonate and vinsol resin based admixtures on the air bubbles. Therefore, most of the followed concrete mixes were batched with either a binary combination of AEA and HRWR or a ternary combination of AEA, HRWR, and WRA.

5. EXPERIMENTAL PROGRAM

The experimental program included measuring the fresh properties of concrete, testing their strength characteristics, and evaluating their durability performance.

All concrete mixes were batched according to ASTM C192/AASHTO T 126. Each concrete mix combination required 18 ft^3 (0.5 m^3) of fresh concrete that was divided into three 6 ft^3 (0.17 m^3) batches to cast the specimens for the strength and durability study. The first batch was used to cast twenty 6 × 12 in. (150 × 300 mm) concrete cylinders to measure the compressive strength gain in concrete. The second batch was used to cast ten 6 × 6 × 21 in. (150 × 150 × 525 mm) concrete prisms to measure the flexural strength gain in concrete. The third batch was used to cast the required specimens for the durability study which included two 6 × 12 in. concrete cylinders to measure the hardened air parameters, 3 × 4 × 16 in. (75 × 100 × 400 mm) prisms to evaluate the freeze/thaw performance of concrete, nine 7 × 7 × 5 in. (175 × 175 × 125 mm) concrete prisms to measure the water penetration per DIN 1048 test, twelve 4 × 8 in. (100 × 200 mm) concrete cylinders to measure the rapid chloride ion penetration per ASTM C1202, three 3 × 12 × 16 in. (75 × 300 × 400 mm) concrete slabs for salt ponding to determine the chloride ion profile, and three additional 6 × 12 in. (150 × 300 mm) concrete cylinders to measure the compressive strength at 360 days.

The acceptance criteria for each batch were based on the specified values for air content and slump. The batches that failed to meet the specified values were rejected, and new batches were made. The mixer used in this study is shown in Figure 5-1.

Figure 5-1. Concrete mixer (7 cubic ft capacity).

5.1. Fresh concrete properties

The fresh properties of concrete included measuring the slump per ASTM C143, the fresh air content per ASTM C231, the unit weight per ASTM C138, the initial and final times of setting of concrete by penetration resistance per ASTM C403. In addition, the concrete and ambient temperatures as well as the relative humidity were measured to ensure that the concrete mixtures were batched and cured in a controlled room temperature environment of 73 ± 3 ºF (23 ± 2 ºC) and with 50% relative humidity.

Table 5-1. Test Methods for Measuring the Fresh Properties of Concrete

Test Method	Testing Times	Sample Size	Number of Samples	
			Per Test	Per Mix
Slump ASTM C143/AASHTO T 119	after mixing & 12 minutes after mixing	slump cone	1	2
Unit Weight ASTM C138/AASHTO T 121	after mixing	cylindrical container, volume=0.25 cubic ft	1	1
Air Content ASTM C231/AASHTO T 121	after mixing & 12 minutes after mixing	measuring bowl	1	2
Setting Time, ASTM C403 AASHTO T 197	time to first reading (40 psi), hr. testing time then until initial set (500 psi) and final set (4000 psi), hr.	measuring bowl with minimum diameter of 6 in.	1	1

5.2. Mechanical Properties of Concrete

The mechanical properties were measured in terms of the compressive and flexural strength tests. The tests were conducted according to ASTM C39/AASHTO T 22 and ASTM C78/AASHTO T 97, respectively, at 3, 7, 14, 28, and 56 days of age. The concrete specimens were cast at the UIC laboratory. The compressive specimens were capped with plastic covers, and the flexural specimens were covered with wet burlaps and stored indoors under ambient temperature for 24 hours after casting. The specimens were then demolded and stored in the moisture room under a controlled temperature of 73°F (23°C) and 100% relative humidity (according to ASTM C511/AASHTO M 201) until the testing dates. Figure 5-2 and Figure 5-3 depict the compressive and flexural strength tests.

Figure 5-2. Test configuration for the compressive strength per ASTM C39

Figure 5-3. Test configuration for the flexural strength of concrete per ASTM C78

5.3. Durability Properties of Concrete

The durability performance of concrete was evaluated in terms of the cyclic freezing and thawing in correlation with the hardened air void parameters, water penetration test per DIN 1048, rapid chloride ion penetration per ASTM C1202, and the salt ponding test per ASTM C1543 for the chloride ion profile per ASTM C1151 and ASTM C1218. These methods of evaluations were chosen because they predicted the overall behavior and durability of concrete. A summary of the durability test methods is presented in Table 5-2.

Table 5-2. Test Methods for the Durability Characteristics of Concrete

Test Method	Testing Times	Sample Size	Number of Samples	
			Per Test	Per Mix
Freeze/Thaw, Procedure A, ASTM C666/AASTHO T161 and ASTM C215	Relative dynamic modulus (RDM) and mass loss readings every 35 cycles	3 × 4 × 16 in. prisms	5 runs	5
Hardened air, ASTM C457	at 56 days	Concrete samples sliced vertically from 6 × 12 in. cylinder	2 runs	2
DIN 1048, Water penetration test	Measure penetration of water at 56, 180, and 360 days	7 × 7 × 5 in. cubes	3 runs	9
Rapid chloride ion permeability, ASTM C1202/AASHTO T 277	at 56, 180, 360 days	4 × 2 in. discs sliced from 4 × 8 in. cylinders	3	9
Salt ponding test, AASHTO T 259 ASTM C1543	Salt pond for 90 days but will continue for 360 days	12 × 12 × 3 in. slab	1	3
Chloride measure for salt ponding, AASHTO T 260 ASTM C1151, ASTM C1218	at 90, 180, 360 days 3 drill holes/slab 6 depths/hole	Measure at ¼, ½, 1, 1½ , 2, and 2½ in. across the slab depth	6 runs	18

5.3.1. Hardened Air Content

5.3.1.1.Background

The concrete must be air-entrained to provide resistance to cyclic freezing and thawing encountered in Illinois. Air entrainment provides void space in which ice crystals can expand without subjecting the concrete material to pressure and inducing cracking. Voids in concrete are classified into four types: capillary voids, entrained air voids, entrapped air voids, and water pockets. Capillary voids occupy the space between the cement gels after hydration. They are irregularly shaped, less than 5 μm in size, and have no contribution to the air-void system. Air-entrained voids are created by the addition of surfactants with stabilized foam (air-entraining admixture) and they are the main contributors to resist the cyclic attack of freezing and thawing. The Virginia Transportation Research Council (VTRC) defines the air-entrained void as spherical in shape, larger than the capillary void, and smaller than 1 mm when measured on a saw-cut lapped surface (Ozyildirim, 1998). Larger bubbles are classified as entrapped air and water pockets and are less evenly distributed than the entrained air. Entrapped air voids are influenced by the physical properties of the aggregate and the workability and improper consolidation of the mix. Water pockets result from the water that fails to bleed to the surface because of an aggregate or hardening paste. The entrapped and water pockets hardly contribute to the freeze/thaw resistance and have undesirable effect on the concrete strength.

5.3.1.2.Method of Preparation and Procedure

In this test, specimens were prepared then air void was determined in accordance with ASTM C457, following the linear-traverse method, through an automated concrete analysis system (CAS 2000). For each concrete mix combination, two 6 × 12 in. (150 × 300 mm) concrete cylinders were cast. The concrete cylinders were subject to curing in the moisture room for 28

days and were then left to dry for another 28 days in the laboratory before testing. Two 6 × 1 in. (150 × 25 mm) concrete disks were cut from the 6 × 12 in. (150 × 300 mm) concrete cylinders using a diamond blade concrete saw. Specimens were then lapped on a sanding machine until a desired surface for microscopic determination was reached as shown in Figure 5-4. The testing setup for the hardened air measurement is shown in Figure 5-5.

Figure 5-4. Concrete specimen prepared for air void measurement.

Figure 5-5. Microscopic determination of air void system parameters (ASTM C457).

In the linear traverse method, traverse lines are developed at equal intervals where the operator measures the length of all the voids across each traverse line. This will allow the user to determine the total length traversed, the length of the voids traversed, as well as the number of voids. These data can be used to determine the air content and various other parameters that determines the distribution of air bubbles within the concrete specimen. The hardened entrained air results were recorded according to the following parameters:

- Void frequency (per in. [per cm]) or void per unit length, which represents the number of air voids intercepted by a traverse line divided by the length of that line. It is suggested to have 8 per in. (3.15 per cm) minimum void frequency.

- Specific surface (1/in. [1/mm]), which is the surface area of the air voids divided by their volume. It gives an indirect indication of the size and distribution of air

bubbles in the specimen. It is suggested to have 500 1/in. (20 1/mm) minimum specific surface.

- Spacing factor (in. [mm]), this measure was proposed by Powers (1949), which designates the distance needed for water to travel from the cement paste to the periphery of the air void. It is suggested to have a maximum spacing factor less than 0.01 in. (0.254 mm).

5.3.2. Freeze/Thaw Evaluation of Concrete

The freeze/thaw test is conducted in accordance with ASTM C666, Procedure A. The setup for the freeze/thaw test is shown in Figure 5-6. For each concrete mix combination, five 3 × 4 × 16 in. (75 × 100 × 400 mm) specimens were cast for freeze/thaw testing. The beams were cured for 56 days prior to testing of which they were moist cured at room temperature (73 ºF [23°C] and 100% RH) in the first 49 days followed by complete immersion in water for seven days at room temperature prior to testing. Testing was conducted until each specimen passed 300 cycles of freezing and thawing. Each cycle ranged between 3 and 3 ½ hours with 2 to 2 ½ hours freezing and 1 hour thawing.

Figure 5-6. Freeze/thaw test cabinet, ASTM C666, procedure A.

The damage assessment caused by freeze/thaw was evaluated in accordance with ASTM C215 (Fundamental Transverse, Longitudinal, and Torsional Resonant Frequencies of Concrete Specimens). The test determines the resonant frequency of prismatic or cylindrical concrete specimens through the resonance impact method described in ASTM C215. The method can be used to assess the deterioration in the concrete specimen subject to freeze/thaw based on its dynamic response or resonant frequency.

The test consists of a hammer and accelerometer that is connected to a data acquisition system for frequency measurement. The test conditioning depends on the shape and size of the specimens. Small specimens are usually placed on a two point support bed while large specimens such as 6 × 12 in. (150 × 300 mm) concrete cylinders or 6 × 6 × 21 in. (150 × 150 × 525 mm) concrete beams can be supported on a special flat sponge (see Figure 5-7). The accelerometer is then mounted on the surface of the specimen at a specific position depending on the mode of vibration (longitudinal, transverse, or torsional) of the resonant frequency that

needs to be determined. The vibration is then excited by striking the hammer at the proper impact point. (see Figure 5-8).

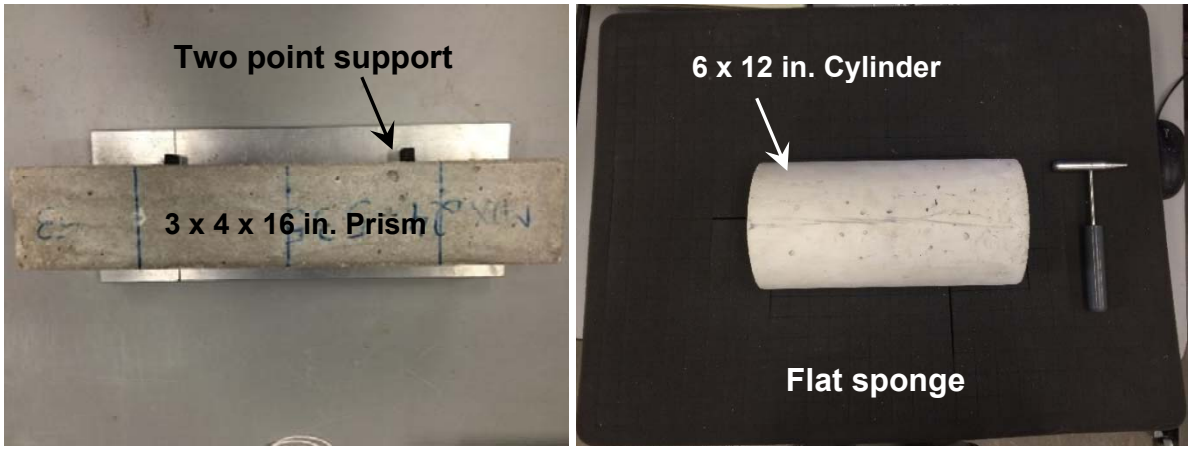

Figure 5-7. Supported specimens for dynamic modulus (E_D) measurement

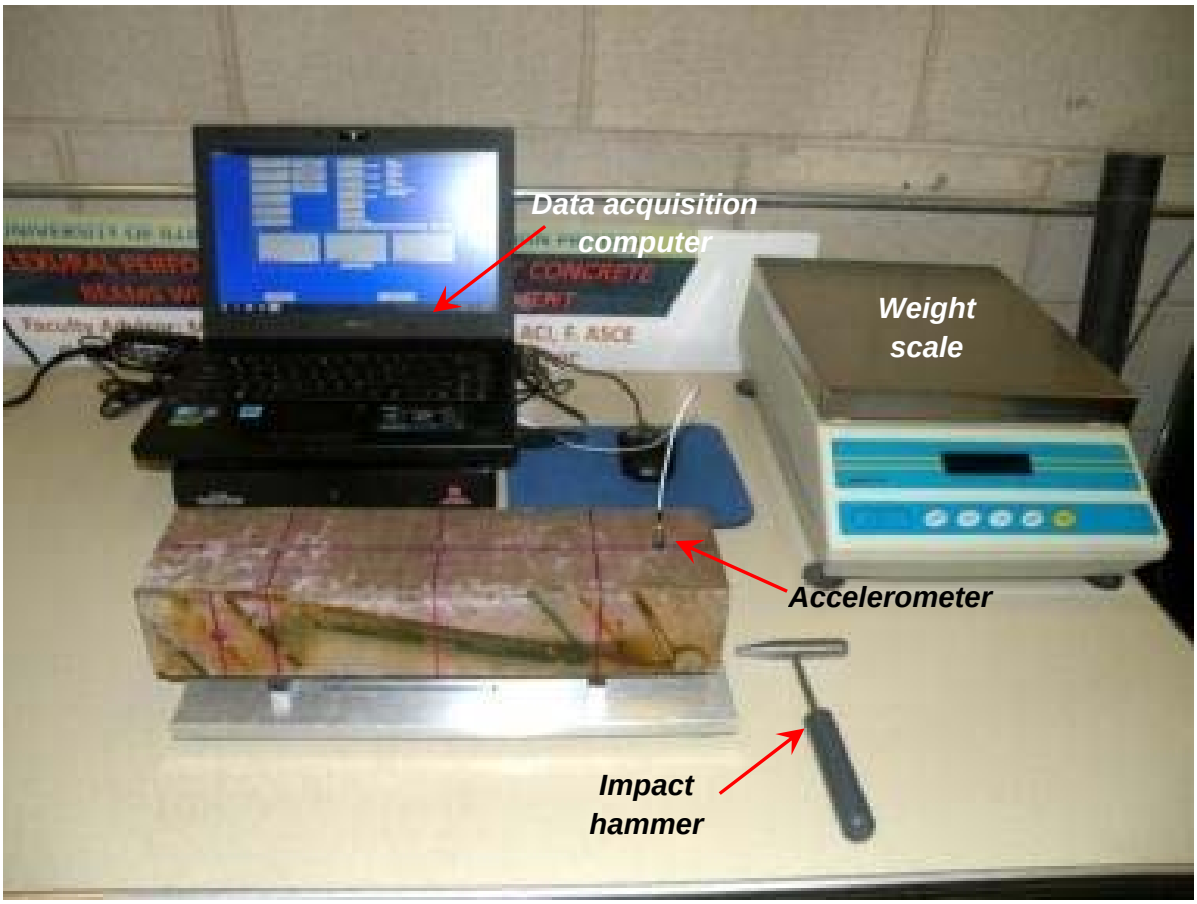

Figure 5-8. DK 5000 dynamic resonance frequency tester, ASTM C215.

Then the software displays the resonant frequency by transforming the recorded accelerometer signal into the frequency domain. The frequency domain is displayed in a chart with the horizontal axis as the frequency and vertical axis as the amplitude. The resonant frequency is represented by the peak amplitude as shown in Figure 5-9.

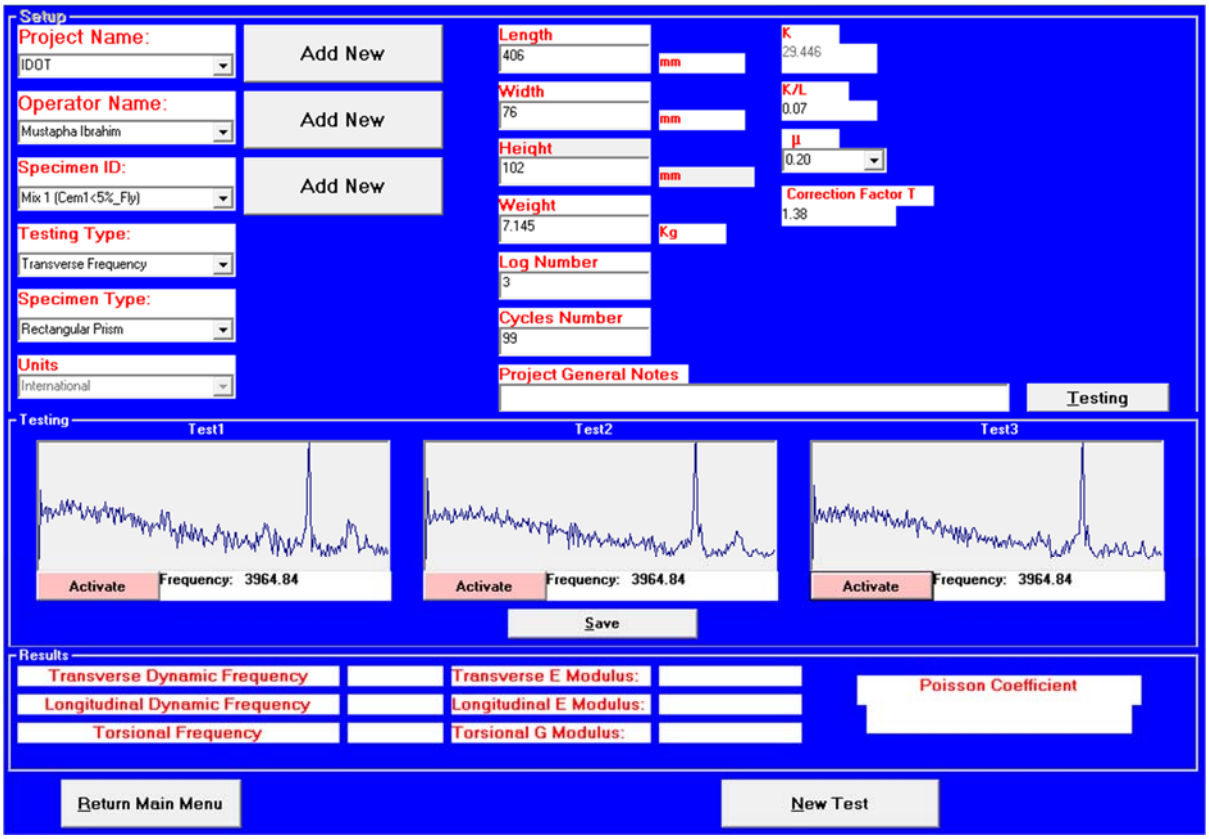

Figure 5-9. Example of a recorded resonant frequency in the DK 5000 software

The resonant frequency for all the freeze/thaw specimens was measured based on the transverse method. Once the transverse resonant frequency is measured the E_D can be calculated as follows:

$$E_D = CMn^2 \qquad \text{Eq. 5.1}$$

Where:

E_D = the dynamic modulus of elasticity, Pa,

M = mass of specimen, Kg,

n = fundamental transverse frequency, Hz,

C = 1.6067 (L^3T/d^4) for a cylinder, or 0.9464 (L^3T/bt^3) for a prism, m^{-1},

L = length of specimen, m,

d = diameter of cylinder, m,

t = thickness (depth) of prism, m,

b = width of prism, m,

T = correction factor based on radius of gyration K (d/4 for a cylinder and t/3.464 for a prism) and Poisson's ratio μ found from Table 1 of ASTM C215.

Testing was repeated at regular intervals ranging between 30 and 36 cycles and the E_D was recorded at each interval and after 300 cycles. The damage due to freeze/thaw is assessed as follows:

$$P_c = \frac{E_{Dc}}{E_{Di}} \times 100 \qquad \text{Eq. 5.2}$$

Where:

E_{Dc} = the dynamic modulus after c cycles,

E_{Di} = the initial dynamic modulus before initiating the freeze/thaw test (0 cycles),

P_c = percentage of drop in the dynamic modulus of elasticity after c cycles.

The total damage after 300 cycles is evaluated as follows:

$$DF = \frac{E_{D300}}{E_{Di}} \times 100 \qquad \text{Eq. 5.3}$$

Where:

E_{D300} = the dynamic modulus after 300 cycles,

DF = the durability factor which represents the total damage after 300 cycles.

The *DF* should be higher than 80% for the concrete mix to have acceptable resistance against freeze/thaw attack. ASTM C494 (Standard Specification for Chemical admixtures for Concrete) states that when chemical admixtures are used in air-entrained concrete, the concrete *DF* should be minimum 80% after 300 cycles of freeze/thaw testing.

5.3.3. Rapid chloride penetration tests (ASTM C1202/AASHTO T 277)

The rapid chloride penetration (RCP) test gives a quick indication of the chloride ion penetration into concrete through the electrical conductance or resistance. Twelve 4 × 8 in. (100 × 200 mm) cylinders were cast for each concrete mix. The cylinders were divided into three sets. The samples were tested at 56, 180, and 360 days of age where they were removed from the moisture room and stored in a room temperature dry environment 28 days before the day of testing.

The RCP test was conducted in accordance to ASTM C1202. For each testing day, 2 in. (50 mm) thick concrete slices were cut from four 4 × 8 in. (100 × 200 mm) cylinders. The slices were vacuum saturated, deaerated, and then soaked in water for 18 ± 2 hours prior to testing. Samples were then secured into test cells consisting of two reservoirs, where one reservoir was filled with 3% NaCl solution (cathode), and the other with 0.3N NaOH solution (anode). The test was conducted by applying 60 Volts potential difference to allow the transfer of chloride ions through concrete from the negative terminal with NaCl solution (cathode) to the positive terminal with NaOH solution (anode). A typical test setup is shown in Figure 5-10. The test was performed for a six hour period, during which the current and the temperature were measured every five minutes. The total charge passing was measured in Coulombs and the average value of four samples was reported.

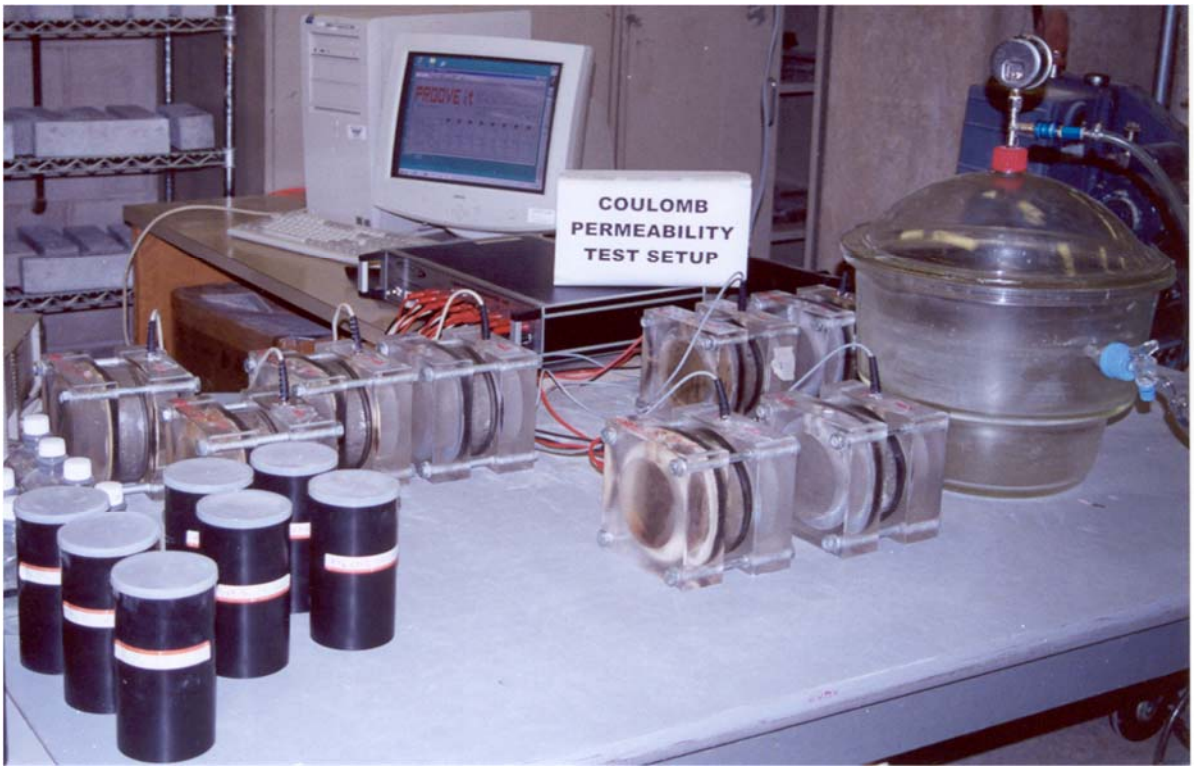

Figure 5-10. Rapid chloride permeability test, ASTM C1202/AASTHO T 277.

Table 5-3 provides a correlation between the level of chloride ion penetration and the charge passed. The table, copied from ASTM C1202, is used as a base for determining the validity of the concrete mix against chloride penetration.

Table 5-3. Chloride Ion Penetrability Based on Charge Passed

Charge Passed (Coulombs)	**Chloride Ion Penetrability**
> 4,000	High
2,000 – 4,000	Moderate
1,000 – 2,000	Low
1000– 1,000	Very Low
< 100	Negligible

5.3.4. Water Penetration Test (DIN 1048)

For the water penetration test, nine 7 × 7 × 5 in. (175 × 175 × 125 mm) prisms were cast for each concrete mix. The concrete prisms were divided into three sets. Each set was cured in the moisture room (73°F [23°C] and 100% humidity) for 28, 152, and 332 days, respectively, and was then subject to 28 days of dry curing before testing. The DIN 1048, better known as water penetration test, was conducted at 56, 180, and 360 days and was carried out on three specimens for each testing period. The test assembly is shown in Figure 5-11.

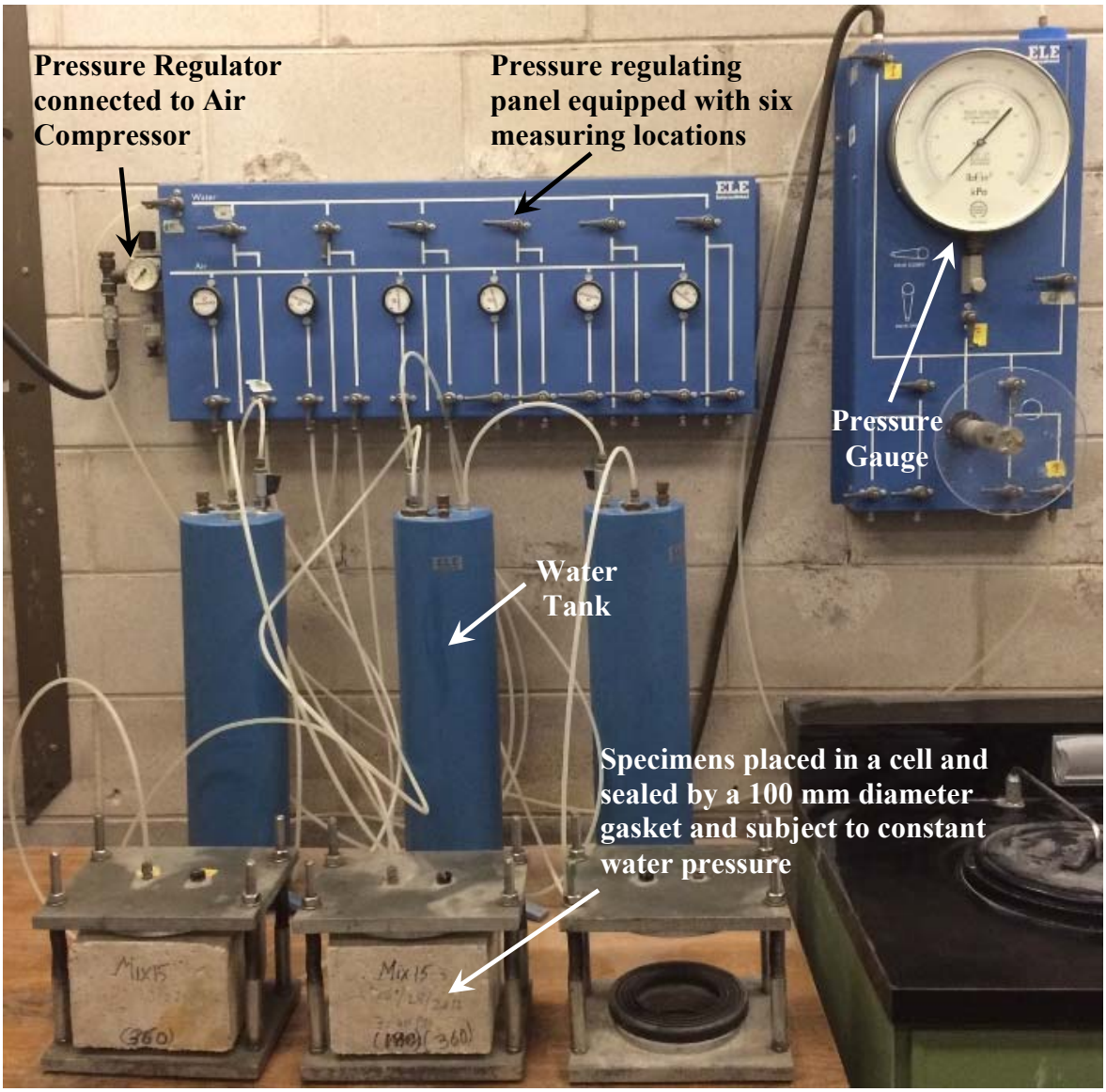

Figure 5-11. DIN 1048 (Water penetration) test setup

Prior to the test, the top surface of the concrete specimens was wire brushed, following the DIN 1048 standard, until the aggregates were exposed. This was recommended by Hedegaard and Hansen (1992), who observed less discrepancy in the penetration results upon removing the specimen's surface. Each specimen was secured into a cell consisting of a rubber gasket with a 4 in. (100 mm) diameter opening placed on top of the wire brushed surface to prevent leakage while applying water pressure. The water pressure imposed on the top surface of the sample is generated by way of compressed air applied to the integral water tank and controlled by a pressure regulator with a pressure gauge. The water pressure was applied for a period of 4 days with 100 kPa (1 bar [14.5 psi]) pressure for the first 48 hours, followed by 300 kPa (3 bar [43.5 psi]) and 700 kPa (7 bar [101.5 psi]) for 24 hours consecutively (Hedegaard and Hansen, 1992). The specimen was then split into two halves, perpendicular to the injected face, where the wetted region was marked and the maximum depth of penetration was recorded. A typical water penetration sample is shown in Figure 5-12.

Figure 5-12. Depth of water penetration in split DIN 1048 specimens

5.3.5. Salt Ponding and Chloride Ion Penetration Test

The salt ponding test was conducted per ASTM C1543 and the chloride ion penetration test was performed by two different methods to measure the acid soluble chloride per ASTM C1152 and water soluble chloride per ASTM C1218.

5.3.5.1. Concrete Sampling

Three concrete slabs for each concrete mixture of 3 × 12 × 16 in. (75 × 300 × 400 mm) were cast and cured at room temperature (73 ºF [23 ºC]) for 24 hrs before unmoulding and transferring them to a controlled moisture curing room at 73 ± 3 ºF (23 ± 2 ºC) temperature and 100% relative humidity. The slabs were moist cured for 14 days followed by 14 days of drying before salt ponding. Prior to salt ponding, the sides of slabs were sealed to prevent

evaporation from those surfaces and to control the direction of chloride penetration. Specimens were then salt ponded for three different periods of 90, 180, and 360 days. Following the recommendations of ASTM C1543, the slabs from each concrete mix were subsequently ponded with three percent sodium chloride solution at a minimum depth of 13 mm. A cover was placed over the solution pond to prevent water evaporation. The ponded slabs were stored in a room temperature controlled environment at 50% relative humidity for the entire exposure period. Figure 5-13 shows concrete slabs subject to salt ponding.

Figure 5-13. Salt ponding test (chloride content across the slab depth).

5.3.5.2.Sample Preparation Procedure

Following the end of the salt ponding period, six samples of at least 10 g (0.35 oz) each were collected from each slab. The samples were taken at depths ranging from 0 – ½ in. (0 – 12.5 mm), ½ – 1 in. (12.5 – 25 mm), 1 – 1½ in. (25 – 37.5 mm), 1½ – 2 in. (37.5 – 50 mm), and 2

– 2½ in. (50 – 62.5 mm). The samples that were measured between 2 to 2½ in. (50 to 62.5 mm) were taken as the initial chloride content in concrete. Both the acid-soluble and water soluble chloride method were performed for measuring the chloride ion concentration in the concrete.

Acid-Soluble Method:

Three grams of the drilled sample were measured and placed in a beaker with 10 ml distilled water. The sample was stirred thoroughly to bring the powder into suspension, then 3 ml of nitric acid HNO_3 was added to the beaker and the solution was diluted with hot H_2O up to 50 ml. This was followed by adding five drops of methyl orange indicator. A total of 3 ml of H_2O_2 were added to samples containing blast furnace slag before adding the methyl orange indicator. More HNO_3 drops were added to the solution, which showed yellow/orange color, until a permanent pink/ red color was seen. The beaker was covered with a watch glass and was heated to boiling on a hot-plate/magnetic stirrer using a small magnet. The mixture was boiled for five minutes and was then allowed to stand for 24 hours in an HCl fume-free atmosphere. The clear supernatant liquid was filtered through double filter paper (Whatman No. 41 over No. 40, or equivalent) into a 250 ml beaker. The filter papers and the funnel were washed with hot distilled water until a total volume of 125 to 150 ml was maintained in the beaker. Figure 5-14 shows the test apparatus.

Water-Soluble Method

Three grams of the drilled sample were placed in a beaker and 60 – 70 ml of distilled water was added to the beaker. The beaker was kept in a HCl fume-free atmosphere for 24 hours, then it was heated to boiling for five minutes on a hot-plate/magnetic stirrer. The sample beaker was filtered using double filter paper (Whatman No. 41 over No. 40, or equivalent) and was placed on a magnetic stirrer. While stirring the solution, one to two drops of methyl orange

indicator were added, followed by drops of HNO_3 until a permanent pink to red color was seen. A total of 3 ml of H_2O_2 were added to samples containing blast furnace slag before adding the methyl orange indicator.

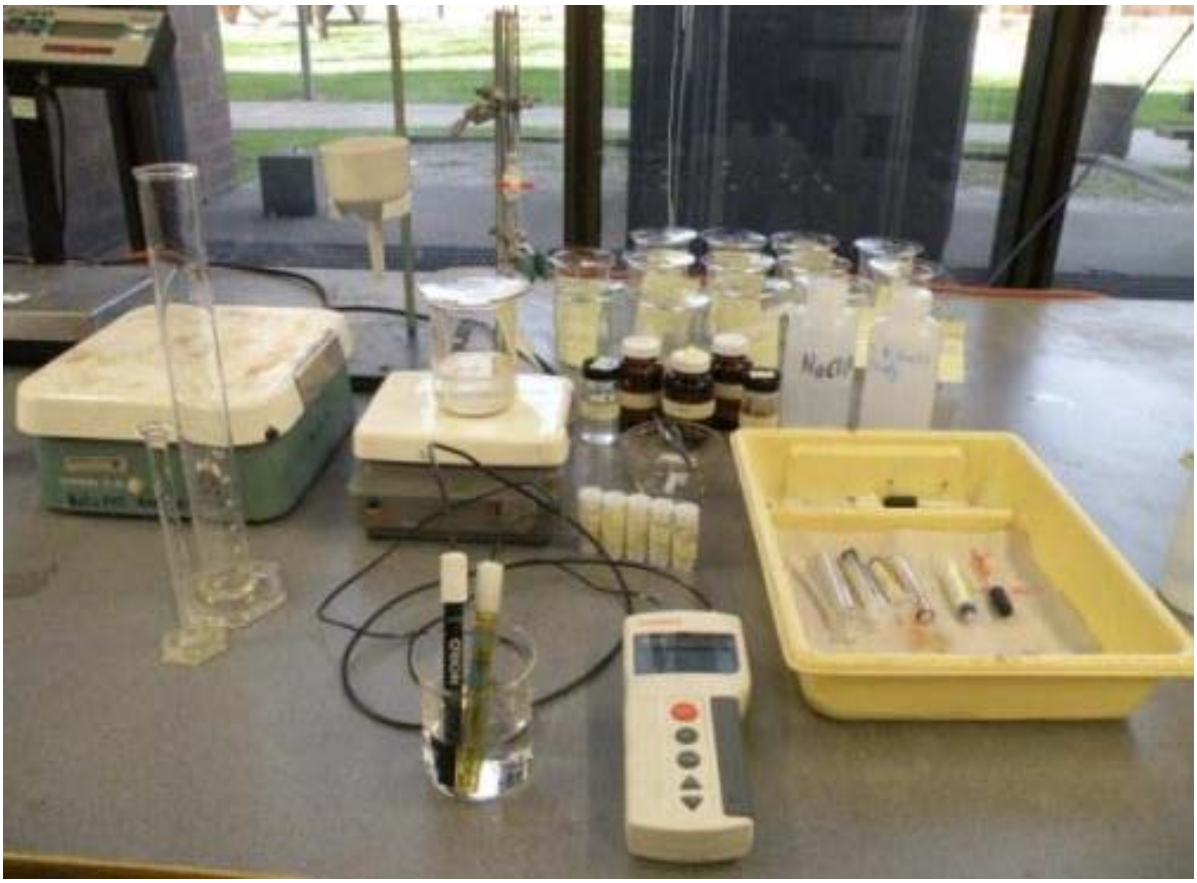

Figure 5-14. Apparatus for testing chloride concentration

5.3.5.3.Potentiometric Titration

The electrode was calibrated with the solutions recommended by the manufacturer. A total of 4.0 ml of 0.01 N NaCI was added to the cooled sample beaker while swirling. The electrode was removed from the beaker of distilled water and was wiped with absorbent paper. The electrode was then immersed into the sample solution. The beaker-electrode assembly was placed on a magnetic stirrer and gently stirred. Using a calibrated buret, a standard 0.01 N $AgNO_3$ solution was added in 0.10 ml increments and a millivoltmeter reading was recorded

after each addition. As the equivalence point was approached, equal additions of $AgNO_3$ solution caused increasingly larger changes in the millivolt reading. These changes decreased once the equivalence point passed. The titration procedure continued until the millivoltmeter reading was at least 40 mv past the approximate equivalence point. The end point of titration, usually near the approximate equivalence point in distilled water, was determined by plotting the volume of AgN03 solution added versus the millivoltmeter readings.

5.3.5.4.Calculations

The endpoint of titration was determined by plotting the volume of $AgNO_3$ solution versus the millivolt reading. This end point corresponds to the inflection point of the resultant smooth curve. The percentage of chloride ions was calculated according to the following equation:

$$Cl^- = 3.5453\frac{(V_1N_1 - V_2N_2)}{W} \qquad \text{Eq. 5.4}$$

Where

V_1 = the end point of $AgNO_3$ in ml,

V_2 = the volume of NaCI solution added in ml,

N_1 = the normality of $AgNO_3$,

N_2 = the normality of NaCI solution, and

W = the weight of original concrete sample in grams.

6. FRESH PROPERTIES OF CONCRETE

A summary of the fresh properties for the durability, compression, and flexure batches for each concrete mix combination are presented in Table 6-1 to Table 6-6. The fresh properties are presented in terms of the slump (workability), fresh air content, unit weight of fresh concrete, ambient and concrete temperature and humidity. The fresh air content were measured twice for all the mixtures, 12 minutes after discharging the concrete from the concrete mixer and after filling all the molds. This practice was adopted after experiencing high air loss in the entrained air content. The reported air content in the tables is based on the final air content after filling the molds. As shown in the tables, the fresh air content ranged from 6.4 to 7.5%. In addition the fresh unit weight of concrete were in the range of 144.5 lb/ft^3 (2315 Kg/m^3) and 146.3 lb/ft^3 (2343 Kg/m^3).

Table 6-1. Fresh Properties of the Durability Mixes batched with Natural Sand

Mix Designation	Dosage, US fl. oz/yd³			W/CM	Slump, in.	Air Content, %	Unit Weight, lb/yd³	Conc. Temp., °F	Lab Temp., °F	Lab Hum., %
	WRA	HRWR	AEA							
C1-F-NS1	–	–	5.0	0.40	3.70	7.2	144.7	78	78	71
C1-F-NS2	8.7	–	10.6	0.42	4.00	6.5	146.0	79	79	72
C1IP1-F-NS	–	–	1.7	0.40	3.25	7.1	145.1	74	73	67
C1IP2-F-NS	10.6	–	2.1	0.42	4.00	7.0	145.1	74	74	71
C1-S-NS1	5.6	5.6	4.8	0.42	3.50	7.1	145.1	72	73	40
C1-S-NS2	48.2	6.9	4.8	0.42	3.50	6.8	145.4	73	73	38
C1IP1-S-NS	11.9	10.4	6.4	0.42	3.50	7.1	145.9	72	73	41
C1IP2-S-NS	48.2	6.4	11.6	0.42	3.25	6.7	145.8	72	74	40
C2-F-NS	8.0	7.2	4.8	0.42	3.50	6.7	145.6	71	70	34
C2IP-F-NS	8.0	7.2	4.8	0.42	3.75	6.7	145.6	71	71	36
C2-S-NS	48.2	12.1	8.8	0.42	4.50	6.8	145.6	70	70	26
C2IP-S-NS	48.2	12.1	8.0	0.42	5.75	6.6	146.1	70	71	30
C3-F-NS	–	–	3.9	0.40	3.75	7.2	144.9	73	71	57
C3IR-F-NS	–	–	3.5	0.40	3.50	7.4	144.5	73	71	60
C3-S-NS	7.2	–	0.8	0.42	3.50	7.3	144.7	73	71	64
C3IR-S-NS	7.2	–	0.5	0.42	4.00	7.3	144.7	72	71	65

1 US fl. oz/yd^3 = 0.04985 L/m^3; 1 lb/yd^3 = 0.593276 Kg/m^3; 1 in. = 25.4 mm

Table 6-2. Fresh Properties of the Durability Mixes batched with Combined Sand

Mix Designation	Dosage, US fl. oz/yd^3			W/CM	Slump, in.	Air Content, %	Unit Weight, lb/yd^3	Conc. Temp., °F	Lab Temp., °F	Lab Hum., %
	WRA	HRWR	AEA							
C1-F-CS	16.9	21.7	33.7	0.42	5.25	6.9	145.1	78	79	70
C1IP1-F-CS	21.7	19.3	35.4	0.42	4.75	7.1	145.0	78	79	70
C1-S-CS	16.9	21.7	57.9	0.44	4.50	7.5	144.5	76	77	71
C1IP1-S-CS	21.7	21.7	57.9	0.44	5.50	6.9	145.4	76	75	67
C2-F-CS	20.9	19.3	35.4	0.42	4.25	6.8	145.6	78	79	70
C2IP-F-CS	21.7	18.5	37.0	0.42	5.50	7.1	146.2	78	79	70
C2-S-CS	19.3	21.7	57.9	0.44	4.25	7.2	145.0	76	77	67
C2IP-S-CS	21.7	21.7	57.9	0.44	4.00	6.8	145.1	76	77	67
C3-F-CS	21.7	24.9	24.1	0.42	4.00	7.3	144.5	71	72	42
C3IR-F-CS	21.7	26.5	24.1	0.42	5.00	7.4	144.8	71	70	42
C3-S-CS	24.1	28.9	69.9	0.44	5.25	7.2	144.8	73	75	28
C3IR-S-CS	24.1	26.5	71.5	0.44	4.75	7.2	144.7	72	75	29

1 US fl. oz/yd^3 = 0.04985 L/m^3; 1 lb/yd^3 = 0.593276 Kg/m^3; 1 in. = 25.4 mm

Table 6-3. Fresh Properties of the Compression Mixes batched with Natural Sand

Mix Designation	W/CM	Slump, in.	Air Content, %	Unit Weight, lb/yd^3	Concrete Temperature, °F	Lab Temperature, °F	Lab Humidity, %
C1-F-NS1	0.40	3.50	7.2	144.8	75	78	67
C1-F-NS2	0.42	3.75	7.2	145.0	74	79	67
C1IP1-F-NS	0.40	3.00	6.9	145.2	74	73	72
C1IP2-F-NS	0.42	3.50	7.5	144.5	75	74	73
C1-S-NS1	0.42	3.75	7.1	145.0	74	77	39
C1-S-NS2	0.42	4.00	7.4	144.6	72	76	30
C1IP1-S-NS	0.42	4.00	7.2	144.6	74	77	40
C1IP2-S-NS	0.42	3.75	7.3	144.6	73	76	36
C2-F-NS	0.42	3.50	6.8	145.1	69	69	34
C2IP-F-NS	0.42	3.50	7.0	145.3	70	69	37
C2-S-NS	0.42	3.50	6.5	146.0	69	69	30
C2IP-S-NS	0.42	3.75	7.5	144.8	70	69	30
C3-F-NS	0.40	3.70	6.6	145.9	74	71	70
C3IR-F-NS	0.40	3.00	7.2	145.0	74	71	67
C3-S-NS	0.42	3.60	6.7	145.5	73	71	65
C3IR-S-NS	0.42	3.50	7.2	145.8	73	71	65

1 in. = 25.4 mm; 1 lb/yd^3 = 0.593276 Kg/m^3

Table 6-4. Fresh Properties of the Compression Mixes batched with Combined Sand

Mix Designation	W/CM	Slump, in.	Air Content, %	Unit Weight, lb/yd^3	Concrete Temperature, °F	Lab Temperature, °F	Lab Humidity, %
C1-F-CS	0.42	5.25	7.1	145.0	76	78	68
C1IP1-F-CS	0.42	4.75	7.2	145.0	78	78	69
C1-S-CS	0.44	6.00	6.7	145.2	74	75	67
C1IP1-S-CS	0.44	4.25	7.3	144.7	78	77	72
C2-F-CS	0.42	3.90	6.6	145.6	77	78	68
C2IP-F-CS	0.42	4.50	6.9	145.6	76	76	63
C2-S-CS	0.44	3.50	6.7	145.6	74	75	68
C2IP-S-CS	0.44	5.75	6.7	146.0	75	76	69
C3-F-CS	0.42	5.00	7.0	146.3	72	73	53
C3IR-F-CS	0.42	5.50	6.8	145.5	72	71	41
C3-S-CS	0.44	5.00	7.4	144.6	72	74	29
C3IR-S-CS	0.44	3.50	7.3	144.6	76	76	34

1 in. = 25.4 mm; 1 lb/yd^3 = 0.593276 Kg/m^3

Table 6-5. Fresh Properties of the Flexure Mixes batched with Natural Sand

Mix Designation	W/CM	Slump, in.	Air Content, %	Unit Weight, lb/yd^3	Concrete Temperature, °F	Lab Temperature, °F	Lab Humidity, %
C1-F-NS1	0.40	3.50	7.0	145.1	75	74	70
C1-F-NS2	0.42	3.50	7.4	144.6	75	74	71
C1IP1-F-NS	0.40	3.50	7.1	144.8	74	74	73
C1IP2-F-NS	0.42	3.50	7.5	144.5	75	75	73
C1-S-NS1	0.42	3.75	7.2	144.8	74	77	39
C1-S-NS2	0.42	3.75	7.1	145.1	72	75	30
C1IP1-S-NS	0.42	4.25	6.4	146.0	73	78	41
C1IP2-S-NS	0.42	5.00	7.3	144.8	73	76	36
C2-F-NS	0.42	3.50	6.6	145.6	70	69	35
C2IP-F-NS	0.42	3.75	7.5	144.8	69	70	37
C2-S-NS	0.42	3.50	6.6	145.6	70	70	30
C2IP-S-NS	0.42	3.75	6.9	145.5	70	69	30
C3-F-NS	0.40	3.50	7.2	144.6	74	73	66
C3IR-F-NS	0.40	3.25	6.7	146.0	74	73	66
C3-S-NS	0.42	3.25	7.1	144.8	73	71	64
C3IR-S-NS	0.42	3.50	7.2	145.0	73	71	64

1 in. = 25.4 mm; 1 lb/yd^3 = 0.593276 Kg/m^3

Table 6-6. Fresh Properties of the Flexure Mixes batched with Combined Sand

Mix Designation	W/CM	Slump, in.	Air Content, %	Unit Weight, lb/yd^3	Concrete Temperature, °F	Lab Temperature, °F	Lab Humidity, %
C1-F-CS	0.42	5.00	6.6	145.9	76	77	69
C1IP1-F-CS	0.42	4.50	7.0	145.3	78	78	64
C1-S-CS	0.44	4.50	7.1	144.8	76	76	70
C1IP1-S-CS	0.44	4.50	6.9	145.3	78	77	72
C2-F-CS	0.42	4.25	7.0	146.0	78	78	69
C2IP-F-CS	0.42	5.00	7.0	145.0	78	78	64
C2-S-CS	0.44	5.00	7.0	145.1	75	76	69
C2IP-S-CS	0.44	4.75	7.5	144.5	74	75	67
C3-F-CS	0.42	3.75	6.7	145.7	71	72	39
C3IR-F-CS	0.42	4.75	7.2	146.1	72	71	41
C3-S-CS	0.44	5.00	7.1	145.0	74	74	37
C3IR-S-CS	0.44	5.00	6.9	145.1	75	74	37

1 in. = 25.4 mm; 1 lb/yd^3 = 0.593276 Kg/m^3

6.1. Workability

The slump was measured upon discharging of the concrete mix and 12 minutes afterwards. The concrete mixes were calibrated to achieve the desired slump and air content. The amount of plasticizers varied depending on the workability of the mix and the ability to get the desired slump without exceeding the maximum amount of chemical admixtures recommended per mix. Once the desired slump and air content were met, the required samples were cast for each

concrete mix. Figure 6-1 and Figure 6-2 show the slump versus the total admixture dosage added for concrete mixes batched with natural sand and combined sand, respectively.

Special attention was given to the effect of variables on the performance of concrete mixes when the concrete mixes were calibrated to reach the desired slump and air content. These variables included the cement source, addition of fly ash or slag, and sources of fine aggregates (natural or combined sand).

6.1.1. Effect of Limestone and Inorganic Processing, and Insoluble Residue

Concrete mixes with conventional cement were compared with concrete mixes with modified cement (IPA and IR), such that both mixes had the same material proportion and cement source. Most concrete mixes made with conventional cement required slightly less amount of admixtures to achieve a slump equivalent to mixes made with modified cement. Figure 6-1, showing mixes batched with natural sand, indicates that the mixes made with conventional cement gave slightly higher slump, except for Mix C1IP1-S-NS which required more admixture to retain a slump equivalent to C1-S-NS. Figure 6-2, showing mixes batched with combined sand, indicates inconsistent variation between the slump and admixture dosage for mixes with conventional and modified cement.

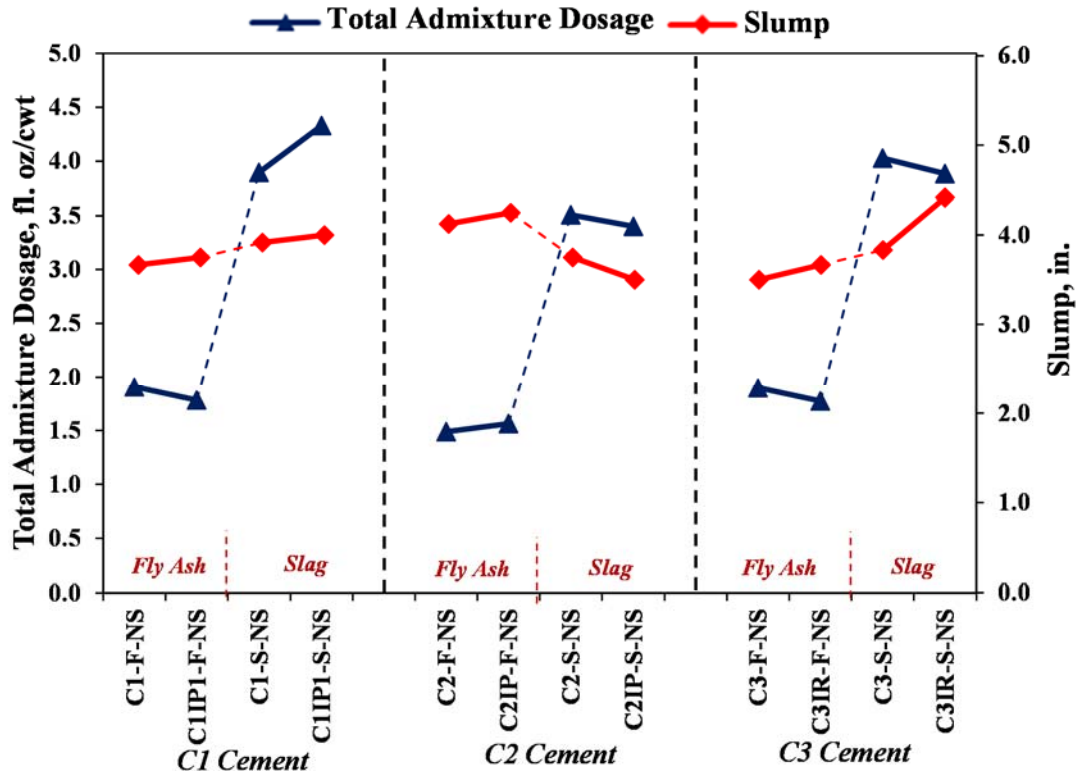

Figure 6-1. Total admixture dosage versus slump for mixes batched with natural sand.

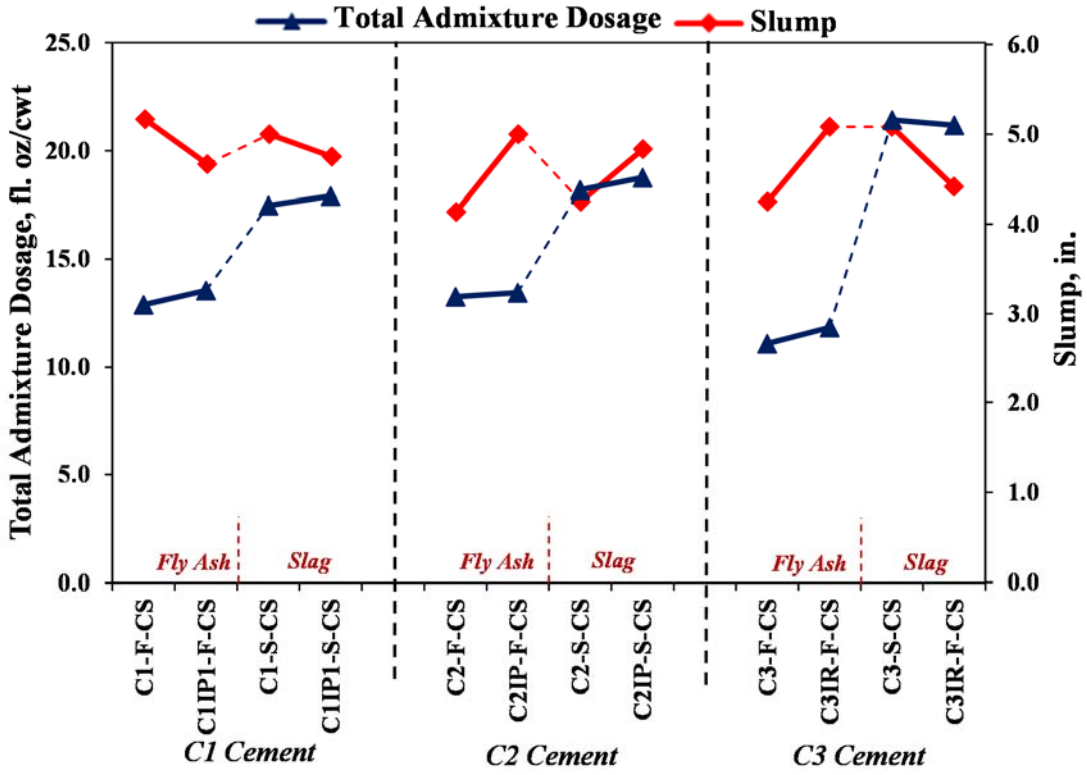

Figure 6-2. Total admixture dosage vs. slump for mixes batched with combined sand.

6.1.2. Effect of Fly Ash or Slag (SCMs)

The use of slag or fly ash affected the workability of concrete as shown in Figure 6-1 and Figure 6-2. Concrete mixes batched with fly ash had 0.02 w/cm less than concrete mixes batched with slag. Moreover, mixes with fly ash required fewer admixtures to maintain the desired slump in comparison to mixes batched with slag. The improved workability of using fly ash in comparison with slag is attributed to the difference in the physical characteristics (specific surface area and surface texture). The specific surface area for fly ash is typically lower than slag, and the surface texture for fly ash is spherical in shape in comparison with slag, which has rough, angular- shaped grains (Kosmatka et al., 2011).

6.1.3. Effect of Fine Aggregate Source (Natural or Combined Sand)

Combined sand required a high dosage of HRWR and AEA to maintain workability. Consequently, the w/cm ratio increased to 0.44 for all mixes made with slag and batched with combined sand. On the other hand, the mixes made with fly ash and natural sand experienced higher slump than desired and the w/cm ratio was, therefore, reduced to 0.40.

6.2. Initial and Final Setting Times

The setting time for all the concrete mixes was measured according to ASTM C403 (Time of concrete mixtures by penetration resistance). The apparatus used for this testing is shown in Figure 6-3. Figure 6-4 through Figure 6-6 show the time setting plots for mixes made with C1, C2, and C3 cement, respectively, and batched with natural sand. Figure 6-7 through Figure 6-9 show the time setting plots for mixes made with C1, C2, and C3 cement, respectively, and batched with combined sand.

Figure 6-3. Penetration resistance testing equipment, ASTM C403.

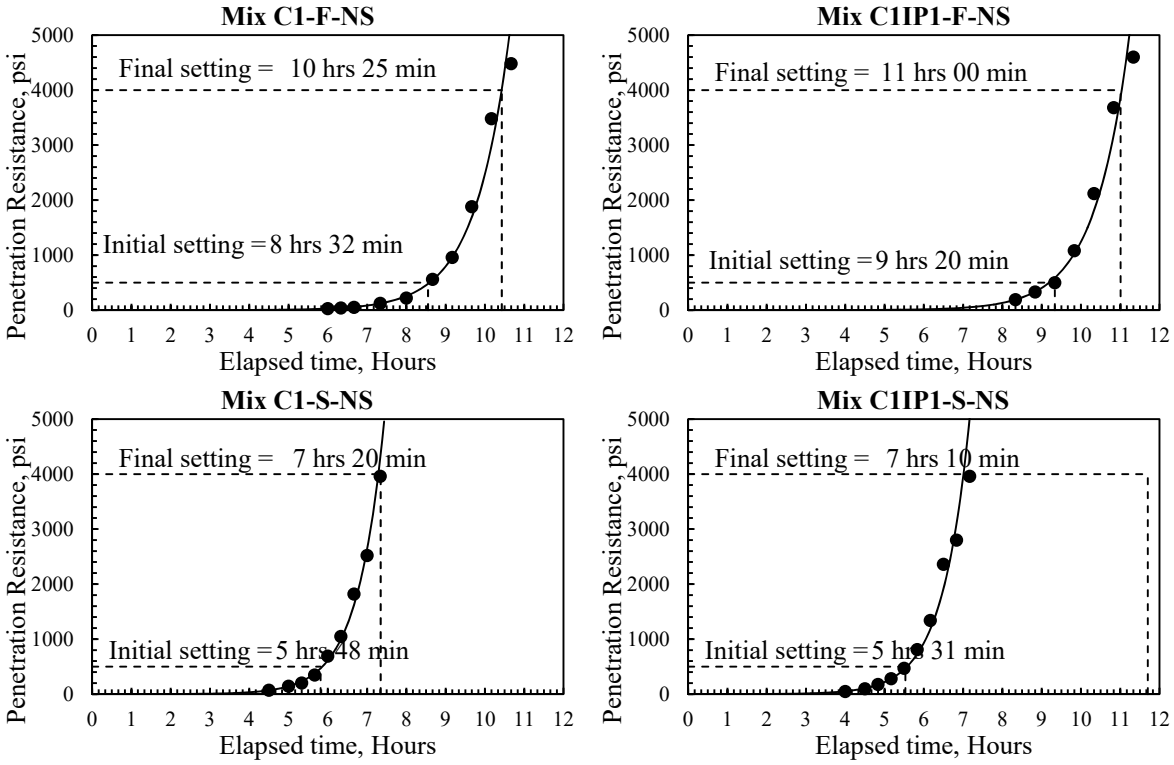

Figure 6-4. Time of setting for concrete mixes made with C1 cement and natural sand

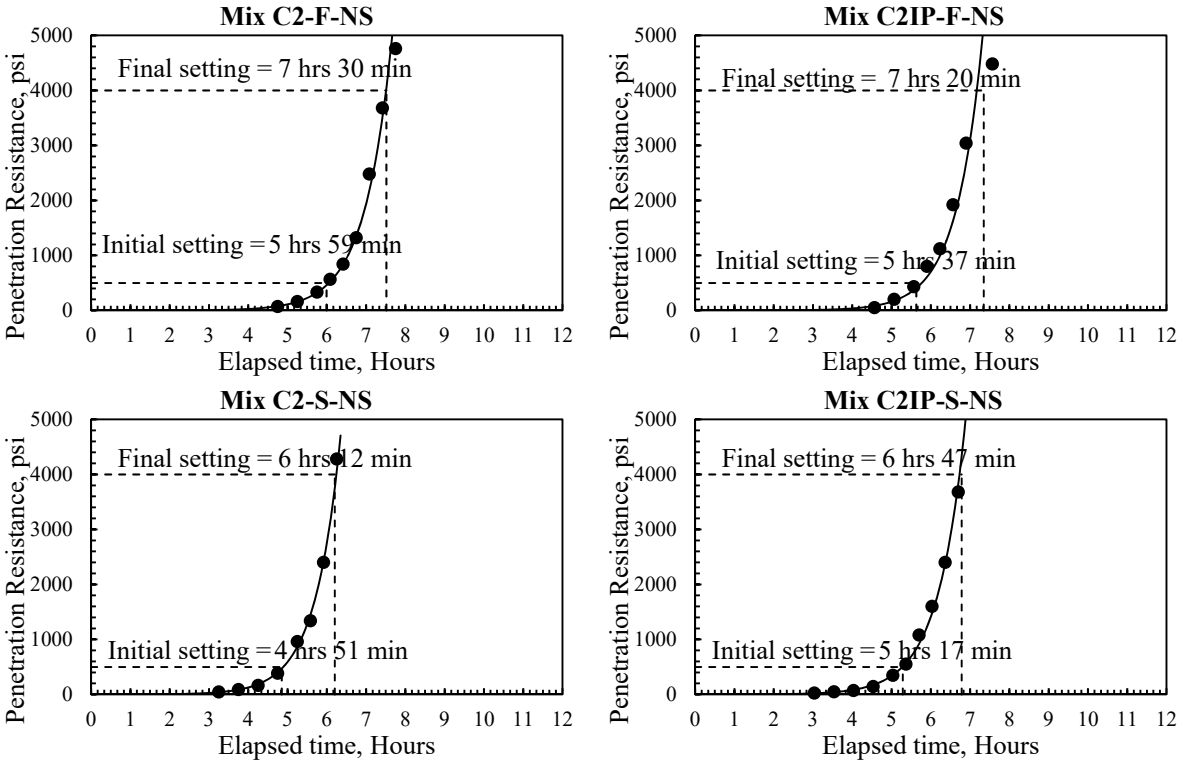

Figure 6-5. Time of setting for concrete mixes made with C2 cement and natural sand

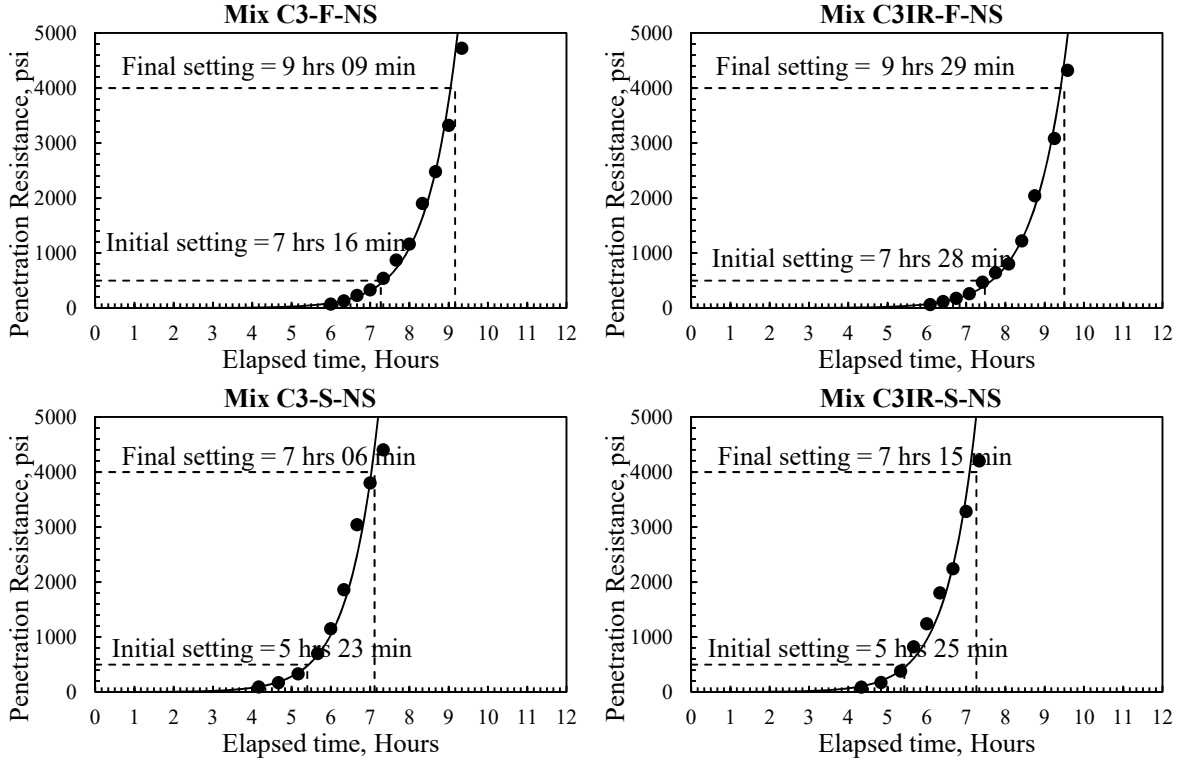

Figure 6-6. Time of setting for concrete mixes made with C3 cement and natural sand

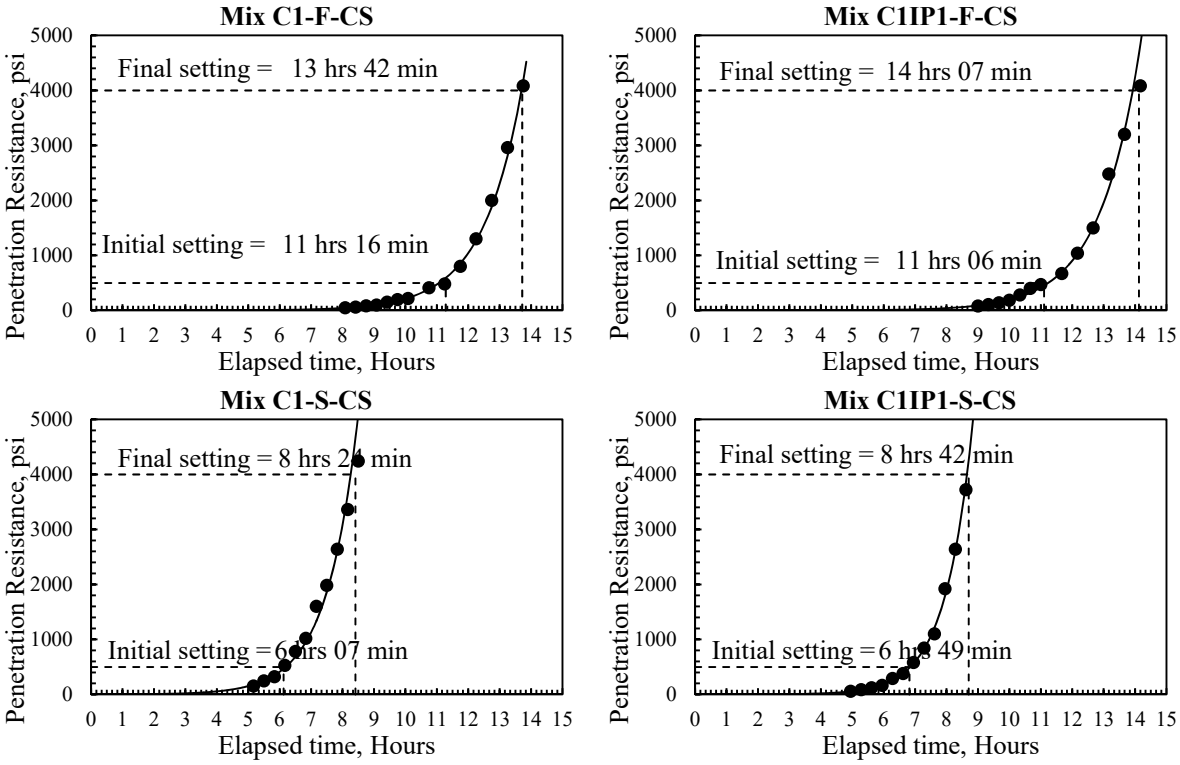

Figure 6-7. Time of setting for concrete mixes made with C1 cement and combined sand

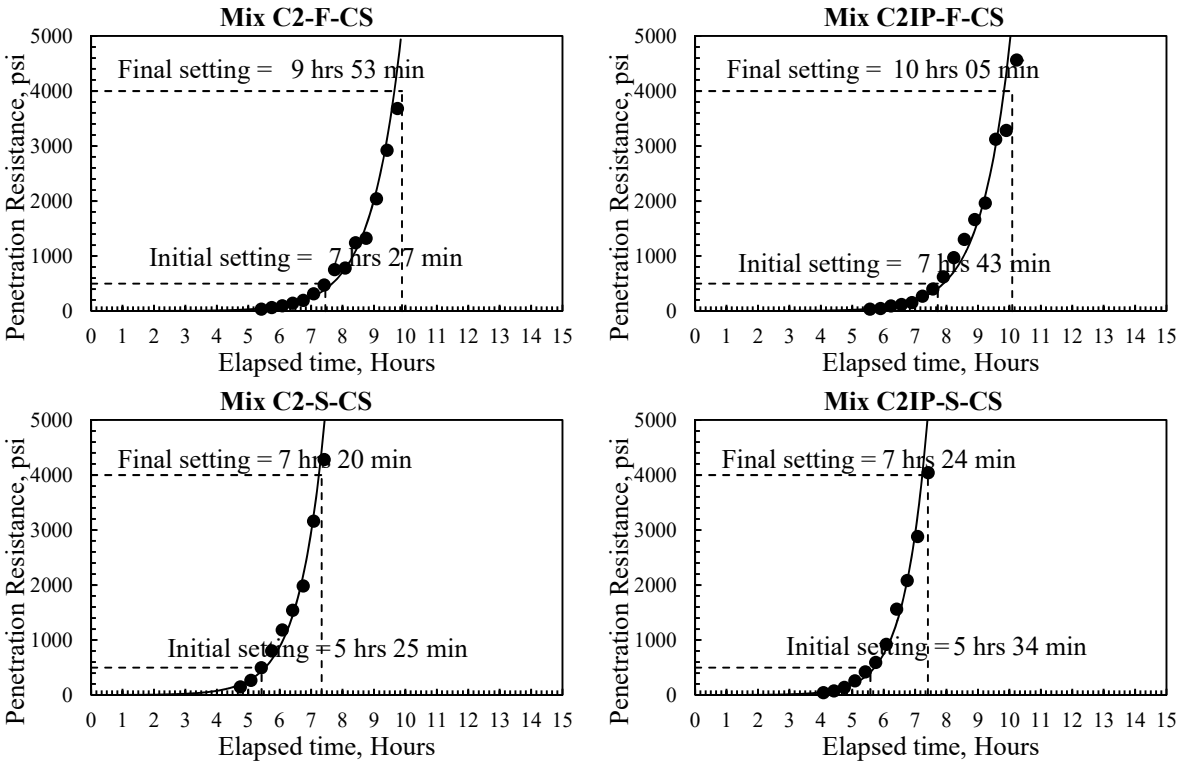

Figure 6-8. Time of setting for concrete mixes made with C2 cement and combined sand

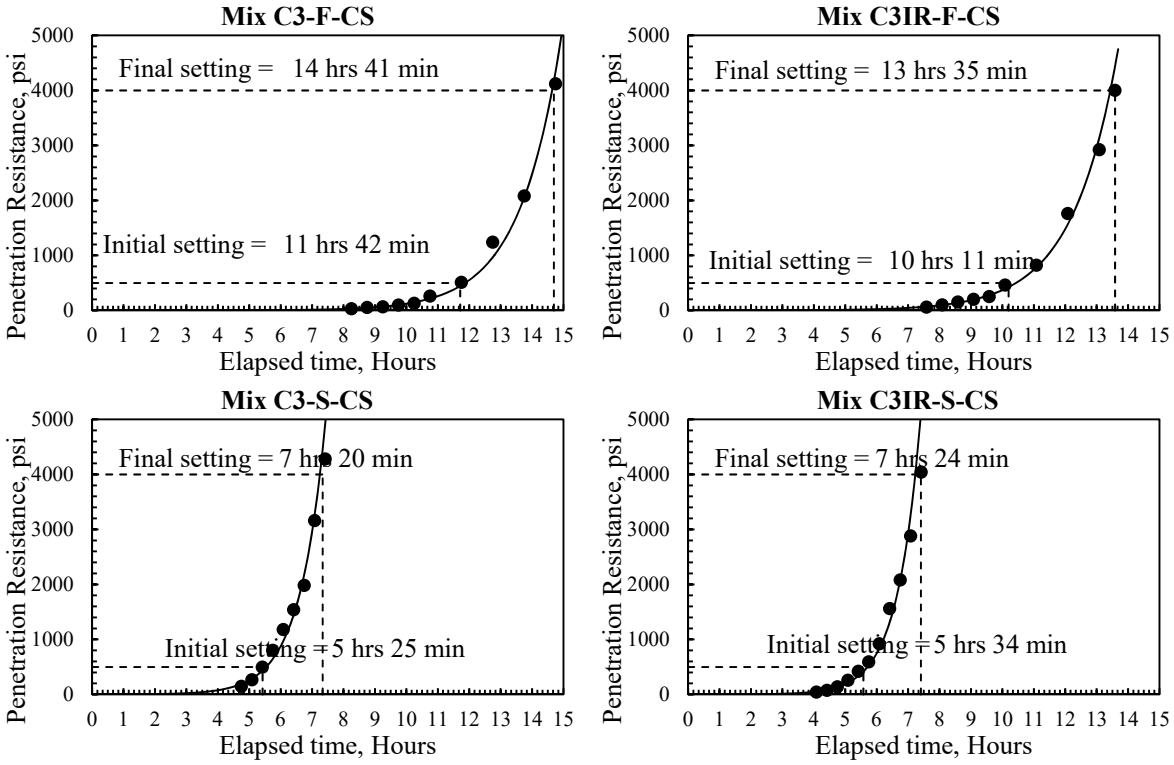

Figure 6-9. Time of setting for concrete mixes made with C3 cement and combined sand

The setting times for all the concrete mixes having the same cement source were prepared and tested on the same day to avoid any inconsistency in the temperature change and the relative humidity. Initial and final setting results indicated ±5% difference for most concrete mixes having the same mix proportioning and cement source with conventional and modified cement However, C3 mixes with combined sand and fly ash showed a decrease in the initial set by 13% and final set by 8% for Mix C3IR-F-CS with respect to Mix C3-F-CS.

6.2.1. Effect of Limestone and Inorganic Processing, and Insoluble Residue

The setting time results for all the mixes indicated that the initial and final set times were slightly higher for concrete mixes with modified cement than concrete mixes with conventional cement (IPA and IR), knowing that both mixes had the same mix proportions. Most concrete mixes made with modified cement experienced a slight increase in initial and final setting

times. This increase is attributed to a slowdown in the hydration process between cement and water because of the addition of more limestone and IPA, and/or insoluble residue. These materials are considered inert and had negligible effect on the chemical reaction of cement paste.

6.2.2. Effect of Fly Ash or Slag (SCMs)

The addition of fly ash or slag to concrete mixes showed a significant difference in setting times. Fly ash prolonged initial and final set times in comparison with slag. Inspection of Figure 6-4 through Figure 6-6 revealed that the average time needed to reach the initial and final set times for concrete mixes batched with fly ash and natural sand was, respectively, 37% and 31% longer than the set times for concrete mixes batched with slag and natural sand. In addition, the average time needed to reach the initial and final set times for concrete mixes batched with fly ash and combined sand was, respectively, 70% and 63% longer than the set times for concrete mixes batched with slag and combined sand, as attested in Figure 6-7 through Figure 6-9.

6.2.3. Effect of Fine Aggregate Source (Natural or Combined Sand)

Natural sand resulted in quicker set time in concrete in comparison with combined sand. The initial and final set times for mixes made with C1 cement were significantly longer in the mixes batched with combined sand (see Figure 6-7) than the mixes batched with natural sand (see Figure 6-4). In addition, the performance of mixes made with C2 and C3 cements was similar to C1 cement mixes. Inspection of Figure 6-4 through Figure 6-9 revealed that the average time needed to reach the initial and final set for concrete mixes batched with fly ash and combined sand was, respectively, 34% and 39% higher than the set times for concrete mixes batched with fly ash and natural sand. Moreover, the average time needed to reach the initial

and final set times for concrete mixes batched with slag and combined sand was, respectively, 8% and 11% higher than the set times for concrete mixes batched with slag and natural sand.

7. TEST RESULTS AND DISCUSSION FOR THE STRENGTH PROPERTIES OF CONCRETE

The compressive and flexural strength results for all the concrete mixes and tested at 3, 7, 14, 28, and 56 days are presented in the tables and charts shown in Appendix B and Appendix C, respectively. The compressive strength results were based on the average of three to four 6 × 12 in. (150 × 300 mm) concrete cylinders and the flexural strength results were based on the average of two 6 × 6 × 21 in. (150 × 150 × 525 mm) concrete prisms. The coefficient of variation (*COV*) for the compressive strength mixes, calculated for each test date, did not exceed 8%, and on average it was within 2.4%. The *COV* for the flexural strength results were slightly higher with an average *COV* of 4% and maximum of 14%.

7.1. Compressive and Flexural Strength Test Results

The average compressive strength tables and charts for all concrete mixes are presented in Appendix B. Table B-1 shows the compressive strength test results for mixes batched with natural sand, and Table B-2 shows the compressive strength test results for mixes batched with combined sand. The compressive strength tables also include fresh air content and unit weight values of each concrete mix. Air content variations between compression concrete mixes having the same cement source and fine aggregate type are less than 1.0%, as shown in Table B-1 and Table B-2. This gives a better understanding of the effect of replacing cement with limestone and IPA, and/or IR on the strength properties of concrete.

Flexural tests are extremely sensitive and test results are usually affected by the way the test is prepared, handled, cured, and conducted. Flexural specimens for all the concrete mixes were tested while wet because drying would yield lower strength. Average flexural

strength tables and charts for all concrete mixes are presented in Appendix C. Table C-1 shows the flexural strength results for mixes batched with natural sand, and Table C-2 shows the results for mixes batched with combined sand. The flexural strength tables also include fresh air content and unit weight values of each concrete mix. For the same cement source, the variation in the air content between each concrete mix for flexural beams batched with natural sand is less than 1.0%, as shown in Table C-1. However, concrete mixes for the flexural beams batched with combined sand were calibrated by dosing high amount of chemical admixtures, which caused a higher variation in air content as shown in Table C-2.

It was observed that the average compressive and flexural strength for all the concrete mixes at 14 day exceeded the minimum target strength specified by IDOT of 3500 psi (24 MPa) and 600 psi (4.1 MPa), respectively.

7.2. Discussion of Test Results

Studies on the addition of limestone and IPA to concrete have shown that the strength properties of concrete are affected by the quality and quantity of limestone and IPA added, production method (i.e. blended or interground with cement), particle size distribution and shape, Blaine fineness, and the addition of SCMs. The Blaine fineness and strength properties of the cement sources used are presented in Table 3-4. The Blaine fineness ranged between 378–408 m^2/Kg. The compressive strength properties were slightly higher for modified cement in comparison with the conventional for C1 source cement, but were slightly lower for C2 cement.

The comparison in the strength properties was based on concrete mixes having the same mix proportioning and batched with conventional or modified cement (IPA and IR). The effect

of using SCMs (slag or fly ash) and fine aggregate source (natural or combined sand) on the strength properties of concrete was analyzed and discussed below.

7.2.1. Compressive Strength

Figure 7-1 and Figure 7-2 show plots for the compressive strength results for concrete mixes batched with natural sand and combined sand, respectively.

7.2.1.1. Effect of Limestone and Inorganic Processing, and Insoluble Residue

For the same cement source and mix proportioning, the compressive strength results for concrete mixes batched with natural sand showed that most mixes with modified cement experienced slightly lower compressive strength at early curing age in comparison with mixes with conventional cement. However, most mixes with modified cement demonstrated slightly better strength gain over a 56 day curing period compared with conventional mixes.

Figure 7-1, showing mixes batched with natural sand, indicates that most of the 3 day compressive strength for mixes made with C1IP, C2IP, and C3IR modified cement was slightly less than the compressive strength of mixes made with C1, C2, and C3 conventional cement, respectively. However, the 56 day compressive strength test results varied for each concrete mix. For instance, mix C1IP-S-NS showed better strength and strength gain at all ages than its counterpart C1-S-NS. In contrast, the compressive strength for mix C3IR-S-NS with modified cement was less at all ages than the strength of its counterpart C3-S-NS with conventional cement. Although the former mix (C3IR-S-NS) demonstrated better strength gain with age than the latter (C3-S-NS).

As shown in Figure 7-2, the compressive strength of concrete mixes batched with combined sand showed similar trends in terms of strength gain to concrete mixes batched with natural sand. For mixes made with C1 cement source, Mix C1-F-CS with conventional cement

demonstrated better 3 and 7 day compressive strength and equivalent 56 day strength compared with its counterpart Mix C1IP1-F-CS with cement containing IPA. Mix C1-S-CS demonstrated slightly lower compressive strength than Mix C1IP1-S-CS at all ages except at 56 day. Similarly, mixes with C2IP cement resulted in slightly higher compressive strength and strength gain at all ages in comparison with their counterpart mixes and made with C2 conventional cement, except for Mix C2IP-S-CS which gave lower 3 day compressive strength than Mix C2-S-CS. Moreover, mixes made with C3IR did not reveal significant difference in the compressive strength at all ages with concrete mixes made with C3 conventional cement and having the same mix proportions. Therefore, this shows that increasing the IR content from 0.75 to 1.5% supports Kiattikomol et al., (2000) findings, who observed insignificant differences with marginal increase in the IR content.

Overall, the compressive strength for concrete mixtures made with the same cementitious combinations and batched with the same sand but with IPA and higher content of IR showed similar compressive strength and strength gain at all times. More differences in the compressive strength were observed after 28 and 56 days; this might be attributed to the difference in the air content, which ranged between 6.4 and 7.5%.

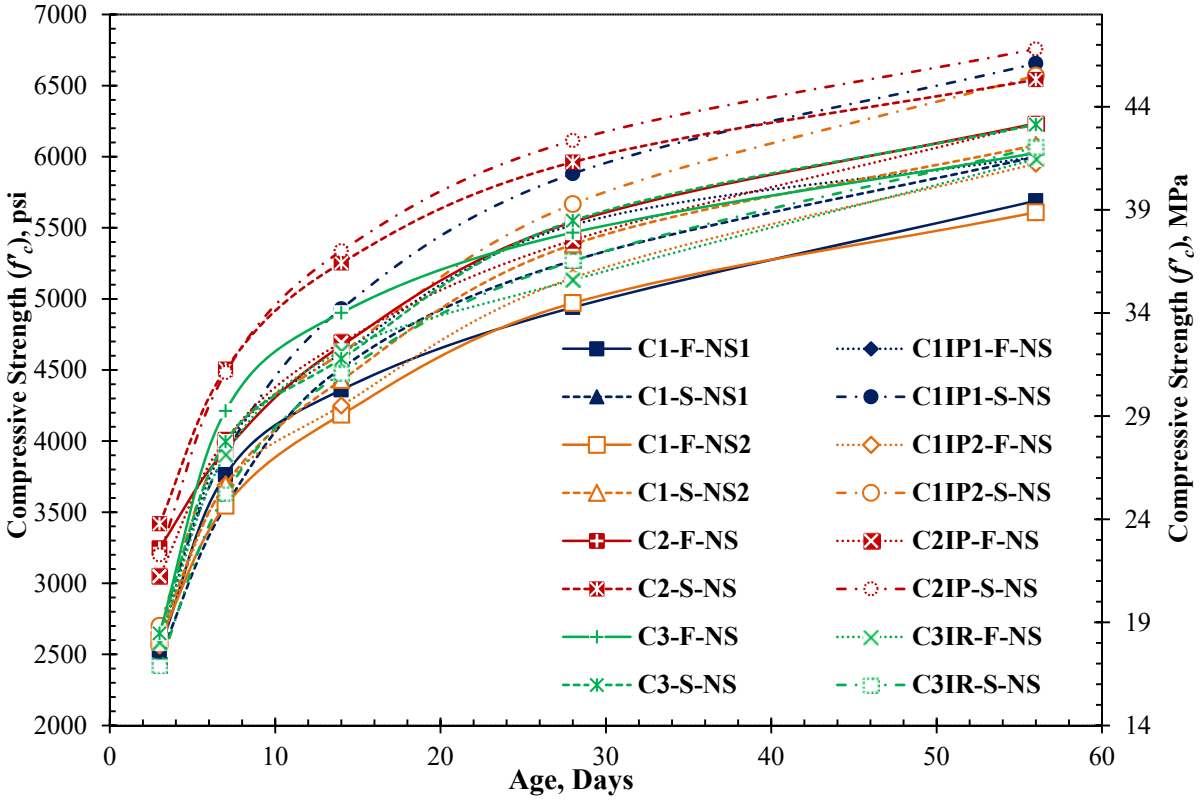

Figure 7-1. Compressive strength for concrete mixes batched with natural sand.

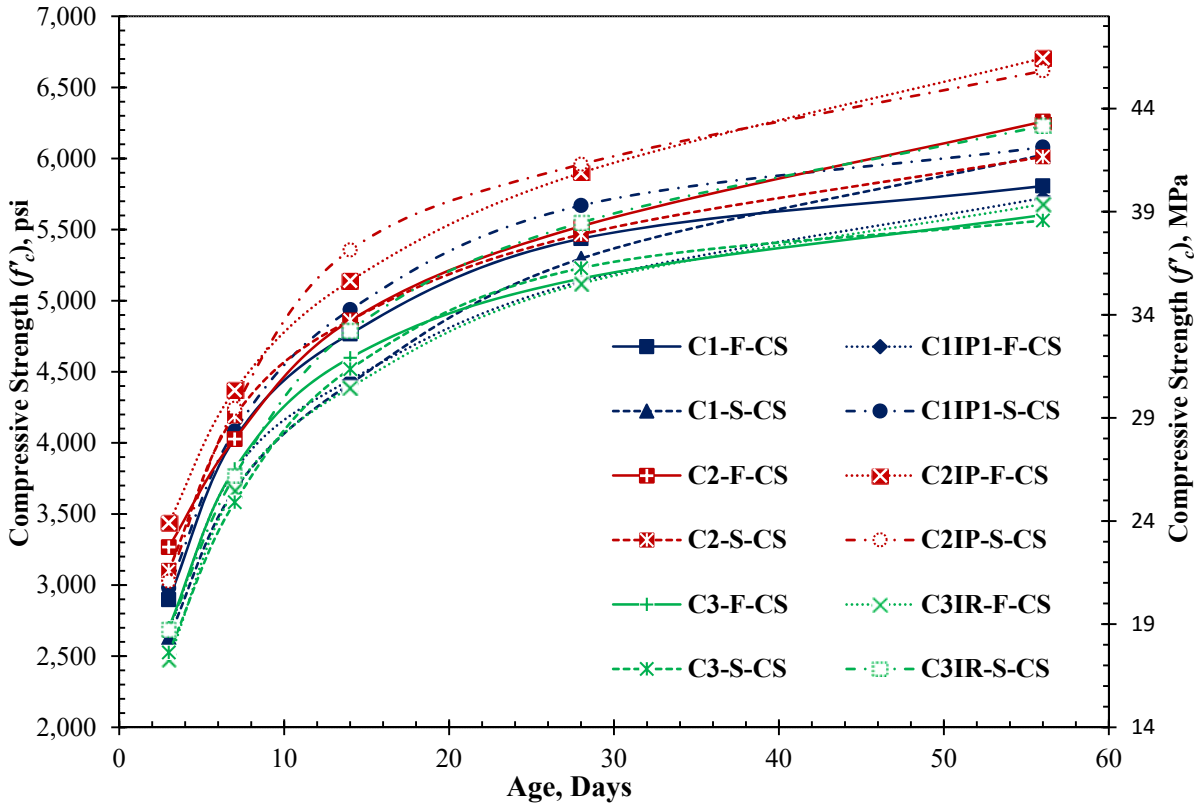

Figure 7-2. Compressive strength for concrete mixes batched with combined sand.

7.2.1.2.Effect of Slag or Fly Ash (SCMs)

It was observed that the compressive strength at ages 3, 7, and 14 days were comparable between concrete mixtures made with Class C fly ash and GGBF slag but it showed favorable performance for GGBF slag at ages 28 and 56 days (see Figure 7-1 and Figure 7-2). The comparison was made between concrete mixes with the same cement source and batched with the same sand type. However, the compressive strength in mixtures made with C3 cement and batched with combined sand did not show a favorable performance for GGBF slag at ages 28 and 56 days. The lower compressive strength, however, was also influenced by the higher w/cm ratio used in GGBF slag (0.44) compared to Class C fly ash (0.42) and the slightly higher air content in Mixes C3-S-CS and C3IR-S-CS in comparison with their counterparts C3-F-CS and C3IR-F-CS, respectively (see Figure 7-2). This observation is in agreement with Burris and Riding (2014) who observed favorable compressive strength performance for concrete mixes tested at 28, 91, and 180 days with w/cm of 0.34 and made with 25% GGBF slag in comparison with 25% Class C fly ash. The improved strength performance in the GGBF slag could be attributed to the higher calcium content (see Table 3-2) which forms more calcium hydroxide to react with silicate thereby creating more calcium silicate hydrate.

7.2.1.3.Effect of Fine Aggregate Sources (Natural or Combined Sand)

The source of fine aggregate used did not show significant effect on the compressive strength. Because of fresh air content and w/cm ratio variations between concrete mixes batched with natural sand and combined sand, it was hard to observe which type of fine aggregate had better effect on the compressive strength and strength gain.

7.2.2. Flexural Strength

Figure 7-3 and Figure 7-4 show plots for the flexural strength results for concrete mixes batched with natural sand and combined sand, respectively.

7.2.2.1. Effect of Limestone and Inorganic Processing, and Insoluble Residue

The flexural strength for all the concrete mixes, having the same cement source and mix proportioning, showed no favorable performance for any concrete mix with modified cement with IPA or higher content of IR in comparison with the conventional cement, as shown in Figure 7-3. For concrete mixes made with C1 cement and batched with natural sand, the strength variation at different ages between Mix C1-F-NS and Mix C1IP1-F-NS and between Mix C1-S-NS and Mix C1IP1-S-NS was inconsistent. Similarly, for the same mix proportion, mixes made with C2 and C3 cement source and batched with natural sand showed inconsistent variation in the flexural strength.

The flexural strength for concrete mixes batched with combined sand, demonstrated similar performance compared with the results for mixes batched with natural sand, as shown in Figure 7-4. No favorable performance observed on whether modified or conventional cement was used. For example, Mix C1-S-NS gave equivalent strength to Mix C1IP1-S-NS at 3 and 28 day and better strength at 7, 14, and 28 day. However, Mix C3-S-CS gave higher strength than Mix C3IR-S-CS at 3 and 7 day and lower strength at 56 day. Therefore, using more than 5% of limestone and IPA, and increasing the insoluble residue content to 1.5% in cement in concrete did not cause significant changes in the flexural strength.

7.2.2.2. Effect of Fly Ash or Slag (SCMs)

When GGBF slag was compared with Class C fly ash for the same cement source and fine aggregate type, it was observed that the majority of concrete mixes batched with slag had

slightly better strength gain than the mixes batched with fly ash. For the same cement source, concrete mixes batched with slag gave better 28 and 56 day flexural strength than the mixes batched with fly ash.

7.2.2.3.Effect of Fine Aggregate Sources (Natural or Combined Sand)

The sand type did not show a notable effect on the flexural strength. For the same cementitious combination, concrete mixtures batched with natural sand showed slightly better flexural strength and strength gain at all ages than mixtures batched with combined sand. This was also influenced by the w/cm ratio for mixtures batched with combined sand which had higher w/cm ratio by 0.02 compared to their counterparts batched with natural sand.

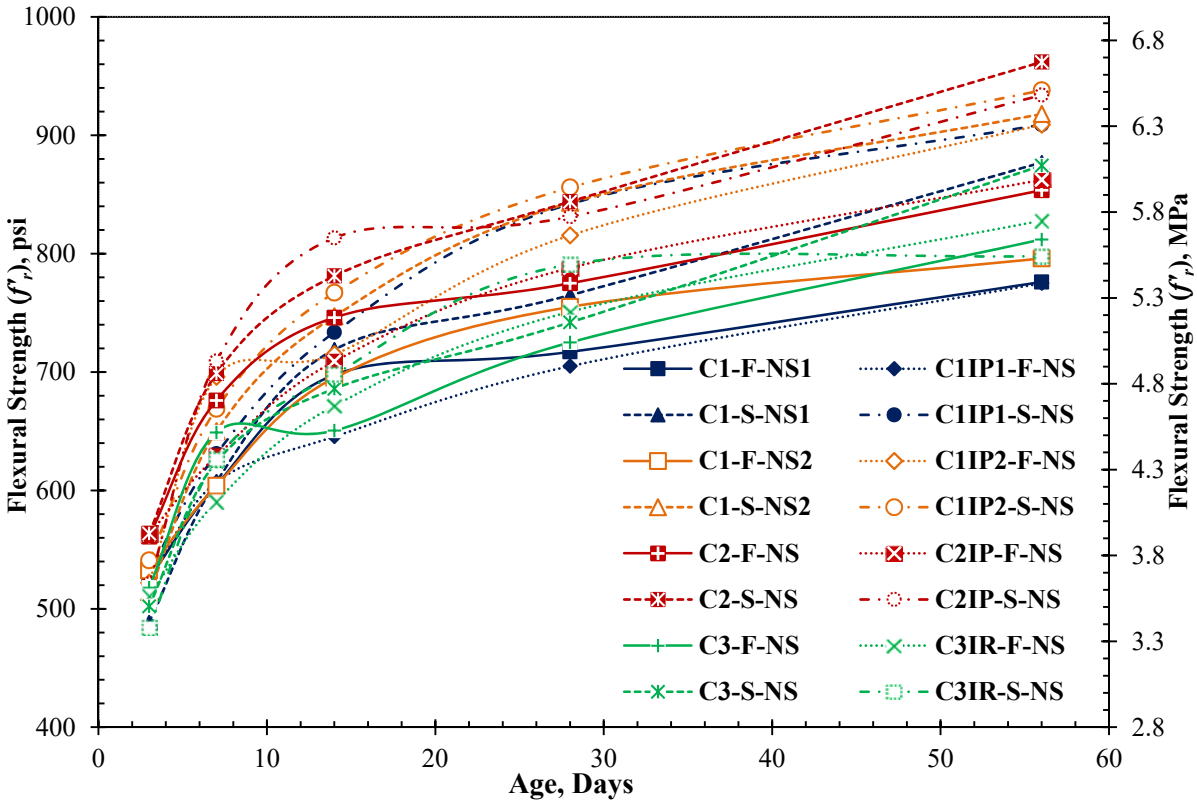

Figure 7-3. Flexural strength for concrete mixes batched with natural sand.

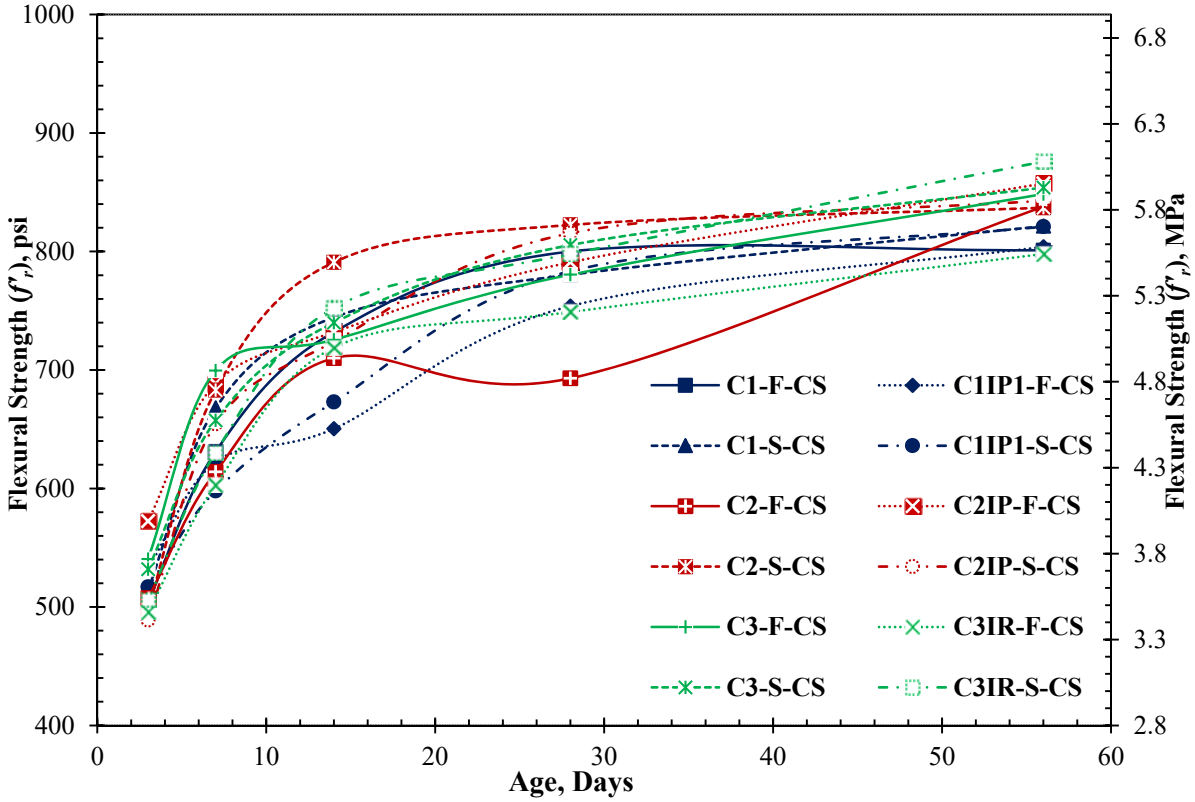

Figure 7-4. Flexural strength for concrete mixes batched with combined sand.

8. EXPERIMENTAL TEST RESULTS FOR DURABILITY OF HARDENED CONCRETE

The hardened properties of concrete include air void system parameters, freeze/thaw tests, rapid chloride penetration resistance (coulomb), water penetration (DIN 1048), and chloride ion penetration (salt ponding).

8.1. Hardened Air Void System Parameters

The hardened entrained air results are presented in Table 8-1 and Table 8-2 for concrete mixes batched with natural and combined sand, respectively. The tables show a summary of the air parameters which included the fresh air content, entrained air content, void per inch (frequency), specific surface, and spacing factor. The highlighted cells indicate that the specimen failed to meet the minimum or maximum requirements set for each parameter.

For mixes batched with natural sand, the amount of air voids in the hardened concrete ranged from 5.66 to 7.92%. The void frequency, spacing factor, and specific surface ranged from 6.1 to 16.82, 0.0036 to 0.0097, and 431 to 955, respectively. For mixes batched with combined sand, the amount of air voids in the hardened concrete ranged from 5.99 to 8.05%. The void frequency, spacing factor, and specific surface ranged from 6.14 to 14.89, 0.0041 to 0.0096, and 367 to 857, respectively. These results indicates that the hardened air content for all the concrete mixes were within the desired range of air between 5 and 8%. Some of the concrete specimens failed to meet the minimum recommended requirements the void frequency and specific surface. However, the spacing factor for all the specimens was less than the maximum recommended target of 0.01. It should be noted that the spacing factor was

observed to give a better indication of the freeze/thaw resistance for concrete than the void frequency and specific surface. This observation is explained in more details in Chapter 9.

Table 8-1. Air Void System Parameters of Hardened Concrete for Mixes with Natural Sand

Mix No.		Fresh Air Content, %	Hardened Air Parameters (ASTM C457)			
			Air Content, %	Void frequency, per inch. (> 8)	Specific Surface, 1/in (> 500)	Spacing Factor, in. (< 0.01)
Mixes batched with natural sand	C1-F-NS	7.2	7.04	16.82	955	0.0036
	C1IP1-F-NS	7.1	7.26	15.03	828	0.0040
	C1IP2-F-NS	7	6.13	6.88	449	0.0088
	C1-S-NS	7.1	7.47	13.41	718	0.0044
	C1IP1-S-NS	7.1	7.92	16.26	822	0.0036
	C1IP2-S-NS	6.7	5.66	6.10	431	0.0097
	C2-F-NS	6.7	6.76	7.58	449	0.0080
	C2IP-F-NS	6.7	6.92	9.41	544	0.0064
	C2-S-NS	6.8	5.90	6.48	439	0.0091
	C2IP-S-NS	6.6	6.72	7.61	453	0.0078
	C3-F-NS	7.2	8.09	12.03	595	0.0050
	C3IR-F-NS	7.4	6.91	12.58	728	0.0048
	C3-S-NS	7.3	7.13	11.70	656	0.0051
	C3IR-S-NS	7.3	7.90	10.25	519	0.0058

1 in. = 25.4 mm

Table 8-2. Air Void System Parameters of Hardened Concrete for Mixes with Combined Sand

Mix No.		Fresh Air Content, %	Hardened Air Parameters (ASTM C457)			
			Air Content, %	Void frequency, per inch. (> 8)	Specific Surface, 1/in (> 500)	Spacing Factor, in. (< 0.01)
Mixes batched with combined sand	C1-F-CS	6.9	7.06	7.62	432	0.0079
	C1IP1-F-CS	7.1	6.99	10.33	591	0.0058
	C1-S-CS	7.5	6.34	6.14	387	0.0096
	C1IP1-S-CS	6.9	5.99	6.97	465	0.0085
	C2-F-CS	6.8	7.39	6.78	367	0.0089
	C2IP-F-CS	7.2	6.46	11.38	704	0.0053
	C2-S-CS	7.8	7.21	8.78	487	0.0067
	C2IP-S-CS	6.8	6.99	10.85	621	0.0055
	C3-F-CS	7.3	6.95	14.89	857	0.0041
	C3IR-F-CS	7.4	6.80	14.01	825	0.0043
	C3-S-CS	7.2	6.91	13.97	809	0.0042
	C3IR-S-CS	7.2	8.05	11.70	582	0.0051

1 in. = 25.4 mm

8.2. Freeze/Thaw Performance of Concrete

Table 8-3 and Table 8-4 present a summary of the hardened air content and the test results for the durability factor (*DF*) after 300 cycles of freezing and thawing for the twenty six concrete mixes batched with natural sand and combined sand. The performance of concrete specimens subjected to freeze/thaw cycles were assessed by two types of deteriorations: The internal micro cracking observed by the *DF* after 300 cycles and the surface scaling examined by visual

inspection. The hardened air content for all the mixes ranged from 5.66% for mix C1IP2-S-NS to 8.05% for mix C3IR-F-CS. This amount of air is considered adequate for the freeze/thaw resistance. However, as shown in Table 8-3 and Table 8-4, some concrete specimens failed to maintain 80% *DF* after 300 cycles of freezing and thawing. Therefore, this premature failure was investigated in Chapter 9 by testing the flexural capacity of the specimens tested for 300 cycles of freezing and thawing, and conducting additional thirty one concrete mixes for freeze/thaw test and flexural strength. The investigation revealed that these premature failures were mainly attributed to aggregate popouts.

8.2.1. Effect of Limestone, IPA, and IR addition

As shown in Table 8-3, mixes made with C1 and C2 cement source and batched with natural sand failed to pass the freeze/thaw test after 300 cycles. However, the *DF* results did not show significant difference or consistent changes between specimens of the same mix proportion and cement source with conventional cement or modified cement containing higher content of limestone and IPA. For example, the *DF* for mix C1-S-NS was higher than the *DF* for mixes C1IP1-S-NS and C1IP2-S-NS; whereas, the *DF* for mix C2IP-S-NS, which had the same mix proportion as C1-S-NS but with C2 cement source, was lower than the *DF* of its counterpart mix (C2-S-NS) and made with conventional cement. Moreover, as shown in Table 8-4, the *DF* for mixes batched with combined sand showed an inconsistent variation in performance based on the use of conventional and modified cement for C1 and C2 cement source. For example, mix C1-F-CS performed better than mix C1IP-F-CS while mix C1IP-S-CS performed better than its counterpart mix C1-S-CS.

Concrete mixes made with C3 cement source showed an excellent performance in contrast of the concrete mixes made with C1 and C2 cement. All the freeze/thaw specimens

for concrete mixes batched with natural sand and combined sand and regardless whether they were made with conventional and modified cement (1.5%) gave an excellent *DF*.

8.2.2. Effect of Class C fly ash and GGBF Slag

The use of slag or fly ash as a replacement to cement showed inconsistent variation in the *DF* results for concrete mixes made with the same cement source and batched with the same sand source. However, it was visually observed that concrete mixes with fly ash experienced more surface scaling than mixes made with slag. Therefore, for the same cement source, most of the concrete mixes made with fly ash experienced greater scaling than concrete mixes made with slag.

8.2.3. Effect of Sand Type

As shown in Table 8-3 and Table 8-4, the combined sand in concrete provided better freeze/thaw performance than natural sand. Total of 63 specimens batched with natural sand and 53 specimens batched with combined sand were tested for freeze/thaw resistance. Only 51% of the specimens batched with natural sand exceeded 80% *DF* whereas 72% of the specimens batched with combined sand exceeded the passing criteria for freeze/thaw. Moreover, concrete mixes batched with natural sand experienced higher scaling than combined sand.

Table 8-3. Summary of the Freeze/Thaw Results for Concrete Mixes batched with Natural Sand

Mix No.		Fresh Air Content, %	Hardened Air Content, %	Spacing Factor, in.	Freeze/Thaw Performance		
					No. of Specimens		Average *DF*
					Total	More than 80% *DF*	
Mixes batched with natural sand	C1-F-NS	7.2	7.04	0.0036	4	3	84.1
	C1IP1-F-NS	7.1	7.26	0.0040	4	4	89.7
	C1IP2-F-NS	7	6.13	0.0088	5	0	69.7
	C1-S-NS	7.1	7.47	0.0044	4	3	78.8
	C1IP1-S-NS	7.1	7.92	0.0036	5	1	67.1
	C1IP2-S-NS	6.7	5.66	0.0097	5	0	50.9
	C2-F-NS	6.7	6.76	0.0080	4	0	69.3
	C2IP-F-NS	6.7	6.92	0.0064	5	0	59.6
	C2-S-NS	6.8	5.90	0.0091	4	0	51.4
	C2IP-S-NS	6.6	6.72	0.0078	5	3	73.9
	C3-F-NS	7.2	8.09	0.0050	4	4	97.1
	C3IR-F-NS	7.4	6.91	0.0048	5	5	98.0
	C3-S-NS	7.3	7.13	0.0051	4	4	93.5
	C3IR-S-NS	7.3	7.90	0.0058	5	5	92.1

1 in. = 25.4 mm

Table 8-4. Summary of the Freeze/Thaw Results for Concrete Mixes batched with Combined Sand

Mix No.		Fresh Air Content, %	Hardened Air Content, %	Spacing Factor, in.	Freeze/Thaw Performance		
					No. of Specimens		Average *DF*
					Total	More than 80% *DF*	
Mixes batched with combined sand	C1-F-CS	6.9	7.06	0.0079	4	2	88.9
	C1IP1-F-CS	7.1	6.99	0.0058	5	5	66.2
	C1-S-CS	7.5	6.34	0.0096	4	0	65.7
	C1IP1-S-CS	6.9	5.99	0.0085	5	1	77.9
	C2-F-CS	6.8	7.39	0.0089	5	5	86.7
	C2IP-F-CS	7.2	6.46	0.0053	4	3	86.0
	C2-S-CS	7.8	7.21	0.0067	4	2	66.5
	C2IP-S-CS	6.8	6.99	0.0055	4	2	72.1
	C3-F-CS	7.3	6.95	0.0041	4	4	96.7
	C3IR-F-CS	7.4	6.80	0.0043	5	5	97.4
	C3-S-CS	7.2	6.91	0.0042	4	4	97.5
	C3IR-S-CS	7.2	8.05	0.0051	5	5	99.1

1 in. = 25.4 mm

8.3. Chloride Ion Concentration per Salt Ponding Test

The test results for the percent of chloride concentration are reported in Appendix D from Table D-1 to Table D-6. The chloride ion concertation was measured at five different depths, from 0 – ½ in. (0 – 12.5 mm) to 2 – 2 ½ in. (50 – 62.5 mm). Both the acid soluble and water soluble methods were measured. The acid-soluble chloride represents the total chloride content in concrete; whereas, water-soluble chloride represents the chloride ions that could be leached

by water such as the sodium chloride. Table D-1 through Table D-3 report the chloride concentration results for acid- and water-soluble for concrete mixes batched with natural sand. These tables include the test results at 90, 180, and 360 days salt ponding for mixes made with C1 (Table D-1), C2 (Table D-2), and C3 (Table D-3) cement, respectively. Because of time restriction, chloride concentration results for mixes C1-F-NS, C1IP1-F-NS, C1-S-NS, and C1IP1-S-NS were measured at 315 days rather than at 360 days of salt ponding. Table D-4 through Table D-6 report the chloride concentration results for acid- and water-soluble for concrete mixes batched with combined sand. These tables include the test results at 90, 180, and 360 days salt ponding for mixes made with C1 (Table D-4), C2 (Table D-5), and C3 (Table D-6) cement, respectively.

The above-mentioned tables show the effect of the duration of salt ponding on chloride concentration and penetration depth. At 90 and 180 days of salt ponding, the majority of mixes showed significant chloride change up to 1 in. in depth, followed by a constant chloride concentration at lower depth ranging between 0.03 – 0.06%, which is observed as the initial chloride level in concrete. At 360 days of salt ponding, the majority of mixes showed chloride penetration change up to 1½ in. (38 mm) in depth, followed by a constant chloride concentration at lower levels.

Studies on the chloride penetration in concrete showed varying results regarding the addition of limestone and IPA to cement in concrete. Some studies indicate increasing chloride penetration with increasing limestone content while others show inconsistent change with limestone and IPA addition.

8.3.1. Effect of Limestone and Inorganic Processing, and Insoluble Residue

Figure 8-1 to Figure 8-3 show the acid-soluble chloride versus depth in concrete for mixes batched with natural sand. Figure 8-1 shows that the percentage of chloride in mixes made with C1 cement at ½ – 1 in. (12.5 – 25 mm) depth were lowest for Mix C1IP1-F-NS (0.092%) at 90 days, Mix C1IP1-S-NS (0.136%) at 180 days, Mix C1-F-NS (0.18%) at 315 days, and Mix C1-S-NS (0.251%) at 360 days, but were highest for Mix C1-F-NS (0.168% and 0.39%) at 90 and 360 days, Mix C1-S-NS at 180 days (0.216%) and 315 days (0.295%).

Figure 8-2 shows that the percentage of chloride in mixes made with C2 cement at ½ – 1 in. (12.5 – 25 mm) depth were lowest for Mix C2IP-S-NS (0.083%) at 90 days and Mix C2-S-NS (0.083% and 0.177%) at 180 and 360 days and highest for Mix C2-F-NS (0.121%) at 90 days, Mix C2IP-F-NS (0.13%) at 180, and Mix C2IP-S-NS (0.331%) at 360 days. Figure 8-3 shows that the percentage of chloride in mixes made with C3 cement at ½ – 1 in. (12.5 – 25 mm) depth were lowest for Mix C3IR-F-NS (0.1% and 0.142%) at 90 and 180 days, and Mix C3-F-NS (0.174%) at 360 days, but were highest for Mix C3IR-S-NS (0.127% and 0.208%) at 90 and 180 days, and Mix C3-S-NS (0.275%) at 360 days. These results indicate the inconsistency of chloride concentration at different depths in concrete mixes made with modified cement either with IPA or higher content of IR in comparison with the conventional cement when batched with natural sand.

Figure 8-4 to Figure 8-6 show the acid-soluble chloride versus depth in concrete for mixes batched with combined sand. Figure 8-4 shows that the percentage of chloride in mixes made with C1 cement at ½ – 1 in. (12.5 – 25 mm) depth were lowest for Mix C1IP1-S-CS (0.139% and 0.083%) at 90 and 180 days, and Mix C1IP1-F-CS (0.213%) at 360 days, but were highest for Mix C1-F-CS (0.154% and 0.207%) at 90 and 180, and Mix C1-S-CS

(0.278%) at 360 days. Similarly, the inconsistent variation in the chloride levels in concrete was also observed in mixes made with C2 and C3 cement, as shown in Figure 8-5 and Figure 8-6, respectively. The inconsistency of these results is yet another indication that limestone and IPA, and the IR levels in cement have a negligible effect on chloride penetration in concrete mixes batched with combined sand.

Therefore, adding modified cement to the concrete mixes measured for chloride concentration did not result in any significant variations compared to conventional cement.

8.3.2. Effect of Fly Ash or Slag (SCMs)

The results failed to indicate a significant variation or consistent trend in the chloride penetration at 90, 180, and 360 days between mixes with same cement source, but blended with Class C fly ash or GGBF slag. The comparison was based on concrete mixes of the same cement source and fine aggregate, but made with slag or fly ash. This shows that the GGBF slag have similar performance to Class C fly ash in contrary to what was observed by Burris and Riding, (2014) who reported better performance against chloride penetration for concrete mixes with Class C fly ash.

8.3.3. Effect of Fine Aggregate Sources (Natural or Combined Sand)

Similarly, no major difference was observed in chloride levels between concrete mixes batched with natural sand and combined sand. The comparison was based on concrete mixes made with same cement source and cementitious combination, but batched with either natural or combined sand. The acid-soluble and water-soluble results showed slightly lower chloride concentration for concrete mixes batched with natural sand because the initial chloride levels in concrete mixes batched with combined sand (~0.06%) were higher than natural sand (~0.04%).

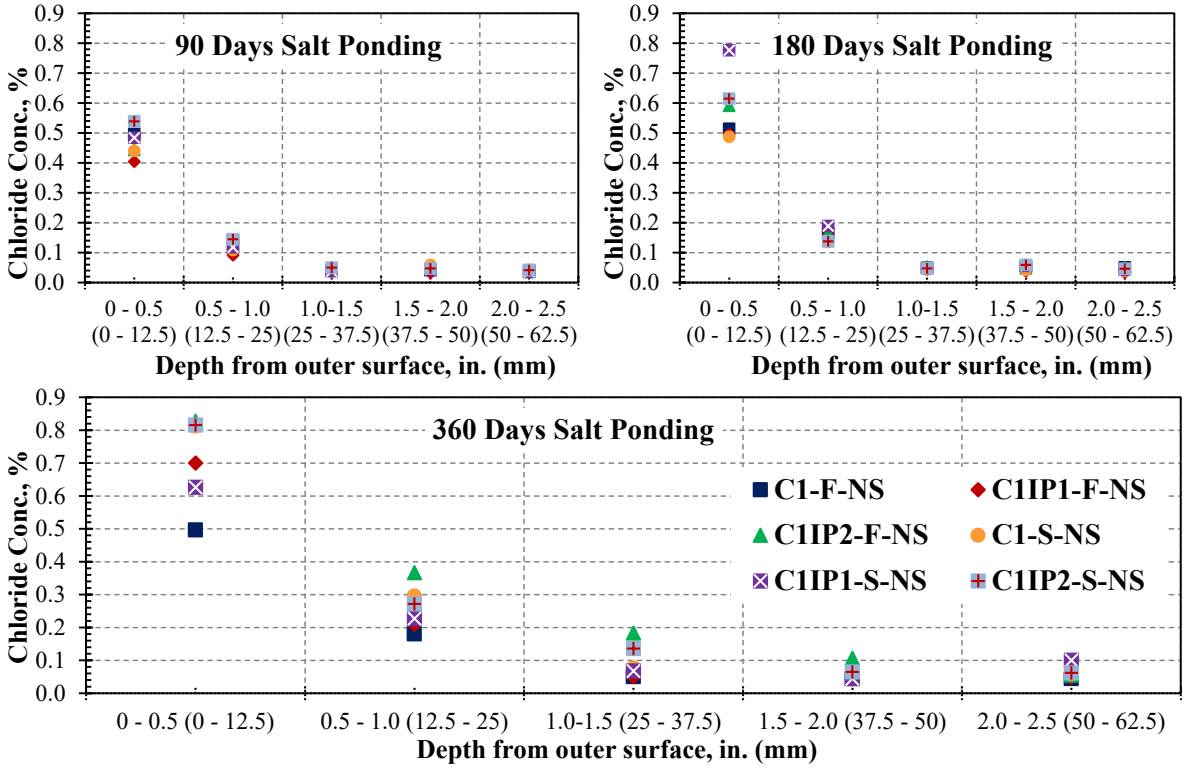

Figure 8-1. Acid-soluble chloride for mixes with C1 and batched with natural sand

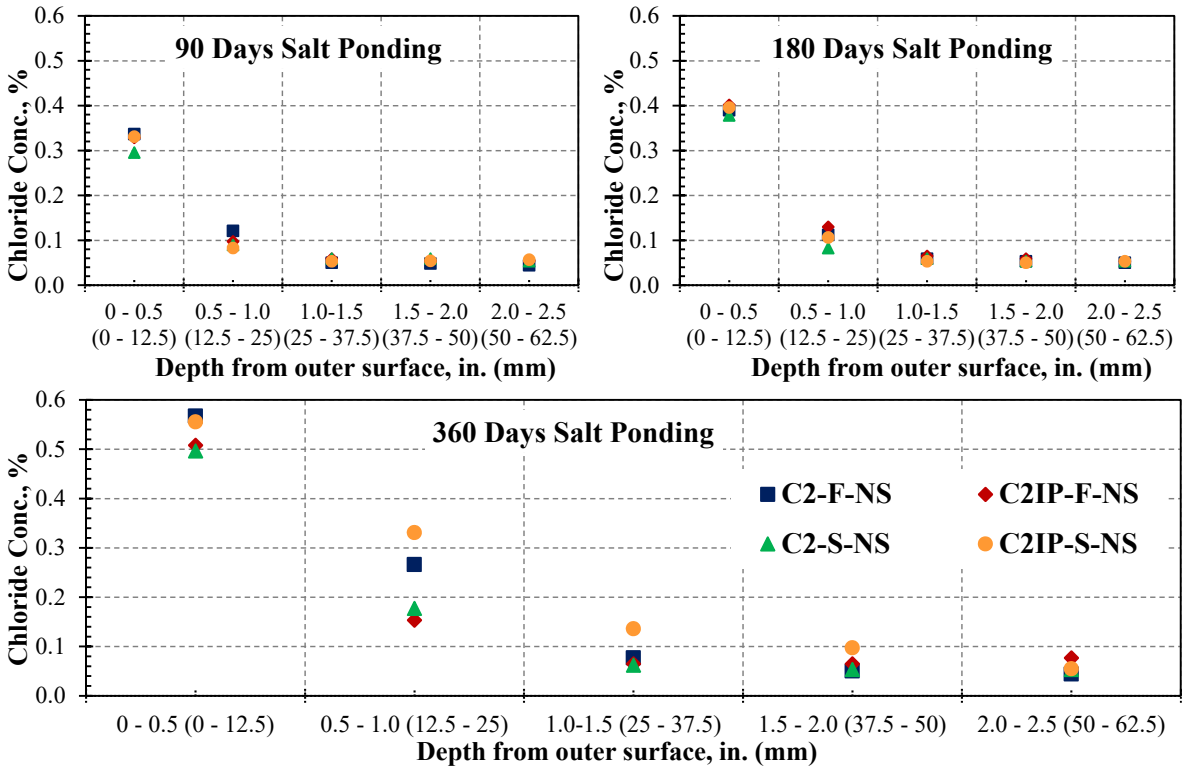

Figure 8-2. Acid-soluble chloride for mixes with C2 and batched with natural sand

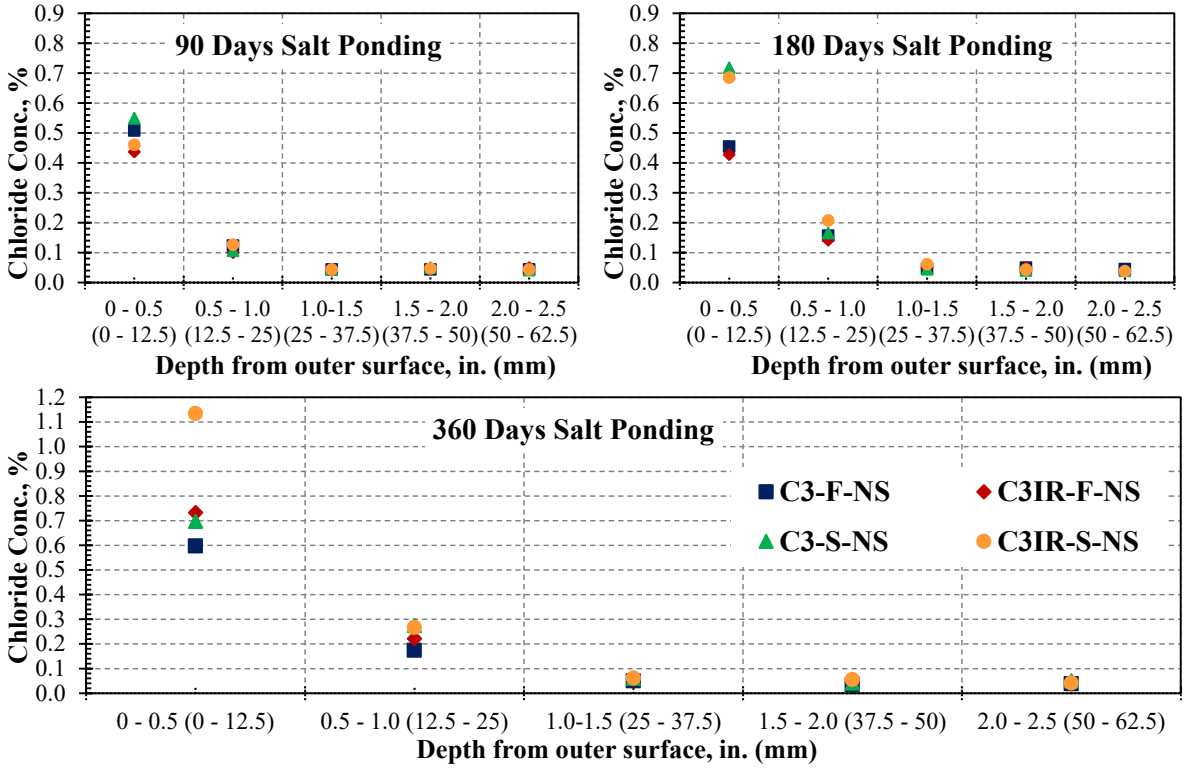

Figure 8-3. Acid-soluble chloride for mixes with C3 and batched with natural sand

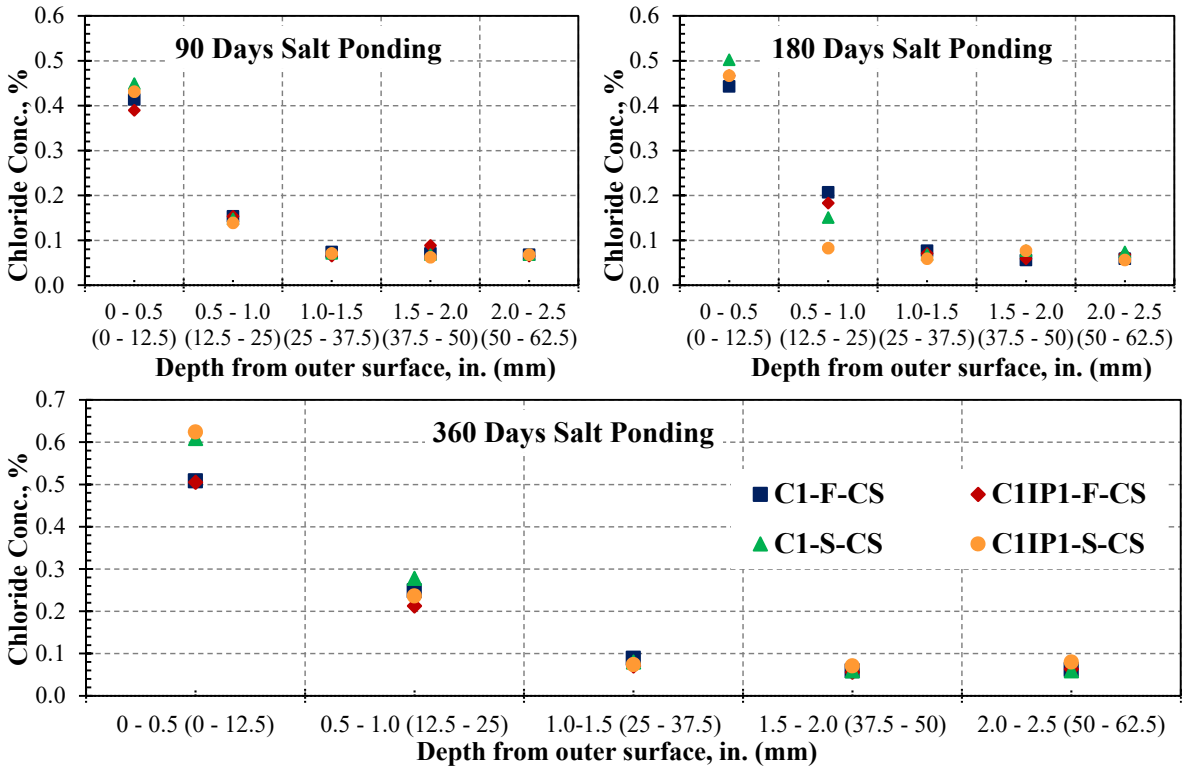

Figure 8-4. Acid-soluble chloride for mixes with C1 and batched with combined sand

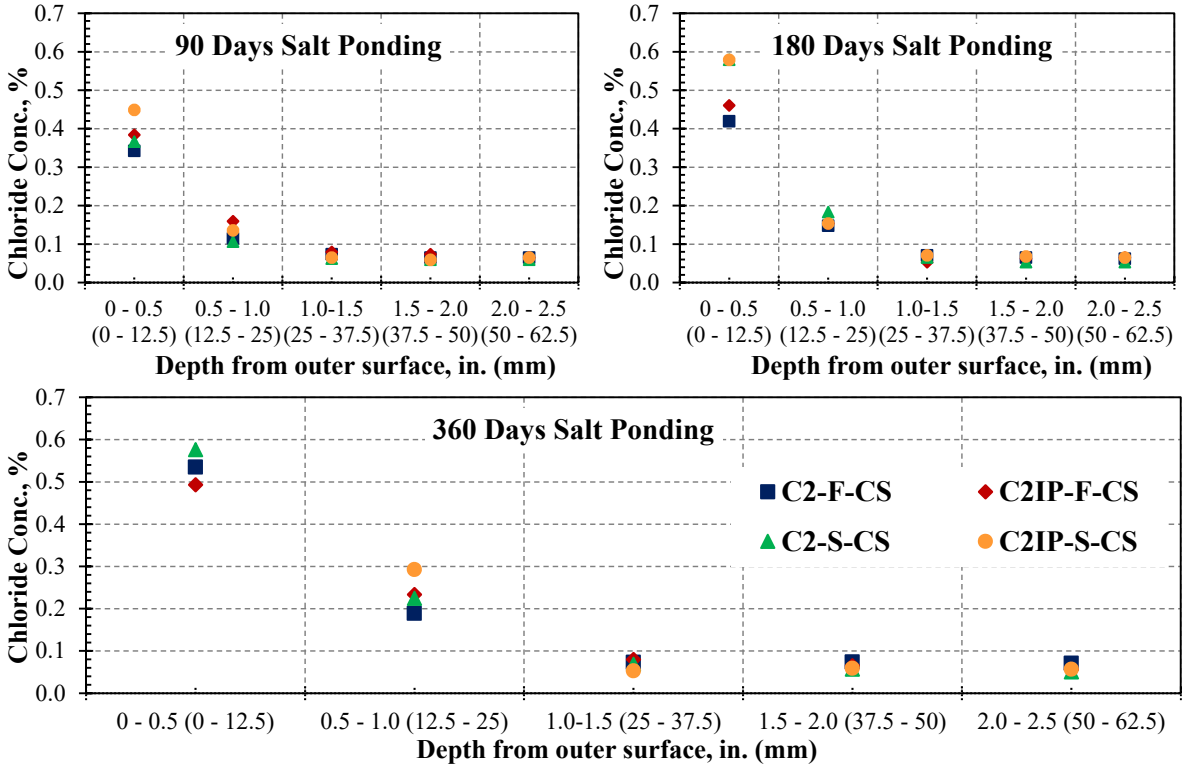

Figure 8-5. Acid-soluble chloride for mixes with C2 and batched with combined sand

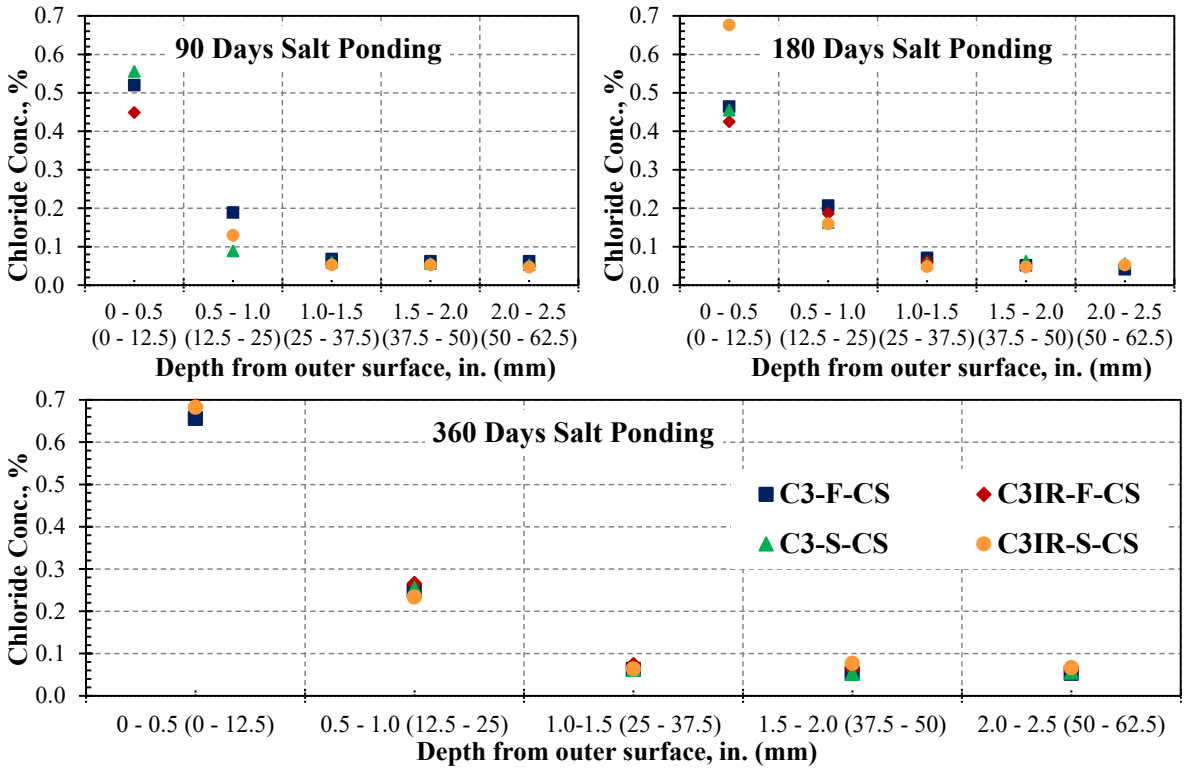

Figure 8-6. Acid-soluble chloride for mixes with C3 and batched with combined sand

8.4. Water Penetration Test Results per DIN 1048

The water penetration results per each specimen for each concrete mix is shown in Appendix E; Table E-1 shows the maximum water penetration depth (x_{max}) for concrete mixes batched with natural sand and Table E-2 shows the results for concrete mixes batched with combined sand. Figure 8-7 and Figure 8-8 present the average of the maximum water penetration depth for concrete mixes batched with natural sand and combined sand, respectively, and measured at 56, 180, and 360 days of age. The results in both figures showed inconsistent variation in the depth of water penetration in mixes with conventional and modified cement.

As expected, the penetration depth decreased with the increase in concrete age at 180 and 360 days. Hedegaard and Hansen (1992) stated that concrete is considered as watertight for all practical purposes when the x_{max} is less than 50 mm (2 in.). Walz (1968) reached the same conclusion after more than 50 years of experience in the water penetration test per DIN 1048 in Germany. All readings indicated less than 50 mm (2 in.) maximum penetration depth at 56 days which ranged from 25 mm (1 in.) for C3-S-CS to 40 mm (1.6 in.) for C2-F-CS and C2IP-S-CS. The results have shown inconsistent variation between conventional cement and cement with IPA and increased IR content. For example, C3-S-NS, batched with natural sand, had higher x_{max} than its counterpart C3IR-S-NS, while the same mixture but batched with combined sand (C3-S-CS) resulted in lower penetration depth than C3IR-S-CS. Similarly, the Class C fly ash did not reveal significant difference in the x_{max} in comparison to GGBF slag. Moreover, the sand type did not show any influence on the penetration depth as it is apparent between mixes batched with natural and combined sand and made with same cementitious combination.

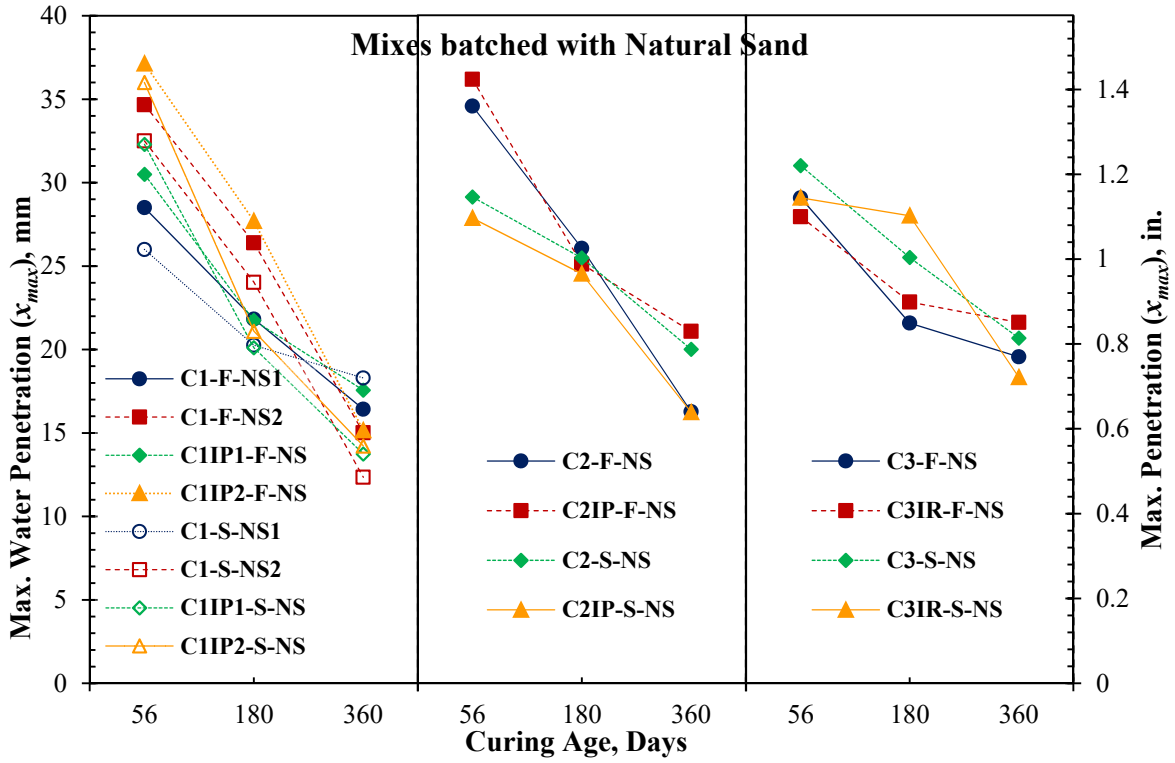

Figure 8-7. Maximum water penetration (x_{max}) results for mixes batched with natural sand.

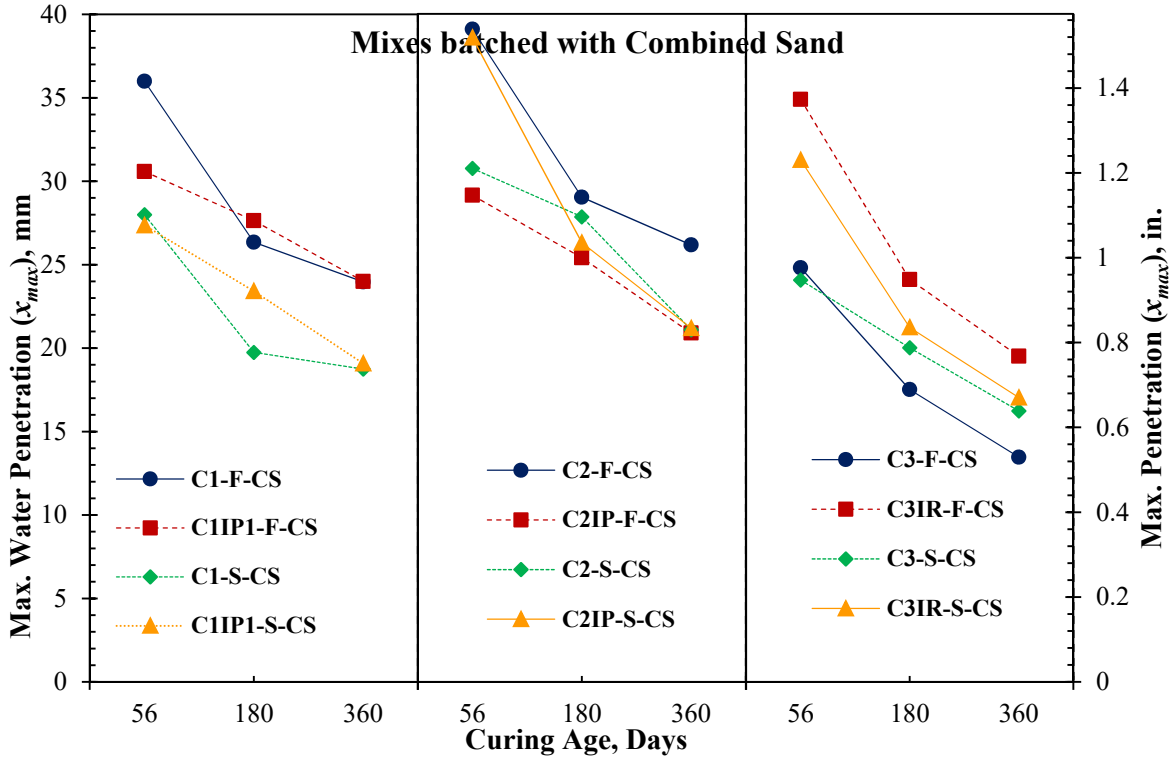

Figure 8-8. Maximum water penetration (x_{max}) results for mixes batched with combined sand.

8.5. Rapid Chloride Penetration Test Results

The RCP test was conducted after 56, 180, and 360 days of age for every concrete mix. Three to four specimens were tested for each period and the average of the specimens was recorded. The Coulomb values of each specimen at all periods are presented in Appendix F; Table F-1 shows the values for concrete mixes batched with natural sand and Table F-2 shows the values for concrete mixes batched with combined sand. A summary of the average RCP results for concrete mixes batched with natural sand and combined sand is shown in Figure 8-9 and Figure 8-10, respectively.

Table 5-3 provides a correlation between the level of chloride ion penetration and the charge passed. The table, copied from ASTM C1202, is used as a base for determining the validity of the concrete mix against chloride penetration. The average charge for the twenty eight concrete mixes ranged between low to moderate at 56 days, very low to low at 180 days, and very low at 360 days, with few exceptions (see Table F-1 and Table F-2).

As expected, the charge decreased with the increase in concrete age with significant reductions at 180 and 360 days for all the mixes. This is attributed to the pozzolanic effect due to the addition of Class C fly ash or GGBF slag that becomes more pronounced at later age of the concrete. It is clear from the data in Figure 8-9 and Figure 8-10 that the inclusion of IPA and higher content of IR had no significant impact on the results. Few mixtures such as C2IP-F-NS, C3IR-F-CS, gave slightly higher results than their counterparts (C2-F-NS and C3-F-CS) at 56 and 180 days, but revealed similar results at 360 days. The Class C fly ash did not reveal any notable influence on reducing the charge passed in comparison to GGBF slag at all ages. The comparison was based on concrete mixtures with same cement source and sand type. The

sand type did not show any influence on the results as it is apparent between mixes batched with natural and combined sand and made with same cementitious combination.

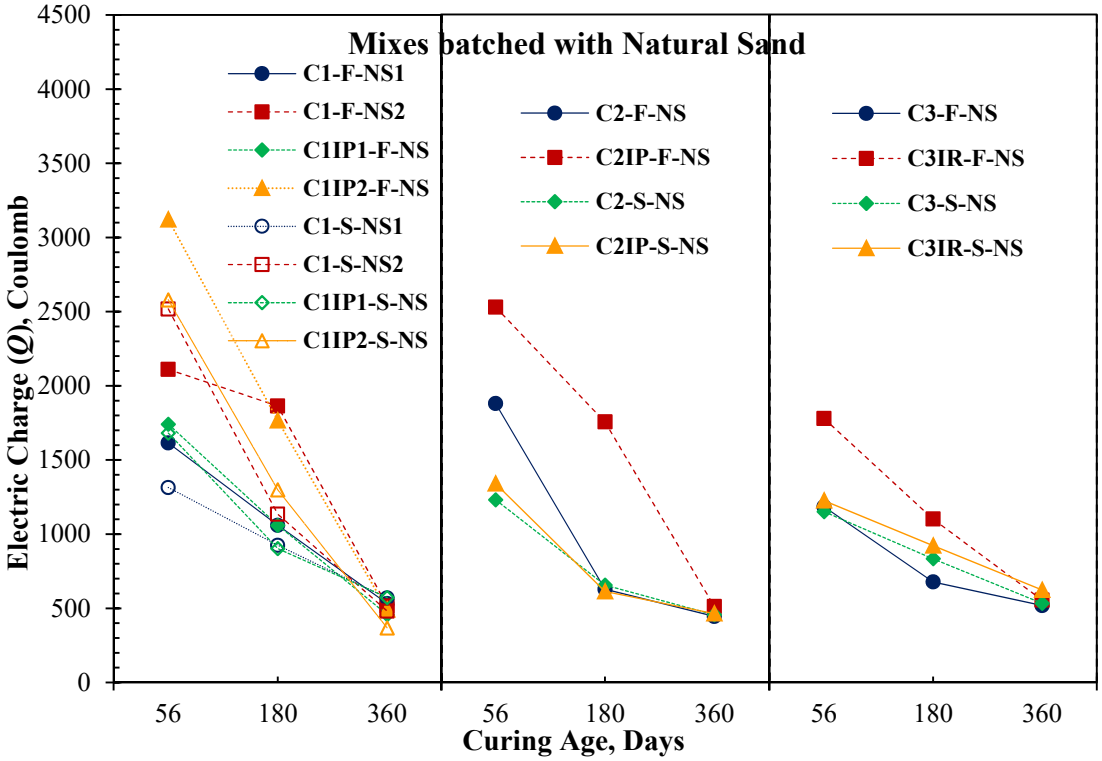

Figure 8-9. Coulomb charge passed per RCP test for mixes batched with natural sand.

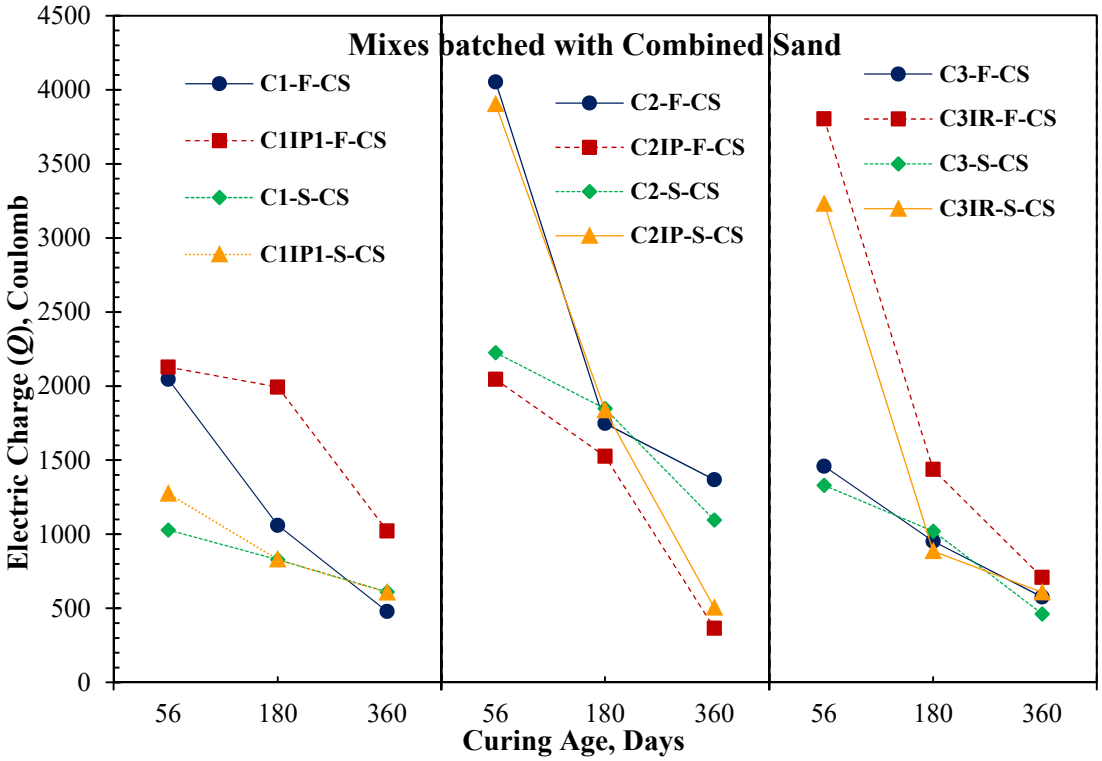

Figure 8-10. Coulomb charge passed per RCP test for mixes batched with combined sand.

9. EVALUATION OF THE FREEZE/THAW PERFORMANCE OF CONCRETE: A CASE STUDY

9.1. Introduction

Deterioration of concrete under freeze/thaw cycles is related to the expansion of water inside the concrete. As water freezes, it expands in volume creating excessive pressure inside the capillary pores and causing them to expand and eventually crack. The freeze/thaw damage in concrete is a very complicated phenomenon and, till today, there is no well-defined theory that explains its mechanism yet. Many theories have been proposed but only two gained wide acceptance: hydraulic pressure theory (Powers, 1945) and osmotic pressure (Powers and Helmuth, 1953) or combination of both. Powers (1945) explained the hydraulic pressure theory by stating that when the water freezes it accumulates hydraulic pressures by preventing unfrozen water to flow in the capillary pores of the cement paste. Powers and Helmuth (1953) explain the osmotic pressure theory such that when water freezes the water molecules move from the gel to the capillary pores through diffusion along concentration gradients (theory of osmosis). Both proposed theories are essential to understand the role of entrained air voids to resist freeze/thaw attacks.

The entrained air void system is the most commonly accepted measure for freeze/thaw resistance. The amount, type, shape, size, and distribution of the entrained air in concrete are the main factors contributing to the resistance of concrete against repeated cycles of freezing and thawing. The amount/volume of entrained air is essential for freeze/thaw resistance. However, it is not a solely sufficient measure for freeze/thaw resistance, but rather it is how well-distributed the air voids within the cement paste. ASTM C457 describes these

characteristics in terms of the entrained air content, spacing factor, void frequency, and specific surface. These parameters are considered the most reliable characteristics for freeze/thaw resistance indication in concrete. However, the parameters associated with this characterization and the results do not always reflect the observed field performance nor do they consider the possible effects on other concrete properties that can be influenced by many factors which include but not limited to: (1) concrete mix components such as cement type and composition, supplementary cementitious materials, type of chemical admixture, aggregate type and quality, and aggregate size; (2) practices used for proportioning, mixing, and placing the concrete mix; and (3) field conditions.

This chapter investigates the cause of a series of premature failures occurred in the freeze/thaw specimens tested in accordance with ASTM C666, Procedure A when the concrete mixes had sufficient entrained air content. Also, the effect of lignosulfonate based water reducing admixture on the fresh and hardened properties of air content was examined.

9.2. Experimental Program

In addition to the twenty six concrete mixes that were made to investigate the effect of limestone and IPA and the increase in IR content, thirty one concrete mixes were added in attempt to investigate series of premature failures in the freeze/thaw specimens that were mainly attributed to aggregate popout.

The cementitious content was 535 lbs/yd^3 (317 Kg/m^3) for the twenty six concrete mixes, which is the minimum amount required for central mixing by the Illinois Department of Transportation (IDOT) for concrete pavement and bridge decks. For the rest of the mixes, same mortar factor, coarse to fine aggregate ratio, and same cementitious combination was

used with cementitious content of 535 lbs/yd^3 (317 Kg/m^3) for twenty three mixes and 600 lbs/yd^3 (356 Kg/m^3) for eight mixes.

From each concrete mix, five 3 × 4 × 16 in. (75 × 100 × 400 mm) concrete prisms and six 6 × 12 in. (150 × 300 mm) concrete cylinders were cast. The experimental program included conducting the freeze/thaw test per ASTM C666, the damage assessment test for freeze/thaw per ASTM C215, the hardened air entrained test per ASTM C457, and the compressive strength measured at 360 days of age. In addition the four point bending test was conducted on the freeze/thaw specimens to measure their flexural capacity after 300 cycles of freezing and thawing.

9.3. Discussion and Correlation

This section includes investigating the relationship between the compressive strength and the fresh and hardened air parameters of concrete, the relationship between the Durability Factor (*DF*) and the hardened air parameters, and the relationship between the flexural capacities of the freeze/thaw specimens with their corresponding dynamic modulus (E_D) measured based on the resonant frequency method.

9.3.1. Fresh and Hardened Air Content versus Compressive Strength Relationship

The compressive strength for the fifty seven concrete mixes was tested at 360 days of age. The strength results ranged from 5500 to 8100 psi (38 MPa to 56 MPa). The fresh air content for all the mixes ranged from 6.5% to 8.1% while the hardened air content measured according to ASTM C457, linear traverse method, ranged from 3.9% and 8.3%. Accordingly, there was quite some variation between the fresh and hardened air content. To investigate this variation, the fresh and hardened air contents were correlated with the compressive strength as shown in Figure 9-1. Inspection of Figure 9-1 revealed that the hardened air content correlated well with

the compressive strength with a correlation coefficient (R^2) of 0.73 and based on the fitting trendline, the compressive strength roughly decreased at a rate of 600 psi (4.1 MPa) for every 1% increase in the air content. In contrary, there was a very weak correlation and inconsistent trend between the compressive strength and the fresh air content. This indicates that some of the concrete mixes experienced high rate of air loss. Further investigation revealed that the use of lignosulfonate based water reducing admixture had major contribution to the air loss in concrete. As shown in Figure 9-2, the difference between the fresh and hardened air content increased with the increase in the use of lignosulfonate WRA. When the amount of lignosulfonate WRA used was less than 10 US fl. Oz/yd^3 (0.5 L/m^3) of concrete, the difference in the air content did not increase beyond 1.0% but as the WRA addition increased the rate of air instability increased and reached more than 3% between the fresh and the hardened air when more than 40 US fl. Oz/yd^3 (2.0 L/m^3) WRA was added. This air instability at the fresh stage in concrete is explained through the effect between the lignosulfonate based WRA and the vinsol resin based AEA. This reaction enhanced the air bubbles, but it increased the instability of air content in the mix and the variation in the rate of air loss.

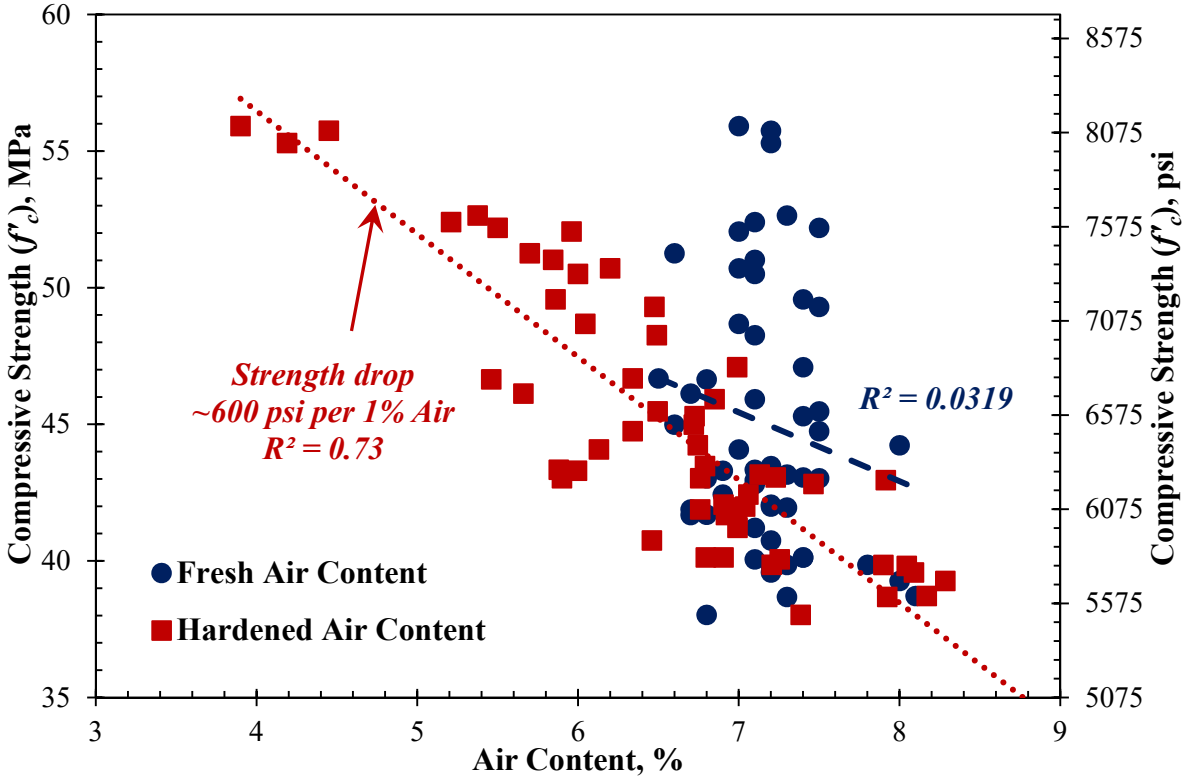

Figure 9-1. Relationship between compressive strength and air content.

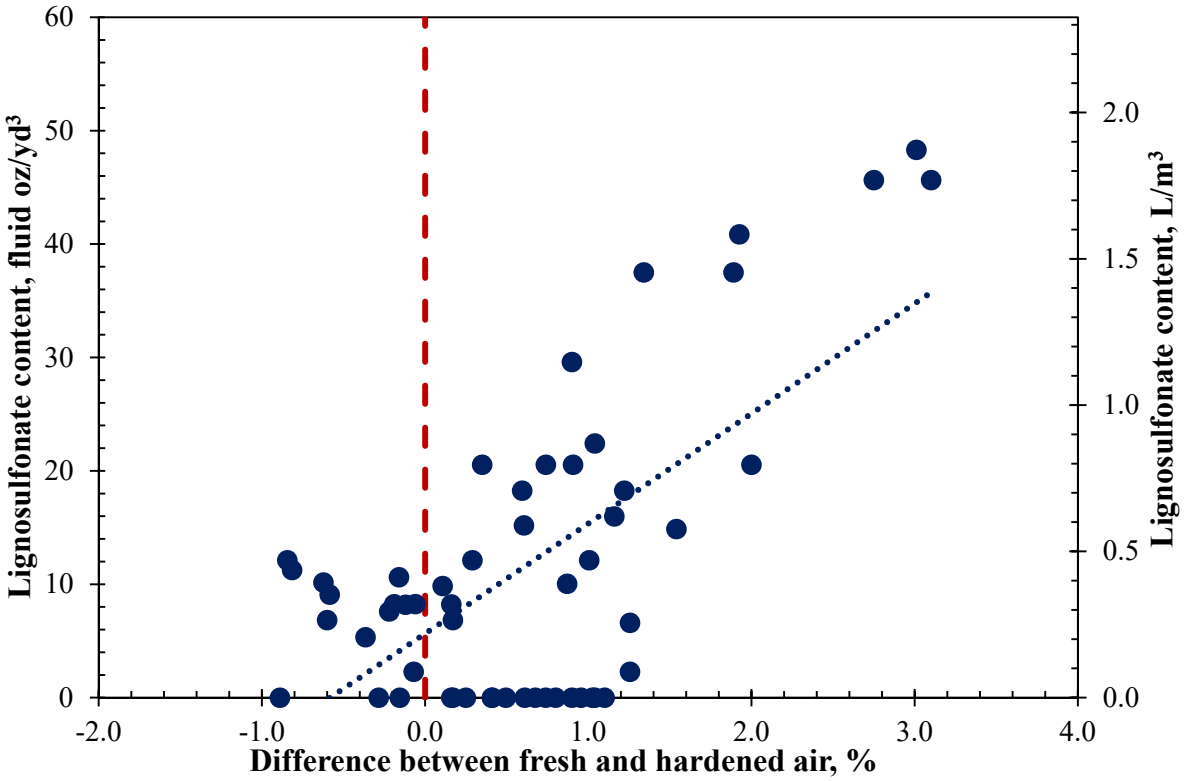

Figure 9-2. Effect of lignosulfonate based WRA on the fresh and hardened air content.

9.3.2. Durability Factor versus Hardened Air Parameters

The concrete resistance to freeze/thaw is directly related to the entrained air content and their distribution in concrete. Therefore, the hardened air parameters per ASTM C457 were correlated with the *DF* of concrete prisms tested for 300 cycles of freeze/thaw for the fifty seven concrete mixes as shown in Figure 9-3. Inspection of Figure 9-3, revealed that there is an inconsistent trend between the *DF* on one hand and the hardened air content, spacing factor, void frequency, and specific surface on the other hand. Some of the specimens experienced very low *DF* even though their hardened air parameters were adequate to resist the hostility of freezing and thawing.

A visual inspection was performed to characterize the damage in the concrete freeze/thaw specimens to further understand the inconsistency in the *DF* versus the hardened air parameters. It was concluded that specimens that failed to maintain good *DF* experienced failure in the coarse aggregate rather than the cement paste as shown in Figure 9-4. Figure 9-4, shows typical aggregate popout in concrete specimens that had adequate air content but with very low *DF*. Further investigation of the aggregate popouts revealed that these failures were attributed to the presence of small quantities (less than 5%) of two main types of particles in the coarse aggregate in the form of chert and calcareous ironstone. These particles were distinguished as the source of expansion and severe cracking and deterioration in the freeze/thaw concrete prisms.

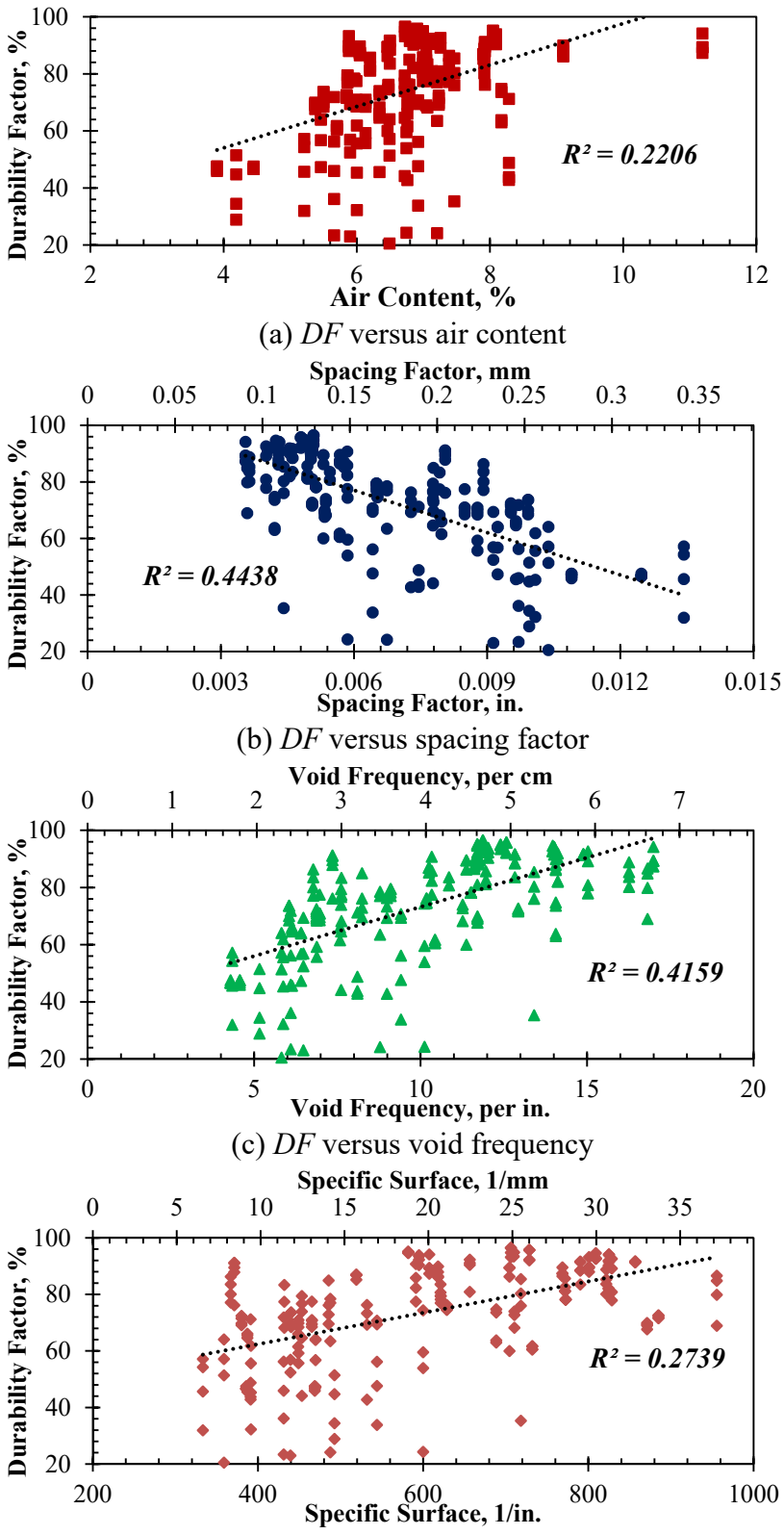

(a) *DF* versus air content

(b) *DF* versus spacing factor

(c) *DF* versus void frequency

(d) *DF* versus specific surface

Figure 9-3. Relationship between the Durability Factor (*DF*) and the hardened air parameters of for all the freeze/thaw specimens

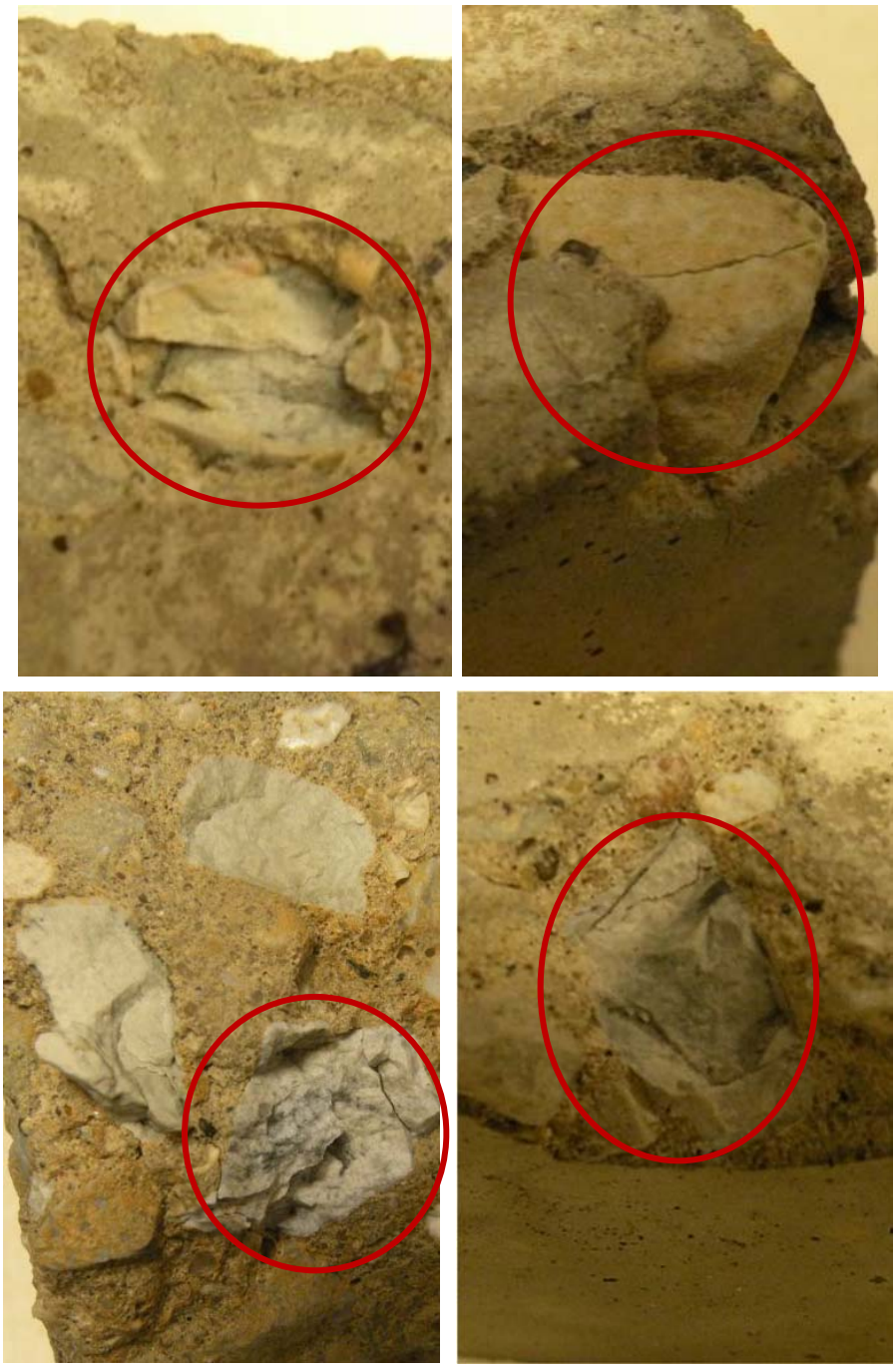

Figure 9-4. Typical aggregate popout in Freeze/thaw specimens

In an attempt to validate the results, the freeze/thaw specimens were sorted out into two categories. The first category included all the specimens that did not experience or show signs of aggregate failure and the second category included all the specimens that experienced

aggregate failure. Then the *DF* were correlated with the hardened air parameters based on the two categories as shown in Figure 9-5. Inspection of Figure 9-5 revealed that there was an acceptable correlation between the DF and hardened air parameters for specimens that did not show signs of aggregate failure, whereas, the results were highly scattered for specimens with aggregate failure. In addition, most of the specimens with aggregate failure performed poorly against freeze/thaw although their hardened air parameters were presumably above the minimum requirements for air content and below the maximum recommended limit for spacing factor.

The *DF* and hardened air parameters relationship was quite interesting for specimens without signs of aggregate failure. As shown in Figure 9-5(a), the *DF* ranged from 45 to 97 for concrete mixes with air content between 5% and 8%. This indicates that some of the specimens with adequate air content had a poor distribution of the air bubbles. As shown in Figure 9-5(b) and (c) a better correlation is rendered for the *DF* with the spacing factor and void frequency than the air content while being more pronounced for the spacing factor. This relationship emphasizes on the importance of the spacing factor as the most reliable measure for qualifying the freeze/thaw performance of concrete. The specific surface relationship with *DF*, however, was less consistent than the other hardened air parameters as it was shown that some of the freeze/thaw specimens showed excellent performance with a specific surface as low as 370 in^{-1} while other specimens failed to maintain adequate *DF* with specific surface as high as 870 in^{-1} (Figure 9-5d).

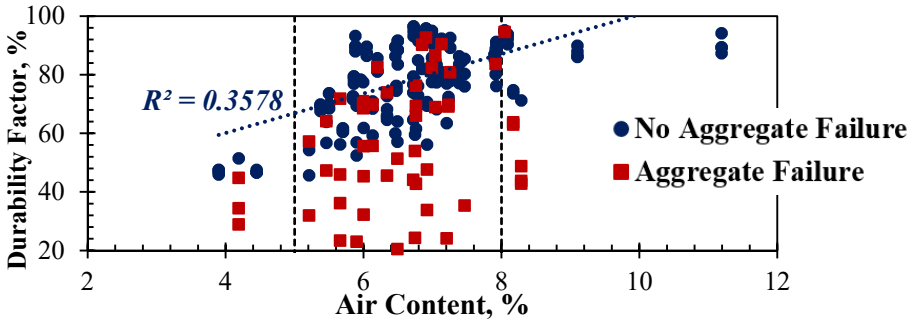

(a) *DF* versus air content

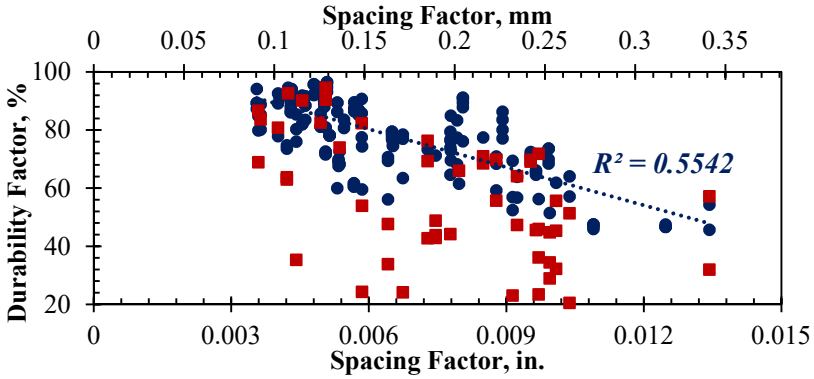

(b) *DF* versus spacing factor

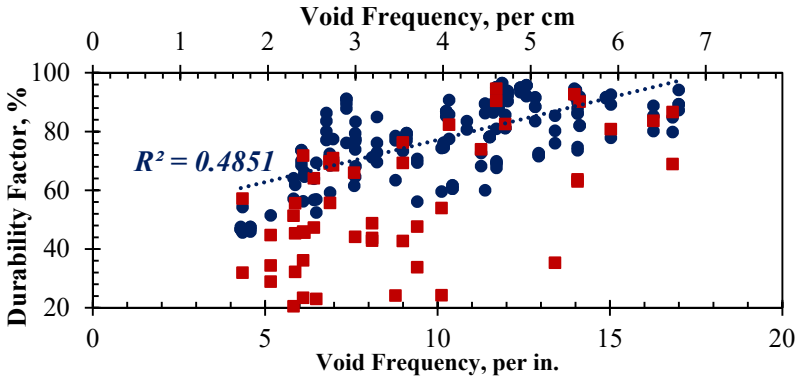

(c) *DF* versus void frequency

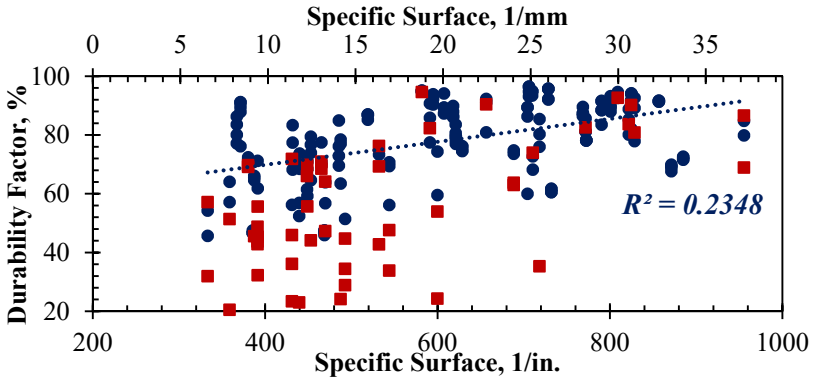

(d) *DF* versus specific surface

Figure 9-5. Durability Factor (*DF*) versus hardened air parameters for freeze/thaw specimens with and without signs of aggregate failure.

9.3.3. Dynamic Modulus versus Flexural Strength Relationship

Further investigation included testing the flexural capacity of freeze/thaw specimens and correlate them with their dynamic modulus of elasticity E_D measured at the 300th freeze/thaw cycle. Total of 225 freeze/thaw specimens for the fifty seven concrete mixes were tested in third point bending mode to measure the flexural capacity. Figure 9-6, shows the flexural strength of the concrete prisms versus their E_D values. An exponential best fitting curve was applied and it revealed that there exist a relationship between the flexural strength and the E_D. However this relationship is observed to be poor (R^2 = 0.49) owing to inconsistent trend between the flexural strength and E_D for some of the freeze/thaw specimens.

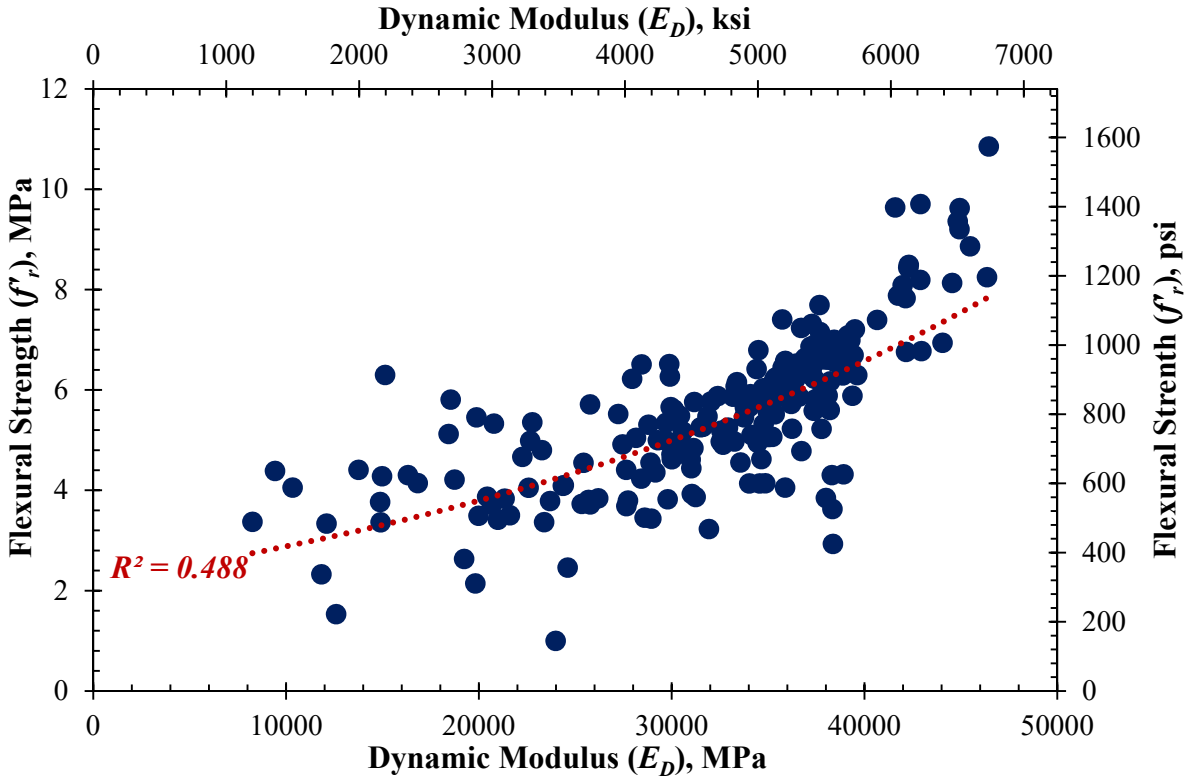

Figure 9-6. Relationship between the flexural strength (f'_r) and dynamic modulus (E_D) for all concrete freeze/thaw specimens

To better understand this inconsistency, specimens that were classified with aggregate popouts were again sorted separately and the flexural strength versus E_D relation were plotted for

specimens without signs of aggregate failures or with aggregate failures as shown in Figure 9-7(a) and (b), respectively. Of the 225 specimens tested for flexure, 50 specimens were classified with aggregate popouts. As shown in Figure 9-7(a), there exist a strong correlation (R^2 = 0.83) between the flexural strength and E_D for specimens that did not show signs of aggregate failure. However, Figure 9-7(b) showed highly scattered results for specimens with aggregate popouts. Although the strength characteristics of concrete are directly related to its dynamic modulus, this inconsistency is attributed to two factors: (1) the localized failure in the specimens due to aggregate popout tend to reduce the resonant frequency of the concrete but does not necessarily affect its strength characteristics, and (2) the location of the failed aggregate within the specimen tested in third point bending which tend to affect the flexural capacity.

In order to validate these observations, an exponential best fitting curve was applied between the flexural strength (f'_r) and E_D in Figure 9-7(a) in the form of $f'_r = ae^{bE_D}$, where a and b are constant coefficients and were found equal to 1.56 and 3.8×10^{-5}, respectively. Then the fitting curve was plotted against the experimental results for specimens with aggregate failures as shown in Figure 9-8. An upper and lower bound curves were plotted for the fitting curve as shown in Figure 9-8 indicating the range of distribution of the experimental results for specimens without aggregate failure. The upper and lower limits were determined by first finding the difference between the experimental and modeled flexural strength results based on their corresponding E_D values. Then the absolute mean and standard deviation were calculated for the difference in the flexural strength results. The mean and standard deviation were then added to the modeled f'_r to determine the upper limit and subtracted from the f'_r for the lower limit.

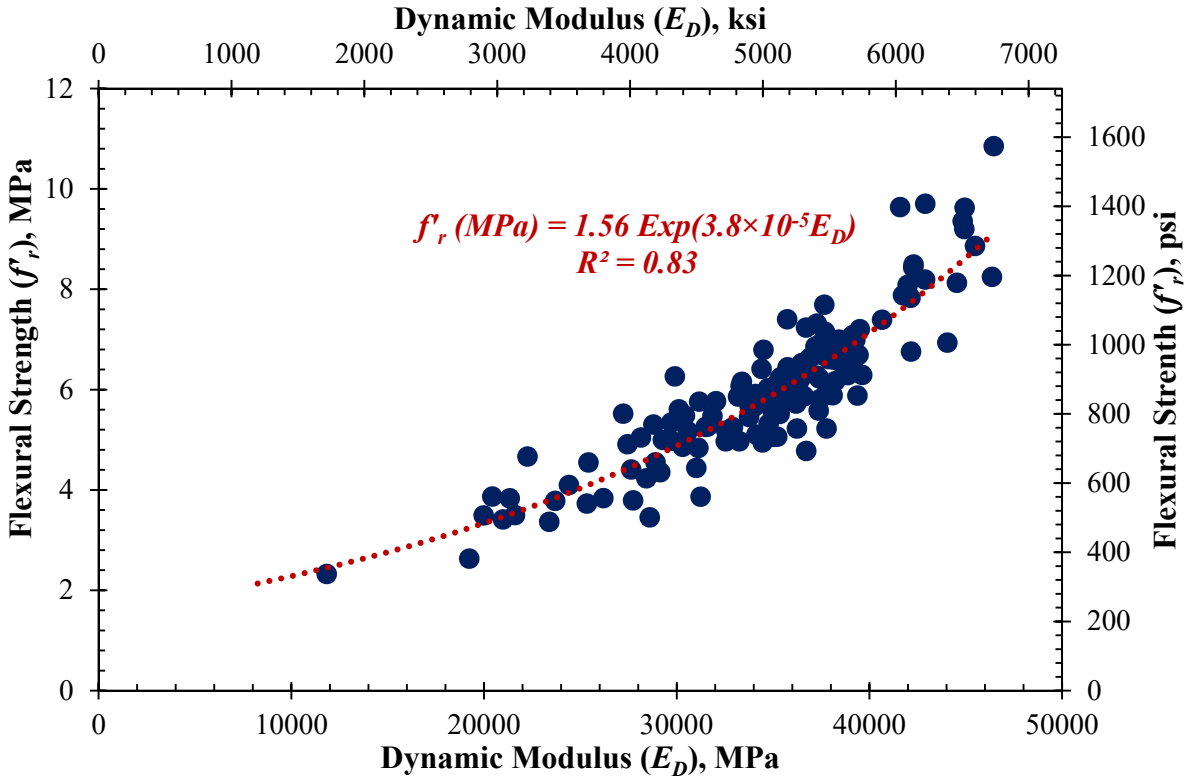

(a) without aggregate failure

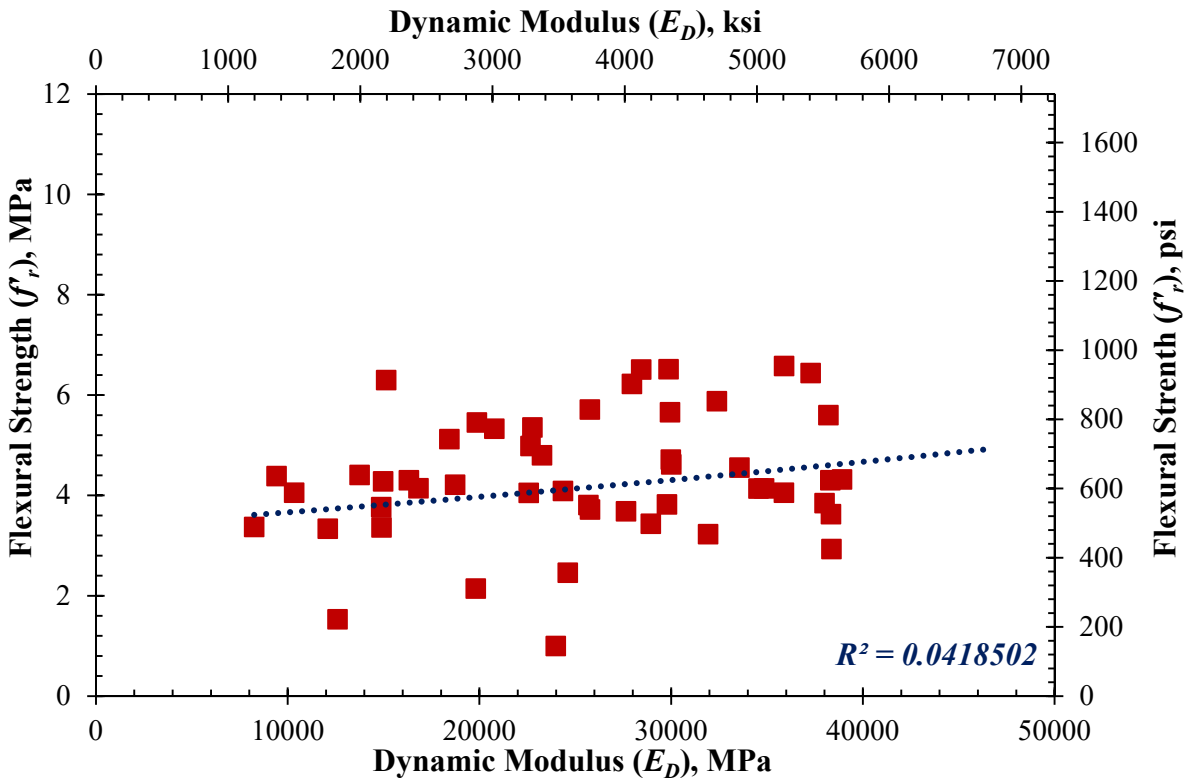

(b) with aggregate failure

Figure 9-7. Relationship between the flexural strength (f'_r) and dynamic modulus (E_D)

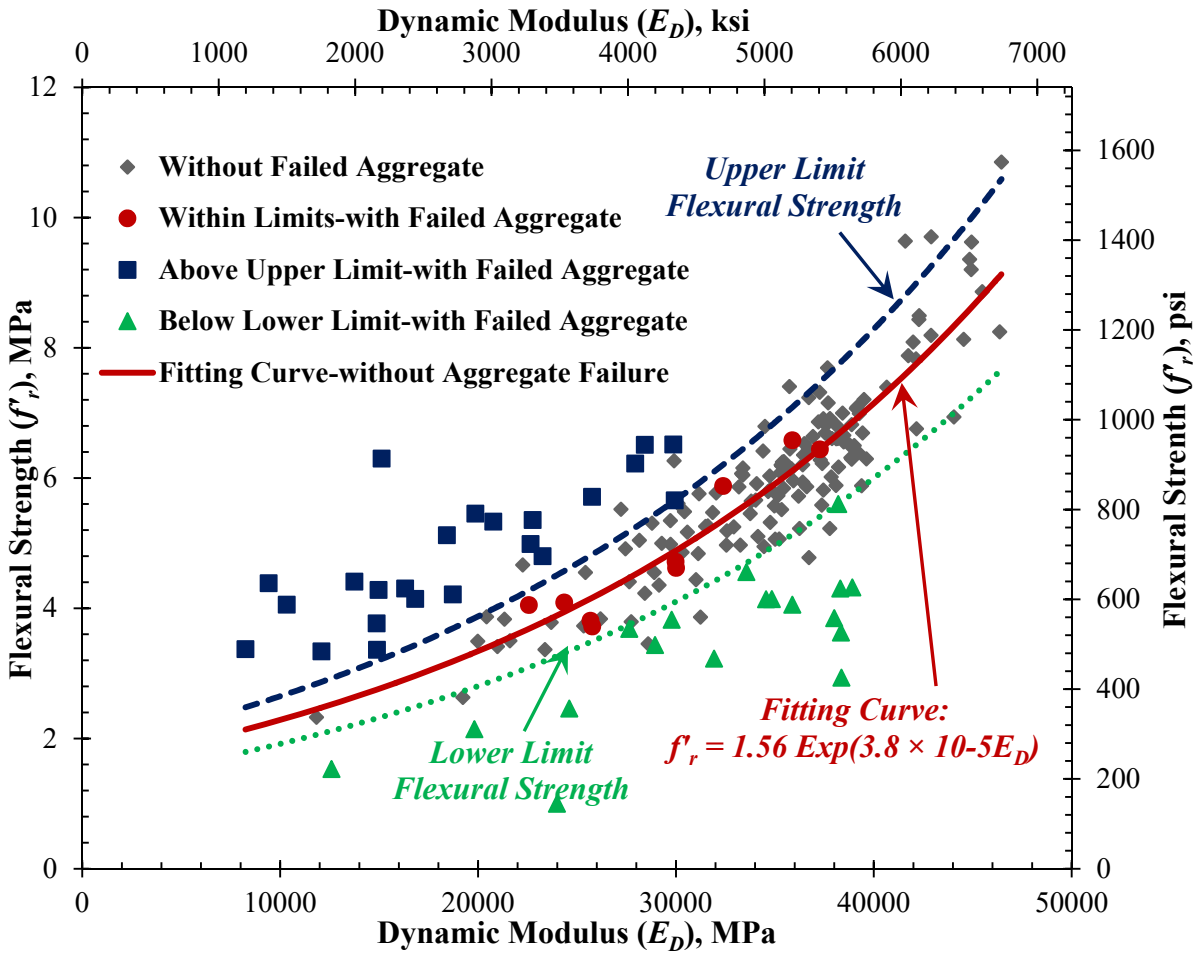

Figure 9-8. Distribution of the f'_r vs. E_D for specimens with aggregate failures

Consequently, specimens with aggregate failure were divided into three categories. The first category included all the results (23 specimens) with f'_r exceeding the upper limit flexural strength as shown in Figure 9-8; the second category included all the results (9 specimens) that were within the lower and upper limits of f'_r; and the third category included all the results (18 specimens) that fell below the lower limit of f'_r (see Figure 9-8). Then the fractured surface of the split specimens tested for flexural strength was examined in an attempt to correlate the inconsistent trend between f'_r and E_D for specimens with signs of aggregate failures. A picture was taken for the fractured surface as shown in Figure 9-9 and Figure 9-10 for concrete specimens with f'_r above the upper limit and below the lower limit, respectively, such that the

upper half of the surface was subject to compression and the lower half to tension under the flexure bending test. Inspection of Figure 9-9 revealed that some of the specimens with f'_r exceeding the upper limit did not have failed aggregate in the fractured surface while other specimens showed aggregate failure but were located either at the neutral axis or in the compression zone. This indicates that the location of the failed aggregate did not affect the modulus of rupture of concrete but affected the resonant frequency measurement which lessened its dynamic modulus of elasticity. In contrast, inspection of Figure 9-10 revealed that that concrete specimens with f'_r that fell below the lower limit showed multiple aggregate failures at the fractured surface and most of them were located in the tension zone of the specimen which explains the reduced flexural capacity with the corresponding modulus of elasticity.

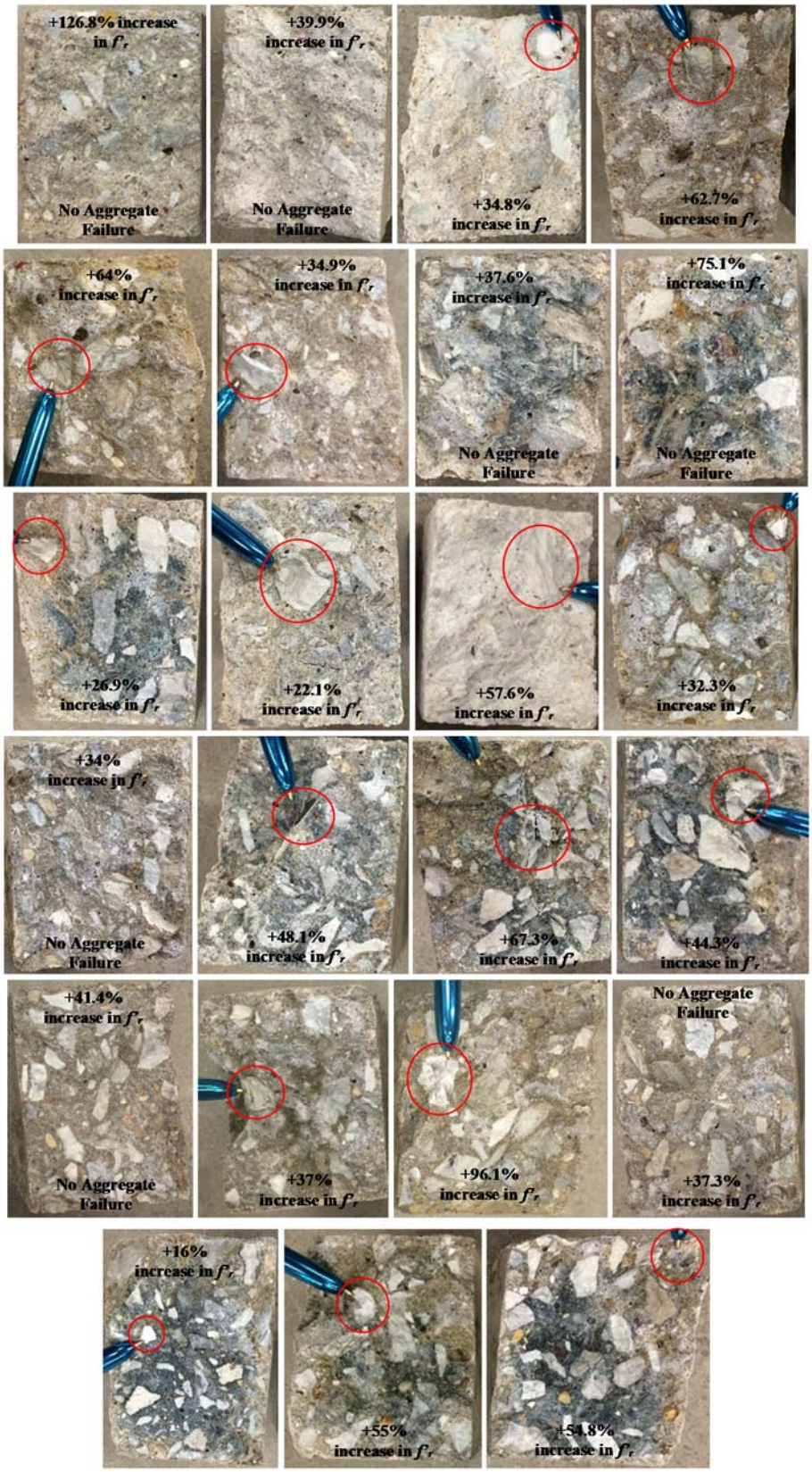

Figure 9-9. Inspection of the fractured surface after the flexure testing for freeze/thaw specimens with f'_r above the upper limit

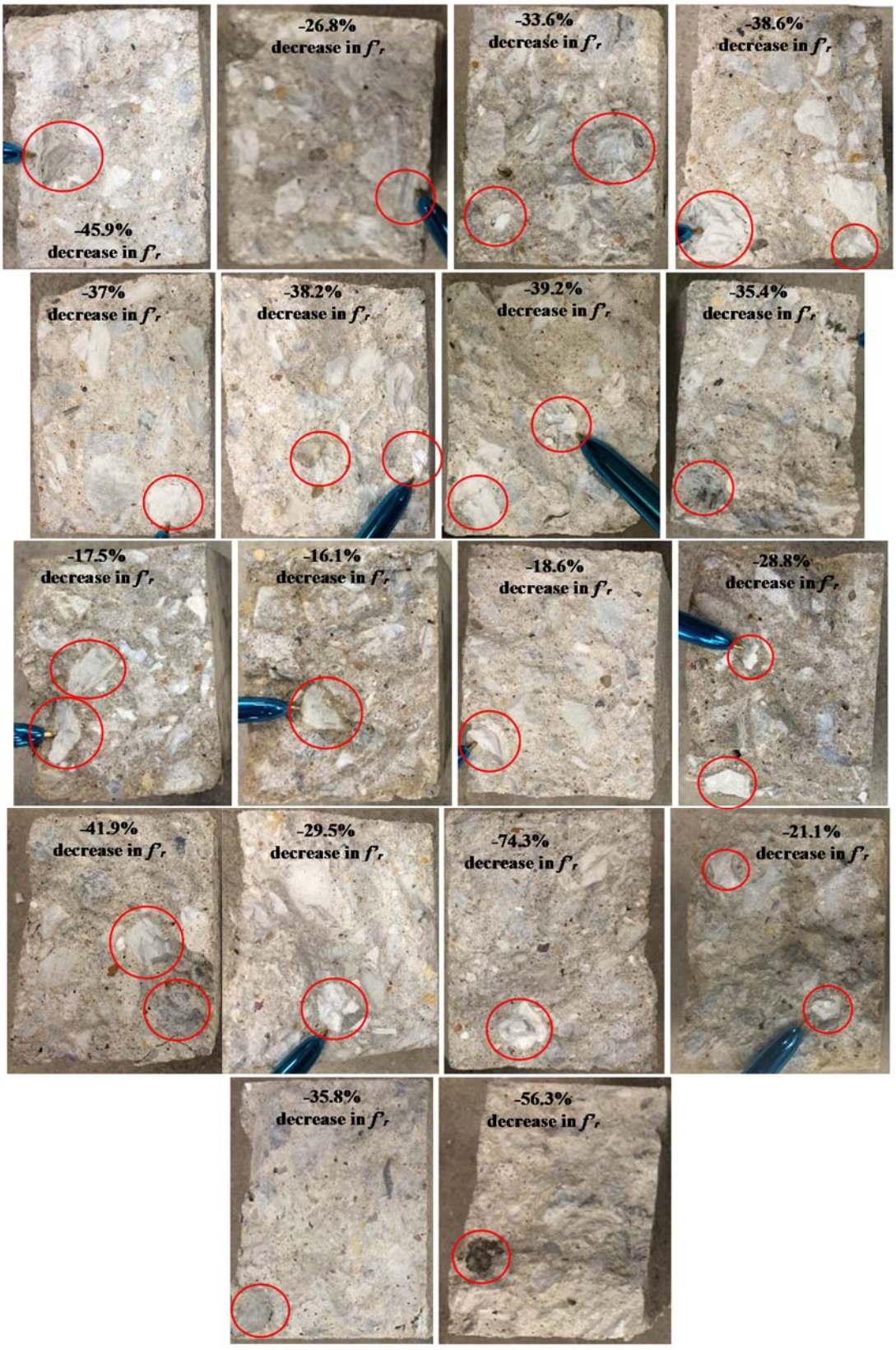

Figure 9-10. Inspection of the fractured surface after the flexure testing for freeze/thaw specimens with f'_r below the lower limit

10. ANALYTICAL EVALUATION OF THE RAPID CHLORIDE PENETRATION AND WATER PENETRATION IN CONCRETE

In this chapter, the penetration coefficient (K_w) of water penetrating in unsaturated concrete under hydrostatic pressure per DIN 1048 was estimated based on the average depth rather than the maximum depth of penetration. In addition, the equivalent-steady state diffusion coefficient (D_{c_rm}) based on the chloride migration rate per RCP test was estimated using the Nernst-Plank equation. By using this equation, the Arrhenius correction factor was applied to account for the "Joule effect". The results showed a reasonable relationship between the K_w and D_{c_rm}. Overall, a reliable method was established to predict the K_w based on the DIN 1048 test and a simplified equation based on the charge passed in RCP test was developed to estimate the D_{c_rm}.

10.1. Introduction

Transport of chloride into concrete is considered as one of the most dangerous mechanisms affecting the durability and service life of the structure. Chloride is primarily responsible for accelerating the initiation of corrosion in the reinforcing steel. The time to corrosion initiation can be predicted by calculating the diffusion coefficient. Concrete samples are collected at different depths to obtain a chloride profile, then the diffusion coefficient can be calculated by applying Fick's Second Law (Crank 1975). The problem with this method is the long periods of chloride exposure needed prior to testing, which deems it impractical for performance based applications.

In this study, the diffusion coefficient based on the RCP test and the penetration coefficient based on the DIN 1048 test were determined based on theoretical approaches by

taking into considerations the external factors that have been observed to influence the test results. The penetration properties were measured using the rapid chloride penetration (RCP) test in accordance to ASTM C1202, which gives an electrical indication for the concrete to resist chlorides, and DIN 1048 test (German standard) that measures the water penetration under hydrostatic pressure through unsaturated concrete. This chapter is aimed to provide an estimate of the transport coefficients based on the RCP and DIN 1048 test results in an attempt to define a reliable empirical method and practical approach.

10.2. Analytical Methods for Chloride and Water Penetration

10.2.1. Calculation of Equivalent Diffusion Coefficient (D_c) for RCP test

The RCP test is known to have three major limitations:

(1) The current passed does not distinguish between the chloride and total ions in the pore solution (Suryavanshi et al., 2002),

(2) The duration period is not long enough (6 hours) to allow a steady-state migration to be achieved, and

(3) The current flow due to the high generated voltage (60 V) can result in what is known as the "Joule effect", which causes an increase in the temperature leading to an increase in the Coulomb charge passed (Betancourt and Hooton, 2004).

Accordingly, in order to predict the equivalent diffusion coefficient (D_c) based on the RCP test results, it's essential to make some corrections due to the aforementioned limitations.

The total chloride-ion flux due to migration, in steady-state conditions, can be expressed as follows:

$$J = \frac{zF}{RT} D_i C_i \frac{\partial E}{\partial x} \qquad \text{Eq. 10.1}$$

Where:

J = the flux of the chloride ion,

z = the valency of chloride ion (z = 1),

F = the Faraday constant value,

R = the universal gas constant (8.314 *Joule/mole/K*),

T = the absolute temperature in Kelvin (*K*),

D_i = the chloride ion diffusion coefficient,

C_i = the chloride ion concentration (2.05 mole/l [58.06 mole/ft^3]), and

E = the electric potential.

More than one solution has been proposed for the chloride diffusion. Ghosh et al. (2011) revealed that the Nernst-Plank equation for D_c is most reliable among others and can be expressed as follows:

$$D_c = \frac{RTkV}{zC_iF(E/L)A} \qquad \text{Eq. 10.2}$$

Where

k = the chloride migration rate,

V = the volume of the solution in the RCP test cell (250 ml),

A = the cross-sectional area exposed to the chloride ion,

E = the RCP test electric potential (60 V), and

L = the thickness of the specimen (50 mm [2 in.]).

The chloride migration rate (k) can be calculated based on the flux J as shown in Eq. (10.3):

$$k = J\frac{A}{V} \qquad \text{Eq. } 10.3$$

Where the flux, J, can be calculated based on the current i as shown in Eq. (10.4):

$$J = \frac{i}{zFA} \qquad \text{Eq. } 10.4$$

As mentioned earlier, the rate of diffusion is increased at higher temperature. To account for the temperature rise, an Arrhenius type equation was used to find the diffusion coefficients at room temperature (23 ºC [73 ºF]), as expressed in Eq. (10.5):

$$D_{c\_rm} = D_c e^{-\frac{E_a}{R}\left(\frac{1}{T_r}-\frac{1}{T_{avg}}\right)} \qquad \text{Eq. } 10.5$$

Where:

D_{c_rm} = the corrected diffusion coefficient at room temperature

E_a = the activation energy,

T_{avg} = the average temperature of the RCP specimens in K, and

T_r = the room temperature expressed in K.

The E_a values used for the 28 concrete mixes were taken from a study conducted by Poole et al. (2007). A summary of the activation energy values from Poole et al. (2007) for different amount of Class C fly ash and Grade 100 Slag replacement to cement is shown in Table 10-1. The E_a for mixtures with w/cm of 0.44 and made with 30% Class C fly ash (23% CaO) and 30% Grade 100 GGBF slag are 35,840 and 37,080 *Joule/mole*, respectively (Poole et al. 2007).

Table 10-1. Activation Energy, E_a, for Cementitious Combinations (Poole et a. 2007)

Material	CaO, %	W/CM Ratio	% by Mass of Total Cementious Material	E_a, J/mol
Class C Fly ash	23.1	0.44	20	34,437
	23.1	***0.44***	***30***	***35,836***
	23.1	0.44	40	36,747
Grade 100 Slag	—	***0.44***	***30***	***37,080***
	—	0.44	40	36,936
	—	0.44	50	39,928

The temperature was recorded for 130 RCP specimens with Q values ranging from 370 to 4050 Coulomb. Figure 10-1 shows the relationship between the Q and the T_{avg} for the 130 RCP specimens. A linear increasing trend with a good correlation coefficient ($R^2 = 0.92$) was observed between T_{avg} and Q. Based on this finding, the T_{avg} was expressed as a function of Q in Eq. (10.6):

$$T_{avg} = 0.00384Q + 23\ ℃ \qquad \text{Eq. 10.6}$$

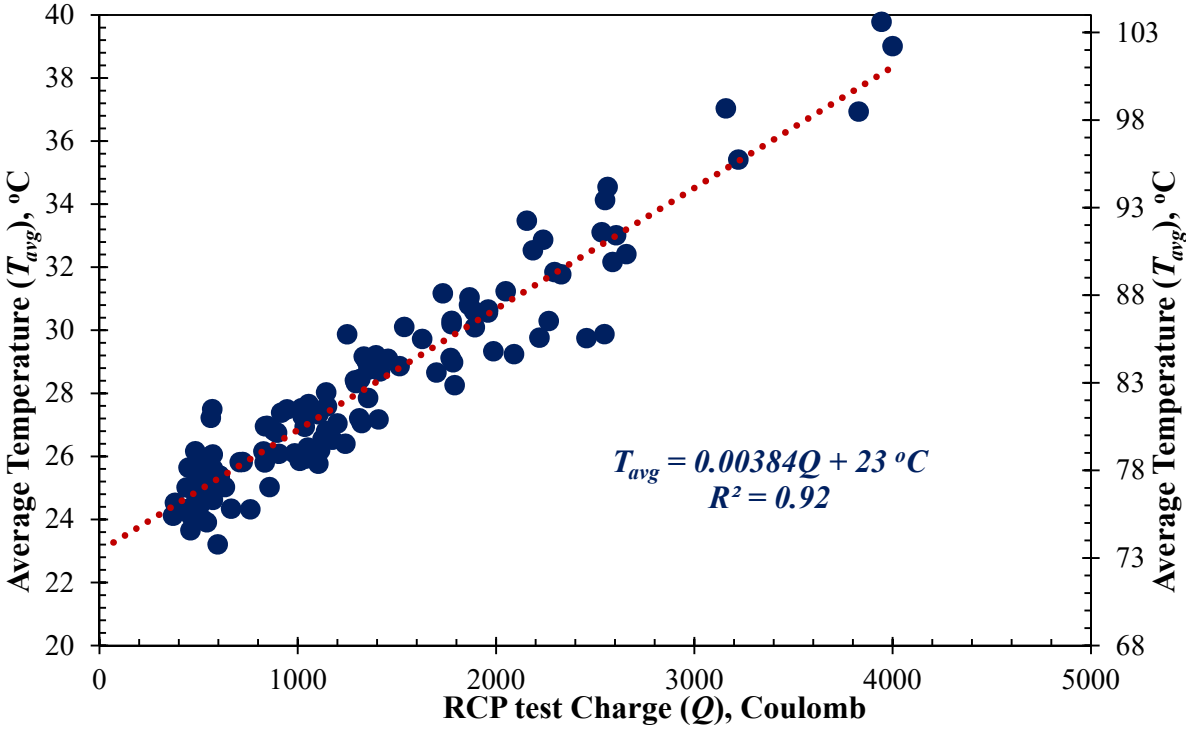

Figure 10-1. Relationship between the average temperature (T_{avg}) and Q in the RCP test

10.2.2. Calculation of Water Penetration Coefficient (K_w) for DIN 1048 Test

The water penetration into concrete generally depends on many features such as the porosity, tortuosity, connectivity between the pores, and the micro cracks. These parameters among others are influenced by the w/cm ratio, the age of the concrete, and the granulometry of the cementitious materials (Phung et al., 2013). In fully saturated concrete, water penetration, better known as permeation, is usually associated with steady flow. Several methods were proposed to measure the permeability in cementitious materials by simply applying Darcy's law and assuming that the flow is steady and uniform (Phung et al., 2013; Scherer et al., 2007; Loosveldt et al., 2002; Ludirdja et al., 1989). In unsaturated concrete as per DIN 1048 test, the water penetration under external hydraulic pressure is associated with sorptivity and unsteady flow. This makes modeling the water penetration more complicated in unsaturated concrete. Several mathematical equations have been suggested for water penetration in unsaturated concrete (Hall, 1977; Fagerlund, 1982; Bamforth et al., 1985; Ho and Lewis, 1987). Reinhardt (1992) proposed a formula for the penetration coefficient (K_w) under the combined effect of capillary tension and hydraulic pressure, and is expressed as follows:

$$K_w = \frac{r}{2}\sqrt{\frac{P_e + P_c}{\eta}t} \qquad \text{Eq. 10.7}$$

Where

r = the radius of the capillary pores,

P_e = the capillary tension; P_c is the hydraulic pressure,

η = the water viscosity, and

t = the time.

This approach is hard to model due to the complexity of obtaining some of the parameters. Others (Vuorinen, 1985; Hedegaard and Hansen, 1992) suggested calculating the K_w by applying Darcy's law and assuming that the flow of water through the concrete pores is stationary and laminar. This assumptions holds true for water penetration in saturated concrete and was validated by several researches (Phung et al., 2013; Scherer et al., 2007; Loosveldt et al., 2002; Ludirdja et al., 1989). Based on these assumptions, eq. (10.8) applies for K_w:

$$\frac{dx}{dt} = K_w \frac{h}{x} \qquad \text{Eq. 10.8}$$

Where

x = the depth of water penetration (m),

t = the time (s),

h = the external pressure head (m),

K_w = expressed in (m/sec).

Then, the K_w can be obtained by integrating Eq. (10.8) to yield Eq. (10.9):

$$K_w = \frac{{x_t}^2}{2ht} \qquad \text{Eq. 10.9}$$

Where

x_t = the penetration depth at time t.

When n pressure levels are applied at n different periods, the equation can become as follows:

$$K_w = \frac{x_t^2}{2 \sum_{i=1}^{n} h_i t_i} \qquad \text{Eq. 10.10}$$

Hedegaard and Hansen (1992) expressed the x_t as the maximum penetration depth (x_{max}). Since the water flow is unsteady and associated with sorptivity, this assumption does not provide an accurate prediction for the K_w. A more reasonable approach is to use the average depth of

penetration (x_{avg}) to calculate K_w. The x_{avg} for the DIN 1048 specimens was calculated by first measuring the area (A_w) and maximum width (w_{max}) of the wetted region for the two split sections using a CAD software (see Figure 10-2).

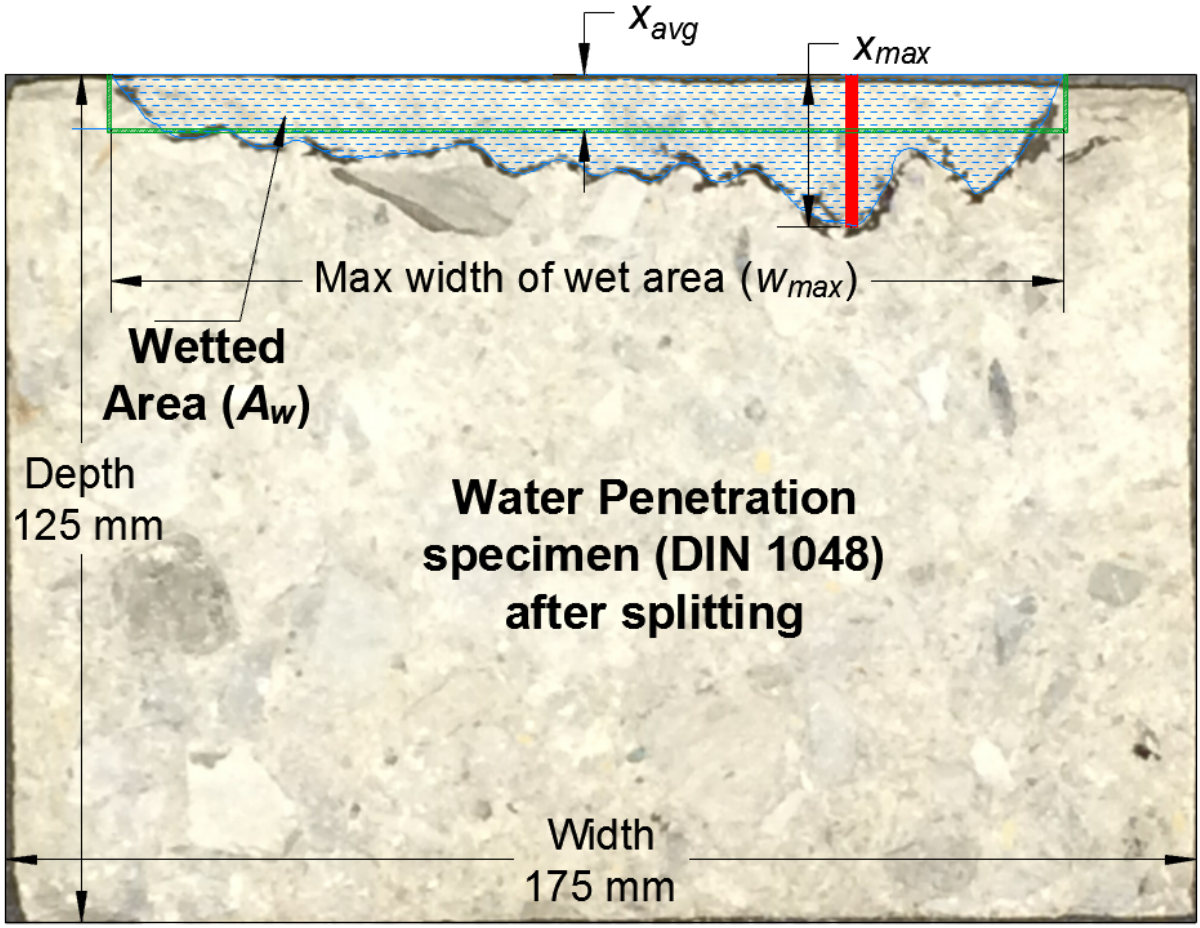

Figure 10-2. Method for calculating the average depth (x_{avg}) in the wetted region

Then x_{avg} was taken as the average of the A_w divided by w_{max} for each half. A relationship was developed between the x_{avg} and x_{max} in the form:

$$x_{avg} = Cx_{max} \qquad \text{Eq. 10.11}$$

Where C is the ratio of the x_{avg} to x_{max}. This ratio can be dependent on many parameters such as the cementitious content, w/cm ratio, interfacial transition zone between the cement paste and the aggregate, maximum aggregate size, and micro cracks. By substituting x_t with x_{avg}, Eq. (10.11) can be expressed as a function of C and x_{max} as follows:

$$K_w = C^2 \frac{x_{max}^2}{2 \sum_{i=1}^{n} h_i t_i} \qquad \text{Eq. 10.12}$$

10.3. DISCUSSION AND CORRELATIONS

10.3.1. DIN 1048: Maximum versus Average Penetration Depth

The purpose of measuring the average depth (x_{avg}) is to have a better prediction for the penetration coefficient of concrete (K_w). The relation between the average and maximum penetration depth for all the concrete specimens and tested at all ages is shown in Figure 10-3. Inspection of Figure 10-3 reveals that there is a trend between the x_{max} and x_{avg}. This trend is observed to be linear with an acceptable correlation coefficient ($R^2 = 0.85$). Based on the best fitting trendline, the ratio of the x_{avg} to x_{max} is roughly $C = 0.61$. This finding is disputable depending on the x_{max} value. For specimens with $x_{max} \leq 20$ mm (0.79 in.), it was observed that the increase in the x_{avg} was very consistent with the x_{max} increase; while for $x_{max} > 20$ mm (0.79 in.), the data is shown to be more scattered with a poor correlation coefficient. From the tested DIN 1048 specimens, it was observed that for larger water penetration depths, the flow can either become more evenly spread along the exposed surface or more oriented towards a specific location. Based on the relationship between x_{max} and x_{avg}, it was not influenced by the fine aggregate type and the cementitious combination when 30% fly ash or slag were used as a replacement to cement. Further investigation is required to study the effect of the w/cm ratio, the cementitious combination and content, curing regime, and the inclusion of aggregates and the maximum aggregate size. It is worth mentioning that the inclusion of aggregates can increase the water penetration in concrete in comparison to cement paste and mortar when having the same w/cm ratio. This can be attributed to the presence of micro cracks, generally

larger than the capillary pores, at the interfacial transition zone between the aggregates and the cement paste (Mehta and Monteiro, 2014).

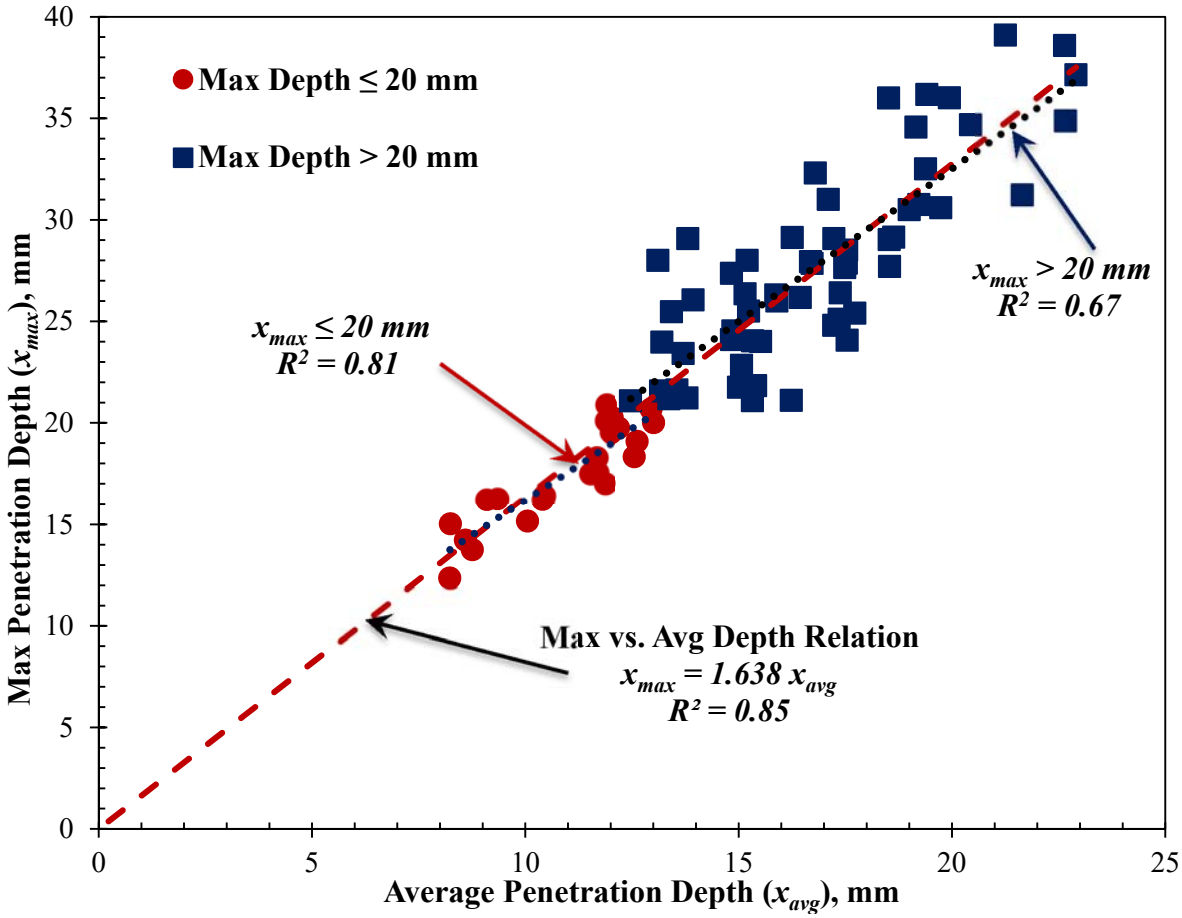

Figure 10-3. Maximum versus average penetration depth per DIN 1048

In order to provide a better insight on the advantage of using x_{avg} for K_w coefficient calculation, the x_{avg} and x_{max} were correlated with the charge passed (Q) based on the RCP test results from the same concrete mixes and tested for the same age. The results are shown in Figure 10-4 and they reveal that there exists a trend between the charge passed and the depth of water penetration. The correlation of the charge passed with the x_{avg} seemed to be more consistent with less scattering and better correlation coefficient ($R^2 = 0.86$) than with the x_{max} ($R^2 = 0.75$); this is based on a logarithmic best fitting curve.

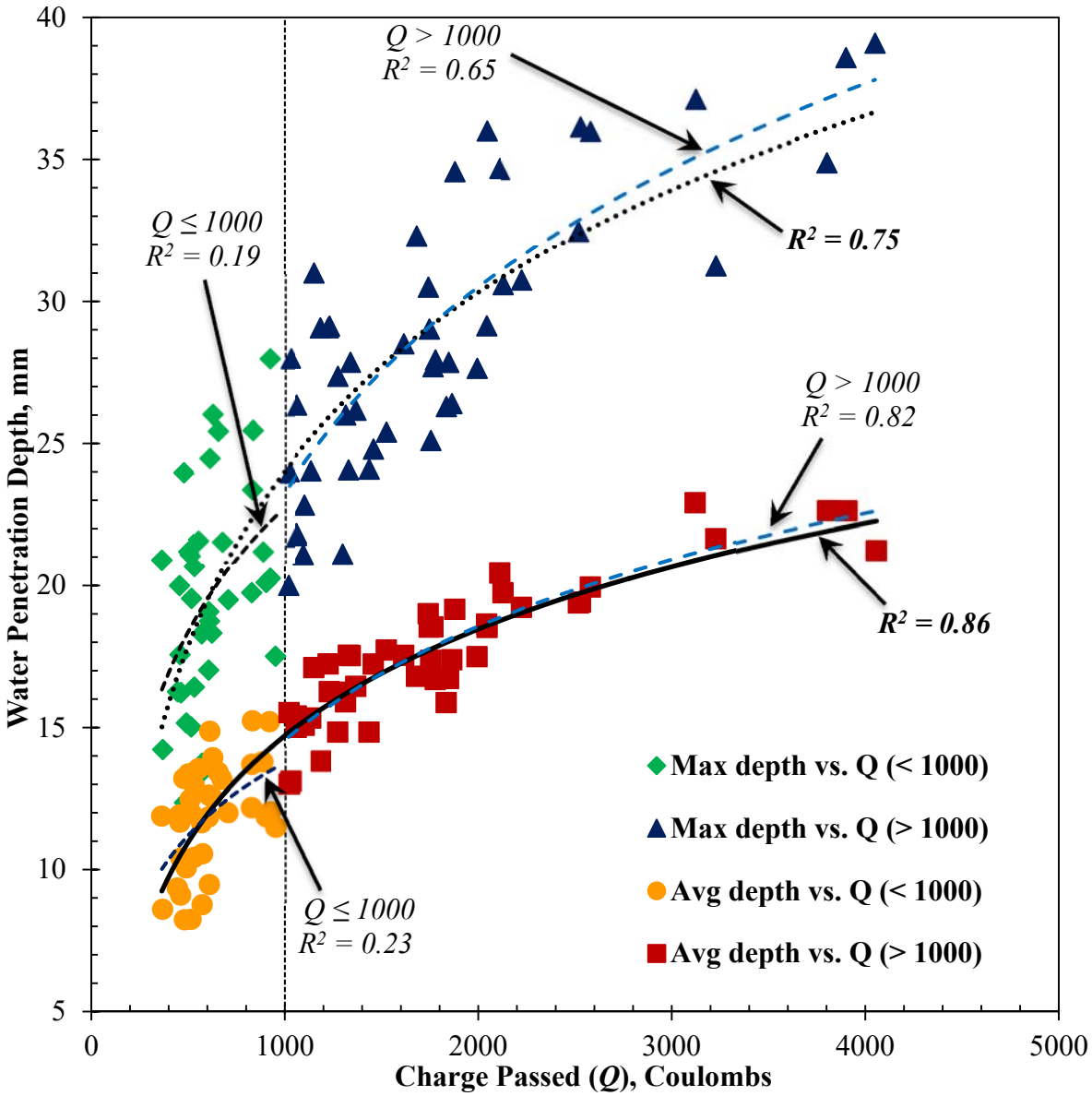

Figure 10-4. Penetration depth per DIN 1048 versus charge passed per RCP test

It is noteworthy to mention that when the charge passed was less than 1000 Coulombs, it seemed that there is no correlation of the Coulomb values with the water penetration depth results as Figure 10-4 demonstrates a poor relation with x_{max} and x_{avg}. Nevertheless, this is not an indication of whether the water penetration values are more reliable than the RCP test results. Several studies tried to correlate the RCP test with other transport mechanisms most notable for the chloride diffusivity into concrete (Issa and Khalil, 2010; Sherman et al., 1996;

Ozyildirim, 1998; Pfeifer, 2000). These studies were in agreement that no correlation exists between the chloride diffusion based on the chloride ion penetration test and the Coulomb values when the Coulomb results are very low.

10.3.2. RCP Test: Equivalent Diffusion Coefficient (D_c) versus Charge Passed (Q)

The equivalent diffusion coefficient (D_c) based on the RCP test results and use of the Nernst-Plank equation is shown in Figure 10-5. It is revealed that the D_c increases linearly with the increase in the charge passed. To confirm this relation, Ghosh et al. (2011) D_c results are compared with the existing results as shown in Figure 10-5; they show very consistent trend with the existing results. After applying the Arrhenius correction factor, it was observed that the D_c values were reduced depending on the charge passed. It is clear from the results that the change in D_c was insignificant for Q values less than 1000 Coulombs. However, as the Q is increased, the reduction in D_c value increased drastically to the point that it was reduced by more than 50% for Q values above 4000 Coulombs.

Based on these findings, a simplified approach is developed to calculate the D_{c_rm} which can be solely based on the Q values. First, from the $D_c - Q$ relation, a best fitting trendline with the following equation can be obtained:

$$D_c = 6.5Q \times 10^{-16} \qquad \text{Eq. } 10.13$$

Where D_c is expressed in m^2/sec. Since the E_a depends on the w/cm ratio and the cementitious combination of the concrete mix, the D_{c_rm}, based on the Arrhenius correction factor, can be predicted by substituting Eq. (10.13) for D_c and Eq. (10.6) for T_{avg} (K) into Eq. (10.5) for D_{c_rm}. This yields the following equation:

$$D_{c\_rm} = 6.5Q \times exp\left[-E_a\left(\frac{Q}{1.95 \times 10^8 + 296Q}\right)\right] \times 10^{-16} \qquad \text{Eq. } 10.14$$

Where D_{c_rm} is expressed in m^2/s, Q in Coulombs, and E_a in *Joule/mole*. A handful selection of E_a values for concrete mixes with different cementitious combinations can be obtained from Poole et al. (2007). It should be noted that this equation is dependent on the T_{avg} which was developed based on the relationship presented in Figure 10-1. Further investigation is needed to validate this relationship with wider range of testing that could include different cementitious combinations and contents, w/cm ratios, and curing conditions.

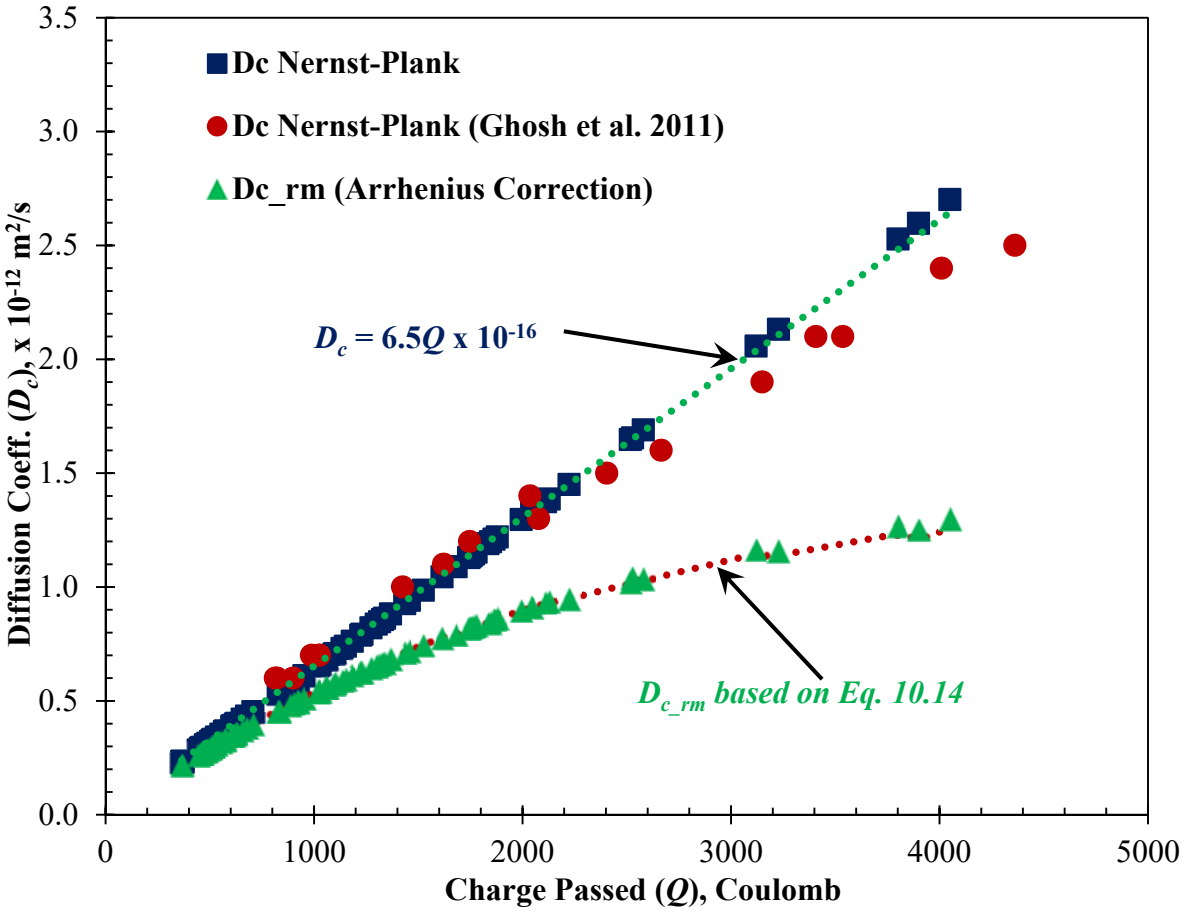

Figure 10-5. Equivalent diffusion coefficient (D_c) vs. the charge passed (Q) in RCP test.

10.3.3. Diffusion Coefficient (D_c) vs. Water Penetration Coefficient (K_w)

The D_c values based on the RCP test results were correlated with the K_w, which was calculated based on the x_{avg} in the DIN 1048, as shown in Figure 10-6. The relation between the K_w and the D_c based on the Nernst-Plank equation before applying the Arrhenius correction factor shows that the D_c increases at an exponential rate with respect to the K_w; whereas, the D_{c_rm} exhibited a consistent linear relationship with the K_w with a zero intercept. The exponential increase in D_c can be explained as a result of the Joule's effect, which causes an increase in the temperature and thereby the Q values. The diffusion mechanism occurs due to chloride concentration gradient and the water penetration in unsaturated concrete occurs due to the combined effect of pressure gradient and capillary suction. Although the K_w and D_c are coefficients for two different transport mechanisms, the relationship between them shows that both mechanisms are dependent on the pore structure and the interconnectivity between the pores. Zhang and Zong (2014) correlated the diffusion coefficient with the water penetration in unsaturated concrete and observed that there is a consistent trend between them. However, this trend was not linear and showed that the rate of increase in water penetration was higher than the chloride diffusion. Their relationship, however, was based on the effect of five different curing regime. Therefore, further investigation is needed to validate this relationship with wider range of testing that could include different cementitious combinations and contents, w/cm ratios, and curing conditions.

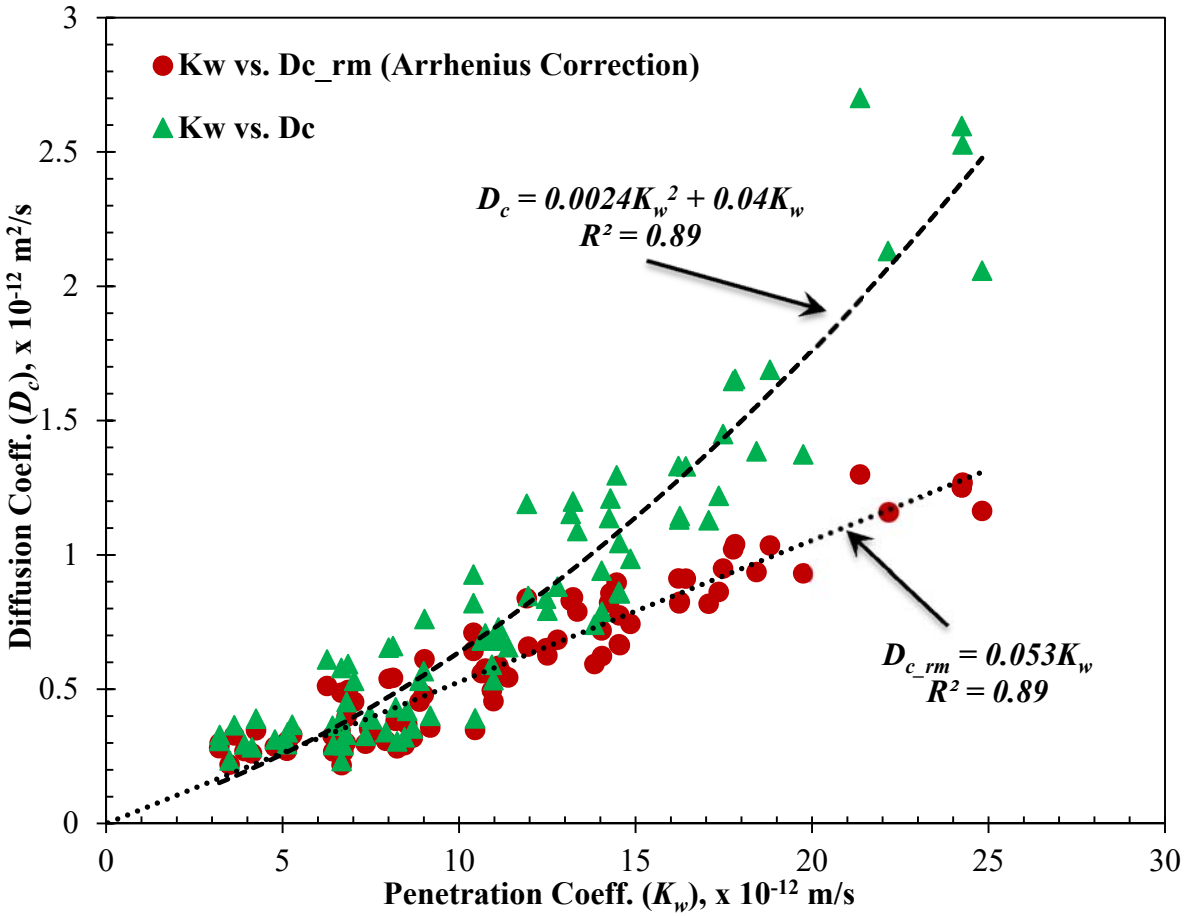

Figure 10-6. Diffusion Coefficient (D_c) vs. Water Penetration Coefficient (K_w)

10.3.4. Compressive Strength, D_c, and K_w Relations

In an attempt to validate the K_w per DIN 1048 and D_c per RCP test, it is worthwhile to correlate the transport coefficients with the strength properties of concrete. The compressive strength for the permeability concrete mixes was measured at 360 days, where they ranged from 5500 to 6700 psi (38 MPa to 46 MPa). Accordingly, the K_w and D_c coefficients for the specimens tested at 360 days were correlated with the compressive strength as shown in Figure 10-7. Inspection of Figure 10-7 reveals a weak correlation between f'_c and K_w based on x_{avg} and x_{max} and f'_c and D_c. This weak link is attributed to the difference in the air content in the concrete mixes which ranged from 6.5 to 7.5%. The air content, better expressed as the entrained air

affects the compressive strength without necessarily influencing the transport mechanism into concrete. However, it can be inferred that there is a decreasing trend in the compressive strength with the increase in K_w and D_c. Moreover, the K_w based on x_{avg} had an improved correlation in comparison to x_{max}, while the D_c per RCP test was the weakest.

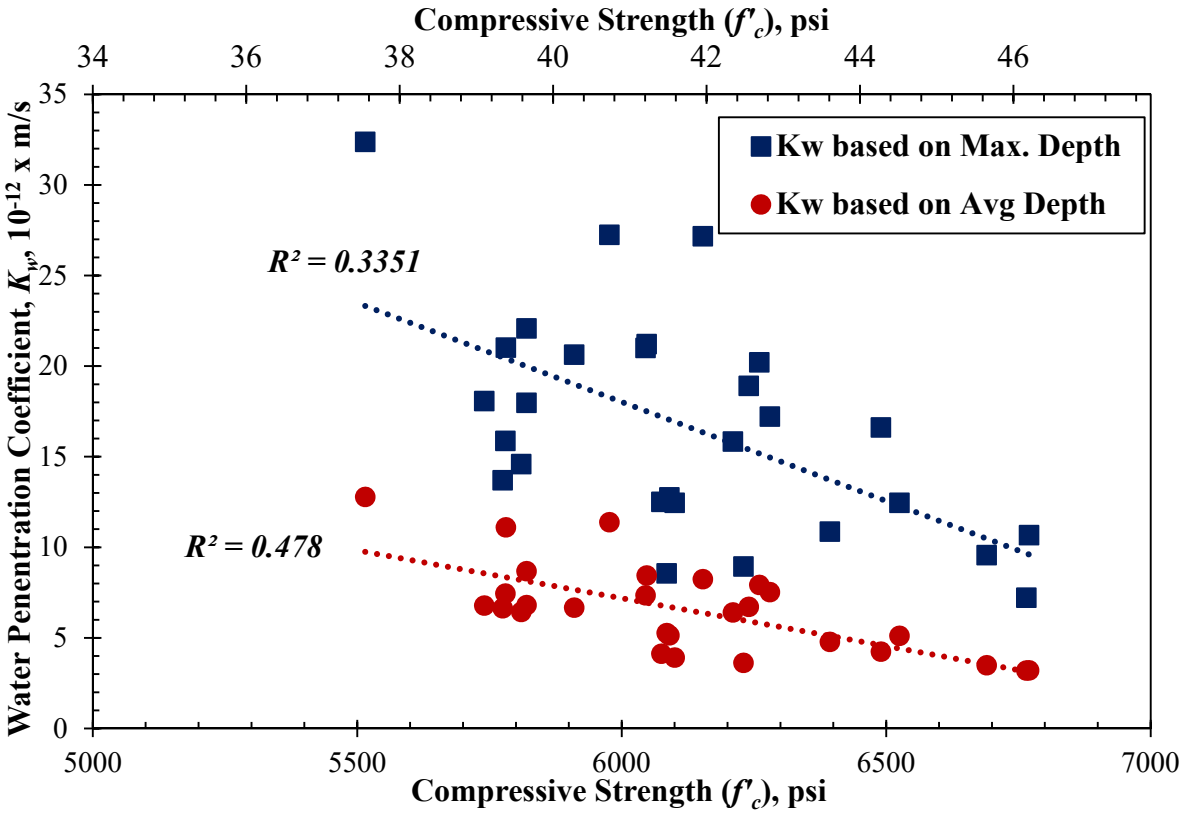

(a) K_w versus compressive strength

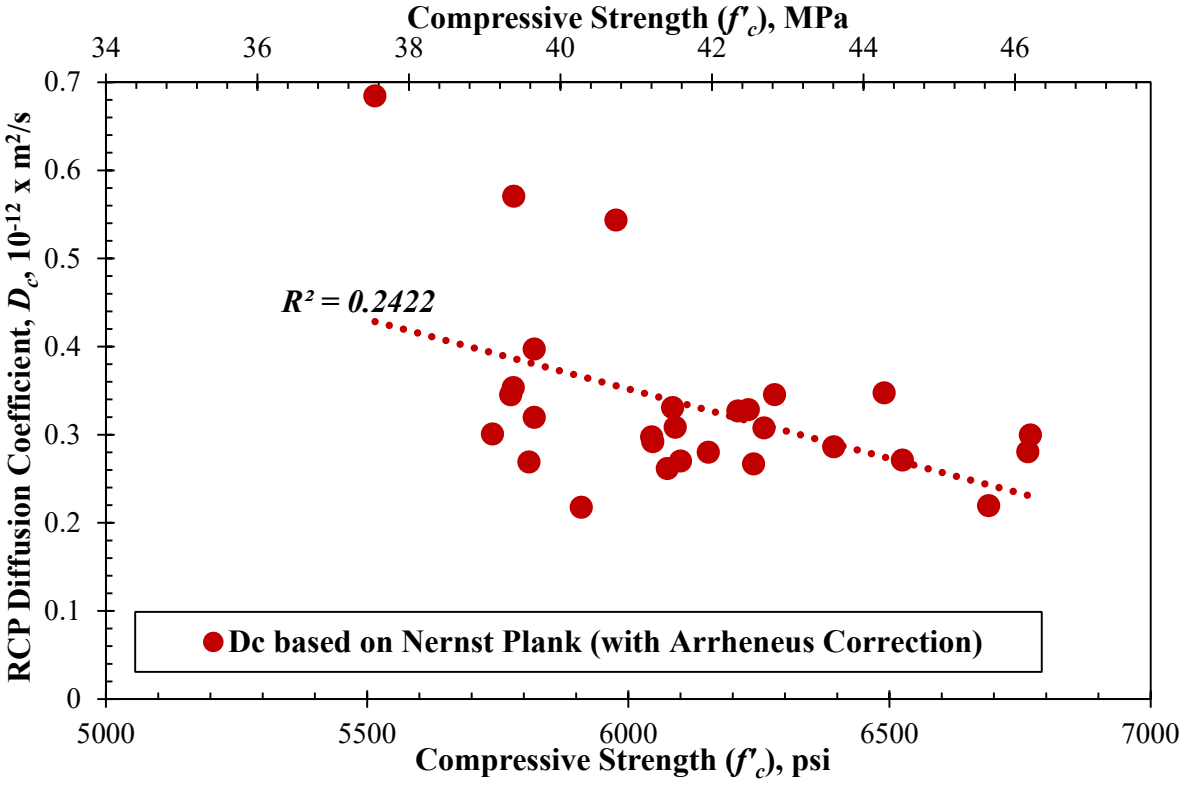

(b) D_c versus compressive strength

Figure 10-7. Transport coefficients versus the compressive strength at 360 days

11. TIME DEPENDENT DIFFUSION MODELING OF CONCRETE WITH CEMENT CONTAINING LIMESTONE AND IPA

This chapter investigates the effect of adding IPA and increasing IR on the diffusivity characteristics of concrete. Also, the effect of replacing cement with supplementary cementitious materials while batching them with two sand types was demonstrated. To show the effect of these materials, the chloride diffusion test was conducted on twenty-six concrete mixes with different proportions that were salt ponded for 90, 180, and 360 days. The IPA addition and increase in IR did not show any notable influence on concrete diffusivity. On the basis of the experimental results, a diffusion model with time dependent surface chloride and diffusion coefficient was developed. The proposed model was compared with existing service life prediction software and models and showed promising results, while the current equations adopted by the software were very conservative.

11.1. Introduction

Chloride induced-corrosion is one of the main deterioration mechanisms affecting the lifespan of bridge decks and other concrete structures. The physical characteristics of concrete such as its porous structure and its chemical properties through its high alkalinity provide the protection needed for the steel reinforcement from chloride penetration. The chloride depassivates the steel and accelerates the time to corrosion initiation process.

The transport of chloride into concrete can occur through different processes: diffusion, permeation, migration, and convection, with diffusion being the dominant transport mechanism. The process where chloride ions in concrete are transported from a region of higher concentration to a region of lower concentration is known as diffusion (Poulsen and

Mejlbro, 2006). The diffusion of chloride in concrete is influenced by many factors including the cement type, supplementary cementitious materials (SCMs) characteristics and replacement quantities, aggregate characteristics, w/cm ratio, exposure conditions and curing methods (Bentz et al., 1999; Oh and Jang, 2007; Yang, 2005).

In this study, the diffusion characteristics of concrete with various inorganic process additions (IPA) and insoluble residue (IR) contents in cement exceeding what's required by ASTM C150 is investigated. The experimental work also describes the effect of using SCMs (Class C fly ash, and Grade 100 GGBF slag) and batching with different sand types. Supplementary cementitious materials such as fly ash and GGBF slag have been shown to improve the porous structure in concrete and reduce the diffusion of chlorides (Thomas et al., 1999; Burris and Riding, 2014). Two types of sand were batched with concrete: (1) natural sand and (2) combined sand. The combined sand is a combination of 50% natural sand and 50% manufactured sand obtained as leftovers from the crushed limestone coarse aggregate quarries.

Very limited research has investigated the effect of IPA and IR on the chloride penetration and diffusivity properties of concrete. Predicting the long-term chloride diffusion process through short-term tests has been the subject of many researchers and engineers. Studies have shown that the diffusion coefficient (D_a) and surface chloride concentration (C_s) are time dependent variables (Tang and Nilson, 1992; Maage et al. 1995; Frederiksen et al. 1997; Takewaka and Mastumoto, 1988; Mustafa and Yusof, 1994; Swamy et al., 1998; Costa and Appelton, 1999; Uji et al., 1990; Purvis et al., 1994; Kato et al., 2005; Shin and Kim, 2002). Accordingly, extrapolating the short-term results requires taking into consideration the changes in C_s and D_a over time. However, none have developed an easy and reliable method

that can effectively predict the chloride diffusion on the long-term based on short-term data. Accordingly, a practical chloride diffusion model with time dependent C_s and D_a can provide a better understanding of the chloride diffusion processes into concrete and can be of great benefit for researchers and engineer.

11.2. RESEARCH SIGNIFICANCE

This study sheds the light on the chloride diffusivity of binary concrete mixtures when adding limestone and IPA to cement and increasing the IR content more than what is specified by ASTM C150. A new mathematical model for chloride diffusion was developed on the basis of time dependent diffusion coefficient and surface chloride concentration. The C_s and D_a time dependent formulas were derived using the experimental results. The experimental results were used in the proposed and some existing models to study their service life and verify the accuracy of the proposed model. The authors believe that the proposed model can be very useful for researchers and engineers due to its simplicity and can open new doors for future research on the chloride diffusion modeling.

11.3. Experimental Program

The experimental program included conducting the salt ponding test and measuring the chloride ion penetration per ASTM C1543 and ASTM C1152. The same concrete slabs for the salt ponding test were used for the chloride diffusion. For each concrete mix, concrete slabs were salt ponded for a period of 90, 180, and 360 days. For the diffusion calculation, the samples were taken from depths of 3 mm (1/8 in.), 6.5 mm (1/4 in.), 12.5 mm (1/2 in.), 19 mm (3/4 in.), 25 mm (1 in.), and 37.5 mm (1½ in.). Also samples were collected between 50 to 62.5 mm (2 to 2½ in.) to measure the initial chloride in concrete. The acid-soluble chloride method

was performed in accordance to ASTM C1152 for measuring the chloride ion concentration in the concrete.

11.4. Chloride Diffusion Methodology

The diffusion of chloride in concrete is calculated using Fick's second law of diffusion as shown in Eq. (11.1):

$$\frac{\partial C}{\partial t} = \frac{\partial}{\partial x}\left\{D\frac{\partial C}{\partial x}\right\} \qquad \text{Eq. 11.1}$$

Where:

t = the time,

x = the depth from the top surface of the concrete,

C = the chloride concentration at time t and depth x, and

D = the diffusion coefficient.

It should be noted that the above equation is applicable for one dimensional problem where the chloride ions are confined to diffuse in the governing direction which is the direction of gravity. The more generalized case is when the chloride diffuses in vertical and horizontal directions. However, studies have shown that the rate of chloride diffusion in the horizontal direction is influenced by the w/cm ratio. The higher the w/cm ratio, the higher is the horizontal diffusion (Swamy et al., 1998; Suryavanshi et al., 1998). It was also observed that for concrete slabs with w/cm less than 0.45, the chloride diffusion in the horizontal direction of the slab was negligible compared to the chloride penetration along its depth (Swamy et al., 1998; Suryavanshi et al., 1998). Since all the concrete mixes were conducted with a w/cm less than

0.45, the chloride diffusion was predicted by assuming that the chloride penetration is confined in one direction.

The general mathematical solution adopted by the ASTM C1556 assumes that the surface chloride concentration and diffusion coefficients are constants. Based on these assumptions the solution becomes as shown in Eq. (11.2), where C_i is the initial chloride content in the concrete before being exposed to external chloride attack:

$$C(x,t) = C_s - (C_s - C_i)erf\left(\frac{x}{\sqrt{4Dt}}\right) \qquad \text{Eq. 11.2}$$

Where:

C(x,t) = the % of chloride concentration by weight of concrete, measured at depth *x* and time *t*,

C_s = chloride concentration at the surface of the concrete,

C_i = initial chloride-ion concentration before chloride exposure,

x = depth of chloride penetration,

D = chloride diffusion coefficient, m^2/s,

t = the time of chloride exposure, sec, and

erf = the error function which is described as follows:

$$erf(z) = \frac{2}{\sqrt{\pi}}\int_0^z exp(-u^2)du \qquad \text{Eq. 11.3}$$

Studies have shown that the diffusion coefficient decreases and the surface chloride concentration increases with time depending on the exposure condition and duration of the chloride exposure. Both the C_s and D_a are time dependent. However, the change in the chloride

diffusion coefficient decays with time and becomes almost negligible after 20-30 years when exposed to chloride laden environment, while the surface chloride of concrete reaches its maximum value after 5-10 years when submerged in seawater or exposed to the marine splash (Poulsen and Mejlbro, 2006). Based on these observations, the current model was developed by considering the time dependency for a period ranging from 5 to 10 years for C_s and 20 to 30 years for D_a of the life of the concrete. Accordingly, the chloride exposure in concrete was divided into three different periods:

- Period 1: having an increase in the surface chloride and a decrease in the diffusion coefficient,
- Period 2: having a decrease in D_a with constant C_s, and
- Period 3: both the C_s and D_a become constants.

Thus, based on these exposure periods, it is not applicable to predict the chloride diffusion process using a single model. Accordingly, three different models were used for the three different periods. The first period is the most complicated to model since both the C_s and D_a are time dependent. Several models have been developed for the diffusion coefficient using a time dependent exponential decay model as shown in Eq. (11.4) [Tang and Nilsson, 1992; Maage et al., 1995; Frederiksen et al., 1997; Takewaka and Mastumoto, 1988]:

$$D_a = D_r \left(\frac{t_a}{t_r}\right)^{-m} \qquad \text{Eq. 11.4}$$

Where:

D_a = the diffusion coefficient at time t_a,

D_r = a factor which can be explained as the value of the achieved chloride diffusion coefficient after a time t_r.

The D_r is typically found by conducting the chloride profile at time t_r, however, it has been suggested in literature that the D_r at a certain period (i.e. 28 days or 1 year) can be modeled as a function of the w/cm ratio and cementitious combination. The m is the decay coefficient, an age parameter which is dependent on the concrete composition and its environment.

The surface chloride build-up with time have been observed by researchers in three different forms. Mustafa and Yusof (1994), Swamy et al. (1998), Costa and Appelton (1999), and Meira et al. (2010), observed a linear trend in the surface chloride buildup with time. Uji et al. (1990), Purvis et al. (1994), Kato et al. (2005), and Shin and Kim (2002) observed that the surface chloride increase is proportional to the square root of the time. Swamy and Laiw (1995) have showed through a comprehensive investigation that it is most accurate to assume that the surface chloride is increasing with time as a power function. There exist simple solutions for the Fick's Second Law in the case where the surface chloride buildup with time follows either a linear or a square root trend (Crank, 1975); however, it is far more complicated to find a solution based on the power function buildup of surface chloride

In this study, the time dependent $D_a(t)$ and $C_s(t)$ functions were modeled based on the D_a and C_s values at 90, 180, and 360 days chloride profiles and that were calculated using Eq. (11.2). The D_a and C_s values were determined using the least square method by means non-linear regression analysis. For full details of D_a and C_s calculations using Matlab® software, see Appendix G.

The initial chloride was less than 0.04% for all the specimens and so it was assumed to be zero. The D_a results are presented in Table 11-1 and Table 11-2 for concrete mixes batched with natural sand and combined sand, respectively, and the C_s results are presented in Table 11-3 and Table 11-4 for concrete mixes batched with natural sand and combined sand,

respectively. Although Eq. (11.2) assumes a constant D_a and C_s, it was apparent that the D_a decreased while the C_s increased with the increase in the chloride exposure period. Thus, using a constant D_a and C_s will not lead to accurate chloride prediction especially when the concrete contains SCMs (Mendham et al., 2000; Stanish and Thomas, 2003). Based on the D_a results at 90, 180, and 360 days a best fitting curve was applied in the form of a power function as shown below:

$$D(t) = k_D t^{-m} \qquad \text{Eq. 11.5}$$

The k_D and m are the coefficients of the best fitting curve function and were found for each concrete mix as shown in Table 11-1 and Table 11-2. The C_s was found to have a power function as a best fit curve with time based on the 90, 180, and 360 days chloride profiles; however, since it's quite complicated to model the chloride diffusion using $C_s(t)$ as a power function, a square root function with time was applied as shown in Eq. (11.6).

$$C_s(t) = k_C\sqrt{t} \qquad \text{Eq. 11.6}$$

The coefficient k_C for each concrete mix is presented in Table 11-3 and Table 11-4 for concrete mixes batched with natural and combined sand, respectively. An example of the best fitting curves for C_s and D_a versus time is shown in Figure 11-1 for mixes made with C2 cement source and batched with combined sand. Both the $D(t)$ and the $C_s(t)$ functions showed acceptable correlation coefficient (R^2) with time (see Table 11-1 to Table 11-4) which indicates that these functions can be relied upon for extrapolating the chloride profiles at different periods. Few mixes however (C2IP-S-NS, C3-F-NS, C3IR-S-NS, and C3-F-CS) did not show an acceptable correlation with time for either $D(t)$ or $C_s(t)$ due to inconsistency in the experimental D_a and C_s values measured at 90, 180, and 360 days of chloride exposure.

Table 11-1. Experimental D_a based on ASTM C1556 with $D(t)$ Equation for Concrete Batched with Natural Sand

Mix Designation		W/CM ratio	Diffusion Coefficient (D_a), m^2/s					
			Chloride Exposure, Days			$D(t) = k_D t^{-m}$		
			90	180	360	k_D	m	R^2
Mixes batched with Natural Sand	C1-F-NS	0.40	2.58E-12	1.99E-12	1.02E-12	7.14E-11	0.722	0.91
	C1IP1-F-NS	0.40	1.73E-12	1.35E-12	8.07E-13	2.68E-11	0.598	0.93
	C1IP2-F-NS	0.42	2.34E-12	1.53E-12	1.20E-12	2.01E-11	0.484	0.98
	C1-S-NS	0.42	1.94E-12	1.65E-12	1.00E-12	2.12E-11	0.518	0.88
	C1IP1-S-NS	0.42	2.05E-12	1.28E-12	7.10E-13	9.20E-11	0.838	0.98
	C1IP2-S-NS	0.42	2.26E-12	1.61E-12	7.92E-13	7.22E-11	0.756	0.96
	C2-F-NS	0.40	2.81E-12	1.91E-12	1.25E-12	3.96E-11	0.587	1.00
	C2IP-F-NS	0.40	1.71E-12	1.16E-12	5.85E-13	5.89E-11	0.775	0.98
	C2-S-NS	0.42	1.85E-12	1.06E-12	7.55E-13	3.29E-11	0.647	0.98
	C2IP-S-NS(1)	0.42	1.50E-12	1.20E-12	1.26E-12	N/A	N/A	N/A
	C3-F-NS(1)	0.40	2.28E-12	1.20E-12	6.38E-13	N/A	N/A	N/A
	C3IR-F-NS	0.40	1.81E-12	1.13E-12	6.99E-13	3.97E-11	0.686	1.00
	C3-S-NS	0.42	1.71E-12	1.19E-12	9.60E-13	1.09E-11	0.417	0.98
	C3IR-S-NS(1)	0.42	2.29E-12	1.38E-12	5.54E-13	N/A	N/A	N/A

Note: 1 $m^2/s = 3.154 \times 10^{13}$ $mm^2/year = 10.7639$ ft^2/s

(1) The D_a did not show a consistent decreasing trend with the increase in exposure periods for mixes C2IP-S-NS, C3-F-NS, and C3IR-S-NS. Therefore, the test results were not used in the proposed model

R^2: Correlation Coefficient

Table 11-2. Experimental D_a based on ASTM C1556 with $D(t)$ Equation for Concrete Batched with Combined Sand

Mix Designation		W/CM ratio	Diffusion Coefficient (D_a), m^2/s					
			Chloride Exposure, Days			$D(t) = k_D t^{-m}$		
			90	180	360	k_D	m	R^2
Mixes batched with Combined Sand	C1-F-CS	0.42	2.85E-12	2.39E-12	1.22E-12	4.83E-11	0.611	0.90
	C1IP1-F-CS	0.42	2.87E-12	1.54E-12	8.95E-13	1.25E-10	0.841	1.00
	C1-S-CS	0.44	2.25E-12	1.24E-12	1.09E-12	2.19E-11	0.523	0.88
	C1IP1-S-CS	0.44	1.61E-12	1.17E-12	7.81E-13	1.72E-11	0.524	1.00
	C2-F-CS	0.42	1.85E-12	1.34E-12	6.81E-13	5.06E-11	0.722	0.96
	C2IP-F-CS	0.42	3.32E-12	1.46E-12	1.12E-12	1.04E-10	0.785	0.92
	C2-S-CS	0.44	1.92E-12	1.17E-12	9.25E-13	1.96E-11	0.526	0.96
	C2IP-S-CS	0.44	2.28E-12	1.23E-12	1.06E-12	2.51E-11	0.551	0.89
	C3-F-CS(1)	0.42	4.05E-12	1.91E-12	9.05E-13	N/A	N/A	N/A
	C3IR-F-CS	0.42	2.35E-12	1.88E-12	8.71E-13	6.46E-11	0.716	0.91
	C3-S-CS	0.44	1.53E-12	1.18E-12	7.45E-13	1.63E-11	0.518	0.97
	C3IR-S-CS	0.44	1.75E-12	1.12E-12	6.79E-13	3.86E-11	0.685	1.00

Note: 1 $m^2/s = 3.154 \times 10^{13}$ $mm^2/year = 10.7639$ ft^2/s

(1) The D_a did not show a consistent decreasing trend with the increase in exposure periods for mix C3-F-CS. Therefore, the test results were not used in the proposed model

R^2: Correlation Coefficient

Table 11-3. Experimental C_s based on ASTM C1556 with $C_s(t)$ Equation for Concrete Batched with Natural Sand

Mix Designation		W/CM ratio	Surface Chloride (C_s), %				
			Chloride Exposure, Days			$C_s(t) = k_C\sqrt{t}$	
			90	180	360	k_C	R^2
Mixes batched with Natural Sand	C1-F-NS	0.40	0.528	0.637	0.861	0.074	0.99
	C1IP1-F-NS	0.40	0.425	0.534	0.740	0.067	1.00
	C1IP2-F-NS	0.42	0.468	0.638	0.861	0.065	1.00
	C1-S-NS	0.42	0.484	0.543	0.869	0.071	0.97
	C1IP1-S-NS	0.42	0.540	0.673	0.861	0.079	0.99
	C1IP2-S-NS	0.42	0.583	0.646	0.816	0.074	0.95
	C2-F-NS	0.40	0.332	0.395	0.570	0.043	0.98
	C2IP-F-NS	0.40	0.321	0.422	0.522	0.049	0.97
	C2-S-NS	0.42	0.300	0.385	0.506	0.044	0.98
	C2IP-S-NS[(1)]	0.42	0.347	0.410	0.556	0.046	0.98
	C3-F-NS[(1)]	0.40	0.466	0.562	0.628	0.061	0.92
	C3IR-F-NS	0.40	0.479	0.567	0.772	0.070	0.98
	C3-S-NS	0.42	0.597	0.696	0.756	0.075	0.90
	C3IR-S-NS[(1)]	0.42	0.501	0.742	1.301	0.100	1.00

Table 11-4. Experimental C_s based on ASTM C1556 with $C_s(t)$ Equation for Concrete Batched with Natural Sand

Mix Designation		W/CM ratio	Surface Chloride (C_s), %				
			Chloride Exposure, Days			$C_s(t) = k_C\sqrt{t}$	
			90	180	360	k_C	R^2
Mixes batched with Combined Sand	C1-F-CS	0.42	0.402	0.439	0.482	0.042	0.87
	C1IP1-F-CS	0.42	0.366	0.457	0.497	0.045	0.92
	C1-S-CS	0.44	0.431	0.501	0.609	0.053	0.95
	C1IP1-S-CS	0.44	0.488	0.489	0.654	0.057	0.93
	C2-F-CS	0.42	0.333	0.428	0.520	0.048	0.96
	C2IP-F-CS	0.42	0.380	0.443	0.479	0.043	0.89
	C2-S-CS	0.44	0.377	0.560	0.613	0.053	0.95
	C2IP-S-CS	0.44	0.449	0.616	0.722	0.064	0.97
	C3-F-CS[(1)]	0.42	0.427	0.536	0.666	0.057	0.97
	C3IR-F-CS	0.42	0.449	0.459	0.677	0.057	0.96
	C3-S-CS	0.44	0.502	0.607	0.807	0.072	0.98
	C3IR-S-CS	0.44	0.706	0.718	0.788	0.081	0.83

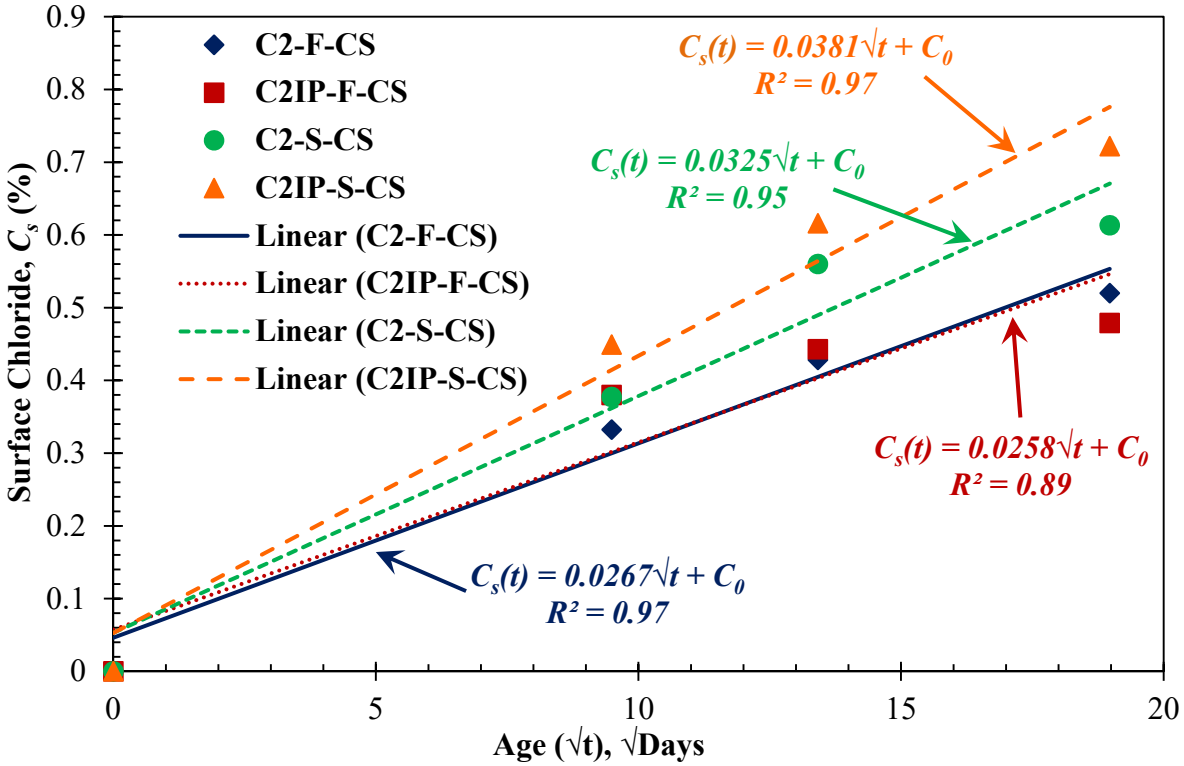

(a) C_s versus square root of the time

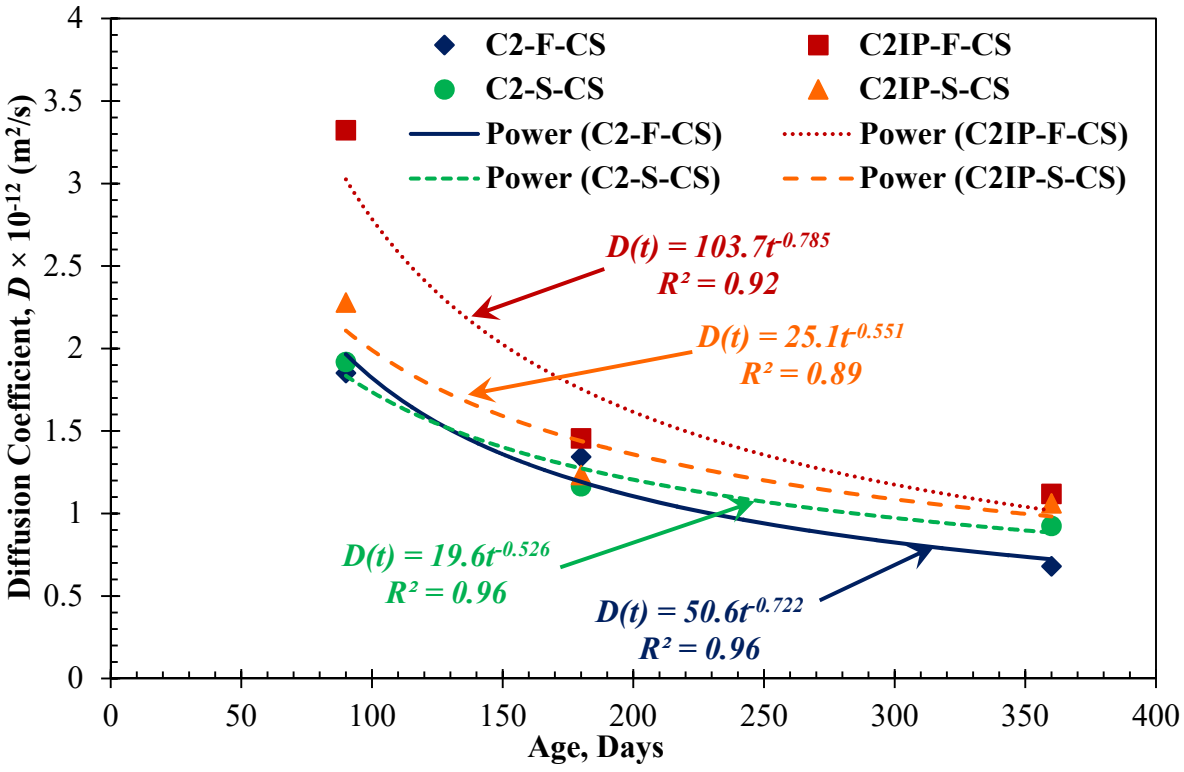

(b) D_a versus time

Figure 11-1. Modeling the diffusion coefficient (D_a) and surface chloride C_s with time (t)

11.4.1. Period 1: C_s is increasing and D_a is decreasing

In the first period, both the diffusion coefficient and surface chloride are assumed to be time dependent. The model can be developed based on Crank (1975) solution for a semi-infinite media with a constant D_a and C_s varying with respect to the square root of the time. The solution is presented in Eq. (11.7) and is also adopted by the ACI 365.1R:

$$C(x,t) = C_i + k_C\sqrt{t}\left\{exp\left(-\frac{x^2}{4D_a t}\right) - \frac{x\sqrt{\pi}}{2\sqrt{D_a t}}erfc\left(\frac{x}{2\sqrt{D_a t}}\right)\right\} \qquad \text{Eq. 11.7}$$

Where:

k_C is the coefficient of $C_s(t)$ in Eq. (11.6), and

erfc is the complementary error function where $erfc(x) = 1 - \text{erf}(x)$.

In order to account for the time-dependent diffusion coefficient $D(t)$, Eq. (11.7) can be used under the condition that the D_a is independent of other variables (Crank, 1975). In this case the Fick's second law of diffusion equation (Eq. 11.1) becomes

$$\frac{\partial C}{\partial t} = D(t)\frac{\partial^2 C}{\partial x^2} \qquad \text{Eq. 11.8}$$

By introducing T as the new time variable such that

$$dT = D(t)dt \qquad \text{Eq. 11.9}$$

Then Eq. (11.8) reduces to

$$\frac{\partial C}{\partial T} = \frac{\partial^2 C}{\partial x^2} \qquad \text{Eq. 11.10}$$

Integrating Eq. (11.9), and assuming an initial boundary condition of $T=0$ when $t=0$, will yield the following:

$$T = \frac{k_D}{m+1} t^{m+1} \qquad Eq.\ 11.11$$

The equation of T can be used in Eq. (11.7) to replace $D_a t$. Accordingly, this will yield the final form of the Fick's chloride diffusion equation for Period 1 (Eq. 11.12):

$$C = C_i + k_C \sqrt{t} \left[exp\left(-\frac{(m+1)}{4k_D} \frac{x^2}{t^{m+1}} \right) - \frac{1}{2} \sqrt{\frac{\pi(m+1)}{k_D}} \frac{x}{\sqrt{t^{m+1}}} erfc\left(\frac{1}{2} \sqrt{\frac{m+1}{k_D}} \frac{x}{\sqrt{t^{m+1}}} \right) \right] \qquad \text{Eq. 11.12}$$

In order to confirm the accuracy of Period 1 model, the modeled chloride profile for each concrete mix was compared with the experimental profiles after 90, 180, and 360 days of chloride exposure. Figure 11-2 shows an example for the fitting curves versus the experimental for Mix C2-S-CS. It can be observed that the model shows a good fit with the experimental chloride profiles.

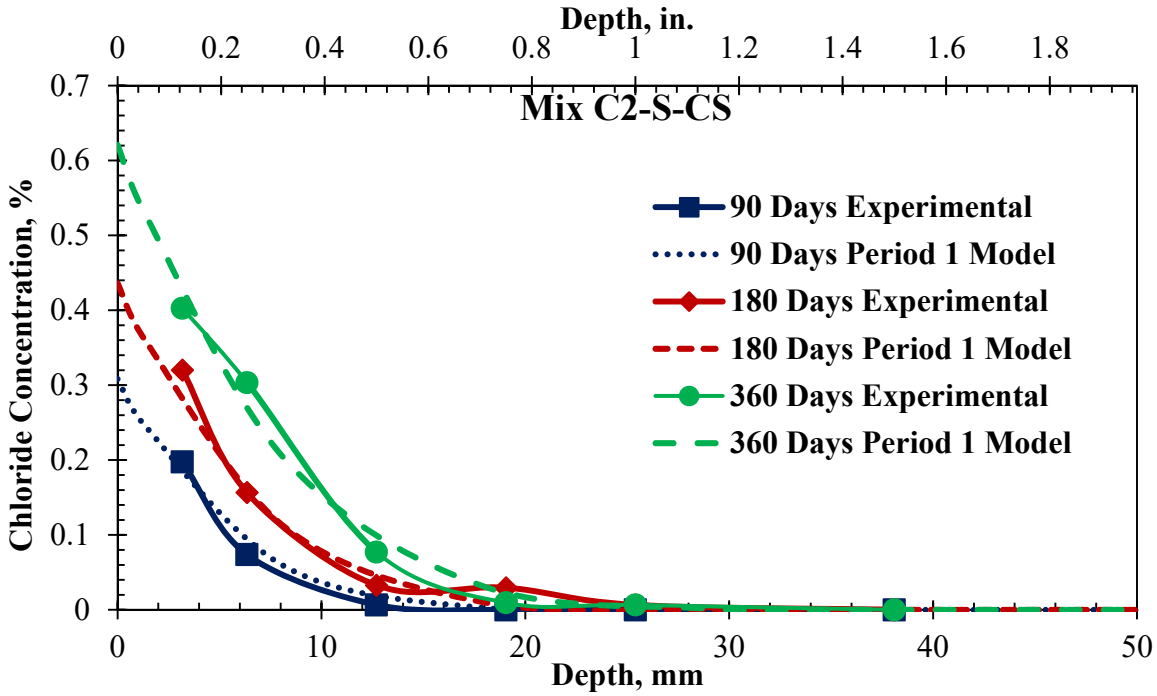

Figure 11-2. Experimental chloride profile vs. Period 1 model for Mix C2-S-CS

11.4.2. Period 2: C_s is constant while D_a decreases

The second period will experience a further decay in the diffusion coefficient without an increase in the surface chloride. The diffusion model for this period was developed in a similar fashion to Period 1 model, but using Eq. (11.2) where both the D_a and C_s are constants. By assuming that D_a is time-dependent and following the steps from Eq. (11.8) to Eq. (11.10), the final form of the Fick's chloride diffusion equation for Period 2 will be as shown in Eq. (11.13):

$$C = C_i + (C_{s1} - C_i) erfc\left(\frac{1}{2}\sqrt{\frac{m+1}{k_D}}\frac{x}{\sqrt{t^{m+1}}}\right) \qquad \text{Eq. 11.13}$$

Where C_{s1} is the surface chloride profile at the end of Period 1 and is considered constant in the following periods. Since the boundary conditions has changed in Period 2, the current equation will not yield the same chloride profile as obtained from Period 1 at the same exposure period. Therefore, an equivalent time at the start of Period 2 should be determined that yield the same chloride at the end of Period 1, while the D_a will continue to decrease for Period 2. Zhou (2014) used a constant equivalent time that results in an approximate but not exact equivalent chloride profile. It was observed that the equivalent time is dependent on the depth of the chloride profile. Accordingly, a more rigorous approach was used to obtain a relation between the equivalent time and the depth of the chloride profile at the end of Period 1. The equivalent time at each depth x is obtained by equating the chloride profile at the end of Period 1 (Eq. 11.12) with the chloride profile at the start of Period 2 (Eq. 11.13). This will result in the equation shown below:

$$t_{1.2eq.} = \left[2\sqrt{\frac{k_D}{m+1}}\frac{x}{inverfc\left(\frac{C_{s1}-C_i}{C_1-C_i}\right)}\right]^{\frac{2}{m+1}} \qquad \text{Eq. 11.14}$$

Where k_D and m are the coefficients of the D_a function in Eq. (11.5), i*nverfc* is the inverse of the complementary error function (*erfc*), and C_1 is the chloride concentration at each depth x at the end of Period 1. Figure 11-3(a) shows the trend of the equivalent time versus the depth of chloride (x) for mixes made with C2 cement and combined sand. It is observed that the equivalent time at the start of Period 2 increases linearly with respect to the depth of the chloride. Therefore, for each concrete mix, a linear equation was used to interpret the equivalent time as a function of the depth (x) of chloride in concrete (see Figure 11-3a). The equivalent time equation was then used in Eq. (11.13) to determine the equivalent chloride profile at the start of Period 2. Inspection of Figure 11-3(b) reveals a perfect fit between the chloride profiles at the end of Period 1 (using Eq. 11.12) and at the beginning of Period 2 (using Eq. 11.13) for mixes C2-F-CS and C2IP-F-CS.

Using the equivalent time, however, might not lead to accurate chloride profile prediction at later age since the rate of chloride buildup with time depends on the age of chloride exposure. Figure 11-4 shows an example of the chloride buildup with time for Mix C2-F-CS and based on ASTM C1556, using D_a and C_s computed after 360 days of chloride exposure. Inspection of Figure 11-4, reveals that the rate of chloride buildup decreases with the increase in the age of chloride exposure. For instance, the increase in chloride content between 7.5 years and 25 years is higher than between 25 and 50 years. Accordingly, in order to accurately predict the chloride profile at anytime t_2 within Period 2, an equivalent time $t_{2eq.}$ can be calculated such that:

$$t_{2eq.} = \frac{t_2}{t_{1.2}} t_{1.2eq.} \qquad \text{Eq. 11.15}$$

Where $t_{1.2}$ is the real time at the beginning of Period 2 and $t_{1.2eq.}$ is the equivalent time of $t_{1.2}$ based on Eq. (11.14).

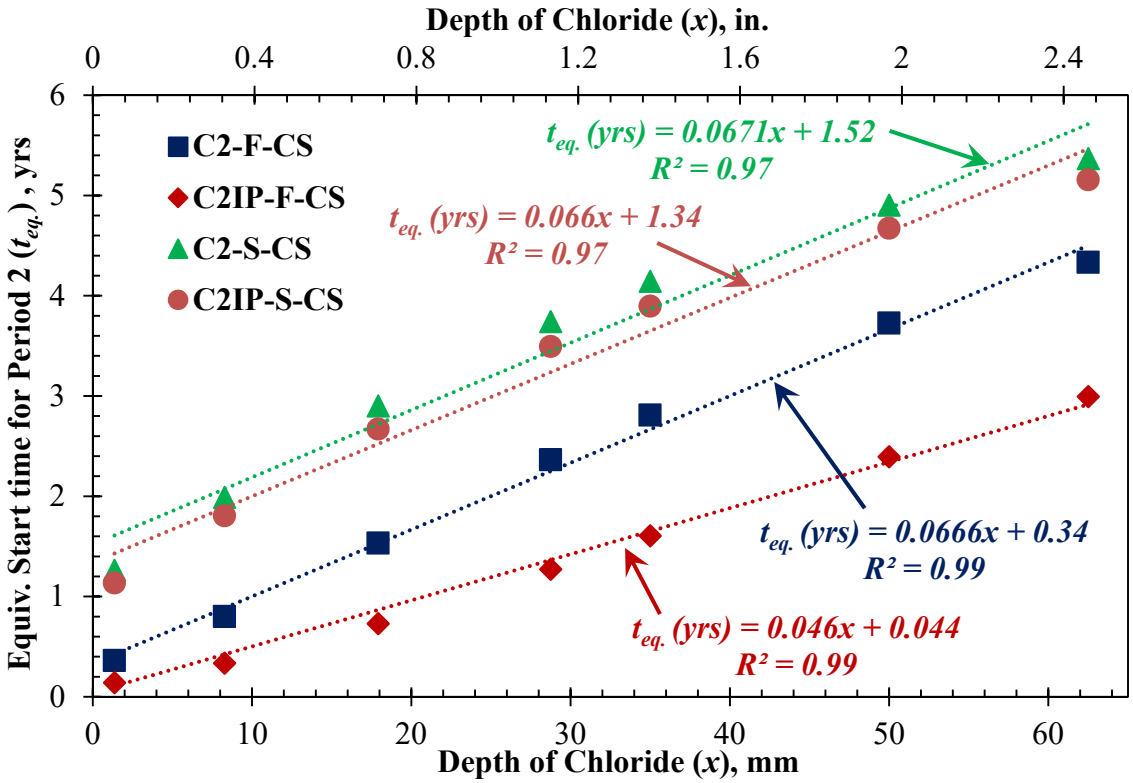

(a) Equivalent time vs. depth of chloride

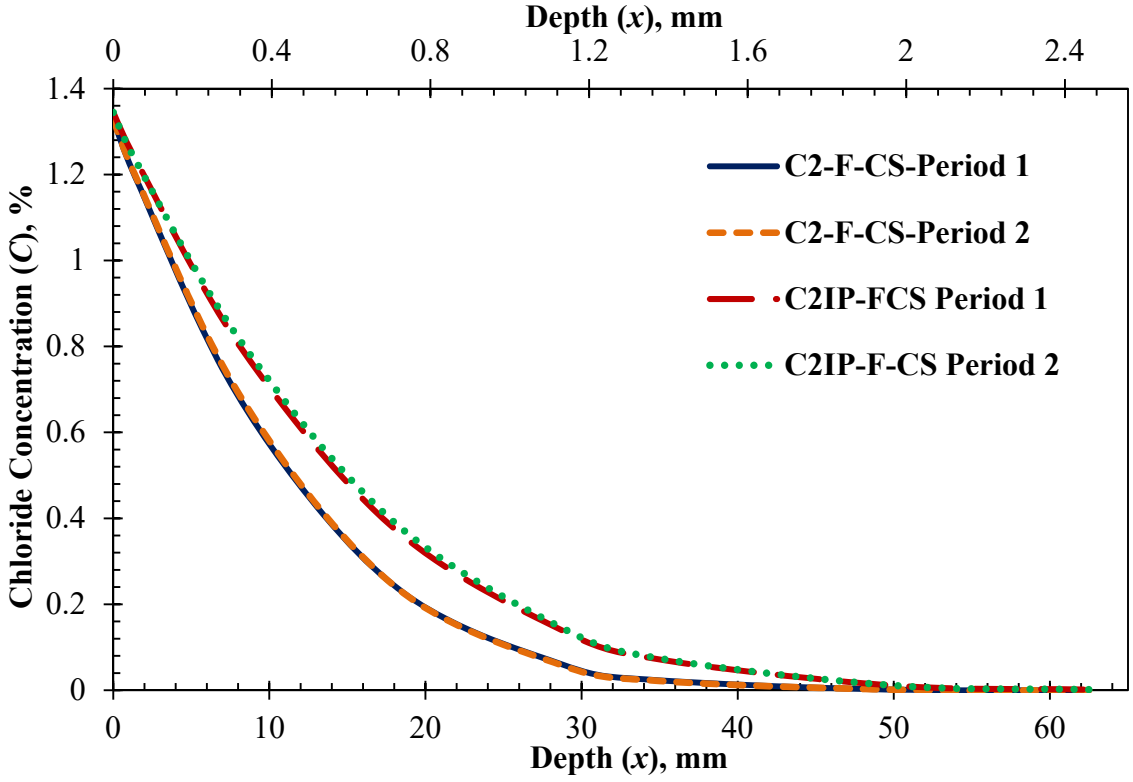

(b) Period 2 vs. Period 1 chloride profiles

Figure 11-3. Time equivalent ($t_{eq.}$) for transition from Period 1 to Period 2 model

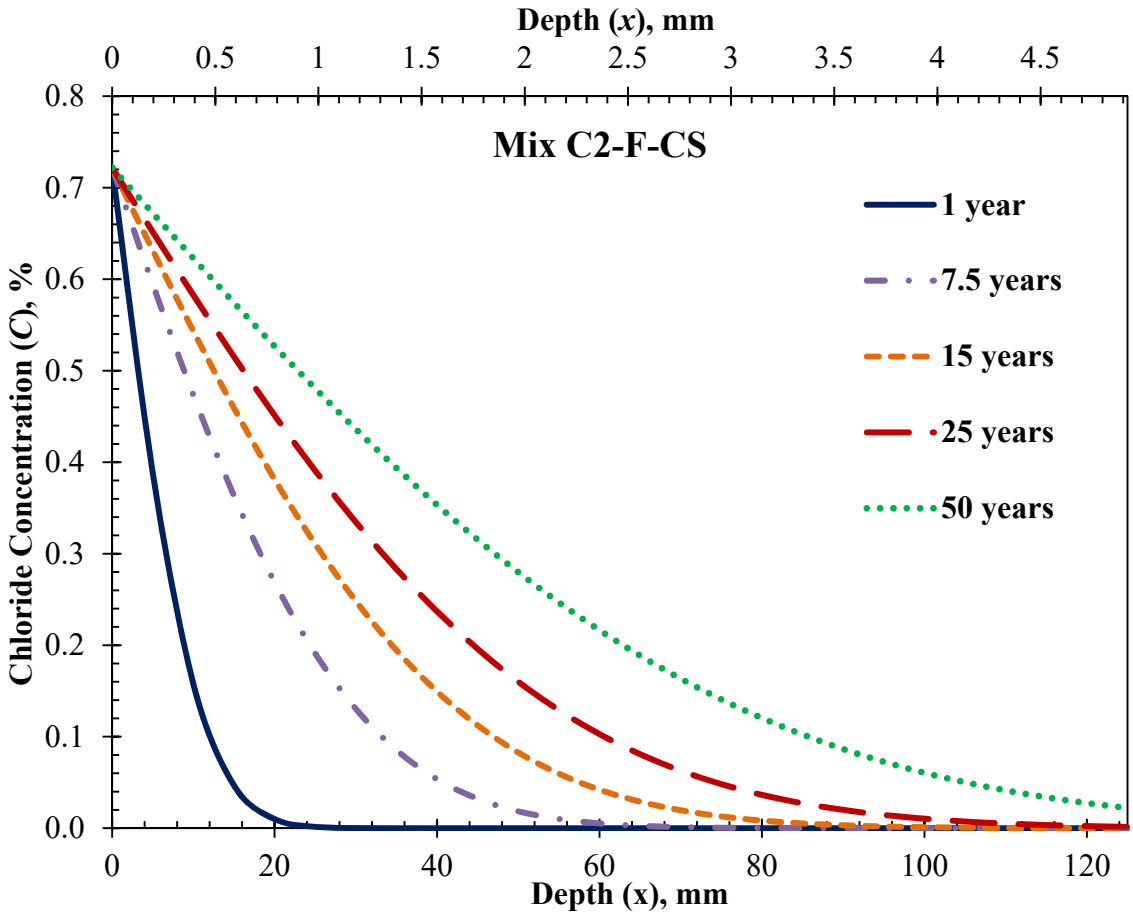

Figure 11-4. Example of chloride profile buildup for mix C2-F-CS and based on Eq. (10.2)

11.4.3. Period 3: C_s and D_a are constants

In Period 3, both the C_s and D_a are considered constant with time. Therefore, Eq. (11.2) can be applied directly with the exception that a time equivalent should be obtained to get a similar profile at the beginning of Period 3 to that at the end of Period 2 (using Eq. 11.13). The equivalent time for the start of Period 3 can be obtained in a similar fashion to the equivalent time obtained for the start of Period 2. Therefore, the time equivalent equation for this period as a function of the depth of chloride (x) is shown below:

$$t_{2.3eq.} = \left[\frac{1}{D_2}\frac{x}{inverfc\left(\frac{C_2 - C_i}{C_{s1} - C_i}\right)}\right]^2 \qquad \text{Eq. 11.16}$$

Where D_2 is the constant diffusion coefficient obtained at the end of Period 2 from Eq. (11.5) and C_2 is the chloride concentration at each depth x at the end of Period 2. For each concrete mix, a linear equation was used to interpret the equivalent time at the beginning of Period 3 as a function of the depth (x) of chloride in concrete. In order to accurately predict the chloride profile at anytime t_3 after the beginning of Period 3, an equivalent time $t_{3eq.}$ can be calculated such that:

$$t_{3eq.} = \frac{t_3}{t_{2.3}} t_{2.3eq.} \qquad \text{Eq. 11.17}$$

Where $t_{2.3}$ is the real time at the beginning of Period 3 and $t_{2.3eq.}$ is the equivalent time of $t_{2.3}$ based on Eq. (11.16).

11.5. Service Life Prediction Models:

Chloride-ion penetration into concrete will cause corrosion initiation once the chloride ion reaches the threshold value at the level of steel reinforcement. The tested concrete mixes were designed for concrete pavements and bridge decks. Six different service life predictions were performed. The first service life prediction (Model 1) was obtained based on the experimental results after 360 days salt ponding and using constant C_s and D_a according to ASTM C1556. The second one (Model 2) was performed based on the newly developed model incorporating the three different periods.

The third service life prediction (Model 3) was performed using Life-365 software (Bentz and Thomas, 2014). The diffusion and decay coefficients for the Life-365 were predicted using Eq. (11.18) and Eq. (11.19) [Bentz and Thomas, 2014].

$$D(t) = D_{28}\left(\frac{t_{28}}{t}\right)^{m} \qquad \text{Eq. 11.18}$$

$$m = 0.2 + 0.4\left(\frac{FA}{50} + \frac{SG}{70}\right) \qquad \text{Eq. 11.19}$$

Where D_{28} is the diffusion coefficient after 28 days of curing (t_{28}) and is calculated using Eq. (11.20) [Bentz and Thomas, 2014]:

$$D_{28} = 10^{(-12.06+2.4w/cm)} \quad (m^2/s) \qquad \text{Eq. 11.20}$$

FA and *SG* are the percent replacement by weight of Class C fly ash and GGBF slag, respectively.

The fourth model (Model 4) used Life-365 software but by applying decay and 28 days diffusion coefficient equations proposed by Riding et al. (2013) shown in Eq. (11.21) and Eq. (11.22).

$$m = 0.26 + 0.4\left(\frac{FA}{50} + \frac{SG}{70}\right) \qquad \text{Eq. 11.21}$$

$$D_{28} = 2.17 \times 10^{-12} e^{(3.584 \cdot w/cm)} \quad (m^2/s) \qquad \text{Eq. 11.22}$$

The fifth and sixth service life predictions (Models 5 and 6) were performed on the new model by using the *m* and D_{28} suggested by Life-365 (Bentz and Thomas, 2014) and Riding et al. (2013), respectively. It should be noted that Models 5 and 6 were performed for comparison with the Life-365 software (Models 3 and 4).

The analysis for the Life-365 were modeled for an urban highway bridge with 2.5 in. concrete cover above the steel reinforcement subject to deicing salt in Chicago, IL. The same

assumptions for the periods that are used in the Life-365 were used in the proposed models. Period 1 lasted 7.1 years, while Period 2 ranged from 7.1 to 25 years, after which it is transferred to Period 3. Wide range of threshold values are reported in the literature. Daigle et al. (2004) suggested using chloride threshold about 0.11% by weight of concrete for concrete with SCMs which was used by Issa and Khalil (2010) who predicted the service life for binary and ternary concrete mixes designed for bridge decks.

11.6. Results and Discussion

11.6.1. Diffusion Test Results based on ASTM C1556

The apparent diffusion coefficients and surface chloride concentrations presented in Table 11-1 through Table 11-4 varied depending on the cement source, the addition of limestone, IPA, and/or IR, the type of SCM used, and the sand type. It is expected that concrete with lower diffusion coefficient will have better resistance to chloride penetration because it indicates that less chloride ions will diffuse into the concrete.

11.6.1.1. Effect of Limestone, IPA, and IR Addition on the Diffusion Parameters

The limestone and IPA were added to C1 and C2 cements to produce C1IP and C2IP, respectively. Inspection of Table 11-1, reveals that the D_a at 360 days for mixes made with C1 and fly ash, and batched with natural sand was lowest for C1IP1-F-NS and highest for C1IP2-F-NS. The latter has higher content of limestone and IPA but had a higher w/cm of 0.42 compared to its counterparts that are made with 0.40. The D_a at 90 and 180 days, however, for C1IP2-F-NS was lower than the D_a in C1-F-NS. This indicates that the diffusion coefficient decayed at a faster rate for mix C1-F-NS. The surface chloride buildup for mixes made with C1 and natural sand was quite consistent and was not influenced by the cementitious combination. Similarly, mixes made with C2 and natural sand showed lower D_a for C2IP in

comparison to C2 mixes except for mix C2IP-S-NS, which did not show a consistent decay in the D_a with time after 90, 180, and 360 days chloride exposure. In addition, the D_a for mixes made with C1 source and batched with combined sand (see Table 11-2) was lower for C1IP compared to C1 cement. In contrary, mixes with C2 cement source and combined sand were the only ones to show higher D_a for C2IP cement at all ages, though the decay coefficient m was higher for mixes with C2IP. Higher decay coefficient values will lead to lower diffusion coefficients and indicates that the cement matrix becomes less porous with time. It is expected that the cement with IPA will experience lower chloride diffusion since the IPA was blended with the cement in the form of GGBF slag which, as a result, improved the porous structure.

The effect of increasing the insoluble residue (IR) in C3 cement (0.75% IR) to produce C3IR cement with 1.5% IR did not show a notable difference on the D_a for comparable concrete mixes batched with natural sand or combined sand, except for C3IR-S-NS, which showed much lower D_a at 360 days and higher decay coefficient. This shows that raising the IR content from 0.75 to 1.5% have negligible effect on the chloride diffusivity into concrete.

11.6.1.2. Effect of Class C fly ash and GGBF Slag

Each cement source used in the twenty six concrete mixes was partially replaced by 30% by weight with Class C fly ash or GGBF slag. Fly ash and slag are known to have a beneficial effect in reducing the diffusivity in concrete over time and improving the service life of reinforced concrete structures. The diffusion coefficients shown in Table 11-1 reveal that both the fly ash and slag have comparable diffusion coefficients after 90, 180, and 360 days of chloride exposure. It is noteworthy to mention that concrete mixes with slag had an increase in w/cm ratio by 0.02 compared to their counterparts made with fly ash. It is revealed from Table 11-1, that both the slag and fly ash did not show a consistent difference in the diffusion

coefficient for concrete mixes with C1 cement and natural sand and at all chloride exposure ages; i.e. the diffusion coefficients for mixes C1-F-NS and C1-S-NS had the same diffusion coefficient after 360 days of chloride exposure with 1.02×10^{-12} and 1.0×10^{-12} m^2/sec, respectively. This inconsistent difference was also apparent in concrete mixes made with C2 and C3 cement and batched with natural sand. Mixes C2-F-NS and C3IR-F-NS had slightly higher D_a after 360 days of chloride exposure than their counterparts C2-S-NS and C3IR-S-NS. On the contrary, mixes C2IR-S-NS and C3-S-NS had slightly higher D_a after 360 days of chloride exposure than their counterparts C2IR-F-NS and C3-F-NS. In addition, it is revealed that there wasn't a notable difference in the decay coefficient m with some mixes with fly ash or slag having higher m than their counterparts.

The chloride exposure after 90 and 180 days for concrete mixes batched with combined sand resulted in higher D_a for mixes with fly ash but slightly higher or similar D_a to concrete mixes with slag after 360 days of exposure, except for mix C2-F-CS which had slightly lower D_a than its counterpart C2-S-CS (see Table 11-2). Nevertheless, it was apparent that the decay coefficient m was higher for all concrete mixes with fly ash. This indicates that the D_a for mixes with fly ash decreased at a faster rate with time when batched with combined sand. This faster decay can also be attributed to the slightly lower w/cm ratio in the mixes with fly ash.

11.6.1.3. *Effect of Sand Type*

Concrete mixes batched with combined sand had an increase in w/cm ratio by 0.02 compared to their counterparts batched with natural sand. The diffusion coefficients after 90 and 180 days of chloride exposure for similar concrete mixes batched with either natural or combined sand were slightly inconsistent. Some of the concrete mixes from both sand types resulted in higher D_a than their counterparts. However, the D_a after 360 days of chloride exposure was

quite similar between the two sand types for same concrete mixes. Although both natural and combined sand revealed comparable results, it could be concluded that the combined sand can slightly reduce the chloride diffusion over time since all the combined sand mixes were made with slightly higher w/cm ratio than their counterparts. The improved D_a in the concrete mixes batched with combined sand can be attributed to the inclusion of the limestone by-product in the combined sand that part of it can perform as an added limestone filler to the total cementitious content, thereby affecting the tortuosity of the cementitious matrix (Hornain et al., 1995). This reduction was also observed by Akrout et al. (2010) in mortar mixes batched with limestone sand in comparison to siliceous sand.

11.6.2. Service Life Prediction Results

One of the reasons for increasing the amount of limestone and IPA as well as the IR in cement is to reduce the carbon foot print in cement production. However, this might result in affecting the service life of concrete and increase the diffusion of chlorides which will lead to reduce the time to initiation of corrosion at the level of steel reinforcements. Service life prediction analysis was performed in order to have a better understanding of the effect of the limestone, IPA, and IR on the time to initiation to corrosion. Six different models were used to assess the service life of the twenty six concrete mixes including the model proposed in this study. Table 11-5 and Table 11-6 present the time to threshold for all the models and the decay coefficients for the proposed model (Model 2), the Life-365 software model (Model 3), and the model based on Riding et al. (2013) [Model 4] for concrete mixes batched with natural sand and combined sand, respectively. As shown in both tables, the decay coefficients for the proposed model which are based on the diffusion coefficients for the 90, 180, and 360 days experimental chloride profiles were higher than all the values predicted by Eq. (11.19) and most of the values

predicted by Eq. (11.21). This indicates that these equations are very conservative in predicting the time to threshold. The time to threshold results for the twenty six concrete mixes based on the six models in Table 11-5 and Table 11-6 are shown in Figure 11-5 and Figure 11-6 for mixes batched with natural and combined sand, respectively.

Table 11-5. Decay Coefficients and Time to Initiation of Corrosion (Time to Threhold) for Concrete Mixes Batched with Natural Sand

Mix Designation	Model 1	Model 2				Model 3(1)		Model 4(1)		Model 5(1)	Model 6(1)
	ASTM C1556 for 360 days chloride profiles	Proposed Model				Life-365 software		Riding et al. D_{28} and m using Life-365 software		Prop. Model with Life-365 D_{28} and m	Prop. Model with Riding et al. D_{28} and m
	$T_{th.}$	C_s	k_D	m	$T_{th.}$	m	$T_{th.}$	m	$T_{th.}$	$T_{th.}$	$T_{th.}$
C1-F-NS	26.9	2.51	7.14E-11	0.722	50.7	0.440	21.4	0.500	50.8	31.8	34.9
C1IP1-F-NS	38.0	2.15	2.68E-11	0.598	65.2	0.440	22.9	0.500	50.8	31.8	34.9
C1IP2-F-NS	23.0	2.39	2.01E-11	0.484	39.2	0.440	19.2	0.500	46.8	28.9	32.8
C1-S-NS	27.4	2.44	2.12E-11	0.518	46.0	0.371	13.8	0.431	31.2	21.2	25.7
C1IP1-S-NS	38.8	2.54	9.20E-11	0.838	64.3	0.371	13.6	0.431	31.2	21.2	25.7
C1IP2-S-NS	36.1	2.26	7.22E-11	0.756	61.7	0.371	14.2	0.431	31.2	21.2	25.7
C2-F-NS	30.3	1.44	3.96E-11	0.587	52.1	0.440	29.9	0.500	50.8	31.8	34.9
C2IP-F-NS	69.7	1.34	5.89E-11	0.775	103.0	0.440	31.4	0.500	50.8	31.8	34.9
C2-S-NS	55.7	1.28	3.29E-11	0.647	93.6	0.371	18.9	0.431	31.2	21.2	25.7
C2IP-S-NS	30.5	N/A	N/A	N/A	N/A	0.371	17.5	0.431	31.2	21.2	25.7
C3-F-NS	54.5	N/A	N/A	N/A	N/A	0.440	25.7	0.500	50.8	31.8	34.9
C3IR-F-NS	42.5	2.12	3.97E-11	0.686	76.7	0.440	23.5	0.500	50.8	31.8	34.9
C3-S-NS	31.4	2.16	1.09E-11	0.417	45.3	0.371	14.4	0.431	31.2	21.2	25.7
C3IR-S-NS	38.8	N/A	N/A	N/A	N/A	0.371	12.8	0.431	31.2	21.2	25.7

(1) The C_s is based on the default value of 0.85% for urban highway bridges in Chicago, IL and based on the Life-365 Software

Table 11-6. Decay Coefficients and Time to Initiation of Corrosion (Time to Threshold) for Concrete Mixes Batched with Combined Sand

Mix Designation	Model 1	Model 2				Model 3(1)		Model 4(1)		Model 5(1)	Model 6(1)
	ASTM C1556 for 360 days chloride profiles	Proposed Model				Life-365 software		Riding et al. D_{28} and m using Life-365 software		Prop. Model with Life-365 D_{28} and m	Prop. Model with Riding et al. D_{28} and m
	$T_{th.}$	C_s	k_D	m	$T_{th.}$	m	$T_{th.}$	m	$T_{th.}$	$T_{th.}$	$T_{th.}$
C1-F-CS	36.1	1.36	4.83E-11	0.611	52.1	0.440	26.2	0.500	46.8	28.9	32.8
C1IP1-F-CS	47.8	1.37	1.25E-10	0.841	68.6	0.440	26.2	0.500	46.8	28.9	32.8
C1-S-CS	32.7	1.63	2.19E-11	0.523	55.5	0.371	15.2	0.431	28.7	18.2	24.0
C1IP1-S-CS	43.1	1.75	1.72E-11	0.524	67.0	0.371	14.7	0.431	28.7	18.2	24.0
C2-F-CS	60.2	1.33	5.06E-11	0.722	93.5	0.440	27.6	0.500	46.8	28.9	32.8
C2IP-F-CS	39.6	1.34	1.04E-10	0.785	64.6	0.440	27.6	0.500	46.8	28.9	32.8
C2-S-CS	38.3	1.70	1.96E-11	0.526	61.3	0.371	14.7	0.431	28.7	18.2	24.0
C2IP-S-CS	29.4	1.97	2.51E-11	0.551	53.7	0.371	13.6	0.431	28.7	18.2	24.0
C3-F-CS	36.7	N/A	N/A	N/A	N/A	0.440	22.5	0.500	46.8	28.9	32.8
C3IR-F-CS	37.6	1.75	6.46E-11	0.716	63.3	0.440	23.2	0.500	46.8	28.9	32.8
C3-S-CS	38.7	2.16	1.63E-11	0.518	61.6	0.371	13.0	0.431	28.7	18.2	24.0
C3IR-S-CS	43.2	2.41	3.86E-11	0.685	74.1	0.371	12.5	0.431	28.7	18.2	24.0

(1) The C_s is based on the default value of 0.85% for urban highway bridges in Chicago, IL and based on the Life-365 Software

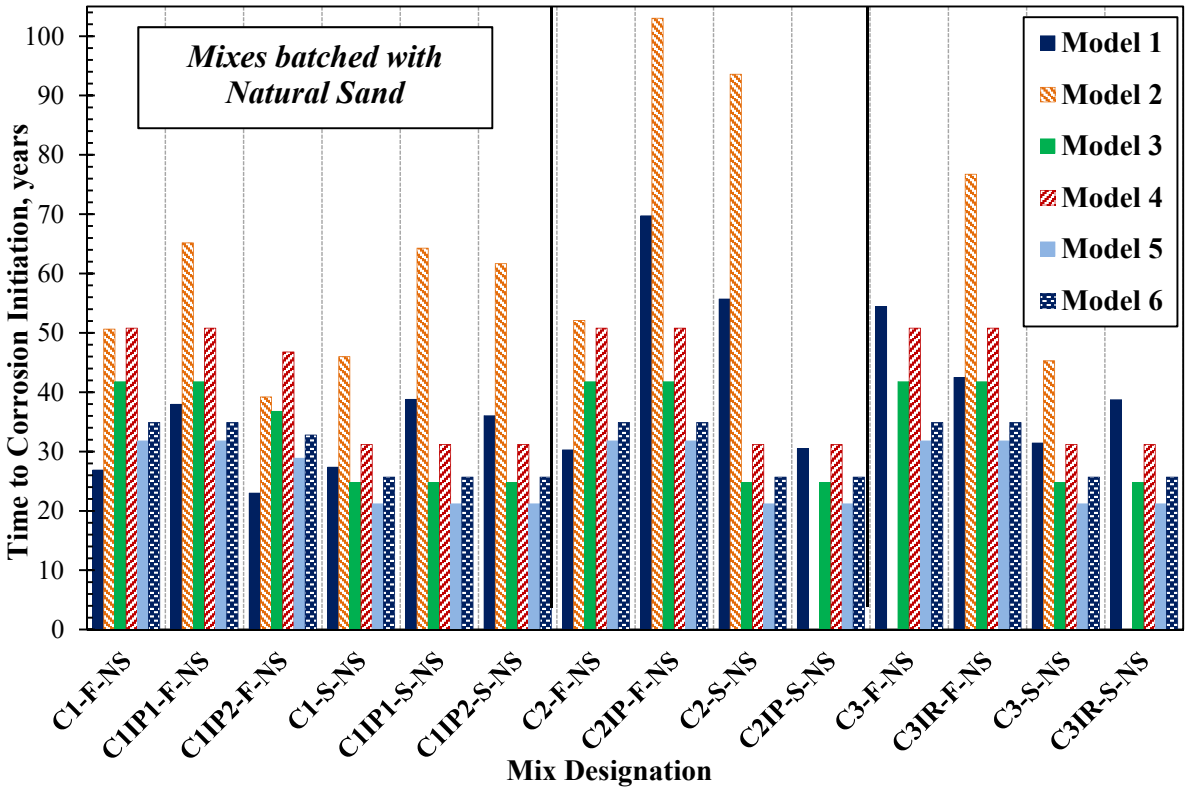

Figure 11-5. Service life prediction comparison between mixes batched with natural sand

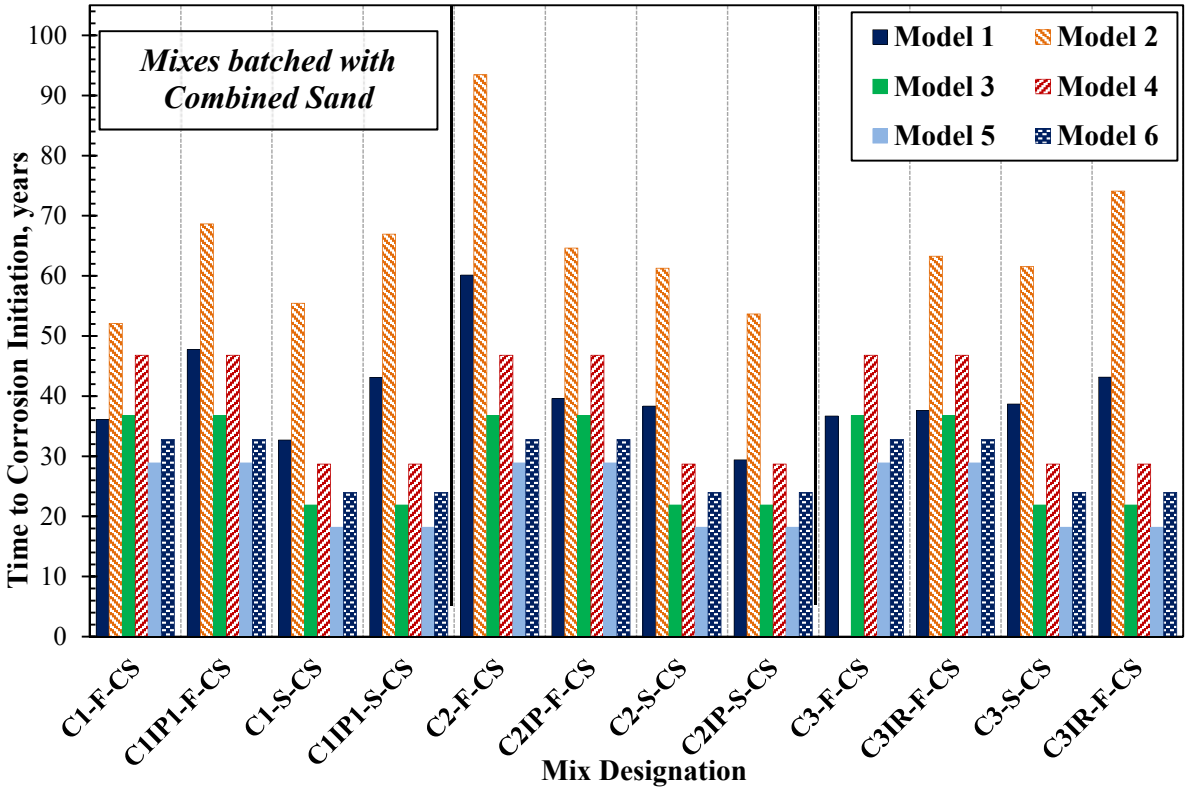

Figure 11-6. Service life prediction comparison between mixes batched with combined sand

The limestone, IPA, and IR additions did not seem to have notable influence on the time to thresholds based on Models 1 and 2, as shown in Figure 11-5 and Figure 11-6. In fact, some of the mixes with modified cement revealed better service life in Model 2 than their counterparts such as C2IP-F-NS which had the highest time to threshold of 103 years in comparison to C2-F-NS with 52 years; C3IR-F-NS and C3IR-F-CS revealed higher time to threshold as well. In addition, no notable difference was observed between the use of class C fly ash and GGBF slag knowing that most of the mixes with slag had higher w/cm by 0.02 than those with fly ash. This might appear in contrast to many findings including Burris and Riding (2014) who observed that concrete mixes with 25% GGBF slag replacements had much lower service life than their counterparts with Class F and Class C fly ash. This might be attributed to the fact that the chemical composition and physical properties of fly ash varies depending on their source of production Siddique and Khan (2011). In addition, most mixes batched with combined sand gave better service life prediction, as shown in Models 1 and 2, than their counterpart mixes batched with natural sand, although most of the mixes with combined sand were made with a w/cm ratio higher by 0.02.

Inspection of Figure 11-5 and Figure 11-6 reveals that the time to threshold for Model 1 was very conservative compared to Model 2. This is expected because Model 1 is based on the D_a and C_s after 360 days of chloride exposure that are assumed constant, while Model 2 results were based on time dependent C_s and D_a. On average, Model 2 results increased by 65% with a 12% standard deviation in comparison to Model 1 results. An excellent relation exists between Model 2 and Model 1 time to thresholds as shown in Figure 11-7. This suggests that the increase in the time for Model 2 was consistent for most of the concrete mixes and it was interdependent on both time variables D_a and C_s.

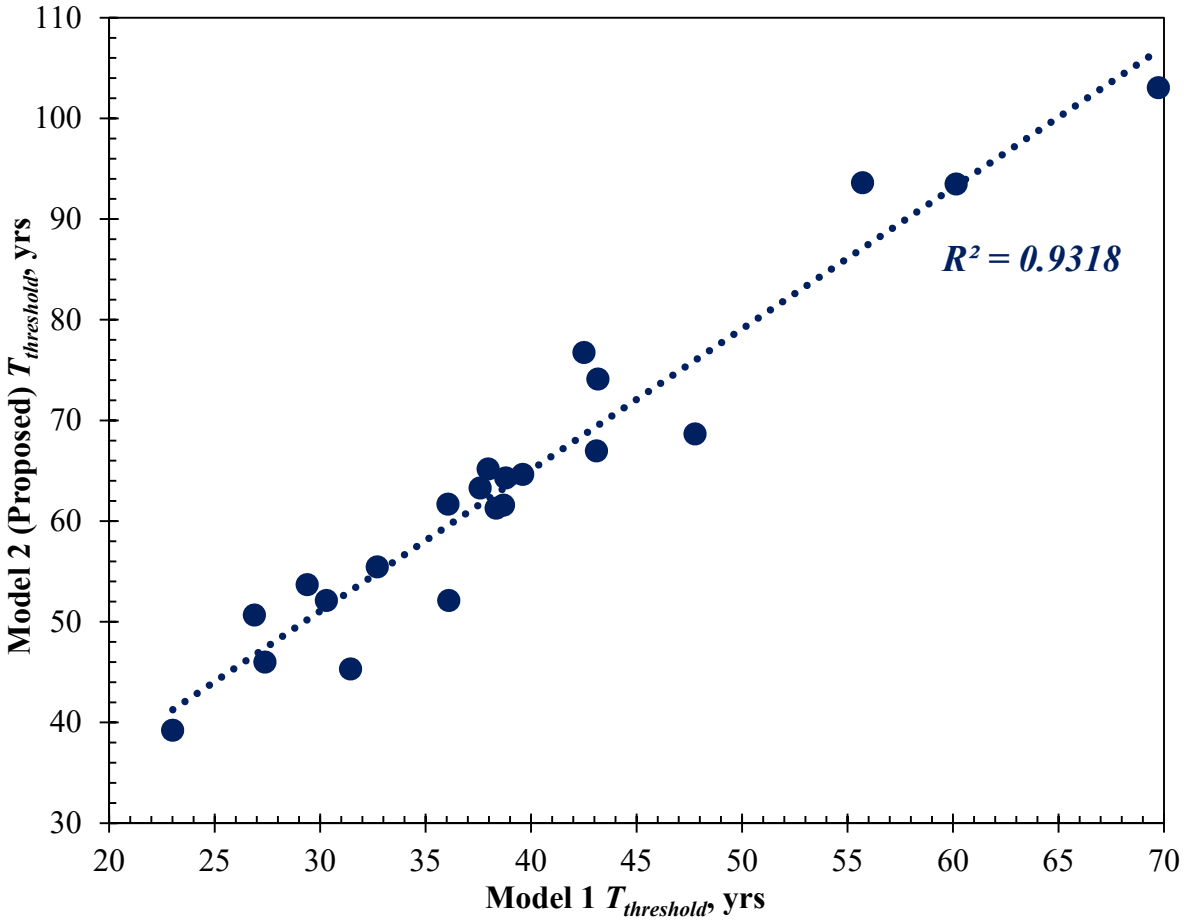

Figure 11-7. Relation between Model 1 and Model 2 time to threshold ($T_{th.}$)

The equations for Models 3 and 4 were applied to Life-365 software where the surface chloride was set by default to reach 0.85% after 7.1 years. Model 3 results were very conservative compared to Model 2 while Model 4 showed better prediction especially with mixes made with Class C fly ash owing to the increase in the decay coefficient in Eq. (11.21) and the better advantage of fly ash over GGBF slag.

In order to validate the use of the proposed model, Models 5 and 6 were applied on the proposed model using Eq. (11.19) and Eq. (11.20) for Life-365 and Eq. (11.21) and Eq. (11.22) for Riding et al. (2013), respectively. The surface chloride was assumed to be square root time dependent with 7.1 years to reach maximum C_s of 0.85%. The results for Models 5 and 6 have shown more conservative predictions than Models 3 and 4. This is attributed to the difference

in the surface chloride buildup between the proposed model and Life-365 software, which is based on the Crank Nicolson finite difference method (Crank, 1975). The latter assumes a linear surface chloride buildup with time in comparison to square root buildup with time in the proposed model. This indicates that the surface chloride in the proposed model is higher than the Life-365 before the maximum surface chloride is reached. It is noteworthy to mention that a similar approach to the proposed model can be used to develop a method based on linear surface chloride buildup with time.

12. SUMMARY AND CONCLUSION

12.1. Research Summary

This research was conducted to evaluate the performance of concrete mixes designed for pavements and bridges decks and made with cement with higher quantities of limestone and inorganic process additions (IPA) and with increased amount of insoluble residue (IR) exceeding what is recommended by the ASTM C150 standard specification for hydraulic cement.

A total of twenty eight concrete mix combinations were prepared. Two sources of cement were used, with less or exceeding 5% of limestone and IPA each (C1 and C2). A third source was introduced by blending C1 conventional cement, having less than 5% of limestone and IPA, with fly ash to produce C3 cement with 0.75 and 1.5% IR levels. In addition, each cement source was replaced by Class C fly ash and grade 100 GGBF slag with 30% replacement of the cementitious materials content levels by weight. The mixes were batched with one source of coarse aggregate (crushed limestone) and two sources of fine aggregates (natural or combined sand). The w/cm ratio specified for the concrete mixes ranged from 0.4 to 0.44.

The concrete mixes were batched according to ASTM C192/AASHTO T 126. The IDOT PCC Mix Design Version V2.1.2 was used to select the mix proportioning for each mix combination. Trial batches were made to calibrate each concrete mix to yield 5 to 8% air content and approximately 2 – 4 in. slump.

The fresh properties, including the measurement of slump, unit weight, air content (pressure meter), setting times, concrete mix temperature, ambient temperature, and humidity,

were successfully determined. The strength properties were tested for both compressive and flexural strengths. The compressive and flexural strengths for the 24 concrete mix combinations indicated acceptable results and exceeded the minimum target of 3500 and 600 psi (24 and 4.1 MPa) at 14 day. The durability properties included the measurement of the freeze/thaw test, hardened air content parameters, chloride ion penetration in concrete, water penetration test (DIN 1048), and rapid chloride penetration (RCP) test.

12.2. Conclusion

12.2.1. Effect of Limestone and IPA, and IR

The results of this study showed that increasing the amount of limestone and IPA in cement in quantities exceeding 5% by weight, and the increase of IR to 1.5% had negligible effect on the strength and durability properties of concrete. The performance of concrete mixes with modified cement is summarized as follows:

1. The modified cement improved the workability in concrete but slightly prolonged its initial and final setting times.
2. The modified cement had a negligible effect on the compressive and flexural strength properties concrete.
3. The modified cement had a negligible effect on the chloride ion concertation, water penetration, and rapid chloride concentration in concrete.
4. No notable influence was observed on the chloride diffusivity in concrete and the threshold time to corrosion initiation between conventional and modified cement.
5. The performance of concrete against freeze/thaw was comparable between concrete mixes made with conventional and modified cement.

12.2.2. Effect of Supplementary Cementitious Materials

The effect of slag and fly ash replacements is summarized as follows:

1. The use of Class C fly ash improved the workability of the concrete mix, but extended the initial and final setting periods for concrete.
2. The difference in the strength properties between concrete mixes with Class C fly ash or Grade 100 GGBF slag was inconsistent indicating neither of the SCM type used showed superiority in improving the strength in concrete.
3. The permeability properties in terms of chloride ion concentration, water penetration and rapid chloride concentration were comparable between concrete mixes with Class C fly ash and Grade 100 slag.
4. The difference in the diffusivity and time to threshold between concrete mixes with Class C fly ash or GGBF slag was inconsistent indicating neither of the SCM type used showed superiority in reducing the diffusivity in concrete.
5. Concrete mixes made with Grade 100 slag experienced less surface scaling than concrete mixes made with Class C fly ash under a freeze/thaw attack.

12.2.3. Effect of Sand Type

The effect of the sand type whether natural sand or combined sand was used is summarized as follows:

1. Concrete mixes batched with natural sand required much less admixture dosage for workability and reached the initial and final sets earlier than mixes batched with combined sand.

2. The difference in the strength properties between concrete mixes batched with natural sand or combined sand was inconsistent indicating neither of the sand type used showed superiority in improving the strength in concrete.
3. The permeability properties in terms of chloride ion concentration, water penetration and rapid chloride concentration were comparable between concrete mixes batched with natural sand or combined sand.
4. The use of combined sand slightly improved the diffusivity in concrete relative to the natural sand. This is attributed to the inclusion of limestone by-products in the combined sand where the very fine portion of it performed as an added limestone filler to the total cementitious content.
5. Concrete mixes batched with combined sand showed better resistance against freeze/thaw and less surface scaling than concrete mixes batched with natural sand.

12.2.4. Evaluation of the Freeze/Thaw Performance in Concrete

The full investigation of the freeze/thaw performance of concrete has yielded the following conclusions:

1. Lignosulfonate based water reducing admixture tends to increase the instability of the fresh air content when mixed with vinsol resin based air entraining admixture. This has led to inconsistent relationship between the compressive strength and the fresh air content of concrete.
2. Although the hardened air parameters are regarded as the most reliable source to predict the freeze/thaw performance of concrete, they don't seem to correlate well with the durability factor in the presence of localized aggregate failures and popouts.

3. The flexural strength versus dynamic modulus relationship revealed that this correlation is dependent on the type and mode of failure of the freeze/thaw specimen and the flexure test configuration. It was revealed that the flexural strength correlated well with the dynamic modulus properties of the freeze/thaw prisms when no aggregate failures were present, while a very poor relationship was observed for specimens with signs of aggregate failures.
4. The series of premature failures has raised some speculations on the adequacy of the minimum total cementitious content (535 lbs/yd^3 [317 Kg/m^3]) to resist the freeze/thaw hostility. Based on the results of this study the IDOT has raised the bar for the minimum amount of Portland cement content from 375 lbs/yd^3 (222 Kg/m^3) to 400 lbs/yd^3 (237 Kg/m^3) when 30% of fly ash or slag are used to replace the cement by weight of the total cementitious content.

12.2.5. Analytical Evaluation of the RCP and Water Penetration in Concrete

Based on the findings of the analytical investigation of the RCP and water penetration tests the following conclusions can be made:

1. The average depth of water penetration seemed to provide a reasonable measure for the water penetration coefficient prediction when compared with the maximum depth of water penetration. This was validated through the better relationship between the K_w based on the average depth of water penetration, charge passed, diffusion coefficient per RCP test, and compressive strength.
2. The Arrhenius factor revealed that when the charge passed exceeded 4000 Coulombs, the Dc was reduced by more than 50%. In addition, the D_c per RCP test after applying the Arrhenius factor showed a more reasonable relation with the K_w per DIN 1048.

3. On the basis of the test results, an equation was developed to determine the diffusion coefficient (D_c) based on the Nernst-Plank formula with the Arrhenius correction factor. The formula is a function of the charge passed (Q) and the activation energy (E_a).

12.2.6. Time Dependent Diffusion Modeling of Concrete

Based on the developed time dependent diffusion model, the following conclusions can be made:

1. The proposed model which accounts for time dependent diffusion and square root buildup of surface chloride with time was successfully developed. The model can be divided into three separate periods, where in the first period, both the diffusion and surface chlorides are time dependent, and in the following periods with either a decreasing or constant diffusion coefficient.
2. The time to threshold based on the proposed model was the highest amongst the other models, which shows the effect of taking into consideration the surface chloride and diffusion coefficients as time dependents.
3. The proposed model can be modified to account for both linear and square root buildup of surface chloride with time. It is expected that the Life-365 software will give similar results to the proposed model with linear buildup of surface chloride.

12.3. Recommendation for Future Work

1. The study have shown similar performance for concrete mixes made with conventional or modified cement when the latter had more than 5% limestone and IPA or 1.5% IR. Further research shall be carried out to investigate the possibility of increasing the limestone and IPA and/or IR in cement. This can also include increasing the Blaine

fineness in the modified cement to overcome the loss in the strength at early age due to the added raw materials.

2. The freeze/thaw evaluation performed in this study, reported the effect of lignosufonate on the air content and the performance of freeze/thaw specimens with aggregate failures and popouts. Future research needs to investigate how to improve the freeze/thaw performance against aggregate popouts. This can include investigating the effect of different concrete mix components such as cement and cementitious content, supplementary cementitious materials, type of chemical admixture (WRA, HRWR, and AEA), aggregate type and quality, and aggregate size.
3. Future research can be expanded to verify the validity of the analytical approaches to calculate the water penetration coefficient and equivalent-steady state diffusion based on the rapid chloride penetration test. Future investigation shall include studying the effect of the w/cm ratio, maximum aggregate size, cementitious content and combinations on the water penetration coefficient relationship and the equivalent-steady state diffusion coefficient.
4. Future research need to be carried out to determine the validity of the time dependent diffusion model for application by researchers and engineers. Moreover, the effect of diffusion and convection combined can be investigated as well as the binding of chlorides by the products of hydration on the time to initiation period.

CITED REFERENCES

- AASHTO M 327, "Standard Specification for Processing Additions for Use in the Manufacture of Hydraulic Cements," American Association of State and Highway Transportation, Washington, DC, 2011, 9 pp.

- AASHTO M 85, "Standard Specification for Portland Cement," American Association of State and Highway Transportation, Washington, DC, 2012, 14 pp.

- ACI Committee 116, "Cement and Concrete Terminology," American Concrete Institute, Farmington Hills, MI, 2000, 73 pp.

- ACI Committee 365, "Service-Life Prediction–State-of-the-Art Report," American Concrete Institute, Farmington Hills, MI, 2000, 44 pp.

- Aitcin P.C. "Binders for Durable and Sustainable Concrete." Modern Concrete Technology 16. Taylor & Francis, London. 2008.

- Akrout, K., Ltifi, M., and Ouezdou, M.B., "Chloride Diffusion in Mortars-Effect of the Use of Limestone Sand; Part II: Immersion Test," *International Journal of Concrete Structures and Materials*, V. 4, No. 2, 2010, pp. 109-112.

- Albeck, J., and Sutej, B. "Characteristics of concretes made of Portland-limestone cement." *Beton*, Vol. 41, No. 5, 1991, pp. 240-244 (in German. English translation by Susan U. Lauer available from Portland Cement Association library).

- Alunno-Rosetti, V., and Curcio, F. "A contribution to the knowledge of the properties of Portland-Limestone Cement concretes, with respect to the requirements of European and Italian design code." *Proceedings of the 10th International Congress on the Chemistry of Cement*, Gothenburg, Sweden, Ed. H. Justnes, 1997, 6 pp.

- ASTM C1152/1152M, "Standard Test Method for Acid-Soluble Chloride in Mortar and Concrete," ASTM International, West Conshohocken, PA, 2004, 4 pp.

- ASTM C1202, "Standard Test Method for Electrical Indication of Concrete's Ability to Resist Chloride Ion Penetration," ASTM International, West Conshohocken, PA, 2012, 7 pp.

- ASTM C1218, "Standard Test Method for Water-Soluble Chloride in Mortar and Concrete," ASTM International, West Conshohocken, PA, 1999R08, 3 pp.

- ASTM C138, “Standard Test Method for Density (Unit Weight), Yield, and Air Content (Gravimetric) of Concrete,” ASTM International, West Conshohocken, PA, 2008, 4 pp.

- ASTM C143/C143M, “Standard Test Method for Slump of Hydraulic-Cement Concrete,” ASTM International, West Conshohocken, PA, 2012, 4 pp.

- ASTM C150/C150M, “Standard Specification for Portland Cement,” ASTM International, West Conshohocken, PA, 2011, 9 pp.

- ASTM C1543-10a, “Standard Test Method for Determining the Penetration of Chloride Ion into Concrete by Ponding,” ASTM International, West Conshohocken, PA, 2010, 4 pp.

- ASTM C1556/1556M, “Standard Test Method for Determining the Apparent Chloride Diffusion Coefficient of Cementitious Mixtures by Bulk Diffusion,” ASTM International, West Conshohocken, PA, 2011, 7 pp.

- ASTM C192/C192M, “Standard Practice for Making and Curing Concrete Test Specimens in the Laboratory,” ASTM International, West Conshohocken, PA, 2012, 8 pp.

- ASTM C215, “Standard Test Method for Fundamental Transverse, Longitudinal, and Torsional Resonant Frequencies of Concrete Specimens,” ASTM International, West Conshohocken, PA, 2008, 7 pp.

- ASTM C219/C219M, “Standard Terminology Relating to Hydraulic Cement,” ASTM International, West Conshohocken, PA, 2014, 4 pp.

- ASTM C231/C231M, “Standard Test Method for Air Content of Freshly Mixed Concrete by the Pressure Method,” ASTM International, West Conshohocken, PA, 2010, 10 pp.

- ASTM C39, “Standard Test Method for Compressive Strength of Cylindrical Concrete Specimens.” ASTM International, West Conshohocken, PA, 2012, 7 pp.

- ASTM C403, “Standard Test Method for Time of Setting of Concrete Mixtures by Penetration Resistance,” ASTM International, West Conshohocken, PA, 2008, 7 pp.

- ASTM C457, “Standard Test Method for Microscopical Determination of Parameters of the Air-Void System in Hardened Concrete,” ASTM International, West Conshohocken, PA, 2012, 15 pp.

- ASTM C465, “Standard Specification for Processing Additions for Use in the Manufacture of Hydraulic Cements,” ASTM International, West Conshohocken, PA, 2010, 5 pp.

- ASTM C494/494M, "Standard Specification for Chemical Admixtures for Concrete," ASTM International, West Conshohocken, PA, 2013, 10 pp.

- ASTM C511, "Standard Specification for Mixing Rooms, Moist Cabinets, Moist Rooms, and Water Storage Tanks Used in the Testing of Hydraulic Cements and Concretes," ASTM International, West Conshohocken, PA, 2013, 3 pp.

- ASTM C666, "Standard Test Method for Resistance of Concrete to Rapid Freezing and Thawing," ASTM International, West Conshohocken, PA, 2003, 6 pp.

- ASTM C672, "Standard Test Method for Scaling Resistance of Concrete Surfaces Exposed to Deicing Chemicals," ASTM International, West Conshohocken, PA, 2012, 3 pp.

- ASTM C78, "Standard Test Method for Flexural Strength of Concrete (Using Simple Beam with Third-Point Loading)." ASTM International, West Conshohocken, PA, 2009, 3 pp.

- Bamforth P.B., Pocock D.C., and Robery, P.C., "The sorptivity of concrete," *Conference: Our World in Concrete and Structures*, Singapore, 1985.

- Bentz, D.P., Garboczi, E.J., Haecker, C.J., and Jensen, O.M., "Effects of Cement Particle Size Distribution on Performance Properties of Portland Cement-Based Materials," *Cement and Concrete Research*, V. 29, No. 10, 1999, pp. 1663-1671.

- Bentz, E.C., and Thomas, M.D.A., "Life-365 Service Life Predic-tion Model, Version 2.2.1," 2014, http://www.life-365.org/. (last accessed January 15, 2014)

- Betancourt, J.G.A., and Hooton, R.D., "Study of the Joule Effect on Rapid Chloride Permeability Values and Evaluation of Related Electrical Properties of Concrete," *Cement and Concrete Research*, V. 34, No. 6, 2004, pp. 1007-1015.

- Bonavetti, V., Donza, H., Menéndez, G., Cabrera, O., and Irassar, E.F., "Limestone filler cement in low w/c concrete: A rational use of energy," *Cement and Concrete Research*, V. 33, 2003, pp. 865–871.

- Bucher, B., Radlinska, A., and Weiss, W.J, "Preliminary Comments on Shrinkage and Shrinkage Cracking Behavior of Cement Systems that Contain Limestone," *Portland Cement Association*, Skokie, IL, 9 pp.

- Burris, L.E., and Riding, K.A., "Diffusivity of Binary and Ternary Concrete Mixture Blends," *ACI Materials Journal*, V. 111, No. 4, 2014, pp. 373-382.

- Burrows, R.W. 1999. *The Visible and Invisible Cracking of Concrete*. ACI Monograph. No. 11, 78 pp.

- CAN/CSA A 3000, "Cementitious materials compendium," CSA Group, Toronto, ON, Canada, 2013, 282 pp.

- Costa, A., and Appleton, J., "Chloride Penetration into Concrete in Marine Environment—Part 1: Main Parameters Affecting Chloride Pene-tration," *Materials and Structures*, V. 32, 1999, pp. 252-259.

- Cramer, S. M., and C. Sippel. 2005. *Effects of Ground Granulated Blast Furnace Slag in Portland Cement Concrete*. Report No. WI/SPR-05-04, Wisconsin Department of Transportation Technical Report.

- Crank, J. *The Mathematics of Diffusion*. Second edition, Clarendon Press, Oxford, UK, 1975, 424 pp.

- Daigle, L., Lounis, Z., Cusson, D., and Smithson, L.D., "Numerical Prediction of Early-Age Cracking and Corrosion in High Performance Concrete Bridges-Case Study," *In Innovations in Bridge Engineering Session*, The 2004 Annual Conference of the Transportation Association of Canada. Quebec City, QC, Canada, 2004.

- Dhir, R., "The potential of fly ash: the future looks bright," *Concrete* V. 40, No. 6, 2006, pp. 68–70.

- Dhir, R.K., "Additional Materials and Allowable Cements in Cement," *Euro-Cements Impact of ENV 196 on Concrete Construction*, eds R.K. Dhir and M.R. Jones, E & F Spon, University of Dundee, Dundee, Scotland, 1994, pp. 51-63.

- Dhir, R.K., Limbachiya, M.C., McCarthy, M.J., and Chaipanich, A., "Evaluation of Portland-limestone cements for use in concrete construction." *Materials and Structures*, V. 40, 2007, pp. 459-473.

- DIN 1048, "Testing Concrete: Testing of Hardened Concrete (Specimens prepared in mould)," Beton und Stahlbeton 1, Deutscher Ausschuß für Stahlbeton of the Normenausschuß Bauwesen, UDC, 1991.

- El-Didamony, H., Salem, T., Gabr, N., and Mohamed, T., "Limestone as a retarder and filler in limestone blended cement," *Ceramics–Silikaty*, V. 39, No. 1, 1995, pp. 15–19.

- Ezziane, K., Kadri, E.H., Hallal, A., and Duval, R., "Effect of mineral additives on the setting of blended cement by the maturity method," *Materials and Structures*, V. 43, 2010, pp. 393-401.

- Fagerlund, G., "On the Capillary of concrete," *Nordic Concrete Research*. Oslo. Pub. No. 1, 1982.

- Frederiksen, J.M., Nilsson, L.O., Poulsen, E., Sandberg, P., Tang L., and Andersen, A., "HETEK, A System for Estimation of Chloride Ingress into Concrete, Theoretical Background," The Danish Road Directorate, Report No. 83, 1997, 107 pp.

- Gebhardt, R.F., "Survey of North American Portland Cements: 1994." *Cement, Concrete, and Aggregates*, ASTM International, V. 17, No. 2, 1995, pp. 145-189.

- Ghosh, P., Hammond, A., and Tikalsky, P.J., "Prediction of Equivalent Steady-State Chloride Diffusion Coefficienets." *ACI Materials Journal*, V. 108, No. 1, 2011, pp. 88-94.

- Hall, C., "Water movement in porous building materials-I." *Building and Environment*, V. 12, 1977, pp. 117-125.

- Hedegaard, S.E., and Hansen, T.C., "Water permeability of fly ash concretes." *Materials and Structures*, V. 25, 1992, pp. 381-387.

- Heikal, M., El-Didamony, H., and Morsy, M.S., "Limestone-filled pozzolanic cement," *Cement and Concrete Research*, V. 30, 2000, pp. 1827–1834.

- Ho, D.W.S., and Lewis, R.K., "The water sorptivity of concrete: the influence of constituents under continuous curing." *Durability of Building Materials*, 4, 241-252

- Hooton, D., Ramezanianpour, A., and Schutz, U., "Decreasing the clinker component in cementing materials: Performance of Portland-limestone cements in concrete in combination with SCMs," *2010 Concrete Sustainability Conference*, NRMCA, Arizona State University, Tempe, AZ, 2010, 15 pp.

- Hooton, R. D. and Thomas, M. D. A., "Portland-Limestone Cements for Use in Concrete CSA A23.1-09 Ballot (Changes to Section 4.2.1 and Table 6)," PowerPoint presentation for the CSA Webex, Canadian Standards Association, 2009.

- Hooton, R.D., Nokken, M., and Thomas, M.D.A.T. *Portland-Limestone Cement: State-of the-Art Report and Gap Analysis for CSA A 3000*. Cement Association of Canada, Ottawa, ON, 2007, 60 pp.

- Hornain, H., Marchand, J., Duhot, V., Moranville-Regourd, M., "Diffusion of Chloride Ions in Limestone Filler Blended Cement Pastes and Mortars," *Cement and Concrete Research*, V. 25, No. 8, 1995, pp. 1667-1678.

- Irassar, E.F., Bonavetti, V.L., Menhdez, G., Donza, H., and Cabrera, O., "Mechanical properties and durability of concrete made with PortlandPortland-limestone cement," *Proceedings of the 3rd CANMET/ACI International Symposium on Sustainable Development of Concrete*, ACI SP-202. American Concrete Institute, Detroit, MI, 2001, pp. 431–450.

- Issa, M.A. *Effect of Portland Cement (current ASTM C150/AASHTO M85) with Limestone and Process Addition (ASTM C465/AASHTO M327) on the Performance of Concrete for Pavement and Bridge Decks*. Report No. FHWA-ICT-14-005, Illinois Department of Transportation, Illinois Center of Transportation, Schaumburg, Illinois, 245 pp.

- Issa, M.A. and Khalil, A.A., "Diffusivity and Permeability of High-Performance Concrete (HPC) for Bridge Decks," *PCI Journal*, Precast/Prestressed Concrete Institute, V. 55, No. 2, 2010, pp. 82-95.

- Kato, E., Kato, Y., and Uomoto, T., "Development of Simulation Model of Chloride Ion Transportation in Cracked Concrete," *Journal of Advanced Concrete Technology*, V. 3, 2005, pp. 85-94.

- Kiattikomol, K., Jaturapitakkul, C., and Tangpagasit, J., "Effect of insoluble residue on properties of Portland cement," *Cement and Concrete Research*, V. 30, 2000, pp. 1209-1214.

- Kosmatka, S.H., and Wilson, M.L. *Design and Control of Concrete Mixes Portland*. EB001, 15th edition. Portland Cement Association, Skokie, IL, 2011.

- LaBarca, I. K., Foley, R.D., and S.M. Cramer. *Effects of Ground Granulated Blast Furnace Slag in Portland Cement Concrete (PCC)-Expanded Study*. Report No. WI/SPR-05-01, Wisconsin Department of Transportation Technical Report, 2007.

- Loosveldt, H., Lafhaj, Z., and Skoczylas, F., "Experimental study of gas and liquid permeability of a mortar," *Cement and Concrete Research*, V. 32, No. 9, 2002, pp. 1357–1363.

- Ludirdja D., Berger, R.L., and Young, J.F., "Simple method for measuring water permeability of concrete," *ACI Materials Journal*, V. 86, No. 5, 1989, pp. 433–439.

- Maage, M., Poulsen, E., Vennesland, O. and Carlsen, J.E. *Service life model for concrete structures exposed to marine environment*. LIGHTCON Report No. 2.4, STF70 A94082 SINTEF, Trondheim, Norway, 1995.

- Malhotra, V.M., "High-performance high-volume fly ash concrete," *Concrete International*, V. 24, No. 7, 2002, pp. 30–34.

- Marceau, M.L., Nisbet, M.A., and VanGeem, M.G. *Life Cycle Inventory of Portland Cement Manufacture*. PortlandSN2095b, Portland Cement Association. Skokie, IL, 2006.

- Matthews, J.D., "Performance of limestone filler cement concrete," *In Euro-Cements Impact of ENV 197 on Concrete Construction* (Ed. R.K. Dhir and M.R. Jones). E&FN Spon, London, 1994, pp. 113–147.

- Mehta, P.K., "Concrete technology for sustainable development," *Concrete International*, 1999, pp. 47–53.

- Mehta P.K., and Monteiro, P.J.M. *Concrete: Microstructure, Properties, and Materials*. Fourth Edition, McGraw-Hill, New York, 2014, 660 pp.

- Meira, G.R., Andrade, C., Alonso, C., Borb, J.C. Jr., and Padilha, M.Jr., "Durability of Concrete Structures in Marine Atmosphere Zones—The Use of Chloride Deposition Rate on the Wet Candle as an Environ-mental Indicator," *Cement and Concrete Composites*, V. 32, No. 6, 2010, pp. 427-435.

- Mendham, J., Denney, R.C., Barnes, J.D., and Thomas, M.J.K. *Vogel's Textbook of Quantitative Chemical Analysis*. Sixth edition, Prentice Hall, Singapore, 2000, 836 pp.

- Moir, G.K., and Kelham, S., "Durability 1. Performance of Limestone-Filled Cements: Report of Joint BRE/BCA/Cement Industry Working Party," Building Research Establishment, Garston, Watford, England, 1993.

- Moir, G.K., and Kelham, S., "Developments in the Manufacture and Use of Portland-limestone cement. *ACI Special Publication*, SP 172-42, 1997, pp. 797–819.

- Mounanga, P., Khokhar, M.I.A., El Hachem, R., and Loukili, A., "Improvement of the early-age reactivity of fly ash and blast furnace slag cementitious systems using limestone filler," *Materials and Structures*, V. 44, No. 2, 2010, pp. 437–453.

- Mustafa, M.A., and Yusof, K.M., "Atmospheric Chloride Penetra-tion into Concrete in Semi-Tropical Marine Environment," *Cement and Concrete Research*, V. 24, No. 4, 1994, pp. 661-670.

- Neville, A.M. *Properties of Concrete*. Fourth Edition, Pitman Book, London, 1995, 844 pp.

- O'Brien, K., Ménaché, J., and O'Moore, L., "Impact of fly ash content and fly ash transportation distance on embodied greenhouse gas emissions and water consumption in concrete," *International Journal of Life Cycle Assessment*, V. 14, No. 7, 2009, pp. 621-629.

- Oh, B.H., and Jang, S.Y., "Effects of Material and Environmental Parameters on Chloride Penetration Profiles in Concrete Structures," *Cement and Concrete Research*, V. 37, No. 1, 2007, pp. 47-53.

- Ondova, M., and Stevulova, N., "Benefits of fly ash utilization in concrete road cover," *Theoretical Foundations of Chemical Engineering*, V. 46, No. 6, 2012, pp. 713-718.

- OPS LS-412, "Scaling Resistance of Concrete Surfaces Exposed to De-icing Chemicals," Ontario Provisional Standard for Roads and Public Works, Ontario, Canada, 5 pp.

- Ozyildirim, C., "Permeability Specifications for High-Performance Concrete Decks," *Transportation Research Record*, V. 1610, 1998, pp. 1-5.

- Pfeifer, D.W., "High Performance Concrete and Reinforcing Steel with a 100-Year Service Life," *PCI Journal*, V. 45, No. 3, pp. 46-54.

- Phung Q.T., Maes, N., Schutter, G.D., Jacques, D., and Ye, G., "Determination of water permeability of cementitious materials using a controlled constant flow method," *Construction and Building Materials*, V. 47, 2013, pp. 1488-1496.

- Poole, J.L., Riding, K.A., Folliard, K.J., Juenger, M.C.G., and Schindler, A.K., "Methods for Calculating Activation Energy for Portland Cement," *ACI Materials Journal*, V. 104, No. 1, 2007, pp. 303-311.

- Poulsen, E. and Mejlbro, L. *Diffusion of Chloride in Concrete: Theory and Application, Modern Concrete Technology*. First edition, CRC Press, United States, 2006, 480 pp.

- Powers, T.C., "A Working Hypothesis for Further Studies of Frost Resistance of Concrete," *Journal of the American Concrete Institute*, V. 16, No. 4, 1945, pp. 245-272.

- Powers, T.C., "The Air Requirement of Frost Resistant Concrete," *Proceedings of the Highway Research Board*, V. 29, 1949, pp. 184- 211.

- Powers, T.C., and Helmuth, R.A., "Theory of Volume Changes in Hardened Portland Cement Paste during Freezing Highway," *Highway Research Board Proceedings*, V. 32, 1953, pp. 285-297.

- Purvis, R.L., Babaei, K., Clear, K.C., and Markow, M.J., "*Life-Cycle Cost Analysis for Protection and Rehabilitation of Concrete Bridges Relative to Reinforcement Corrosion*. Strategic Highway Research Program, SHRP-S-377, National Research Council, Washington DC, 1994, 289 pp.

- Reinhardt, H.W., "Transport of Chemicals through Concrete." *Materials Science of Concrete III*, ed. J. P. Skalny, American Ceramic Society, Westerville, OH, 1992, pp. 209–241.

- Riding, K.A., Thomas, M.D.A., and Folliard, K.J., "Apparent Diffusivity Model for Concrete Containing Supplementary Cementitious Materials," *ACI Materials Journal*, V. 110, No. 6, 2013, pp. 705-714.

- Scherer, G.W,, Valenza, J.J., and Simmons, G., "New methods to measure liquid permeability in porous materials," *Cement and Concrete Research*, V. 37, No. 3, 2007, pp. 386–397.

- Schiller, B., and Ellerbrock, H.G., "Grinding and properties of cements with several principal constituents." *ZKG International*, Edition B. V. 45, No, 7, 1992, pp. 325–334.

- Schmidt, M., "Cement with interground additives—Capabilities and environmental relief, Part 1," *Zement-Kalk-Gips*, V. 45, No. 2, 1992a, pp. 64–69 (English translation in Vol. 45, No, 4, pp. 87–92).

- Schmidt, M., "Cement with interground additives—Capabilities and environmental relief, Part 2," *Zement-Kalk-Gips*, V. 45, No. 6, 1992b, pp. 296–301.

- Schmidt, M., Harr, K., and Boeing, R., "Blended cement according to ENV 197 and experiences in Germany," *Cement, Concrete, and Aggregates*, V. 15, No., 2, 1993, pp. 56–164.

- Sherman, M.R., McDonald, D.B., and Pfeifer, D.W., "Durability Aspects of Precast Prestressed Concrete, Part 2: Chloride Permeability Study." *PCI Journal*, V. 41, No. 4, 1996, pp. 75–95.

- Shin, C.B., and Kim, E.K., "Modeling of Chloride Ion Ingress in Coastal Concrete," *Cement and Concrete Research*, V. 32, No. 5, 2002, pp. 757-762.

- Siddique, R. and Khan, M.I. *Supplementary Cementing Materials*. First edition, Engineering Materials, Springer, Berlin, Germany, 2011, 287 pp.

- Siebel, E., and Sprung, S., "Influence of limestone in PortlandPortland-limestone cement on the durability of concrete." Beton, V. 41, No. 3, 1991, pp. 113–117 (in German. English translation by Susan U. Lauer available from Portland Cement Association library).

- Sprung, S., and Siebel, E., "Assessment of the suitability of limestone for producing Portland-limestone cement (PKZ)," *Zement-Kalk-Gips*, V. 44, No. 1, 1991, pp. 1–11.

- Stanish, K., and Thomas, M., "The Use of Bulk Diffusion Tests to Establish Time-Dependent Concrete Chloride Diffusion Coefficients," *Cement and Concrete Research*, V. 33, No. 1, 2003, pp. 55-62.

- Suryavanshi, A.K., Swami, R.N., and Cardew, G.E., "Estimation of Diffusion Coefficients for Chloride Ion Penetration into Structural Concrete." *ACI Materials Journal*, V. 99, No. 5, 2002, 441-449.

- Suryavanshi, A.K., Swamy, R.N., and McHugh, S., "Chloride Penetration into Reinforced Concrete Slabs," *Canadian Journal of Civil Engineering*, V. 25, 1998, pp. 87-95.

- Swamy, R.N., and Laiw, J.C., "Effectiveness of Supplementary Cementing Materials in Controlling Chloride Penetration into Concrete," *Fly Ash, Silica Fume, Slag, and Natural Pozzolans in Concrete*, Proceedings of the Fifth International Conference, SP-153, editor V.M. Malhotra, American Concrete Institute, Farmington Hills, Michigan, 1995, pp. 657-674.

- Swamy, R.N., Suryavanshi, A.K., and Tanikawa, S., "Protective Ability of an Acrylic-Based Surface Coating System against Chloride and Carbonation Penetration into the Concrete," *ACI Materials Journal*, V. 95, No. 2, 1998, pp. 101-112.

- Takewaka, K., Mastumoto, S., "Quality and Cover Thickness of Concrete based on the Estimation of Chloride Penetration in Marine Environments," *ACI Special Publication*, SP 109-17, 1988, pp. 381-400.

- Tang, L., and Nilsson, L.O., "Chloride Diffusivity in High Strength Concrete at Different Ages," *Nordic Concrete Research Publication*, V. 11, 1992, pp. 162-171.

- Taylor, P.C. *Specifications and Protocols for Acceptance Tests on Processing Additions in Cement Manufacturing*. Transportation Research Board, NCHRP Report 607, Washington D.C., 2007, 87 pp.

- Tezuka, Y.,Gomes, D., Martins, J., and Djanikian, J.G., "Durability aspect of cement with high limestone filler content," *Proceedings of the 9th International Congress on the Chemistry of Cement,* New Delhi, India, 1992, pp. 53–59.

- Thomas, M., "Optimizing the Use of Fly Ash in Concrete," *Concrete Thinking for a Sustainable World*, Portland Cement Association, Skokie, Illinois, 2007.

- Thomas, M.D.A., Cail, K., Blair, B., Delagrave, A., and Barcelo, L., "Equivalent performance with half the clinker content using PLC and SCM." *2010 Concrete Sustainability Conference*, NRMCA, 2010a.

- Thomas, M.D.A., Hooton, R.D., Cail, K., Smith, B.A., de Wal, J., and Kazanis, K.G., "Field trials of concretes produced with Portland-limestone cement." *Concrete International*, January 2010b, pp. 35–41.

- Thomas, M.D.A., Shehata, M.H., Shashiprakash, S.G., Hopkins, D.S., and Cail, K., "Use of Ternary Cementitious Systems Containing Silica Fume and Fly Ash in Concrete," *Cement and Concrete Research*, V. 29, No. 8, 1999, pp. 1207-1214.

- Tsivilis, S. Chaniotakis, E., Badogiannis, E., Pahoulas G., and Ilias, A., "A study on the parameters affecting the properties of Portland-limestone cements," *Cement and Concrete Composites*, V. 21, No. 2, 1999a, pp. 107–116.

- Tsivilis, S., Batis, G., Chaniotakis, E., Grigoriadis, G., and Theodossis, D., "Properties and behavior of limestone cement concrete and mortar." *Cement and Concrete Research*, V. 30, No. 10, 2000, pp. 1679–1683.

- Tsivilis, S., Chaniotakis, E., Batis, G., Meletiou, C., Kasselouri, V., Kakali, G., Sakellariou, A., Pavlakis G., and Psimadas, C., "The effect of clinker and limestone quality on the gas permeability, water absorption and pore structure of limestone cement concrete," *Cement and Concrete Composites*, V. 21, No. 2, 1999b, pp. 139–146.

- Tsivilis, S., Tsantilas, J., Kakali, G., Chaniotakis, E., and Sakellario, A., "The permeability of PortlandPortland-limestone cement concrete," *Cement and Concrete Research*, V. 33, No. 9, 2003, pp. 1465–1471.

- Uji, K., Matsuoka, Y., and Maruya, T., "Formulation of an Equation for Surface Chloride Content of Concrete Due to Permeation of Chloride," *Corrosion of Reinforcement in Concrete*, editors C.L. Page, K.W.J. Treadway, and P.B. Bamforth, Elsevier Science, Barking, UK, 1990, pp. 258-267.

- Vuk, T., Tinta, V., Gabrovšek, R., and Kaučič, V., "The effects of limestone addition, clinker type and fineness on properties of Portland cement." *Cement and Concrete Research*, V. 31, No. 1, 2001, pp. 135–139.

- Vuorinen, J., "Applications of diffusion theory to permeability tests on concrete, Part 1: depth of water penetration into concrete and coefficient of permeability." *Magazine of Concrete Research*. V. 37, No. 132, 1985, pp. 153-161.

- Walz, K., "Grundlagen und praktische Bedeutung der Undurchl/issigkeit des Betons gegen Flfissigkeiten," *Bauu. Bauindustrie 3*, 1968, pp. 122-129.

- Yang, C.C., "A Comparison of Transport Properties for Concrete Using the Ponding Test and the Accelerated Chloride Migration Test," *Materials and Structures*, V. 38, No. 3, 2005, pp. 313-320.

- Zhang, S.P., and Zong, L., "Evaluation of Relationship between Water Absorption and Durability of Concrete Materials," *Advances in Materials Science and Engineering*, V. 2014, 2014, 8 pp.

- Zhou, S., "Modeling Chloride Diffusion in Concrete with Linear Increase of Surface Chloride," *ACI Materials Journal*, V. 111, No. 5, 2014, pp. 483-490.

APPENDIX A. SAMPLE OF IDOT PCC MIX DESIGN SHEET

DTT03110 PCC MIX DESIGN Version 2.1.2

PCC MIX #: **MIX 14-CEM1>5%** MATERIAL: **21605** CONCRETE PC ASH EFFECTIVE:
REF MIX#: **UIC** CLASS: **PV** LAST YR USED: TERMINATED:
RESP: **91** DISTRICT 1 LAB: **IP** Independent Plant Site REVIEWED BY: DFLAG:

BATCH CU YD	ADX	H2O% RED	FINE MOD	% AIR	VOIDS	(Z) CEMENT	MORTAR FACTOR	{TYPE} ASH	FA	{GAL/CWT} FA	CA	{ABS. VOL} CA,B	FA,A
1.00	**W**	**8.0**		**6.5**	**0.41**	**5.35**	**0.88**	**C**	**B**	**5.3**	**0.200**	0.401	0.291

MATERIAL	PROD NO	PROD NAME	SP G	% BLEND	%MOIST / REPL	[LBS / CU YD] SSD	[LBS / CU YD] ADJ	[KG / CU M] ADJ
022CA11	**50312-04**	MS THORNTON, (CA)	**2.70**	**100.0**		1823	1823	1082
029FM02	**52010-20**	NATURAL SAND (BLUFF CITY)	**2.64**					
029FM20	**51972-02**	HANSON MS ROMEOVILLE(CS)	**2.67**	**100.0**	**1.70**	1308	1331	790
37801	**52403-02**	LAFARGE PLEASANT PRAIRIE, WI	**2.53**	**29.9**		160	160	95
37601		ST MARY, CEM3	**3.15**	**70.1**		375	375	225
37821	**544-07**	HOLCIM SKYWAY, SLAG GR. 100	**2.90**					
					ADJ. H2O (gal : lbs)	24.5	204	121
					TOTAL BATCH WT (lbs)		3893	2310

{FA + CA} MIX-H2O: 5.50 W/C RATIO: 0.42
RED MIX-H2O: 5.06
TOTAL CEMENTITIOUS MATL: 5.35
THEO. H2O (gal : lbs) 27.1 226

PRODUCER: **1234-56** PROD NAME: **PCC PAVING CO.**
REMARKS:
REMARKS: CONTRACT **ICT Project**

ADDITIONAL INFORMATION: Lab: UIC CONCRETE LAB Location: CHICAGO
Designer: M. ISSA Created: 07/11/12

Adx(s):	Matl Code	Type	Product	Remarks
	42147	AEA	W.R. GRACE DARAVAIR 1400	2 oz/cwt
	43709	A	W.R. GRACE WRDA 82	4 oz/cwt

	Target	Actual	
Slump (in.)	3.5		
Air (%)	6.5		
Strength (psi) 1.	3500		Comp. 14 day
2.	600		Flex. 14 day
3.			
4.			

Printed 8/16/2012

Note: All other mixes can be made by changing the cement source and Indicating weather slag or fly ash is used.

APPENDIX B. EXPERIMENTAL RESULTS FOR COMPRESSIVE STRENGTH

Table B-1. Average Compressive Strength for Mixes Batched with Natural Sand

Mix Designation		W/CM Ratio	Air Content, %	Unit Weight, lb/ft^3	Compressive Strength, psi				
					Age, Days				
					3	7	14	28	56
Mixes batched with Natural Sand	C1-F-NS1	0.42	7.2	144.8	2530	3763	4360	4940	5690
	C1-F-NS2	0.42	7.2	145.0	2600	3545	4185	4971	5609
	C1IP1-F-NS	0.42	6.9	145.2	2590	3967	4617	5520	6000
	C1IP2-F-NS	0.42	7.5	144.5	2563	3691	4250	5149	5952
	C1-S-NS1	0.40	7.1	145.0	2477	3543	4513	5270	6000
	C1-S-NS2	0.40	7.4	144.6	2636	3696	4429	5383	6082
	C1IP1-S-NS	0.42	7.2	144.6	2697	3910	4931	5881	6656
	C1IP2-S-NS	0.42	7.3	144.6	2701	3993	4620	5667	6571
	C2-F-NS	0.40	6.8	145.1	3247	3937	4670	5540	6235
	C2IP-F-NS	0.40	7.0	145.3	3050	4010	4693	5413	6235
	C2-S-NS	0.42	6.5	146.0	3419	4506	5254	5963	6543
	C2IP-S-NS	0.42	7.5	144.8	3200	4483	5338	6115	6758
	C3-F-NS	0.42	6.6	145.9	2644	4213	4902	5467	6027
	C3IR-F-NS	0.42	7.2	145.0	2587	3906	4632	5133	5983
	C3-S-NS	0.42	6.7	145.5	2648	3996	4579	5550	6227
	C3IR-S-NS	0.42	7.2	145.8	2422	3630	4478	5267	6067

Table B-2. Average Compressive Strength for Mixes Batched with Combined Sand

Mix Designation		W/CM Ratio	Air Content, %	Unit Weight, lb/ft^3	Compressive Strength, psi				
					Age, Days				
					3	7	14	28	56
Mixes batched with Combined Sand	C1-F-CS	0.42	7.1	145.0	2897	4030	4767	5437	5807
	C1IP1-F-CS	0.42	7.2	145.0	2687	3807	4443	5137	5723
	C1-S-CS	0.44	6.7	145.2	2630	3670	4417	5297	6027
	C1IP1-S-CS	0.44	7.3	144.7	2980	4083	4937	5670	6080
	C2-F-CS	0.42	6.6	145.6	3267	4027	4860	5523	6260
	C2IP-F-CS	0.42	6.9	145.6	3437	4370	5140	5900	6707
	C2-S-CS	0.44	6.7	145.6	3103	4190	4863	5467	6013
	C2IP-S-CS	0.44	6.7	146.0	3027	4243	5357	5960	6617
	C3-F-CS	0.42	7.0	146.3	2699	3817	4598	5155	5603
	C3IR-F-CS	0.42	6.8	145.5	2473	3667	4390	5120	5680
	C3-S-CS	0.44	7.4	144.6	2527	3583	4520	5230	5565
	C3IR-S-CS	0.44	7.3	144.6	2683	3770	4790	5550	6230

APPENDIX C. EXPERIMENTAL RESULTS FOR FLEXURAL STRENGTH

Table C-1. Average Flexural Strength for Mixes Batched with Natural Sand

Mix Designation		W/CM Ratio	Air Content, %	Unit Weight, lb/ft^3	Flexural Strength, psi				
					Age, Days				
					3	7	14	28	56
Mixes batched with Natural Sand	C1-F-NS1	0.42	7.0	145.1	526	605	698	717	776
	C1-F-NS2	0.42	7.4	144.6	533	604	695	755	796
	C1IP1-F-NS	0.42	7.1	144.8	526	607	646	705	775
	C1IP2-F-NS	0.42	7.5	144.5	522	696	715	816	909
	C1-S-NS1	0.40	7.2	144.8	489	608	719	765	877
	C1-S-NS2	0.40	7.1	145.1	514	650	747	843	918
	C1IP1-S-NS	0.42	6.4	146.0	531	631	734	842	909
	C1IP2-S-NS	0.42	7.3	144.8	541	669	767	856	938
	C2-F-NS	0.40	6.6	145.6	561	676	746	775	854
	C2IP-F-NS	0.40	7.5	144.8	563	629	709	788	863
	C2-S-NS	0.42	6.6	145.6	564	699	781	844	962
	C2IP-S-NS	0.42	6.9	145.5	521	709	813	831	934
	C3-F-NS	0.42	7.2	144.6	518	649	651	725	812
	C3IR-F-NS	0.42	6.7	146.0	511	591	672	751	828
	C3-S-NS	0.42	7.1	144.8	502	624	686	742	875
	C3IR-S-NS	0.42	7.2	145.0	484	626	698	791	798

Table C-2. Average Flexural Strength for Mixes Batched with Combined Sand

Mix Designation		W/CM Ratio	Air Content, %	Unit Weight, lb/ft^3	Compressive Strength, psi				
					Age, Days				
					3	7	14	28	56
Mixes batched with Combined Sand	C1-F-CS	0.42	6.6	145.9	504	631	732	800	801
	C1IP1-F-CS	0.42	7.0	145.3	533	623	651	754	804
	C1-S-CS	0.44	7.1	144.8	515	668	745	781	822
	C1IP1-S-CS	0.44	6.9	145.3	517	598	673	784	821
	C2-F-CS	0.42	7.0	146.0	508	614	710	693	838
	C2IP-F-CS	0.42	7.0	145.0	573	689	732	791	858
	C2-S-CS	0.44	7.0	145.1	499	683	791	823	837
	C2IP-S-CS	0.44	7.5	144.5	489	655	724	816	843
	C3-F-CS	0.42	6.7	145.7	541	700	726	781	849
	C3IR-F-CS	0.42	7.2	146.1	496	603	719	749	798
	C3-S-CS	0.44	7.1	145.0	532	658	740	806	854
	C3IR-S-CS	0.44	6.9	145.1	506	631	753	798	876

APPENDIX D. CHLORIDE CONCENTRATION VERSUS DEPTH BASED ON THE SALT PONDING TEST

Table D-1. Chloride Concentration for Concrete Mixes made with C1 Cement and Batched with Natural Sand

Chloride Concentration (Acid and Water Soluble) in Concrete due to Salt Ponding Test							
% Cl^- by mass of concrete							
Mix No.	Ponding Duration	Titration Method	Depth from outer surface, in. (mm)				
			0 - 0.5	0.5 - 1.0	1.0-1.5	1.5 - 2.0	2.0 - 2.5
C1-F-NS	90 Days	AS	0.496	0.145	0.041	0.041	0.041
		WS	0.470	0.133	0.032		
	180 Days	AS	0.514	0.165	0.050	0.053	0.051
		WS	0.476	0.151	0.035		
	315 Days	AS	0.496	0.180	0.050	0.044	0.044
		WS	0.473	0.162	0.037		
C1IP1-F-NS	90 Days	AS	0.405	0.092	0.038	0.033	0.041
		WS	0.369	0.080	0.032		
	180 Days	AS	0.496	0.160	0.044	0.038	0.034
		WS	0.479	0.142	0.034		
	312 Days	AS	0.700	0.210	0.050	0.044	0.047
		WS	0.656	0.192	0.035		
C1IP2-F-NS	90 Days	AS	0.443	0.133	0.051	0.047	0.035
		WS	0.449	0.124	0.047	0.050	0.044
	180 Days	AS	0.591	0.165	0.053	0.047	0.051
		WS	0.579	0.168	0.044	0.041	0.041
	360 Days	AS	0.827	0.366	0.183	0.106	0.055
		WS	0.827	0.366	0.068	0.095	0.055
C1-S-NS	90 Days	AS	0.440	0.109	0.038	0.059	0.041
		WS	0.422	0.097	0.032		
	180 Days	AS	0.487	0.136	0.044	0.043	0.039
		WS	0.467	0.130	0.035		
	315 Days	AS	0.812	0.295	0.077	0.056	0.059
		WS	0.792	0.278	0.068		
C1IP1-S-NS	90 Days	AS	0.485	0.118	0.038	0.044	0.035
		WS	0.470	0.109	0.032		
	180 Days	AS	0.777	0.189	0.047	0.056	0.043
		WS	0.756	0.167	0.038		
	315 Days	AS	0.626	0.227	0.068	0.044	0.100
		WS	0.597	0.202	0.056		
C1IP2-S-NS	90 Days	AS	0.539	0.145	0.050	0.047	0.041
		WS	0.532	0.139	0.044	0.050	0.044
	180 Days	AS	0.615	0.138	0.047	0.059	0.046
		WS	0.579	0.118	0.047	0.050	0.041
	360 Days	AS	0.815	0.272	0.136	0.065	0.062
		WS	0.745	0.248	0.118	0.053	0.056

AS: Acid soluble chloride method
WS: Water soluble chloride method

Table D-2. Chloride Concentration for Concrete Mixes made with C2 Cement and Batched with Natural Sand

Chloride Concentration (Acid and Water Soluble) in Concrete due to Salt Ponding Test							
% Cl^- by mass of concrete							
Mix No.	**Ponding Duration**	**Titration Method**	**Depth from outer surface, in. (mm)**				
			0 - 0.5 (0 - 12.5)	**0.5 - 1.0 (12.5 - 25)**	**1.0-1.5 (25 - 37.5)**	**1.5 - 2.0 (37.5 - 50)**	**2.0 - 2.5 (50 - 62.5)**
C2-F-NS	90 Days	AS	0.337	0.121	0.050	0.048	0.044
		WS	0.343	0.124	0.050	0.044	0.047
	180 Days	AS	0.390	0.112	0.059	0.053	0.050
		WS	0.384	0.106	0.050	0.047	0.044
	360 Days	AS	0.567	0.266	0.077	0.050	0.044
		WS	0.272	0.239	0.089	0.047	0.041
C2IP-F-NS	90 Days	AS	0.329	0.097	0.059	0.054	0.054
		WS	0.307	0.089	0.053	0.080	0.053
	180 Days	AS	0.402	0.130	0.065	0.059	0.053
		WS	0.390	0.115	0.053	0.056	0.044
	360 Days	AS	0.508	0.154	0.065	0.065	0.077
		WS	0.514	0.154	0.065	0.065	0.077
C2-S-NS	90 Days	AS	0.295	0.090	0.059	0.059	0.053
		WS	0.301	0.083	0.053	0.051	0.041
	180 Days	AS	0.378	0.083	0.059	0.053	0.053
		WS	0.414	0.083	0.062	0.050	0.053
	360 Days	AS	0.496	0.177	0.062	0.053	0.053
		WS	0.496	0.165	0.059	0.059	0.050
C2IP-S-NS	90 Days	AS	0.331	0.083	0.053	0.054	0.057
		WS	0.331	0.077	0.047	0.047	0.041
	180 Days	AS	0.396	0.106	0.053	0.050	0.053
		WS	0.425	0.109	0.053	0.047	0.059
	360 Days	AS	0.555	0.331	0.136	0.097	0.055
		WS	0.573	0.260	0.106	0.157	0.055

AS: Acid soluble chloride method

WS: Water soluble chloride method

Table D-3. Chloride Concentration for Concrete Mixes made with C3 Cement and Batched with Natural Sand

Chloride Concentration (Acid and Water Soluble) in Concrete due to Salt Ponding Test							
% Cl^- by mass of concrete							
Mix No.	**Ponding Duration**	**Titration Method**	**Depth from outer surface, in. (mm)**				
			0 - 0.5 (0 - 12.5)	**0.5 - 1.0 (12.5 - 25)**	**1.0-1.5 (25 - 37.5)**	**1.5 - 2.0 (37.5 - 50)**	**2.0 - 2.5 (50 - 62.5)**
C3-F-NS	90 Days	AS	0.508	0.124	0.044	0.044	0.044
		WS	0.508	0.115	0.038	0.038	0.038
	180 Days	AS	0.455	0.157	0.047	0.050	0.045
		WS	0.421	0.138	0.032		
	360 Days	AS	0.597	0.174	0.050	0.034	0.038
		WS	0.555	0.154	0.038		
C3IR-F-NS	90 Days	AS	0.437	0.100	0.041	0.047	0.050
		WS	0.437	0.124	0.035	0.038	0.041
	180 Days	AS	0.428	0.142	0.050	0.050	0.038
		WS	0.402	0.130	0.038		
	360 Days	AS	0.733	0.222	0.056	0.043	0.041
		WS	0.688	0.204	0.044		
C3-S-NS	90 Days	AS	0.550	0.106	0.044	0.050	0.041
		WS	0.508	0.103	0.038	0.044	0.035
	180 Days	AS	0.718	0.165	0.044	0.040	0.040
		WS	0.653	0.151	0.030		
	360 Days	AS	0.697	0.275	0.060	0.041	0.050
		WS	0.691	0.256	0.050		
C3IR-S-NS	90 Days	AS	0.461	0.127	0.044	0.047	0.044
		WS	0.449	0.124	0.047	0.041	0.038
	180 Days	AS	0.685	0.208	0.062	0.044	0.038
		WS	0.659	0.192	0.050		
	360 Days	AS	1.134	0.267	0.062	0.056	0.042
		WS	1.105	0.249	0.053		

AS: Acid soluble chloride method

WS: Water soluble chloride method

Table D-4. Chloride Concentration for Concrete Mixes made with C1 Cement and Batched with Combined Sand

Chloride Concentration (Acid and Water Soluble) in Concrete due to Salt Ponding Test							
% Cl^- by mass of concrete							
Mix No.	**Ponding Duration**	**Titration Method**	**Depth from outer surface, in. (mm)**				
			0 - 0.5 (0 - 12.5)	**0.5 - 1.0 (12.5 - 25)**	**1.0-1.5 (25 - 37.5)**	**1.5 - 2.0 (37.5 - 50)**	**2.0 - 2.5 (50 - 62.5)**
C1-F-CS	90 Days	AS	0.414	0.154	0.074	0.071	0.068
		WS	0.402	0.154	0.068	0.065	0.068
	180 Days	AS	0.443	0.207	0.077	0.056	0.059
		WS	0.437	0.201	0.077	0.053	0.053
	360 Days	AS	0.508	0.248	0.089	0.059	0.062
		WS	0.476	0.219	0.069		
C1IP1-F-CS	90 Days	AS	0.390	0.154	0.065	0.089	0.065
		WS	0.402	0.154	0.065	0.065	0.065
	180 Days	AS	0.467	0.183	0.071	0.059	0.068
		WS	0.467	0.207	0.071	0.065	0.065
	360 Days	AS	0.505	0.213	0.071	0.056	0.063
		WS	0.479	0.186	0.053		
C1-S-CS	90 Days	AS	0.449	0.148	0.071	0.068	0.068
		WS	0.414	0.151	0.071	0.071	0.071
	180 Days	AS	0.502	0.151	0.068	0.077	0.074
		WS	0.473	0.151	0.059	0.059	0.062
	360 Days	AS	0.609	0.278	0.080	0.059	0.059
		WS	0.588	0.251	0.059		
C1IP1-S-CS	90 Days	AS	0.431	0.139	0.071	0.062	0.068
		WS	0.425	0.136	0.071	0.059	0.065
	180 Days	AS	0.467	0.083	0.059	0.077	0.056
		WS	0.449	0.118	0.050	0.062	0.047
	360 Days	AS	0.624	0.236	0.074	0.071	0.080
		WS	0.615	0.213	0.059		

AS: Acid soluble chloride method

WS: Water soluble chloride method

Table D-5. Chloride Concentration for Concrete Mixes made with C2 Cement and Batched with Combined Sand

Chloride Concentration (Acid and Water Soluble) in Concrete due to Salt Ponding Test							
% Cl^- by mass of concrete							
Mix No.	**Ponding Duration**	**Titration Method**	**Depth from outer surface, in. (mm)**				
			0 - 0.5 (0 - 12.5)	**0.5 - 1.0 (12.5 - 25)**	**1.0-1.5 (25 - 37.5)**	**1.5 - 2.0 (37.5 - 50)**	**2.0 - 2.5 (50 - 62.5)**
C2-F-CS	90 Days	AS	0.343	0.115	0.074	0.065	0.065
		WS	0.331	0.106	0.071	0.065	0.068
	180 Days	AS	0.420	0.148	0.071	0.065	0.062
		WS	0.408	0.136	0.056	0.050	0.050
	360 Days	AS	0.535	0.189	0.073	0.074	0.071
		WS	0.485	0.157	0.057		
C2IP-F-CS	90 Days	AS	0.384	0.160	0.080	0.074	0.065
		WS	0.390	0.142	0.077	0.077	0.068
	180 Days	AS	0.461	0.154	0.053	0.062	0.065
		WS	0.437	0.142	0.047	0.047	0.047
	360 Days	AS	0.493	0.233	0.080	0.065	0.056
		WS	0.473	0.210	0.065		
C2-S-CS	90 Days	AS	0.366	0.106	0.062	0.059	0.059
		WS	0.378	0.112	0.065	0.062	0.062
	180 Days	AS	0.579	0.183	0.065	0.053	0.053
		WS	0.567	0.136	0.053	0.041	0.041
	360 Days	AS	0.576	0.225	0.069	0.057	0.050
		WS	0.567	0.210	0.054		
C2IP-S-CS	90 Days	AS	0.449	0.136	0.065	0.059	0.065
		WS	0.461	0.130	0.065	0.065	0.056
	180 Days	AS	0.579	0.154	0.071	0.068	0.065
		WS	0.615	0.142	0.059	0.059	0.047
	360 Days	AS	0.712	0.292	0.053	0.059	0.057
		WS	0.674	0.271	0.076		

AS: Acid soluble chloride method

WS: Water soluble chloride method

Table D-6. Chloride Concentration for Concrete Mixes made with C3 Cement and Batched with Combined Sand

Chloride Concentration (Acid and Water Soluble) in Concrete due to Salt Ponding Test							
% Cl^- by mass of concrete							
Mix No.	**Ponding Duration**	**Titration Method**	**Depth from outer surface, in. (mm)**				
			0 - 0.5 (0 - 12.5)	**0.5 - 1.0 (12.5 - 25)**	**1.0-1.5 (25 - 37.5)**	**1.5 - 2.0 (37.5 - 50)**	**2.0 - 2.5 (50 - 62.5)**
C3-F-CS	90 Days	AS	0.520	0.189	0.068	0.062	0.062
		WS	0.502	0.177	0.056	0.050	0.050
	180 Days	AS	0.464	0.207	0.071	0.052	0.041
		WS	0.420	0.194	0.056		
	360 Days	AS	0.656	0.248	0.062	0.053	0.053
		WS	0.615	0.225	0.044		
C3IR-F-CS	90 Days	AS	0.449	0.130	0.053	0.053	0.050
		WS	0.437	0.136	0.047	0.041	0.038
	180 Days	AS	0.425	0.187	0.062	0.056	0.051
		WS	0.408	0.171	0.044		
	360 Days	AS	0.685	0.266	0.074	0.062	0.059
		WS	0.637	0.236	0.059		
C3-S-CS	90 Days	AS	0.555	0.089	0.059	0.056	0.053
		WS	0.555	0.106	0.047	0.047	0.044
	180 Days	AS	0.455	0.162	0.057	0.062	0.056
		WS	0.428	0.148	0.043		
	360 Days	AS	0.762	0.254	0.063	0.053	0.056
		WS	0.729	0.232	0.050		
C3IR-S-CS	90 Days	AS	0.733	0.130	0.053	0.053	0.047
		WS	0.721	0.124	0.044	0.044	0.047
	180 Days	AS	0.677	0.160	0.048	0.047	0.053
		WS	0.625	0.143	0.033		
	360 Days	AS	0.682	0.233	0.064	0.077	0.067
		WS	0.635	0.234	0.067		

AS: Acid soluble chloride method

WS: Water soluble chloride method

APPENDIX E. WATER PENETRATION RESULTS PER DIN 1048 (MAX. DEPTH OF PENETRATION)

Table E-1. Maximum Depth of Water Penetration for Concrete Mixes Batched with Natural Sand

Mix Designation		Sample No.	Max. Water Penetration Depth (x_{max}), mm		
			56 Days	180 Days	360 Days
Concrete Mixes Batched with Natural Sand	C1-F-NS1	1	28.2	23.0	14.5
		2	30.7	21.4	16.8
		3	26.6	21.1	18.0
		AVG	**28.5**	**21.8**	**16.4**
	C1-F-NS2	1	36.0	26.1	24.7
		2	34.7	26.4	15.9
		3	33.3	26.6	14.2
		AVG	**34.7**	**26.4**	**15.0**
	C1IP1-F-NS	1	32.5	23.0	17.5
		2	28.5	33.5	19.6
		3	30.5	20.5	15.5
		AVG	**30.5**	**21.8**	**17.5**
	C1IP2-F-NS	1	37.4	28.2	14.7
		2	35.7	29.3	15.1
		3	38.3	25.6	15.6
		AVG	**37.1**	**27.7**	**15.2**
	C1-S-NS1	1	24.0	21.5	15.7
		2	28.0	23.5	17.2
		3	14.0	20.5	18.7
		AVG	**26.0**	**21.8**	**17.2**
	C1-S-NS2	1	30.0	21.9	12.2
		2	33.2	23.0	11.3
		3	34.3	27.1	13.6
		AVG	**32.5**	**24.0**	**12.4**
	C1IP1-S-NS	1	29.9	18.0	12.6
		2	34.6	22.2	13.4
		3	32.5	20.1	15.2
		AVG	**32.3**	**20.1**	**13.7**
	C1IP2-S-NS	1	34.3	19.3	12.4
		2	35.3	20.2	13.6
		3	38.4	23.8	16.6
		AVG	**36.0**	**21.1**	**14.2**

Note: Cells highlighted in red were excluded from the average

Table E-1. (Continued). Maximum Depth of Water Penetration for Concrete Mixes Batched with Natural Sand

Mix Designation		Sample No.	Max. Water Penetration Depth (x_{max}), mm		
			56 Days	180 Days	360 Days
Concrete Mixes Batched with Natural Sand	C1-F-NS1	1	30.3	34.6	16.0
		2	36.0	25.1	18.5
		3	37.3	27.0	14.3
		AVG	**34.6**	**28.9**	**16.3**
	C2IP-F-NS	1	33.4	27.9	22.3
		2	35.2	22.7	20.7
		3	40.0	24.7	20.2
		AVG	**36.2**	**25.1**	**21.1**
	C2-S-NS	1	32.3	25.2	20.7
		2	28.5	25.8	19.2
		3	26.7	14.7	20.1
		AVG	**29.1**	**25.5**	**20.0**
	C2IP-S-NS	1	31.3	27.0	16.1
		2	25.9	23.6	17.6
		3	26.4	22.9	15.0
		AVG	**27.9**	**24.5**	**16.2**
	C3-F-NS	1	30.2	22.5	16.6
		2	24.6	18.6	22.5
		3	32.4	23.7	19.6
		AVG	**29.1**	**21.6**	**19.5**
	C3IR-F-NS	1	31.1	22.9	21.1
		2	27.1	20.7	24.2
		3	25.6	24.9	19.5
		AVG	**27.9**	**22.8**	**21.6**
	C3-S-NS	1	29.0	26.6	21.7
		2	33.0	24.4	23.3
		3	40.8	17.7	17.0
		AVG	**31.0**	**25.5**	**20.7**
	C3IR-S-NS	1	29.7	29.7	17.8
		2	28.5	29.2	19.3
		3	41.8	25.1	17.9
		AVG	**29.1**	**28.0**	**18.3**

Note: Cells highlighted in red were excluded from the average

Table E-2. Maximum Depth of Water Penetration for Concrete Mixes Batched with Combined Sand

Mix Designation		Sample No.	Max. Water Penetration Depth (x_{max}), mm		
			56 Days	180 Days	360 Days
Concrete Mixes Batched with Combined Sand	C1-F-CS	1	35.5	26.4	23.5
		2	30.5	24.5	24.2
		3	34.2	28.2	24.2
		AVG	**33.4**	**26.4**	**24.0**
	C1IP1-F-CS	1	30.0	37.8	22.2
		2	28.6	26.2	23.8
		3	33.1	29.1	26.0
		AVG	**30.6**	**27.6**	**24.0**
	C1-S-CS	1	26.9	18.3	19.1
		2	28.1	20.8	17.9
		3	29.0	20.1	19.3
		AVG	**28.0**	**19.7**	**18.7**
	C1IP1-S-CS	1	28.2	23.5	20.4
		2	26.5	23.4	20.9
		3	35.6	31.2	15.9
		AVG	**30.1**	**26.0**	**19.1**
	C2-F-CS	1	39.8	29.0	26.5
		2	38.4	30.0	27.0
		3		28.1	25.1
		AVG	**39.1**	**29.0**	**26.2**
	C2IP-F-CS	1	32.0	25.1	20.9
		2	28.7	25.7	21.1
		3	26.7	19.1	20.7
		AVG	**29.1**	**25.4**	**20.9**
	C2-S-CS	1	30.7	28.1	30.5
		2	33.0	27.7	21.1
		3	28.5	28.0	21.1
		AVG	**30.7**	**27.9**	**24.2**
	C2IP-S-CS	1	35.9	27.6	21.1
		2	37.4	25.1	22.5
		3	42.5	26.1	19.9
		AVG	**38.6**	**26.3**	**21.2**

Note: Cells highlighted in red were excluded from the average

Table E-2. (Continued). Maximum Depth of Water Penetration for Concrete Mixes Batched with Combined Sand

Mix Designation		Sample No.	Max. Water Penetration Depth (x_{max}), mm		
			56 Days	180 Days	360 Days
Concrete Mixes Batched with Combined Sand	C1-F-CS	1	24.4	24.6	12.8
		2	25.2	17.3	14.1
		3	34.3	17.8	13.4
		AVG	**24.8**	**17.5**	**13.5**
	C3IR-F-CS	1	32.7	22.9	25.8
		2	34.1	23.7	20.1
		3	37.8	25.7	18.9
		AVG	**34.9**	**24.1**	**19.5**
	C3-S-CS	1	22.8	19.7	17.1
		2	25.3	20.3	15.3
		3	30.1	13.7	25.8
		AVG	**24.1**	**20.0**	**16.2**
	C3IR-S-CS	1	29.5	21.6	16.7
		2	32.9	18.8	18.1
		3	31.3	23.3	16.3
		AVG	**31.2**	**21.2**	**17.0**

Note: Cells highlighted in red were excluded from the average

APPENDIX F. RAPID CHLORIDE PENETRATION RESULTS

Table F-1. Charge Passed per RCP Test Results for Concrete Mixes Batched with Natural Sand

Mix Designation		Sample No.	56 Days		180 Days		360 Days	
			Coulomb	Condition	Coulomb	Condition	Coulomb	Condition
Concrete Mixes Batched with Natural Sand	C1-F-NS1	1	1449	Low	1044	Low	598	Very Low
		2	1799		1100		496	
		3	1597		1085		542	
		4	**2404**		1012		496	
		AVG	**1615**		**1060**		**533**	
	C1-F-NS2	1	2176	Moderate	1567	Low	561	Very Low
		2	2079		2000		434	
		3	2079		2025		554	
		AVG	**2111**		**1864**		**516**	
	C1IP1-F-NS	1	1884	Low	923	Low	427	Very Low
		2	1820		1149		519	
		3	1665		1094		420	
		4	1600		1075		466	
		AVG	**1742**		**1060**		**458**	
	C1IP2-F-NS	1	3182	Moderate	1655	Low	470	Very Low
		2	3063		1739		487	
		3	3118		1904		516	
		AVG	**3121**		**1766**		**491**	
	C1-S-NS1	1	1445	Low	848	Very Low	582	Very Low
		2	1167		824		615	
		3	1417		1070		555	
		4	1231		958		532	
		AVG	**1315**		**925**		**571**	
	C1-S-NS2	1	2573	Moderate	1054	Low	424	Very Low
		2	2894		1150		530	
		3	2087		1201		493	
		AVG	**2518**		**1135**		**482**	
	C1IP1-S-NS	1	1785	Low	856	Very Low	557	Very Low
		2	1814		1056		685	
		3	1539		907		520	
		4	1589		794		532	
		AVG	**1682**		**903**		**573**	
	C1IP2-S-NS	1	2454	Moderate	1348	Low	396	Very Low
		2	2551		1362		364	
		3	2735		1186		347	
		AVG	**2580**		**1299**		**369**	

Table F-1. (Continued) Charge Passed per RCP Test Results for Concrete Mixes Batched with Natural Sand

Mix Designation		Sample No.	56 Days		180 Days		360 Days	
			Coulomb	Condition	Coulomb	Condition	Coulomb	Condition
Concrete Mixes Batched with Natural Sand	C1IP2-S-N	1	2454	Moderate	1348	Low	396	Very Low
		2	2551		1362		364	
		3	2735		1186		347	
		AVG	**2580**		**1299**		**369**	
	C2IP-F-NS	1	2181	Moderate	1755	Low	517	Very Low
		2	2542		1849		502	
		3	2862		1660		517	
		AVG	**2529**		**1755**		**512**	
	C2-S-NS	1	1274	Low	669	Very Low	449	Very Low
		2	1167		670		404	
		3	1251		628		515	
		AVG	**1231**		**656**		**456**	
	C2IP-S-NS	1	1488	Low	584	Very Low	435	Very Low
		2	1314		649		481	
		3	1214		606		476	
		AVG	**1339**		**613**		**464**	
	C3-F-NS	1	1364	Low	603	Very Low	566	Very Low
		2	1134		588		490	
		3	775		787		545	
		4	1054		730		470	
		AVG	**1184**		**677**		**518**	
	C3IR-F-NS	1	1795	Low	1001	Low	707	Very Low
		2	1125		1039		563	
		3	1879		1363		419	
		4	1660		1000		527	
		AVG	**1778**		**1101**		**554**	
	C3-S-NS	1	1225	Low	817	Very Low	566	Very Low
		2	1151		808		534	
		3	1150		919		551	
		4	1076		790		482	
		AVG	**1151**		**834**		**533**	
	C3IR-S-NS	1	1267	Low	945	Very Low	637	Very Low
		2	1665		966		589	
		3	1187		880		608	
		4	1219		898		659	
		AVG	**1225**		**922**		**623**	

Table F-2. Charge Passed per RCP Test Results for Concrete Mixes Batched with Combined Sand

Mix No.		Sample No.	56 Days		180 Days		360 Days	
			Coulomb	Condition	Coulomb	Condition	Coulomb	Condition
Concrete Mixes Batched with Combined Sand	C1-F-CS	1	2019	Moderate	980	Low	459	Very Low
		2	2052		1120		483	
		3	2066		1054		486	
		4	1499		1090		489	
		AVG	**2046**		**1061**		**479**	
	C1IP1-F-CS	1	1960	Moderate	2083	Low	964	Low
		2	2236		1980		1002	
		3	2189		1919		1068	
		4	2126		732		1058	
		AVG	**2128**		**1994**		**1023**	
	C1-S-CS	1	1103	Low	880	Very Low	608	Very Low
		2	1114		795		586	
		3	930		825		648	
		4	969		816		601	
		AVG	**1029**		**829**		**611**	
	C1IP1-S-CS	1	1320	Low	792	Very Low	590	Very Low
		2	1238		866		615	
		3	1326		837		593	
		4	1212		824		630	
		AVG	**1274**		**830**		**607**	
	C2-F-CS	1	4219	High	1623	Low	1398	Low
		2	3895		1743		1326	
		3	4036		1875		1378	
		AVG	**4050**		**1747**		**1367**	
	C2IP-F-CS	1	1798	Moderate	1471	Low	328	Very Low
		2	2211		1458		411	
		3	2180		1580		330	
		4	1987		1592		390	
		AVG	**2044**		**1525**		**365**	
	C2-S-CS	1	2310	Moderate	1755	Low	1099	Low
		2	2064		1846		1130	
		3	2297		1939		1109	
		4	1314		543		1042	
		AVG	**2224**		**1847**		**1095**	
	C2IP-F-CS	1	4211	Moderate	1750	Low	497	Very Low
		2	3995		1831		533	
		3	3784		1875		481	
		4	3611		1884			
		AVG	**3900**		**1835**		**504**	

Table F-2. (Continued). Charge Passed per RCP Test Results for Concrete Mixes Batched with Combined Sand

Mix No.	Sample No.	56 Days		180 Days		360 Days	
		Coulomb	Condition	Coulomb	Condition	Coulomb	Condition
C3-F-CS	1	1561	Low	977	Very Low	594	Very Low
	2	1362		1011		535	
	3	1451		961		627	
	4	1095		859		548	
	AVG	**1458**		**952**		**576**	
C3IR-F-CS	1	3523	Moderate	1489	Low	747	Very Low
	2	3962		1590		769	
	3	3919		1292		640	
	4	2435		1373		677	
	AVG	**3801**		**1436**		**708**	
C3-S-CS	1	1383	Low	686	Low	468	Very Low
	2	1324		934		447	
	3	1310		1016		522	
	4	1301		1109		410	
	AVG	**1329**		**1020**		**462**	
C3IR-S-CS	1	3337	Moderate	829	Very Low	573	Very Low
	2	3315		927		605	
	3	3218		886		597	
	4	3042		899		650	
	AVG	**3228**		**885**		**606**	

APPENDIX G. SAMPLE CALCULATION OF CONSTANT SURFACE CHLORIDE AND DIFFUSION COEFFICIENTS

G.1. Method of Calculation of C_s and D

The surface chloride (C_s) and diffusion coefficient (D) were calculated using least square method by means of non-linear regression analysis based on the following equation.

$$C(x,t) = C_s - (C_s - C_i)erf\left(\frac{x}{\sqrt{4Dt}}\right) \qquad \text{Eq. } D.1$$

Where:

$C(x,t)$ = the % of chloride concentration by weight of concrete, measured at depth x and time t,

C_s = chloride concentration at the surface of the concrete,

C_i = initial chloride-ion concentration before chloride exposure,

x = depth of chloride penetration,

D = chloride diffusion coefficient, m^2/s,

t = the time of chloride exposure, sec, and

erf = the error function which is described as follows:

$$erf(z) = \frac{2}{\sqrt{\pi}}\int_0^z exp(-u^2)du \qquad (D.2)$$

The procedure for the Non-Linear Regression Analysis is shown below:

$$S = \sum_{n=2}^{N} \Delta C^2(n) = \sum_{n=2}^{N} (C_m(n) - C_c(n))^2$$

Where:

S = sum of squares of chloride concentration in percent to be minimized, (mass %),

N = the total number of measured chloride samples,

$\Delta C(n)$ = difference in percent between the measured and calculated chloride concentration of the n^{th} layer,

C_m (n) = measured chloride concentration in % at the n^{th} layer.

C_c (n) = calculated chloride concentration in percent at the n^{th} layer

Plot the measured chloride contents at all points versus depth below the surface. Plot the best-fit curve on the same graph (see Figure G-1).

G.2. Example of Detailed Procedure for Calculating of Cs and D (Matlab®)

```
%Non-Linear Regression Analysis using Least Square Method
clear all

tex=-56/365;                %time when the concrete was cast (yr)
ti=0/365;                   %time when concrete was exposed to chloride (yr)
tin=[90]/365;        %time when the chloride profile was determined (yr)
Ci=[0.0];      %Initial Chloride content (% of concrete mix)

x= [1 8 15 25 35];%Depth of chloride measured (mm)
N=size(x,2);           %number of samples

%Measured chloride profile (% of concrete mix)at specified depth x.
Cm=[0.438   0.101   0.000   0.000   0.000
0.550   0.187   0.000   0.004   0.003
0.737   0.231   0.008   0.000   0.000
0.337   0.047   0.000   0.000   0.008
0.445   0.108   0.001   0.005   0.000];

syms Do Co; %Do: Diffusion Coefficient (mm2/yr)
            %Co: % Chloride at surface level at time t=tin

kt=size(tin,2);

for i=1:kt
Cx(i,:)=Ci(i)+(Co-Ci(i))*erfc(0.5*x/sqrt(tin(i)*Do));%Ficks Chloride Equation
end

n=1;
m=n+1;
p=0;

for l=1:kt
k=0;              %number of set of equations to be solved per profile
for i=n:N-1
    for j=m:N
        Sol(l,k+1)=solve(Cx(l,i)==Cm(l,i),Cx(l,j)==Cm(l,j));
    k=k+1;
    p=p+1
    end
    m=m+1;
end
m=n+1;
end

%Solution for Do and Co for all possible equations
D=[Sol.Do];
C=[Sol.Co];

for i=1:k
    for j=1:kt
        Do(i,j)=D(j+(i-1)*kt);
```

```
        Co(i,j)=C(j+(i-1)*kt);
    end
end

%Find the Calculated the Chloride content using Fick's Equation by applying
%all the possible variables calculated for Do and Co.

%Use Non-linear Regression Analysis to select the optimum Do and Co
for l=1:kt
for i=1:k
    for j=1:N

Cx(i,j,l)=Ci(l)+(Co(i,l)-Ci(l))*erfc(0.5*x(j)/sqrt(tin(l)*Do(i,l))); %Ficks Chloride↙
Equation

dC(i,j,l)=Cm(l,j)-Cx(i,j,l); %difference between the measured and calculated chloride↙
concentration at depth x
dC2(i,j,l)=dC(i,j,l)^2;
    end
S(i,l)=sum(dC2(i,:,l));    %sum of squares to be minimized, (mass %)2
end
end

%Eliminate complex numbers in S matrix
for l=1:kt
    for i=1:k
        if abs(imag(S(i,l)))>1e-50;
            S(i,l)=1000;
        end
    end
end

% Minimum sum of least square
for l=1:kt
    km=1;
    for i=1:k-1
        j=i+1;
        if (S(km,l)<S(j,l));
        Smin(l)=S(km,l);
        else
        Smin(l)=S(j,l);
        km=j;
        end
    end
end


%Select the final values for Do and Co
for l=1:kt
[row(l),column(l)] = find(S==Smin(l));
Dof(l)=Do(row(l),column(l));
```

```
Cof(l)=Co(row(l),column(l));
end

%Final Chloride profile equation using Ficks second law with selected Do and
%Co at t=tin

for l=1:kt
xc(1,l)=0;
Cc(1,l)=Ci(l)+(Cof(l)-Ci(l))*erfc(0.5*xc(1,l)/sqrt(tin(l)*Dof(l)));
ni=0.5;
Ni=max(x)/ni;

for i=1:Ni+1
    xc(i,l)=xc(1,l)+i*ni;
    Cc(i,l)=Ci(l)+(Cof(l)-Ci(l))*erfc(0.5*xc(i,l)/sqrt(tin(l)*Dof(l)));
end
end

%plot the chloride profile for the measured vs. calculated
for l=1:kt
    if l<kt
    plot(x,Cm(l,:)); hold on;
    plot(xc(:,l),Cc(:,l),'-.r'); hold on;
    else
    plot(x,Cm(l,:)); hold on;
    plot(xc(:,l),Cc(:,l),'-.r'); hold off;
    end
end
title ('Observed vs. Ficks Model Chloride Profile');
legend('Observed','Ficks Model');
xlabel('Depth, mm');
ylabel('Chloride Concentration, %');

disp(Smin);
disp(Cof);
disp(Dof);
```

The modeled versus the measured chloride profile of this example is shown in Figure G-1.

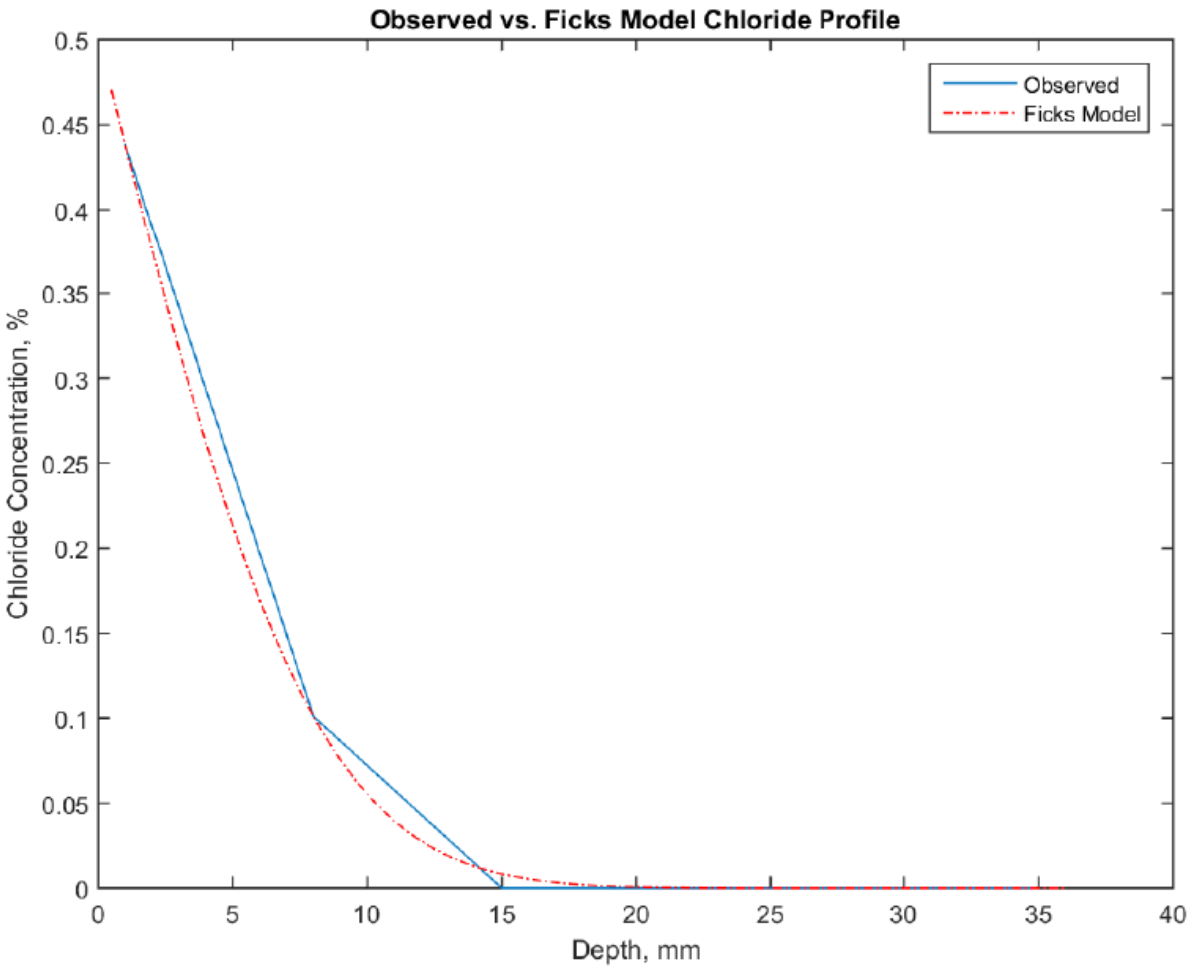

Figure G-1. Modeled versus observed chloride profile.